U. S. Department of Energy
1000 Independence Avenue, S.W.
Washington, D.C. 20585

Fiscal Year 2019: First Quarter

Progress Reports:
Advanced Battery Materials Research (BMR) Program
&
Battery500 Consortium

Released March 2019
for the period of October – December 2018

Approved by

Tien Q. Duong, Program Manager
Advanced Battery Materials Research Program & Battery500 Consortium
Vehicle Technologies and Electrification Program
Energy Efficiency and Renewable Energy

TABLE OF CONTENTS

Advanced Battery Materials Research Program

Battery500 Consortium Program

TABLE OF FIGURES

TABLE OF TABLES

A MESSAGE FROM THE MANAGER: ADVANCED BATTERY MATERIALS RESEARCH PROGRAM AND BATTERY500 CONSORTIUM

The Advanced Battery Materials Research (BMR) Program brings together leading experts from top academic, commercial, and national laboratories to identify novel electrode/electrolyte materials for enhanced battery performance. The goal is greater acceptance of electric vehicles into the consumer market. To aid in this endeavor, state-of-the-art characterization techniques and computational methodologies are used. This document summarizes activities of the BMR Program investigators during the period from October 1, 2018, through December 31, 2018.

A few notable achievements from the BMR investigators this quarter are summarized below:

- **Argonne National Laboratory** (Srinivasan's Group) examined stress distribution in ceramic single-ion conductors using a meso-scale model to determine the reason behind the experimentally observed cracking seen in ceramics despite the high modulus of these materials. The model shows that current focusing at the grain boundary, caused by difference in conductivity as well as mechanical properties, leads to stress build-up past the fracture threshold of the ceramic, causing dendrite growth in the grain boundary region.

- **Pennsylvania State University** (Wang's Group) developed a three-dimensional, cross-linked polyethylenimine lithium-ion-affinity sponge as the Li-metal anode host using electrokinetic phenomena to mitigate the issues associated with the Li-metal anode. They demonstrated that an electrokinetic surface conduction and electro-osmosis process occurring within the high-zeta-potential sponge changes the concentration and current density profiles, enabling dendrite-free plating/stripping of lithium with high Coulombic efficiency.

- **Stanford University** (Cui's Group) employed a dark-field light microscopy (DFLM) technique on a planar electrochemical cell fabricated on a glass slide to visualize the sulfur electrochemistry reactions for a Li/S battery *in operando*.

- **Daikin America** (Hendershot/Sunstrom's Group) measured the dynamic thicknesses of 200 mAh cells utilizing F-containing electrolytes during cycling. Using an optical displacement gauge, the team recorded swelling and contraction in the anode/cathode as a function of charge/discharge. Overall, the full cycling performance benefit of fluoroethylene carbonate (FEC) in the electrolyte was determined to be 10 vol%.

- **Argonne National Laboratory** (Markovic's and Curtiss' Group) investigated cubic garnet $Li_7La_3Zr_2O_{12}$ (LLZO) stabilized with aluminum, niobium, or tantalum dopants for all-solid-state Li-metal batteries. The team focused on comparing the redox stability of the various additives. The study revealed that niobium is reduced throughout the bulk of the garnet LLZO after contacting lithium metal, whereas Zr^{4+} is reduced somewhat near the interface for the dopants. The aluminum showed no significant change before and after reaction with lithium, and the electrochemical impedance spectroscopy (EIS) remained stable for an extended contact time.

Highlights from the Battery500 Consortium team include the following:

- **Keystone Project 1 (Materials and Interfaces).** Team members elucidated the voltage-dependent formation of SEI using cryogenic electron microscopy (cryo-EM) and EIS. The Team also developed a Li-S redox mediator to enable low polarization charging of Li_2S with improved reversible capacity.
- **Keystone Project 2 (Electrode Architectures).** Efforts focused on developing thick electrodes, which are necessary to achieve cell-level energy densities of ≥ 400 Wh/kg. The Team is focusing on studying influence of active mass loading and porosity for both NMC-622 and NMC-811 cathodes.
- **Keystone Project 3 (Cell Fabrication, Testing and Diagnosis).** Protocols for the safe operation and handling of lithium metal were established. This information will be available at the BMR website in the coming months.

We encourage you to follow our progress as we proceed. Our next report is expected to be available in June 2019. If you would like additional information regarding these and other DOE battery projects, we invite you to attend the Vehicle Technology Annual Merit Review (AMR) Meeting. This year it will be held June 10-13, 2019, at the Hyatt Crystal City hotel in Arlington, Virginia. To register for the meeting, please visit the meeting website (https://www.energy.gov/eere/vehicles/annual-merit-review).

Sincerely,

Tien Q. Duong

Tien Q. Duong
Manager, Advanced Battery Materials Research Program & Battery500 Consortium
Vehicle Technologies and Electrification Program
Energy Efficiency and Renewable Energy
U.S. Department of Energy

TASK 1 – Liquid/Polymer Solid-State Electrolytes

Summary and Highlights

The BMR Program goal is to develop long-life batteries superior to commercial Li-ion systems in terms of cost, vehicle range, and safety. The BMR Program addresses the fundamental problems of electrode chemical and mechanical instabilities that have slowed development of affordable, high-performance, automotive batteries. The aim is to identify electrode/electrolyte materials that yield enhanced battery performance and lead to greater acceptance of electric vehicles (EVs). Currently, the U. S. Department of Energy (DOE) Vehicle Technologies Office (VTO) supports ten projects in the BMR Program under this Electrolytes Task. These projects can be categorized into three general topics:

- **Liquid.** The projects for liquid electrolyte aim to develop electrolyte formulations, based on fluoro-chemistries, to achieve significantly improved operating voltage, increased durability, and increased energy density of Li-ion batteries at a reasonable cost. Nonaqueous polyelectrolyte solutions with high Li^+ transference numbers will be developed to achieve high rate capabilities at room temperature. In addition, electrolytes with new polymer binders bearing a pentafluorophenyl group on the backbone will be designed, synthesized, and tested.
- **Polymer.** The targets of polymer electrolyte (PE) projects include inorganic/polymer and polymer/gel hybrid electrolytes that have flexibility, mechanical strength, thermal stability, high ionic conductivity, stable interfaces against lithium metal, and polysulfide-trapping capability enabling energy density Li-S batteries, with comparable cycle life.
- **Self-Forming & Self-Healing.** The self-forming, self-healing electrolyte projects are focused on developing and implementing Li-metal-based metal fluorite and metal iodide batteries, capable of energy densities > 400-500 Wh/kg and 1000 Wh/L.

Highlights

At Daikin, measurement of dynamic thicknesses of cycling 200-mAh cells is in progress. A Keyence optical displacement gauge (one per cell) is used to record swelling in anode/cathode as a function of charging/ discharging the cell. Overall, full cycling performance benefit of fluoroethylene carbonate (FEC) in the electrolyte is realized at a 10 vol%. In addition, based on open circuit voltage (OCV) loss, gas evolution, etc. of NCA cells, the team concludes a significant amount of gassing is an inherent property of the cathode material.

The University of California (UC) at Berkeley group proposed a new polymer as a candidate for attaining high Li^+ transference number liquid electrolytes. They are purifying and characterizing these new polymers in electrolyte solutions. The group published a study of sulfonated polysulfone/poly(ethylene glycol) copolymer dissolved in dimethylsulfoxide (DMSO) and carbonates aimed at better understanding the basic design of polyelectrolyte solutions. They are also investigating effect of additives to sulfonated polyelectrolyte in carbonate solvent systems to improve transport properties and electrode-electrolyte interfacial stability.

At Argonne National Laboratory (ANL), the team shows that the tris(2,2,2-trifluoroethyl)borate (TFEB) additive to lithium polysulfide Li_2S_8 solution in dimethyl ether (DME) reduced the characteristic brown/dark color of polysulfide anions to light color. With further additive addition, all visible color in the solution disappeared, showing rapid interaction between tris(2,2,2-trifluoroethyl)borate (TFEB) and polysulfide anions. This interaction is caused by the Lewis acid-base reaction between the boron and polysulfide anion forming a soluble polysulfide-borate complex. This strong chelation was also observed in electrochemical performance in Li-S cell. To further evaluate the impact of TFEB, a 1-M lithium bis(trifluoromethanesulfonyl)imide (LiTFSI) 1,3 dioxalane / tetrafluoropropyl ether (DOL/TTE) electrolyte was selected instead of DOL/DME electrolyte. With 5% TFEB additive, the cell delivered much higher initial capacity, indicating improved sulfur utilization. However, increased additive amount showed the opposite result. It is conclusive that TFEB is a strong anion-receptor as designed, but suffers from lithium compatibility issue. New stable additives to address this are under development.

At University of Maryland (UMD), computational studies were carried out for understanding lithium nucleation and dendrite growth in the garnet solid electrolyte materials. The team studied the energy barrier of lithium nucleation using classical nucleation theory. They found that overpotential would greatly reduce the activation energy of the nucleation of the lithium particles in solid electrolyte, and that the lithium would preferably fill the pores of garnet rather than growing into garnet, which requires a higher barrier. These results support use of porous garnet framework for Li-metal electrode. They also modeled the electronic potential and ionic transport within the solid electrolyte with different microstructure features during lithium cycling. It was found the interphase layer on nanofibers and interfaces can significantly mitigate the potential hot spot of current concentration and hence provide protections against the lithium dendrite nucleation and growth.

The University of Washington (UW) group has developed improved formulations and fabrication procedures for the gel cathodes and composite separators, and also performed extensive testing on these materials (both in and outside of full-cell configurations) to gain insight into the origins of full-cell cycling behavior. In addition, they showed that the PENDI-350/triPy (PP) polymer when used as a binder increases Li-S battery capacity retention significantly from 43.5% to 74.2% after 100 cycles at C/20. The capacity retention reached close to 100% after 100 cycles at 1C, demonstrating the polysulfide trapping property of the PP polymer. Furthermore, they showed that the (naphthalene diimide) NDI moiety enhances capacity retention in two ways: first, it can be reversibly reduced into NDI^{2-} ions that can trap polysulfides via strong ion-dipole interaction; second, it can also function as a redox-mediator, which promotes the charge transfer and finally increases utilization of sulfur during discharge process. Further characterization of this effect is ongoing in Li-S cell with practical loading sulfur cathode.

At West Virginia University (WVU), composite solid electrolytes (CSEs) with silane-coated $Li_{6.25}La_3Al_{0.25}Zr_2O_{12}$ (s@LLAZO) nanofibers were further studied for investigating their morphologies, mechanical properties, and electrochemical performance. Symmetric Li | pentaerythritol triacrylate (PETA) / (poly(ethylene glycol) diacrylate-70SN (PEGDA-70SN) | Li cell was tested. Density functional theory (DFT) calculations of hydrogen treated $Li_{0.5}La_{0.5}TiO_3$ (LLTO) with different concentration of oxygen vacancy were completed.

The Stanford group has designed artificial solid-electrolyte interphases (SEI) with two distinct concepts that can enable stable deposition of metallic lithium. The two concepts are based on dynamic self-healable polymers (SHP) and single-ion conducting elastomers. Lithium plating efficiency for the different PDMS-SHP coatings with varying size of polydimethylsiloxane (PDMS) blocks were measured. Their data indicate that a higher degree of dynamic bonding is essential for the stabilization of electrodeposition.

The Lawrence Berkeley National Laboratory (LBNL) group, for the first time, was able to achieve the limiting current of 4.5 mA/cm^2 for a hybrid triblock copolymer electrolyte, POSS-PEO-POSS [POSS, polyhedral oligomeric silsesquioxane; PEO, poly(ethylene oxide)]. Due to limitations in triblock polymer material, the systematic study of current density effects was conducted with PS-PEO (115-172), which has been shown to have indistinguishable cycle life compared to equivalent cells fabricated with POSS-PEO-POSS (5-35-5).

At Stony Brook University (SBU), the energy density of the solid state concept was determined and relates to the composition of the electrolyte and the ability to effectively utilize the LiI material in the A cell. With full utilization of the LiI of the current electrolyte/cell chemical composition, the energy density is 450 Wh/kg. An alternative cell design was developed, and preliminary cycling data were collected for this alternative design. Several interfacial modifications were studied and showed increasing Coulombic efficiency (CE) with increased cycle number, including one that showed high CE near 100% over 10 cycles.

At Rutgers, the group further advanced development of the 12-V self-forming architecture by addressing transport (1) using stepped cycling protocols for alleviated stress, (2) at the electrolyte level, (3) at the positive electrode level, and (4) through cell spacing design. Several optimization steps have been translated from the single-cell design to the 12-V architecture with the goal of improving performance. It was determined that diffusion limitations were the ultimate barrier in further progress. To overcome this barrier, three directions will be pursued next quarter. These include a decrease of the electrode spacing with improved electrode morphologies, moderate temperature increase, and hybridization of the electrolyte.

Task 1.1 – Advanced Lithium-Ion Battery Technology: High-Voltage Electrolyte (Joe Sunstrom, Ron Hendershot, and Alec Falzone, Daikin)

Project Objective. The project objective is to identify electrolyte formulations, based on fluoro-chemistries, that will allow significantly improved operating voltage, increased durability, and increased energy density of Li-ion batteries at a reasonable cost. The project seeks to understand the conditions under which the electrolyte degrades, the effect on battery performance, and solutions that can overcome current limitations of the electrolyte. Gassing in Li-ion batteries is one of the most common failure mechanisms and poses the greatest safety risk in consumer devices. This project aims to investigate gas composition as a function of cathode material, electrolyte formulation, and operating voltage, and proposes optimal cell compositions at decomposition voltages.

Project Impact. Developing an understanding of the operating conditions in which gasses form in Li-ion batteries enables the project to propose optimized cell compositions, which operate at higher voltages for a longer period. Different fluorinated electrolyte components and additives may suppress and/or eliminate gas generation at or above hypothesized decomposition voltages. To investigate these topics, it is imperative that the project utilize multiple approaches, including, but not limited to: cathode material, electrolyte composition, operating voltage, and cycle number.

Approach. The evolving composition of the electrolyte in the battery will be examined by various analytical instruments to study volatiles [gas chromatography – mass spectrometry (GC-MS)/thermal conductivity detector (TCD)], liquid [liquid chromatography MS (LC-MS)], and solid [time-of-flight secondary ion mass spectrometry (TOF-SIMS), thermogravimetric analysis MS (TGA-MS), X-ray photoelectron spectroscopy (XPS), and auger electron spectroscopy (AES)] electrolyte decomposition products during battery operation. In the first year, the team addressed the gas composition and kinetics for both hydrocarbon and fluorocarbon as a function of several charge/discharge conditions. In the second year, the project will transition into analysis of the solid-state electrolyte (SSE) decomposition components of its tested batteries to obtain valuable information about SEI layer formation and how it manifests change in both the anode (graphite) and cathode (LCO and NMC). The third year is focused on measuring changes in the solid-state structure of the cathode following high-voltage operation. The project aims to quantify any dissolved metal ions originating from the cathode, and deposited on the anode using inductively coupled plasma – mass spectrometry (ICP-MS). It will also study changes in the cathode structure using powder X-ray diffraction (XRD).

Out-Year Goals. Work will progress toward understanding how electrolyte formulation and cell operation affect the stability of transition metals (TMs) in the cathode structure. Specifically, the project aims to quantify metal ions, if any, dissolved into solution as a function of operating parameters (that is, voltage, time, etc.) and electrolyte formulation. In addition, measurements will be made using powder XRD to detect changes in the crystal structure of the cathode (LCO and NMC). Understanding effects on the solid-state structure in Li-ion batteries will provide valuable information on the required cathode chemistry for increased performance at high voltage.

Collaborations. The project has initiated a collaboration with Dr. Yi Cui (Stanford University) for cryogenic transmission electron microscopy (cryo-TEM) measurements on solid battery components.

Milestones

1. Film composition (elemental) versus time/voltage complete – Milestone 2.2. (Q1, FY 2019; Completed)
2. Battery thickness (non-gas) versus time/voltage complete – Milestone 2.3. (Q2, FY 2019; In progress)

Progress Report

Real-time thickness measurements of anode swelling will be made with Keyence contact sensors. These devices are capable of outputting an analog signal that can be measured using an external device (for example, Arbin battery tester), and have a linear response in the 0-5 mm range. Thickness standards (0-1 mm) were used to generate the calibration curve depicted in Figure 1 (left). For each sensor to account for system variability, it was necessary to generate a calibration curve of thickness versus change in voltage. In addition, the structure of the contact sensor device setup for 200 mAh cells can also be seen in Figure 1 (right).

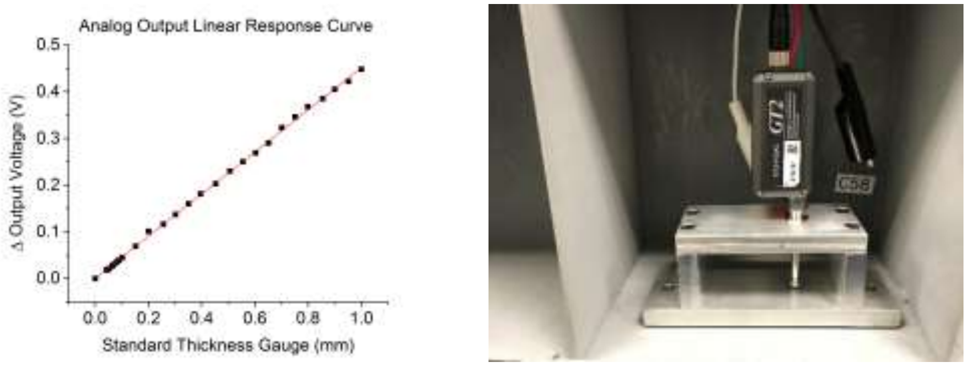

Figure 1. Calibration curve of Keyence contact sensors in the 0-1 mm range (left). Custom device configuration to measure thickness changes in 200 mAh cells (right).

Along with obtaining organic and inorganic fragmentation information of the SEI layer using TOF-SIMS, chemical information can be obtained utilizing XPS. Characteristic binding energies can be obtained by fitting the resulting multiplex spectra. XPS survey spectra of a cycled NMC-622 cathode are depicted in Figure 2, both before (black curve) and after (red curve) a 1-minute sputter cycle to remove adventitious carbon. Characteristic TM energies (nickel, manganese, cobalt) can be seen, in addition to strong carbon, oxygen, and fluorine 1s binding energies.

The fitted carbon 1s multiplex spectrum is displayed in Figure 2 (middle), and represents the carbon present on the surface of the SEI layer. Along with the fluorine 1s and oxygen 1s multiplex spectra, changes in the types of inorganic and organic species as a function of position in the SEI layer can be seen by depth profile experiments using XPS. At the surface of the SEI layer, closest to the liquid electrolyte, carbonate and inorganic fluorides are expected to have the greatest contributions (Figure 2). As proximity in the SEI layer becomes closer to the bulk metal oxide cathode material, the presence of an amorphous carbon layer gains intensity.

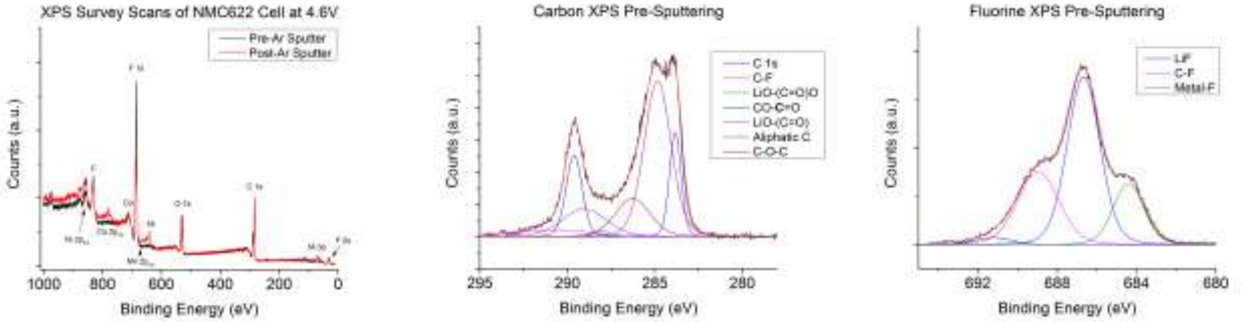

Figure 2. X-ray photoelectron spectra of tested NMC-622 cathode (4.6 V, fluorinated electrolyte, 200 cycles). Survey spectrum (left), carbon 1s (middle), and fluorine 1s (right) fitted spectra are depicted.

In addition, a collaboration with Dr. Yi Cui (Stanford University) began this quarter to utilize cryo-TEM as another method to measure thickness of the SEI layer in tested cells with fluorinated electrolyte at 4.6 V.

Patents/Publications/Presentations

Presentation

- BMR Electrolytes Meeting, LBNL, Berkeley, California (October 11–12, 2018): “Daikin Advanced Lithium Ion Battery Technology – High Voltage Electrolyte”; J. Sunstrom, A. J. Falzone, C. A. Meserole, R. Hendershot, A. Sandoval, A. Haque, E. Grumbles, and M. Costa.

Task 1.2 – Multi-Functional, Self-Healing Polyelectrolyte Gels for Long-Cycle-Life, High-Capacity Sulfur Cathodes in Lithium-Sulfur Batteries

(Alex Jen and Jihui Yang, University of Washington)

Project Objective. The project objective is to develop self-healing and polysulfide-trapping polyelectrolyte gels containing room-temperature ionic liquid (RTIL) for the Li-S battery system. The battery design will be able to achieve gravimetric and volumetric energy densities of ≥ 800 Wh/kg and ≥ 1000 Wh/L, respectively.

Project Impact. The Li-S battery system is currently hampered by poor capacity retention, primarily caused by dissolution of polysulfide reaction intermediates in typical organic electrolytes, as well as poor electrical contact between insulating sulfur and the conductive carbon matrix. This project aims to produce a high-capacity, long-cycle-life Li-S battery system by using rational molecular design strategies to address each capacity loss mechanism directly. A long-cycle-life Li-S battery system with the capability of doubling Li-ion energy density would enable production of lighter, longer range EVs at a cost affordable to the average U. S. household.

Approach. The team will develop Li-S coin cells that utilize self-healing, interpenetrated ionomer gel electrolytes in both the cathode and separator. The team will synthesize necessary starting materials and fabricate components of these gels while testing their relevant electrochemical and mechanical properties. All components will be combined into interpenetrating structures, which will be tested both alone and in cell configurations. Device performance data will be collected and used to further optimize designs of both material and cell, culminating in an optimized Li-S battery design capable of doubling the energy density of traditional Li-ion batteries. During the first year, the team is focusing on (1) synthesis of a variety of precursors for gel electrolytes, (2) fabrication and testing of both baseline materials and novel materials made from these precursors, and (3) iterative validation and improvement of design principles through both materials and device testing.

Out-Year Goals. Work will progress toward developing structure-property relationships for the self-healing, interpenetrated gel ionomer electrolyte and its individual components, as well as successful incorporation of such an electrolyte into a working Li-S cell. The team plans to demonstrate significant improvements in both capacity and retention when using the project's novel materials, as compared to state-of-the-art baseline systems.

Collaborations. This project funds work at the UW. Dr. Alex Jen, principal investigator (PI), focuses on design, synthesis, and testing of novel materials, as well as device-based verification of design principles. Dr. Jihui Yang (co-PI) focuses on optimization of device fabrication and testing, as well as investigation of failure mechanisms in devices using novel materials. Pacific Northwest National Laboratory (PNNL) facilities will be used for detailed study of device operation.

Milestones

1. Provide detailed cell performance data for practical-loading cells containing currently best materials designs, along with conclusions regarding the origin of performance details. (Q2, FY 2019; In progress)
2. Provide detailed cell performance data for concept cells containing currently best materials designs, which should meet or nearly-meet performance targets. (Q4, FY 2019)

Progress Report

Multifunctional Ionomer Gels / Gel Cathode. Previously, the team described integration of the solvate ionogel (SIG) materials into both the cathode and separator of Li-S batteries. This resulted in quasi-solid-state cells that showed excellent specific capacity and retention on cycling at 23°C, but with a significant overpotential, and voltage features that are typical of cells with organic electrolytes. This quarter, the team has developed improved formulations and fabrication procedures for the gel cathodes and composite separators, and also performed extensive testing on these materials (both in and outside of full-cell configurations) to gain insight into the origins of full-cell cycling behavior.

Figure 3a shows the capacity of Li-S concept cells (~1 mg_{sulfur}/cm^2) over 100 cycles at 30°C. At 0.1C rate, the team found that quasi-solid-state cells containing SIG show better capacities than the control material system [PVdF binder + organic liquid electrolyte (DOL/DME) in Celgard 2500], but by a slight amount (~ 100 mAh/g), and exhibit long-term capacity fading at a similar rate. By contrast, cells of typical construction with solvate ionic liquid (SIL) electrolyte showed poorer initial capacity, but with reduced fading. Examining voltage profiles (3rd cycle) for these cells at varying rates revealed major differences between cell types (Figure 3b-c). The team found that the discharge overpotentials of SIG/SIL cells are almost uniformly larger than the control electrolyte, especially during the low-voltage region that accounts for most of the cell capacity. The transition from higher to lower voltage also occurs more gradually for these cells, although the voltage minimum at this transition point, characteristic of a polysulfide-induced "dip" in liquid electrolyte conductivity, is absent for the SIG cells. Similarly, overpotential for SIG/SIL cells during recharge is generally larger, and more sloped for SIG cells. Also notable is the maximum in voltage observed on initiation of recharge, well known to be associated with activation of solid Li_2S deposits. This "bump" is significant for the SIL case, but far less prominent in the SIG case and entirely absent from the control.

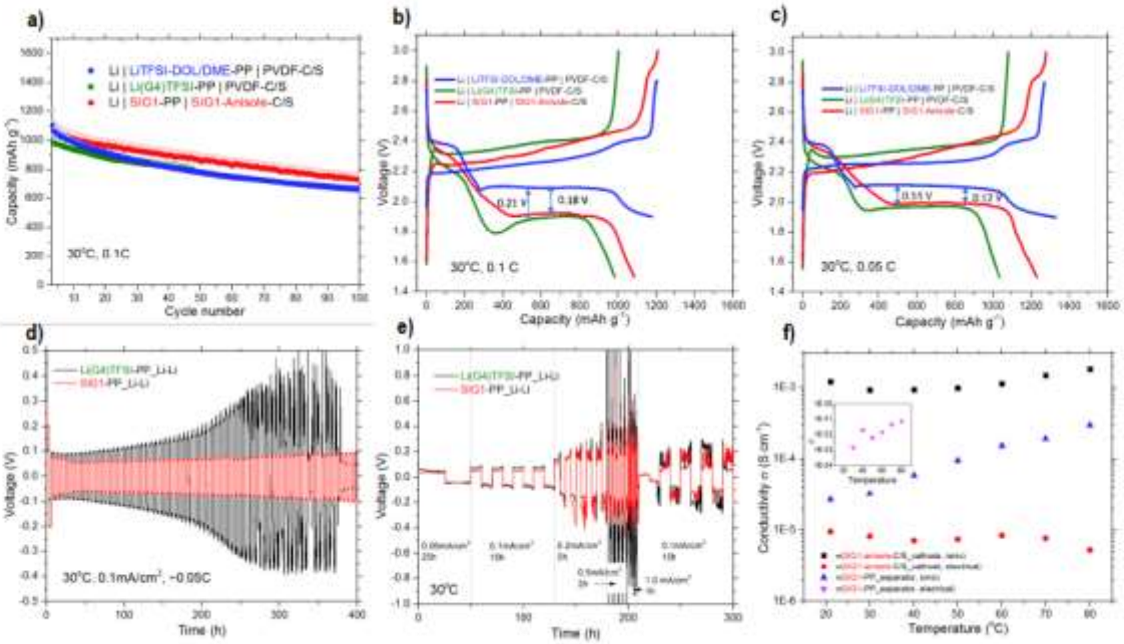

Figure 3. (a) Specific capacity (mAh/g_{sulfur}) for Li-S cells of indicated cell structure [anode | electrolyte-separator | binder/gel-cathode] during galvanostatic cycling at 0.1C (calculated based on 1672 mAh/g_{sulfur} theoretical capacity). (b) 3rd cycle voltage profiles for indicated cells at 0.1C. (c) 3rd cycle voltage profiles for indicated cells at 0.05C. (d) Cycling of symmetric cells [electrolyte-separator-electrodes] at ±0.1 mA/cm^2 using a 6 h cycle period. (e) Cycling of symmetric cells [electrolyte-separator-electrodes] with varying current density and cycle period. (f) Ionic/electrical conductivity versus temperature for gel cathodes and gel separators, extracted from frequency-dependent impedance between stainless-steel blocking electrodes.

To gain further insight, the team fabricated Li|Li symmetric cells containing either SIG composite separators or Celgard 2500 wetted with a similar total volume of SIL. Cyclic stripping and plating at 30°C and 0.1 mA/cm^2 (Figure 3d), roughly equivalent to the current density of the above cells at 0.05C, reveal uniformly lower and more-stable overpotential for the SIG separators (~ 50 mV versus ~ 100 mV). This trend roughly holds at larger current densities (Figure 3e), although the potentials become erratic at 0.2 mA/cm^2 or higher, indicating unstable behavior that will eventually lead to dendrite-related short-circuiting.

These differences at the anode/separator may explain the increased overpotential of full cells with SIL electrolyte as compared to SIG; they cannot explain the differences of both compared to the control, even assuming the anode/separator resistance of the control cell is negligible. While many of these differences may instead relate to altered conversion chemistries in the cathode (which are still being investigated), a significant portion of the overpotential in the SIG cells may be due to poor electrical conductivity in the cathode as well. Impedance analysis of a typical gel cathode sample between blocking electrodes revealed a very poor through-film electrical conductivity of <10^{-5} S/cm (Figure 3f), corresponding to ~ 125mV cell polarization at 0.1C rate. The team is investigating changes to gel cathode composition and fabrication procedures to reduce this electrical resistance.

Self-Healing Materials. Following the previous characterization of the PP SHP system, including its tunable mechanical/self-healing behavior and useful Li$^+$ conductivity, the team continued efforts to characterize effects of this material in a Li-S battery system. As reported earlier, performance improvements are expected from two primary functions of the polymer system: the polysulfide-trapping effect of NDI moieties, and self-healing of mechanical damages of materials during cycling. The PP polymer when used as a binder was shown to increase capacity retention significantly, from 43.5% to 74.2% after 100 cycles at C/20. Capacity retention reached close to 100% after 100 cycles at 1C, which demonstrated the polysulfide-trapping property of the PP polymer.

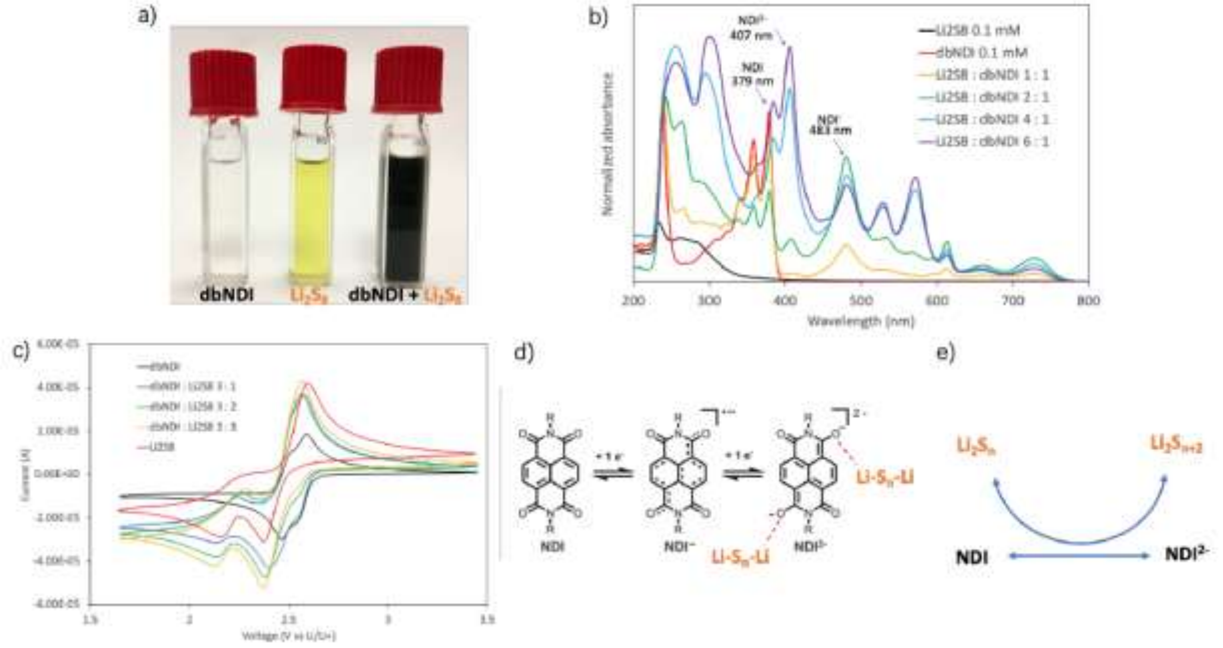

Figure 4. (a) Visual test of the reaction/interaction between Li_2S_8 (1 mM) and dbNDI (1 mM) in DOL/DME (1:1, v:v) with 1 M LiTFSI. (b) Ultraviolet-visible spectra of solutions with various ratios between dbNDI and Li_2S_8 in DOL/DME (1:1, v:v) with 1 M LiTFSI. The concentration of dbNDI was kept constant as 0.1 mM in the mixture. (c) Cyclic voltammetry spectra of dbNDI (10 mM) and Li_2S_8 in DOL/DME (1:1, v:v) with 1 M LiTFSI (scan rate = 10 mV/s). (d) Two-step reductions of NDI moiety and illustration of ion-dipole interaction between NDI moiety and polysulfides. (e) Schematic illustration of redox-mediator effect of NDI moiety.

This quarter, the team performed cyclic voltammetry (CV) and ultraviolet-visible (UV-Vis) studies on dibutyl-NDI (dbNDI) and Li_2S_8 as model compounds to understand details of the polysulfide-trapping mechanism. By simply mixing dbNDI with Li_2S_8 in DOL/DME, the color changed immediately from the yellow of Li_2S_8 to black (Figure 4a). This color change suggests strong interaction/reaction between dbNDI and Li_2S_8. UV-vis studies were conducted of solutions with various ratios between dbNDI and Li_2S_8. As shown in Figure 4b, dbNDI (red line) shows the characteristic peak of the neutral state at 379 nm. After adding Li_2S_8 with a molar ratio of 1:1, the peak of the neutral dbNDI (379 nm) decreases slightly and a peak at 483 nm increases, which corresponds to the existence of $dbNDI^-$ ion. When the ratio of Li_2S_8:dbNDI increases to 2:1, more of the neutral dbNDI is reduced into $dbNDI^-$ ion. Meanwhile, the peak of $dbNDI^{2-}$ ion appears at 407 nm, which increases rapidly with increasing Li_2S_8. In short, the NDI moiety enhances capacity retention in two ways: first, it can be reversibly reduced into NDI^{2-} ions that can trap polysulfides via strong ion-dipole interaction (Figure 4d); and second, it can also function as a redox-mediator (Figure 4e), which promotes the charge transfer and finally increases utilization of sulfur during the discharge process. Further characterization of this effect is ongoing in Li-S cell with practical loading sulfur cathode.

Patents/Publications/Presentations

Publications

- Hubble, D., J. Qin, F. Lin, I. A. Murphy, S.-H. Jang, J. Yang, and A. K.-Y. Jen. “Designing Lithium Solvate Ionogels with Very High Conductivity and Lithium Transference Number.” *Journal of Materials Chemistry A* 6 (2018): 24100–24106. doi: 10.1039/C8TA08808J.
- Qin, J., F. Lin, D. Hubble, Y. Wang, Y. Li, I. A. Murphy, S.-H. Jang, J. Yang, and A. K.-Y. Jen. “Tuning Self-Healing Properties of Stiff, Ion-Conductive Polymers.” In peer review at *Journal of Materials Chemistry A.*
- Li, Y.,* I. A. Murphy,* Y. Chen, F. Lin, X. Wang, S. Wang, D. Hubble, S.-H. Jang, K. T. Mueller, C. Wang, A. K.-Y. Jen, and J. Yang (*co-first author). “Surface Functionalization of Mesoporous Carbon for Polysulfide Trapping in Lithium Sulfur Batteries.” In peer review at *Journal of Materials Chemistry A.*

Task 1.3 – Construct and Test Lithium-Metal/Composite Electrolyte/Lithium-Metal Symmetric Cells (Nianqiang (Nick) Wu, West Virginia University; Xiangwu Zhang, North Carolina State University)

Project Objective. The project objective is to develop SSEs based on the highly conductive inorganic nanofibrous network in the polymer matrix for lithium batteries.

Project Impact. The team will conduct research and development (R&D) on solid-state inorganic nanofiber-polymer composite electrolytes that will not only provide higher ionic conductivity, improved mechanical strength, and better stability than the PEO polymer electrolyte, but also exhibit better mechanical integrity, easier incorporation, and better compatibility with the Li-metal anode than the planar ceramic membrane counterparts. The proposed inorganic nanofiber-polymer composite electrolytes will enable practical use of high-energy-density, high-power-density Li-metal batteries, and Li-S batteries.

Approach. Integration of the highly Li^+-conductive inorganic nanofiber network into the polymer matrix not only provides the continuous Li^+ transport channels, but also kinetically inhibits crystallization from the amorphous state of polymer electrolyte. The inorganic nanofibers will be fabricated with an electrospinning technique; the ionic conductivity of inorganic nanofibers will be improved by chemical substitution or doping. Highly ionic-conductive polymers will be developed by cross-linking and/or creation of a block-copolymer structure. The composition and microstructure of the composite electrolyte will be designed to suppress the lithium dendrite formation.

Out-Year Goals. Work will progress toward synthesis of the inorganic nanofibers and polymer matrix. The goal is to find the optimal synthetic route to achieve the desirable conductivity.

Collaborations. This project funds work at WVU and North Carolina State University (NCSU). Dr. Nianqiang (Nick) Wu at WVU serves as PI, and Dr. Xiangwu Zhang at NCSU acts as co-PI. Peng Zheng and Xuefei Gao (Ph.D. student at WVU), Hui Yang (Postdoctoral Fellow at WVU), Botong Liu (Ph.D. student at WVU), Chaoyi Yan (Ph.D. student at NCSU), and Mahmut Dirican (Postdoctoral Fellow at NCSU) contributed to the project.

Milestones

1. Construct the Li-metal/composite electrolyte/Li-metal symmetric cells – Subtask 3.1.1. (Q4, FY 2019; Completed)
2. Test electrochemical performance of the Li-metal/composite electrolyte/Li-metal symmetric cells, such as interfacial resistance as a function of time derived from impedance spectroscopy and the electrochemical stability window derived from anodic/cathodic scans – Subtask 3.1.2. (Q4, FY 2019; 80% Completed)
3. Investigate interfacial stability under both open-circuit and Li-metal plating-stripping conditions; and measure the end of half-cycle voltage during lithium plating-striping cycling for the symmetric cells – Subtask 3.1.3. (Q4, FY 2019; 50% Completed)
4. Examine effectiveness of composite electrolytes in suppressing formation and growth of lithium dendrites – Subtask 3.1.4. (Q4, FY 2019; 30% Completed)

Progress Report

This quarter, composite solid electrolytes (CSEs) with silane-coated LLAZO (s@LLAZO) nanofibers were further studied for investigating their morphologies, mechanical properties, and electrochemical performance. Symmetric Li|PETA/PEGDA-70SN|Li cell was tested. DFT calculation of hydrogen-treated LLTO with different concentration of oxygen vacancy was finished.

Construct and Test the Li-Metal/Composite Electrolyte/Li-Metal Symmetric Cells

Silane-Coated LLAZO-Incorporated Cross-Linked Polymer Composite Electrolytes. The pristine PEGDA polymer electrolyte showed Young's modulus of 18.1 MPa, tensile strength of 1.36 MPa, and maximum elongation of 7.9%. With the addition of LLAZO nanofibers, the resultant LLAZO-60PEGDA showed increased elongation (21%) and tensile strength (1.74 MPa), but reduced Young's modulus (10.4 MPa) due to the plasticized effect. With silane coating, s@LLAZO(24h)-40PEGDA CSE demonstrated the highest modulus (29.5 MPa) and tensile strength (4.2 MPa) because the binding force between nanofibers and polymer matrix was enhanced.

The electrochemical stability of the s@LLAZO-PEGDA composite electrolytes was also tested. LLAZO-90PEGDA CSE with 10 wt% LLAZO nanofibers in PEGDA showed similar anodic stability (4.7 V) to PEGDA (4.5 V) because of the high PEGDA content. Nevertheless, s@LLAZO-60PEGDA CSE has a higher LLAZO content of 40 wt%, and hence exhibited a higher decomposition onset voltage of 5.3 V owing to the excellent electrochemical stability of inorganic Li-conductor.

As shown in Figure 5b, the ionic conductivities of s@LLAZO(6h)-PEGDA composite electrolytes increased with the increasing the weight content of nanofibers. The ceramic fillers with silane treatment were also fabricated with SiO_2 and TiO_2 nanoparticles for comparison. However, after increasing the SiO_2 or TiO_2 filler content beyond 10 wt%, the ionic conductivity of s@SiO_2(6h)-PEGDA and s@TiO_2(6h)-PEGDA composite electrolytes decreased dramatically. This significant conductivity difference confirmed that the active s@LLAZO nanofiber filler provided significant contribution to Li^+ conduction in the s@LLAZO-PEGDA composite electrolytes.

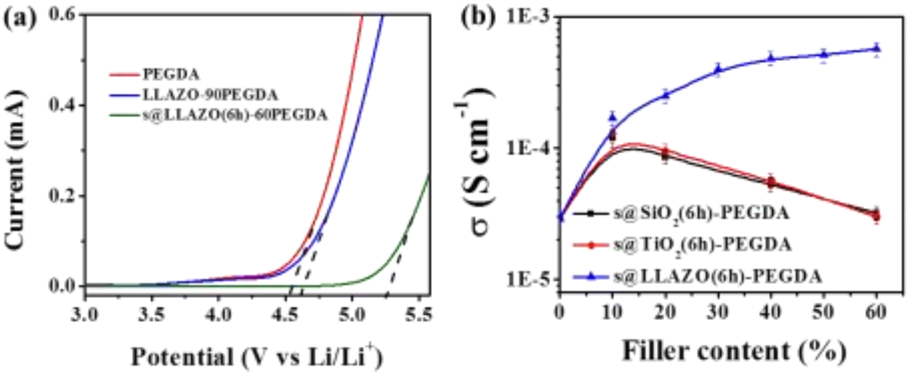

Figure 5. (a) Linear sweep voltammetry curves of PEGDA, LLAZO-90PEGDA, and s@LLAZO(6h)-60PEGDA composite electrolytes. (b) Ionic conductivity of s@LLAZO(6h)-PEGDA, s@TiO_2(6h)-PEGDA, and s@SiO_2(6h)-PEGDA CSEs with different filler contents.

Plastic-Crystal-Based Solid Polymer Electrolytes

A symmetric Li|PETA/PEGDA-70SN|Li cell was assembled to mimic a charging and discharging operation in Li-metal batteries. The cell was periodically charged and discharged for 30 min at a constant current density of 0.1 mA/cm^2 at room temperature. The cell showed stable lithium cycling for 250 h without short-circuiting. The cell overpotential was 38 and 70 mV at current densities of 0.1 and 0.2 mA cm^{-2}, respectively.

DFT Calculation of Hydrogen Treated LLTO with Different Concentration of Oxygen Vacancy

DFT calculation shows that the oxygen vacancies that are created on different sites of perovskite crystalline structures determine the electrochemical performance of the LLTO materials. In the simulation model of $Li_3La_7Ti_{12}O_{36}(Li_{0.25}La_{0.583}TiO_3)$ as shown in Figure 6a, there are three different layers in the LLTO structure, named La-rich layer, Ti-rich layer, and La-poor layer.

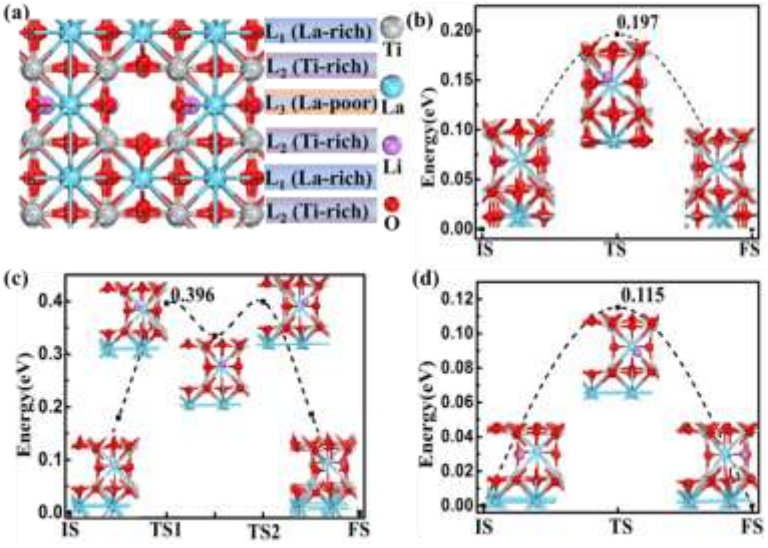

Figure 6. (a) Density functional theory simulation model $Li_3La_7Ti_{12}O_{36}(Li_{0.25}La_{0.583}TiO_3)$. (b) Energy barrier of Li-ion transport through lanthanum vacancy in oxygen vacancy-free model. (c) Simulation model with 16.67% of oxygen vacancy concentration (all oxygen vacancy located in the La-rich layer). (d) Simulation model with 22.22% of oxygen vacancy concentration (six oxygen vacancies located in the La-rich layer and two oxygen vacancies located in the Ti-rich layer, symmetrically).

In the oxygen vacancy-free model, as shown in Figure 6b, the lithium atom is near the La-vacancy site in the transition state and the Li-ion transport barrier is 0.197 eV, which is in agreement with reported values. To study the influence of the oxygen vacancy on the transport of lithium ions, it is crucial to first analyze the location of oxygen vacancies. The oxygen vacancy may occur in any of these layers. The oxygen vacancy energetically prefers to set in La-rich layer for 2.78% concentration (one oxygen vacancy in the model). Then, the team added the oxygen vacancies to six in the model, corresponding to 16.67% of O-vacancy concentration. The results show that all oxygen vacancies will sit in the La-rich layer (energetically favorable state). Thus, the team can conclude that the oxygen vacancy prefers to sit in the La-rich layer if the concentration is smaller than 16.67%, or the oxygen vacancies in the La-rich would occur before the oxygen vacancy is present in other layers. For 16.67% of oxygen vacancies in La-rich layer, the barrier for Li-ion transport is calculated to be 0.396 eV, which is higher than that of the oxygen vacancy-free model. This may be due to a stronger Coulomb force between oxygen and lithium ions. When the oxygen vacancy concentration is higher than 16.67%, the team has simulated the model with 22.22% of oxygen vacancies (eight oxygen vacancies in the model). It shows that six oxygen vacancies are present in the La-rich layer, and two oxygen vacancies are located in the La-poor layer symmetrically. In this case, the barrier for lithium translation is 0.115 eV, which is smaller than that of the oxygen vacancy-free model. The calculation analysis is in accordance with previous results.

Patents/Publications/Presentations

The project has no patents, publications, or presentations to report this quarter.

Task 1.4 – High Conductivity and Flexible Hybrid Solid-State Electrolyte
(Eric Wachsman, Liangbing Hu, and Yifei Mo, University of Maryland)

Project Objective. The project objective is to develop flexible hybrid electrolyte with garnet nanofibers to achieve the following: (1) flexible, with greater mechanical strength (~ 10 MPa) and thermal stability than polymer electrolytes; (2) high room-temperature ionic conductivity, ~ 0.5 mS/cm; (3) stable interface with lithium metal and effective blocking of lithium dendrites at current densities up to 3 mA/cm^2; and (4) battery performance with Li-S chemistry with an energy density of ≥ 450 Wh/kg (and ≥ 1000 Wh/L) and maintaining ≥ 80% of capacity up to 500 cycles.

Project Impact. Instability and/or high resistance at the interface of lithium metal with various solid electrolytes limit(s) the use of the metallic anode for batteries with high energy density, such as Li-air and Li-S batteries. The critical impact of this endeavor will be focused on developing a new type of SSE that is highly conductive, highly flexible, and electrochemically stable. The new SSE will enable Li-metal anodes with excellent interfacial impedance and blocking of lithium dendrite formation.

Approach. The project will synthesize garnet nanofibers, fill the porous region with polymer electrolyte, and characterize the flexible hybrid membrane properties. The flexible hybrid SSE microstructure will be determined using focused ion beam / scanning electron microscopy (FIB/SEM) and integrated with electrochemical methods to investigate the properties and stability with Li-metal anode.

Out-Year Goals. The project will develop a fundamental understanding of the mechanism of Li-ionic diffusion in garnet nanofibers and their mechanical properties, as well as these properties for hybrid garnet-fiber/polymer hybrids. Work will progress toward study of the electrode assembly during electrochemical cycling of the anode.

Collaborations. This project funds work at UMD, College Park. Dr. E. D. Wachsman (PI) will focus on optimizing the garnet network to achieve high ionic conductivity and flexibility using FIB/SEM and electrochemical impedance spectroscopy (EIS) characterization. Dr. L. Hu (co-PI) focuses on synthesis of the hybrid electrolyte and test for Li-metal anode with the hybrid electrolyte. Dr. Y. Mo (co-PI) will lead efforts on computational modeling of the garnet nanofiber hybrid electrolytes for fundamental mechanistic understanding.

Milestones

1. Modeling of lithium dendrite protection: Understand lithium dendrite growth and protection effect of polymer and interphase layers on garnet nanofiber. (Q1, FY 2019; Completed December 2018)

Progress Report

Computational studies based on first principles calculations and continuum modeling were performed for understanding lithium nucleation and dendrite growth in the garnet solid electrolyte materials. The team studied the energy barrier of lithium nucleation using classical nucleation theory. Using the surface and interface energies from first principles calculations, they obtained the energy of lithium particle nucleation as a function of the particle size. Results indicated that the applied overpotential would greatly reduce the activation energy of the nucleation of the lithium particles in solid electrolyte, in consistency with the experimental observations that high overpotential would greatly accelerate lithium dendrite growth. The team also found a low energy barrier and small critical nucleus size of lithium particle, suggesting easy lithium nucleation. In addition, they compared the lithium nucleation inside the preexisting pores of garnet and toward the inside of garnet. The calculations also show that the lithium would preferably fill the pores of garnet rather than grow into garnet, which requires a higher barrier. These results support the use of porous garnet framework for Li-metal electrode.

Since electronic transport is critical in lithium dendrite formation within solid electrolyte, the team also studied various point defects in the garnet solid electrolyte using first principles calculations (Figure 7). The calculations found lithium insertion into garnet may be energetically favorable at Li-rich conditions, in agreement with previous experimental results. In addition, the results suggest oxygen vacancies may form at Li-rich conditions and may aid Li-metal reduction. In addition, the first principles calculations found possible polarons formation inside the garnet, which may provide possible electron transport and aid dendrite formation. The modeling of point defects in garnet provides new insights into lithium dendrite growth mechanism in garnet solid electrolyte.

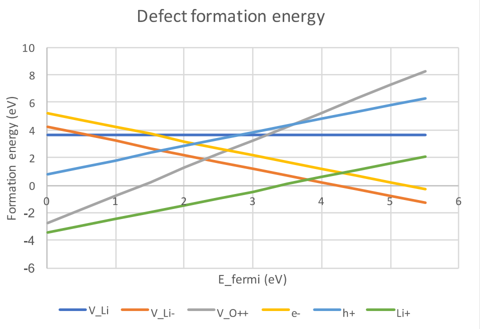

Figure 7. Formation energy of various point defect in lithium garnet.

The team modeled the electronic potential and ionic transport within the solid electrolyte with different microstructure features during lithium cycling. For the lithium dendrite formed inside solid electrolyte, modeling results (Figure 8) show high ion current density near the tip of lithium dendrite, indicating an increase of lithium chemical potential and the driving force for lithium dendrite growth, also known as a hot spot. Similar behavior exists in the grain boundaries of garnet solid electrolyte, caused by slow ionic diffusion and high resistances in grain boundaries. This behavior also suggests a tendency for lithium dendrite growth in grain boundaries of solid electrolyte, consistent with numerous reports in the literature. The team found that the hybrid solid electrolyte with garnet nanofibers exhibits fewer hot spots for lithium dendrite growth because of the well-connected, fast-ion conducting garnet fibers formed inside the hybrid solid electrolyte. This modeling result is consistent with the high current density up to 3 mA/cm^2 observed in the lithium cycling experiments of hybrid garnet solid electrolyte. The modeling is also performed to study the effect of polymer and interphase layers on nanofibers. It was found the interphase layer on nanofibers and interfaces can significantly mitigate the potential hot spot of current concentration and hence provide protections against lithium dendrite nucleation and growth.

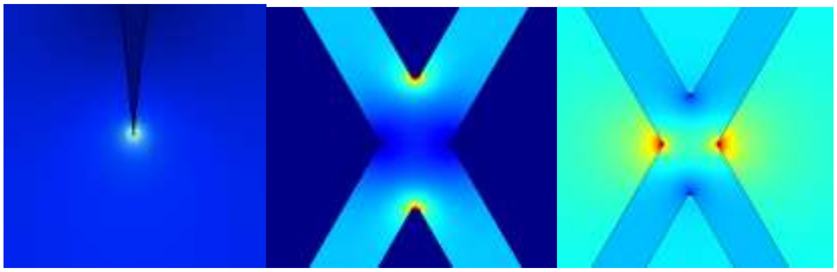

Figure 8. Hot map of lithium dendrite formation in solid electrolyte with various microstructure features.

Patents/Publications/Presentations

Publication

- Nolan, A., Y. Zhu, X. He, Q. Bai, and Y. Mo. "Computation-Accelerated Design of Materials and Interfaces for All-Solid-State Lithium-Ion Batteries." *Joule* 2 (2018): 2016-2046.

Presentations

- Materials Research Society (MRS) Fall Meeting, Boston, Massachusetts (November 26–30, 2018): "Beyond Dendrites, Cycling Li-Metal across Garnet at High Current Densities"; E. Wachsman. Invited.
- Battery Safety/Lithium Battery Materials and Chemistries, Washington, D. C. (2018): "Garnet Based Li-Metal Batteries"; L. Hu. Invited.
- American Institute of Chemical Engineers (AiCHE) Annual Meeting, Pittsburg (November 2018): "Garnet Based Li-Metal Batteries"; L. Hu. Invited.
- MRS Fall Meeting, Boston, Massachusetts (November 2018): "Understanding Fast Ion Diffusion in Super-Ionic Conductors and Computational Materials Design"; Y. Mo. Invited.
- MRS Fall Meeting, Boston, Massachusetts (November 2018): "Design Principles for Solid Electrolyte–Electrode Interfaces in All-Solid-State Li-Ion Batteries: Insight from First-Principles Computation"; Y. Mo. Invited.

Task 1.5 – Self-Forming Thin Interphases and Electrodes Enabling 3D Structured High-Energy-Density Batteries
(Glenn Amatucci, Rutgers University)

Project Objective. The project objective is to develop and implement a novel *in situ* formed Li-metal-based metal fluoride battery that will enable packaged 10-mAh batteries of energy densities > 1000 Wh/L and > 400 Wh/kg at 12 V.

Impact. Successful realization of 3D batteries formed *in situ* with a practical approach to large-scale fabrication would address some of the DOE EV performance goals, including: (1) areal capacity increase, (2) improved rates, and (3) designs to enable high-voltage unit cells.

Approach. The project is divided into two main tasks that focus on advance of the self-forming chemistry concurrent to cell design and fabrication. The self-forming chemistry task is comprised of three subtasks encompassing the negative and positive reactive current collectors, and the bi-ion glass conductor. The cell design and fabrication are targeting development and integration of the bipolar configuration to achieve the 12-V single-cell goal.

Out-Year Goals. Work will continue toward improving reactive current collectors and cell design to optimize electrochemical performance of the cell stack in terms of energy density both gravimetric and volumetric, as well as capacity retention on cycling. A secondary focus will be implementation of bipolar design within the cell structure.

Collaborations. All project tasks will be performed at Rutgers University.

Milestones

1. Design and fabricate 10-mAh cell stack that achieves 12 V and delivers energy densities of 1400 Wh/L and 600 Wh/kg per cell stack. (Q1, FY 2019; In progress)
2. Establish negative current collector compositions that enable high efficiency of lithium plating and stripping in excess of 95% during the *in situ* formation step and > 99% during subsequent cycles. (Q2, FY 2019)
3. Achieve < 30% increase in electrolyte impedance after 50 cycles as characterized by EIS. (Q3, FY 2019)
4. Establish positive current collector compositions that achieve 90% of the theoretical energy density based on complete utilization of the initial amount of the positive reactive current collector. (Q4, FY 2019)
5. *Deliverables:* Deliver 12 baseline and 12 improved packaged cells with 10-mAh capacity. Improved cells will offer > 1000 Wh/L and > 400 Wh/kg, and output voltage of 12 V.

Progress Report

Last quarter, progression of the 12-V self-forming architecture moved to successful charging and discharging of the cell with nominal voltage of 12 V. The studies further demonstrated that diffusion limitations could be improved by increasing surface area through reduced electrode thickness and smaller electrode width. The team was able to achieve a positive electrode utilization of 40% by combining this aspect ratio modification with thicker reactive electrolyte. Overall, the electrode design change helped decrease diffusion length, giving access to more of the reactive chemistry while the additional reactive electrolyte coverage ensured continuity in transport pathways. These modifications were part of the building blocks for the project's research this quarter.

The team has now further advanced development of the 12-V self-forming architecture by addressing transport (1) using stepped cycling protocols for alleviated stress, (2) at the electrolyte level, (3) at the positive electrode level, and (4) through cell spacing design.

Cycling Protocols. Cycling protocols were investigated to include incremental depth of charge to allow systematic formation of the electrochemical cell and alleviate stresses induced by phase transformations. The cells were charged at constant voltage with stepped capacity cutoff. The initial two cycles were used as formation cycles, with capacity cutoffs of 13% and 26% of theoretical capacity, respectively. The third cycle had a capacity cutoff of 52%, which was utilized for all remaining cycles. These protocols were found to improve cycling stability of the 12-V cells from 1-2 cycles last quarter to > 8 cycles (Figure 9). Moving forward with this concept, the team will increase the capacity cutoff to 75% to achieve higher energy densities and positive electrode utilization.

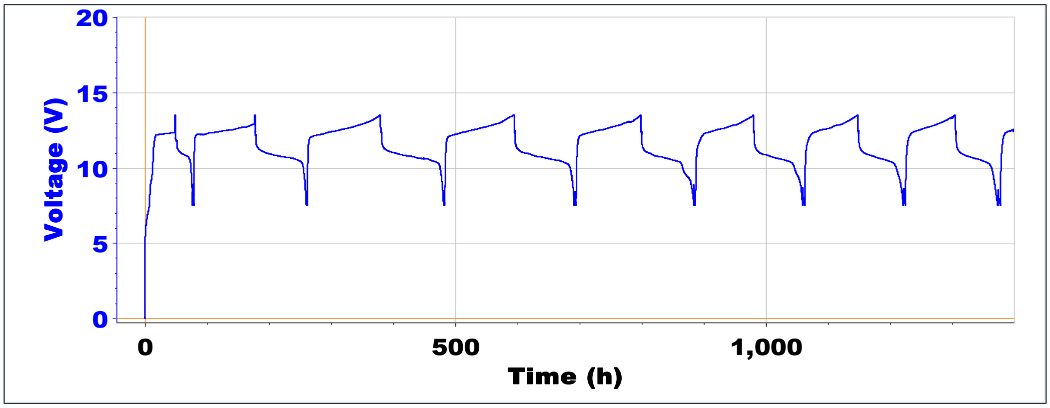

Figure 9. Voltage profile for a 12-V cell architecture with optimized electrode aspect ratio. The cell cycled between 7.5 V and 13.5 V following a charge protocol with incremental capacity cutoffs of 13%, 26%, and 52% of the theoretical capacity in the first 3 cycles and maintaining its maximum cutoff after the 3rd cycle.

Electrolyte Level. The team investigated the incorporation of additives to the reactive electrolyte of the 12-V self-forming architecture to improve its transport properties. Indeed, they had previously reported optimization of conductivity through use of SSE additives to the glass compositions in single-cell experiments and hoped that such gains could be translated to the 12-V architectures. 12-V cells were fabricated with and without electrolyte additives and were cycled between 7.5 and 13.5 V utilizing the above described protocol of stepped capacity cutoffs. As similarly exemplified by studies of the single-cell architecture, the cell with the additives demonstrated distinct improvement in performance, with an increase of roughly 30% in capacity and over 10% increase in utilization, as shown in Figure 10.

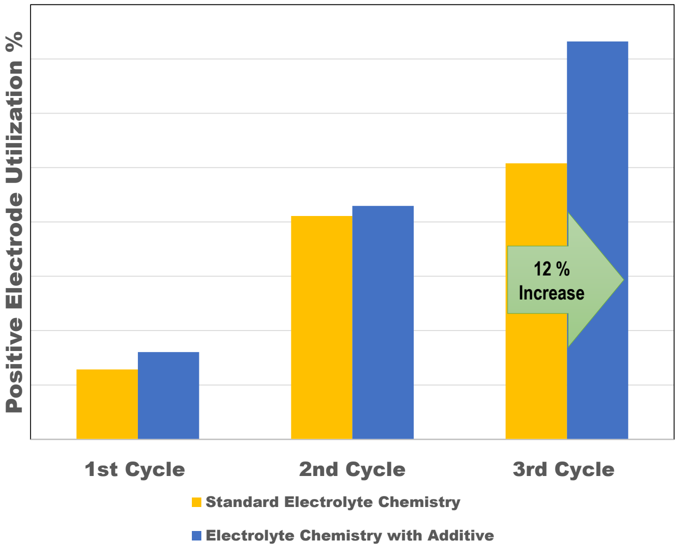

Figure 10. Impact of electrolyte additive on utilization of positive electrode for 12-V self-formed cells cycled between 7.5 and 13.5 V. The cells were charged at constant voltage, with incremental capacity cutoffs of 13%, 26%, and 52% of theoretical capacity in the first 3 cycles showing that when the capacity limitation is lifted, the solid-state electrolyte additive improves the performance significantly.

Positive Electrode Level. To enhance transport properties and improve performance, electronic and ionic conductor additives were incorporated in the project's unique nanolayered positive electrode current collector composite format to provide the base for the composition of the positive electrode composite after formation of the 12-V architectures. These composite architectures were identified in the second quarter of FY 2018 to provide increased transport properties. Although more than a 20% increase was obtained for previously investigated isolated positive electrode designs, when applied to the 12-V architecture, no additional improvements were observed.

Cell Spacing Design. Finally, the team investigated two pathways to decrease diffusion length to further improve transport properties and increase electrochemical performance of the cell. Initially, electrode width was further decreased in an attempt to optimize accessibility of active material in the positive electrode. However, cycling properties for these cells were either equal or less favorable than previous studies. The conclusions for these results implied the electrode mechanical integrity may be approaching its limit with the current fabrication process. Secondly, based on supporting research from a previous project where close to 100% positive utilization was obtained with roughly 70% less spacing between the electrodes, the team decided to pursue decreasing the spacing of electrolyte in the cell design. With the current fabrication technique, the team was able to reduce the spacing between the electrodes by 40%. However, these adjustments did not improve reported performance, most likely due to engineering challenges regarding morphology of the electrode structure associated with the current fabrication process. Therefore, to surpass such limitations and produce a cell design with optimal transport properties, alterations to processing need to be investigated.

In summary, several optimization steps were translated from the single-cell design to the 12-V architecture with the goal of improving performance. Although the team achieved an optimized electrode design, electrolyte of enhanced conductivity, and optimized cycling protocols, it was determined through a more in-depth cell characterization that diffusion limitations were the ultimate barrier in further progress. To overcome this barrier, three directions will be pursued next quarter. These include a decrease of the electrode spacing with improved electrode morphologies, moderate temperature increase, and hybridization of the electrolyte. The aforementioned techniques should promote an increase in rate of diffusion, which will allow for an increase in active material of the positive electrode to ultimately go beyond the current capabilities consistent with what the team has identified with more traditional approaches.

Patents/Publications/Presentations

The project has no patents, publications, or presentations to report this quarter.

Task 1.6 – Dual Function Solid-State Battery with Self-Forming, Self-Healing Electrolyte and Separator
(Esther Takeuchi, Stony Brook University)

Project Objective. The project objective is to demonstrate a solid-state rechargeable battery based on a Li-metal anode and iodine cathode with a self-forming, self-healing electrolyte and separator with high gravimetric and volumetric energy density.

Project Impact. This program will enable demonstration of the proposed rechargeable battery with improved power capability, high energy density, and a self-forming, self-healing SSE/separator. Technical insight will be gained regarding improved conductivity of the solid lithium iodide (LiI) based electrolyte, power capability of the proposed system, the self-healing nature of the LiI layer, the nature of the electrode-electrolyte interfaces, and feasibility of the system to reach the DOE targets.

Approach. The proposed concept is a dual function rechargeable solid-state battery utilizing LiI combined with silver iodide (AgI) as the electrolyte, with lithium metal (and small quantities of silver metal) as the anode and iodine as the cathode with a self-forming, self-healing separator/electrolyte. The battery will be assembled in the discharged state where the anode and cathode will be created during the first formation (charge) step. Initially, silver ion (Ag^+) will diffuse toward the negative electrode and be reduced to silver metal (Ag^0), and iodine ion (I^-) will be oxidized to elemental iodine (I_2) at the cathode side. As the formation of the battery continues, lithium ion (Li^+) will form a Li-metal layer at the anode, with generation of iodine at the cathode. LiI will remain and serve as both the separator and electrolyte.

Out-Year Goals. This is a multiyear program where the effort is divided into three major tasks.

- Year 1 involves electrolyte preparation and characterization including preparation of SSEs and conductivity measurements.
- Year 2 will focus on cell construction and testing including both *in situ* and *ex situ* analysis.
- Year 3 will focus on cell characterization. Under the program, cycle life, efficiency, energy density, and the functional capacity of cells will be determined.

Collaborations. This project collaborates with Amy Marschilok and Kenneth Takeuchi of SBU.

Milestones

1. Determine functional capacity and energy density of construction A cells. (Q1, FY 2019; Completed December 30, 2018)
2. Determine functional capacity and energy density of construction B cells. (Q2, FY 2019; Initiated)

Progress Report

Determine Functional Capacity and Energy Density of Construction A Cells

This quarter's milestone was to determine the functional capacity and energy density of construction A cells. Cell design A included the composite LiI solid electrolyte with LiI(3-hydroxypropionitrile)$_2$ additive, as reported in previous quarters. Cell design A was constructed with four interface variations: A-Interface I (AI-I), A-Interface II (AI-II), A-Interface III (AI-III), A-Interface IV (AI-IV). Variation of the interface was studied to evaluate its effects on CE during charge-discharge cycling.

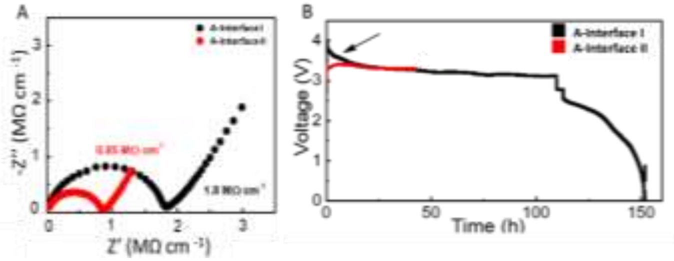

Figure 11. Cell design A: (a) pre-charge AC impedance, and (b) comparison of first cycle charge curve.

Before charging, EIS was obtained. AI-I had an impedance value that was > 2X that of AI-II (1.8 v. 0.85MΩcm^{-1}) (Figure 11a). Initially the cells were activated by a charge step, by charging at constant current (10µA/cm^2) to 5% state of charge (SOC). On charging (arrow, Figure 11b), there is a notable difference (~ 0.7 V) in overpotential observed between the two cell constructions; however, as charge continues, the potentials of the two cells merge.

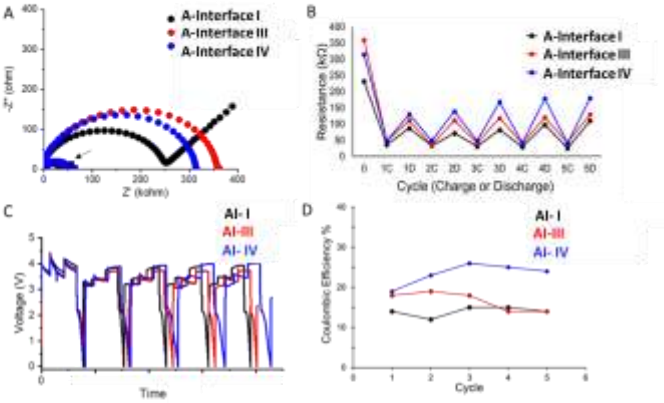

Figure 12. Cell design A: (a) electrochemical impedance spectroscopy, (b) resistance versus cycle, (c) cycling, and (d) Coulombic efficiency versus cycle number.

Additionally, new interfaces (AI-III and AI-IV) were evaluated. Pre- and post- charge impedance was obtained, (Figure 12a, post-charging denoted by arrow) where a substantial decrease after charge was noted. Cells were tested by step-wise charging, where they were charged at 5 µA/cm^2, 10 µA/cm^2, and 20 µA/cm^2 to 5% theoretical capacity and then discharged for a total of five charge-discharge cycles (Figure 12c). The resistance (in K) was shown as a function of charge or discharge with respect to the cycle number, where the resistance was determined by the intersection of the semi-circle on a point on the x-axis in the low frequency region of a Nyquist plot (Figure 12b). While there was an increase in the impedance after discharge, the values remained far lower than the initial impedance of the as-prepared cells. The CE for each cycle was determined, and some differences were observed between cell constructs; however, cell construction A cells demonstrated CE of ≤ 30% (Figure 12d).

The energy density of the solid-state concept was determined, and it relates to composition of the electrolyte and the ability to effectively utilize the lithium material in the cell. With full utilization of the LiI of the current electrolyte/cell chemical composition, the energy density is 450 Wh/kg.

An alternative cell design was developed, and preliminary cycling data were collected for this alternative design. Several interfacial modifications were studied and are denoted as B-I, B-II, B-III and B-IV.

Interestingly, B-II, B-III, and B-IV showed increasing CE with increased cycle number. Notably, B-I showed high CE near 100% efficiency over 10 cycles (Figure 13). This cell design will be studied further, as high CE has been demonstrated.

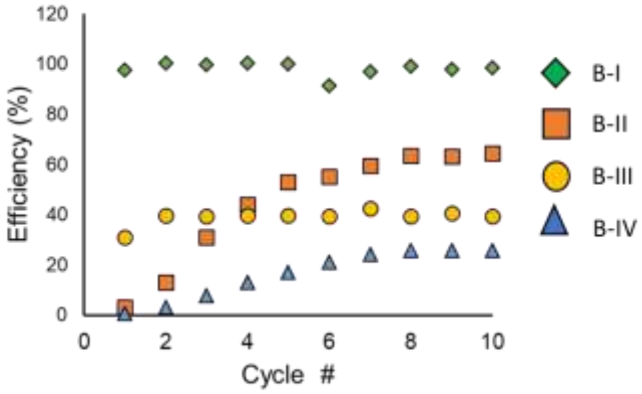

Figure 13. Coulombic efficiency of cell construction B with four different interfacial configurations.

Patents/Publications/Presentations

Presentation

- MRS Fall Meeting, Boston, Massachusetts (November 2018): "Demonstration of a Self-Forming Solid-State Rechargeable Li/I_2 Battery"; A. Abraham, J. Huang, P. F. Smith, A. Marschilok, K. Takeuchi, and E. Takeuchi.

Task 1.7 – High-Conductivity, Low-Temperature Polymer Electrolytes for Lithium-Ion Batteries (Bryan D. McCloskey, University of California at Berkeley)

Project Objective. Design of electrolytes with enhanced transport properties compared to conventional liquid organic electrolytes is key to improving the rate at which a Li-ion battery can be discharged or charged. Ideally, electrolytes would allow high mobility for lithium ions and disallow mobility of inactive ions (for example, the counteranion of the Li^+). However, current liquid electrolyte compositions usually provide higher mobility for the counteranion than Li^+, which results in high concentration polarization that disallows fast charging, particularly in batteries that employ thick porous electrodes, as is necessary for EVs to provide high energy densities. The project objective is to develop a high Li^+ transference number (t_{Li}, the fraction of ionic current carried by Li^+ in an electrolyte of uniform composition) polymer-based electrolyte that, when used in a Li-ion battery, can support current rate capabilities sufficient for EV propulsion at room temperature.

Impact. Development of practical high t_{Li} polymer-based electrolytes for Li-ion batteries would enable safer Li-metal and graphitic anode cycling and thicker porous electrode designs, leading to improved specific and volumetric battery energy densities consistent with the EV Everywhere Grand Challenge. High-energy anode and cathode materials, such as lithium metal, silicon, and high-voltage layered or spinel structures, could be enabled by electrolytes with high t_{Li} and large operating voltage windows, such as those based on sulfones, as proposed here.

Approach. Lowering the operating temperature of polymer electrolytes has been cited as an important challenge to their viability as Li-ion battery electrolytes. The project will address this challenge by using Li^+ neutralized anionically charged polymers as salts in conventional liquid solvents. Using these so-called polyelectrolyte solutions, initial results indicate that the project can access t_{Li} values typical of single-ion conducting polymer electrolytes ($t_{Li} > 0.9$) and conductivity values (> 1 mS/cm at room temperature) that approach those of traditional battery electrolytes.

Out-Year Goals. The optimization of transport and stability properties of these polyelectrolyte systems, through understanding of appropriate polymer and solvent design, is the objective. The goal is to develop new polyelectrolyte compositions that provide superior transport properties (specifically, higher t_{Li} and conductivity) than conventional liquid electrolytes and enable use of high-energy electrode materials, such as lithium metal.

Collaborations. Collaborations on this project include V. Battaglia (porous electrode preparation) and K. Persson (atomistic modeling) at LBNL.

Milestones

1. Complete synthesis and characterization of a new Li^+-neutralized charged polymer (pFTO) with a triflate-like ion ($-CF_2-SO_{3-}$) appended to the polymer backbone to improve ion dissociation. (Q1, FY 2019; Completed October 2018)
2. Complete nuclear magnetic resonance (NMR) transport and viscosity measurements of pFTO dissolved in carbonate-based solvents. Progress measure: Publish an article describing transport properties of polyelectrolyte solutions comprised of sulfonated polysulfone-co-poly(ethylene oxide) in carbonate-based solvents. (Q2, FY 2019; Progress measure completed November 2018.)
3. Complete electrochemical transport measurements of pFTO in symmetric cells with Li-metal electrodes and SSEs. (Q3, FY 2019)
4. Complete characterization of rate capabilities of cells comprised of lithium metal, a porous NMC cathode, and pFTO-containing carbonate solutions during electrochemical cycling. (Q4, FY 2019)

Progress Report

This quarter, the team has focused on several new routes to attain a high Li^+ transference number liquid electrolyte. Last quarter, the project reported the successful synthesis of the polymer shown in Figure 14a (which satisfies this quarter's milestone), though noted the need for further purification and characterization to verify the result. Further examination of the ^{19}F NMR spectrum, and quantification of ion content by inductively coupled plasma – optical emission spectroscopy (ICP-OES), found a range of side reactions and lower than expected lithium content in the final polymer. These issues, as well as the heterogeneous nature of a condensation polymer, suggested the need for alternative routes to a useful polymer. For this reason, the project has purchased the monomers necessary for the polymers shown in Figure 14b, which have only recently become commercially available and are likely to yield ionomers with substantially better performance than the pFTO polymer shown in Figure 14a. These monomers can be polymerized via reversible addition-fragmentation polymerization (RAFT) to yield highly regularly, ion-containing polymers that have previously been investigated for battery applications in the dry state. The team therefore expects these polymers, which are also known to be soluble in carbonates, to be better candidates for further study than the originally proposed pFTO. The team is working to produce and purify these polymers, and future milestones will focus on their characterization in solution.

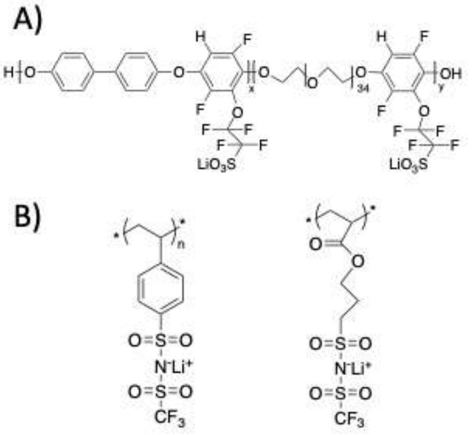

Figure 14. Polymers being studied in this project. (a) Triflate-based ionomer comprised of poly(ethylene oxide) and polysulfone backbones (pFTO). (b) Triflimide-based styrene and acrylate ionomers targeted in FY 2019.

While this work is ongoing, the team has continued work on understanding the basic design of polyelectrolyte solutions. They completed and published a study of sulfonated polysulfone-co-poly(ethylene glycol) dissolved in DMSO and carbonates, which satisfies the progress measure for next quarter. This study was the first report of a polyelectrolyte in carbonate-based solvents, and it elucidated several important design considerations with nonaqueous polyelectrolyte solutions. First, the team found that the dielectric constant is a poor predictor of solution behavior in the new solvent, suggesting additional theoretical work is needed to better describe new solvents. Second, the team demonstrated a disconnect between bulk viscosity measurements and the local environment of ions and molecules that actually dictates solution transport behavior. Third, they demonstrated the need for additional synthetic design of polymers that are both soluble and provide high dissociation of ions in carbonate blend solvents, further motivating a study of the polymers in Figure 14b. Finally, the team demonstrated that salt addition is a potential method to tune transference numbers and conductivity in the case that the polyion is well dissociated.

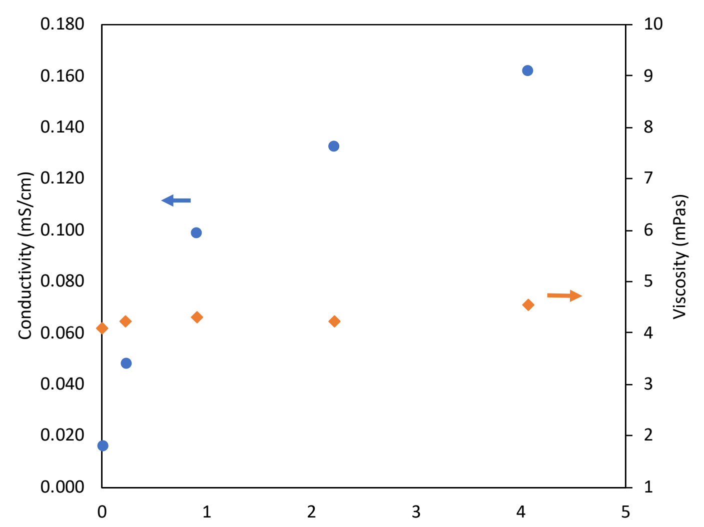

Figure 15. Conductivity and viscosity as a function of added 12-crown-4 ether of a sulfonated polysulfone-co-poly(ethylene glycol) dissolved in 1:1 ethylene carbonate:dimethyl carbonate.

As an extension of this study, the team has begun investigating the effect of additives to sulfonated polyelectrolyte in carbonate solvent systems to improve transport properties and electrode-electrolyte interfacial stability. Figure 15 shows the conductivity and viscosity of sulfonated polysulfone-co-poly(ethylene glycol) at 0.05 M $-SO_3^-$ as a function of the amount of 12-crown-4 (a crown ether) added. At a molar ratio of 4:1 crown:lithium, which corresponds to only 3 vol% crown ether, the team finds nearly an order of magnitude increase in conductivity with no effect on viscosity. NMR diffusion measurements indicate this conductivity increase is a result of increased dissociation of the lithium from the polymer chain. The team found that this increase in conductivity is significantly larger than that from addition of a similar amount of either water or tetraglyme, and it is different from most previous uses of crown ether where a decrease in conductivity was observed. This promising route to a high transference number solution without significant changes in polymer chemistry will be tested in a standard Li-ion cell next quarter.

Patents/Publications/Presentations

Publication

- Diederichsen, K. M., K. D. Fong, R. C. Terrell, K. A. Persson, and B. D. McCloskey. "Investigation of Solvent Type and Salt Addition in High Transference Number Nonaqueous Polyelectrolyte Solutions for Lithium Ion Batteries." *Macromolecules* 51 (2018): 8761–8771.

Presentations

- AIChE Annual Meeting, Pittsburgh, Pennsylvania (October 30, 2018): "Investigation of Solvent Composition and Salt Addition in High Transference Number Nonaqueous Polyelectrolyte Solutions"; K. Diederichsen.
- AIChE Annual Meeting, Pittsburgh, Pennsylvania (November 1, 2018): "Modeling of High Transference Number Electrolytes for Fast Charging Lithium Ion Batteries"; E. McShane.

Task 1.8 – Advanced Polymer Materials for Batteries
(Zhenan Bao and Yi Cui, Stanford University)

Project Objective. This project will develop new polymer materials for batteries. The team will develop polymer coatings with specific mechanical properties that can accommodate the volume expansion and contraction of the Li-metal anode associated with deposition and stripping (charging and discharging).

Project Impact. The cycling stability and CE of Li-metal electrodes will be increased by implementation of a polymer-based protective layer that functions as an artificial SEI with desired properties. The improved performance will enable further development toward practical utilization of Li-metal anodes with higher cycling efficiency and less susceptibility to dendrite-based failure.

Approach. The project uses soft polymer coatings with dynamic crosslinking to give the resulting polymers liquid-like rheological properties and stretchable and self-healing properties. In previous work, the project has shown that such coatings resulted in uniform deposition/stripping of lithium metal and improved cycling stability of Li-metal electrodes. To understand the design rules for effective polymer coatings, the team chose a few representative polymers to systematically understand structure property relationships. Here, the team investigates the correction between surface energy of the polymer and exchange current for lithium deposition.

Out-Year Goals. Work will progress toward further understanding and development of various polymer coatings for protecting Li-metal anodes.

Collaborations. There are no active collaborations this quarter.

Milestones

1. Identify at least two different types of SHPs with promise to suppress dendrites. (Q1, FY 2019; Completed)

Progress Report

Rational design of the electrode-electrolyte interphase is essential to stabilize electrodeposition of metallic lithium. Thus, it is important to design an artificial interfacial layer that can accommodate the stress generation due to the volume changes during battery operation and at the same time maintain ionic continuity. This quarter, the team has designed artificial SEI with two distinct concepts that can enable stable deposition of metallic lithium. The two concepts are based on dynamic SHPs and single-ion conducting elastomers.

Self-Healable Polymeric Architectures

The team hypothesizes that stimuli-responsive polymeric architectures can be effective in preventing morphological instabilities during electrodeposition compared to covalently bonded rigid polymers and crosslinked elastomers, when used as artificial interfaces between the electrode and electrolyte. The fundamental working mechanism of the dynamic polymeric coatings can arise from the spontaneous structural response of the polymer in response to the roughening electrode during electrodeposition. As the polymer coating is free to flow, if there is a ‘hotspot’ (uneven deposit) on the surface of the lithium metal, the dynamic polymer coating can rearrange and cover these regions, resulting in increased overpotential. Thus, successive Li^+ ions deposit on the flatter regions, resulting in uniformity of deposition. Furthermore, the tortuous pathway in the polymeric interface can enable uniform distribution of lithium ions during the charging process, thus leading to uniform deposition.

In this work, the team synthesizes a series of different supramolecular polymers that will be designed comprised of various content of noncovalent interactions and polymer entanglements using polymerization of PDMS with urea linkages. Figure 16a shows the chemical structure of the SHP comprising a PDMS soft block where *n* (number of siloxane monomers) was changed from 10 to 350, while the urea linkages were formed using isophrone diisocyanate units. The data on variation in the ratios between urea units and PDMS blocks are useful in understanding the effect of elasticity and the self-healing property. The team characterized the molecular properties of the SHP using infrared spectroscopy, as shown in Figure 16b. It is observed that the shift in the wavenumber in the –NH and -C=O bond stretching (representing the strength of H-bonding) is nearly identical for all three co-polymers. However, the abundance of H-bonding units differs significantly in the three samples.

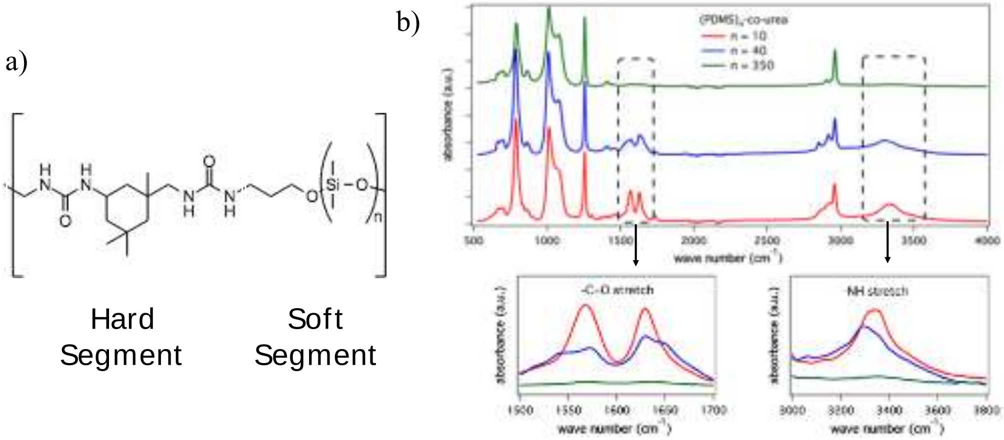

Figure 16. (a) Chemical structure of polydimethylsiloxane (PDMS) self-healing polymer. (b) Fourier transform infrared spectra of the PDMS self-healing polymer, with varying sizes of PDMS soft block in the co-polymer.

The team analyzed electrochemical characteristics of PDMS SHP using CE measurements in Li||PDMS-SHP@Cu cells. Specifically, the current density used in this experiment was $0.5mA/cm^2$ and capacity being $1mAh/cm^2$, while the electrolyte utilized was 1 M $LiPF_6$ in ethylene carbonate/dimethyl carbonate (EC/DMC) along with 10% fluoroethylene carbonate (FEC) additives. Figure 17a shows the comparison of the lithium plating efficiency for the different PDMS-SHP coatings with varying sizes of PDMS blocks. It is observed that the CE values for all coatings were nearly identical at values between 90-95%. However, there appears to be a trend in the relative lifetimes of the cells. It is seen that the PDMS-SHP with the shortest PDMS co-block (n=10) outperforms the other coatings. This indicates that a higher degree of dynamic bonding is essential for the stabilization of electrodeposition. Furthermore, the team compared the performance of the Li||Cu cells with that of the control electrolyte in Figure 17b, where it is clear that while the control cell fails within 100 cycles, the PDMS-SHP coating enables stable cycling for over 150 cycles.

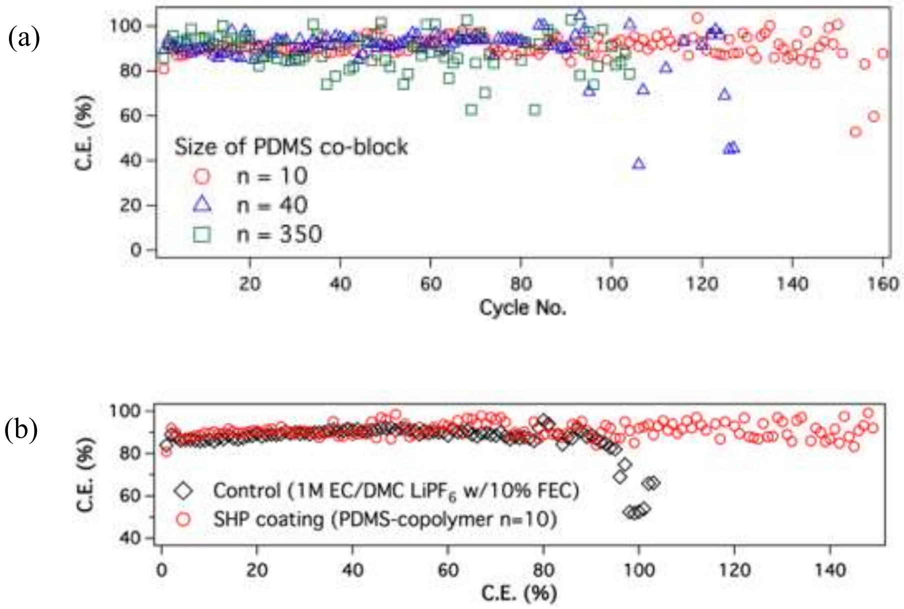

Figure 17. (a) Chemical structure of polydimethylsiloxane (PDMS) self-healing polymer (SHP). (b) Fourier transform infrared spectra of the PDMS SHP with varying sizes of PDMS soft block in the co-polymer.

Patents/Publications/Presentations

Publication

- Tsao, Y., M. Lee, E. C. Miller, G. Gao, J. Park, S. Chen, T. Katsumata, H. Tran, L-W. Wang, M. F. Toney, Y. Cui, and Z. Bao. “Designing a Quinone-Based Redox Mediator to Facilitate Li_2S oxidation in Li-S batteries.” *Joule*. In press.

Task 1.9 – Improving the Stability of Lithium-Metal Anodes and Inorganic-Organic Solid Electrolytes (Nitash Balsara, Lawrence Berkeley National Laboratory)

Project Objective. The project objective is to establish a new hybrid electrolyte that will be stable against cells with a Li-metal anode.

Project Impact. Polymer electrolytes offer increased stability in lithium batteries in comparison to more widely used liquid electrolytes. Nanostructured electrolytes containing both soft, ion-conducting domains and rigid nonconducting domains offer the opportunity to tune both mechanical and electrical properties separately. Such electrolytes are conveniently made by block copolymer self-assembly. Most of the block copolymer electrolytes studied thus far comprise organic polymer chains for both the conducting and rigid domains. The team hopes to synthesize new electrolytes that simulataneously have high transport properties and have greater stability against lithium in comparison to organic diblock copolymers.

Approach. First, the team synthesizes hybrid diblock copolymers by incorporating monomers that contain an inorganic component. Then electrolytes are prepared by mixing these diblock copolymers with salt. Electrochemical and mechanical characterization of these materials is performed before carrying out cycling X-ray tomography experiments. The combination of these approaches enables rational design of materials that exhibit improved stability against lithium metal.

Out-Year Goals. The project will synthesize a new hybrid electrolyte that is designed to be stable against lithium metal. The material is a block copolymer wherein acryloisobutyl polyhedral oligomeric silsesquioxane (POSS) is covalently bonded to the chain. The second block is a conventional polymer electrolyte, PEO. Electrochemical characterization of this polymer will include measurement of all transport properties including conductivity, diffusion coefficient, and the transference number. The stability against lithium metal will be evaluated by CV, while its applications as an electrolyte will be evaluated and visualized using cycling X-ray tomography experiments on symmetric Li-hybrid-Li cells.

Collaborations. There are no active collaborations this quarter.

Milestones

1. Determine limiting current in solid electrolytes. (Q1, FY 2019; Completed)
2. Determine the nature of lithium/electrolyte interface. (Q2, FY 2019)
3. Study the effect of lithium metal purity and failure mechanisms. (Q3, FY 2019)
4. Determine parametric range over which stable lithium electrodeposition is obtained. (Q4, FY 2019)

Progress Report

The limiting current of a hybrid triblock copolymer electrolyte, POSS-PEO-POSS (structure shown in Figure 18) was measured. A 5-35-5 [kg/mol] membrane was fabricated with salt concentration [Li]/[EO] = 0.04.

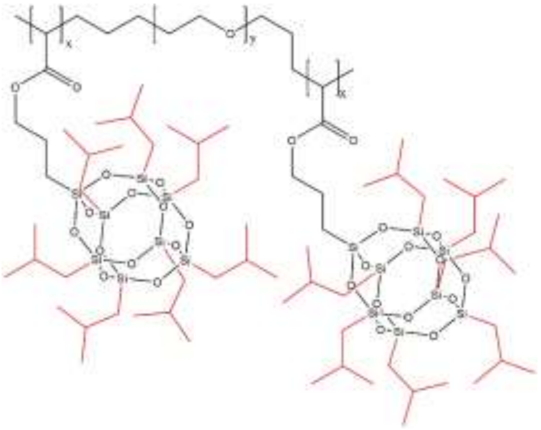

Figure 18. Chemical structure of the POSS-PEO-POSS triblock copolymer.

A routine to test the limiting current of POSS-PEO-POSS was performed and is shown in Figure 19. The measurement was performed by sandwiching a 30-µm-thick, solid, organic-inorganic polymer electrolyte between lithium electrodes. The Li-polymer-Li cells were then polarized to electrodeposit lithium from one electrode to the other. The current density was increased systematically until the potential diverged or the cell short-circuited. The results in Figure 19 show that the POSS-PEO-POSS hybrid triblock electrolyte demonstrated a limiting current above 3.0 mA cm^{-2}. Further experiments on this cell showed an exceptionally high limiting current between 4.5 and 6.0 mA cm^{-2} for a membrane of 30-µm thickness.

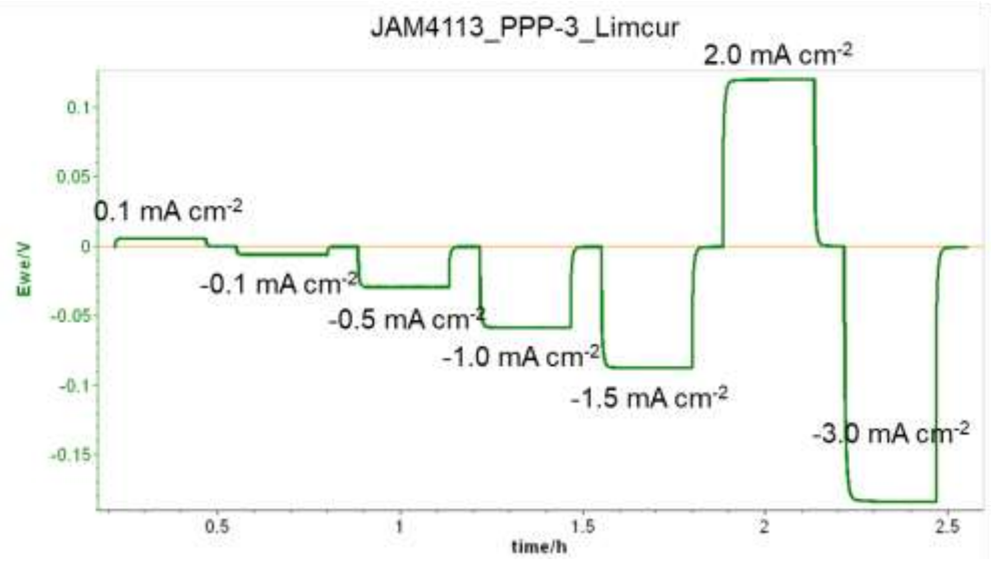

Figure 19. Example of a routine used to test the limiting current of POSS-PEO-POSS (5-35-5).

For the first time, the team was able to experimentally achieve the estimated limiting current of 4.5 mA cm^{-2} based on Monroe and Newman's equation (Equation 1) without an immediate short-circuit.[1]

$$i_L = \frac{2c_B DF}{L(1-t_{Li})} \qquad \text{(Equation 1)}$$

In all previous experiments on all-organic block copolymer electrolytes, the practical limiting current was reached well before the estimated limiting current based on Equation 1 was reached. The team also notes that the estimate of limiting current is not based on complete characterization of solid polymer electrolytes using the Newman approach.

The limiting current is implicated as a normalization factor in the Barai et al. model of the propagation of lithium protrusions through solid polymer electrolytes.[2,3] Thus, it is of relevance to study the effect of current density on nucleation and growth of lithium protrusions. Due to limitations in triblock polymer material, the systematic study of current density effects was conducted with PS-PEO (115-172), which has been shown to have indistinguishable cycle life compared to equivalent cells fabricated with POSS-PEO-POSS (5-35-5).

[1] Monroe, C., and J. Newman. *Journal of Electrochemical Society* 150, no. 10 (2003): A1377–A1384.

[2] Barai, P., K. Higa, and V. Srinivasan. *Journal of Electrochemical Society* 164, no. 2 (2017): 180–189.

[3] Barai, P., K. Higa, and V. Srinivasan. *Physical Chemistry Chemical Physics* 19 (2017): 20493–20505.

Patents/Publications/Presentations

Publications

- Masyln, J. A., W. S. Loo, K. D. McEntush, H. J. Oh, K. J. Harry, D. Y. Parkinson, and N. P. Balsara. "Growth of Lithium Dendrites and Globules through a Solid Block Copolymer Electrolyte as a Function of Current Density." *Journal of Physical Chemistry B* 122, no. 47 (2018): 26797–26804.
- Wang, D. R., D. B. Shah, J. A. Masyln, W. S. Loo, E. J. Nelson, M. L. Latimer, J. Feng, K. H. Wujcik, D. Prendergast, T. A. Pascal, and N. P. Balsara. "Rate Constants of Electrochemical Reactions in a Lithium-Sulfur Cell Determined by *Operando* X-Ray Absorption Spectroscopy." *Journal of the Electrochemical Society* 165, no. 14 (2018): A3487-A3495.

Presentations

- Departmental Colloquium, Department of Chemical Engineering, Notre Dame, South Bend, Indiana (November 13, 2018): "Ohm's Law, Lithium Batteries, and the Clean Energy Landscape."
- Frontiers of Molecular Engineering Symposium, Royal Society of Chemistry, University of Chicago, Chicago, Illinois (September 27, 2018): "Ohm's Law, Lithium Batteries, and the Clean Energy Landscape"; Invited lecture.
- Departmental Colloquium, Department of Chemical Engineering, Louisiana State University, Baton Rouge, Louisiana (September 21, 2018): "Ohm's Law, Lithium Batteries, and the Clean Energy Landscape."

Task 1.10 – Electrolyte/Binder for High Efficiency Lithium-Sulfur Battery: New Materials Design and Computation

(Larry A. Curtiss, Zhengcheng Zhang, and Ahn Ngo, Argonne National Laboratory)

Project Objective. Lithium-sulfur batteries have received great attention because sulfur exhibits an order of magnitude higher theoretical capacity than that achievable with intercalation-type cathode materials in Li-ion batteries and is considered as a promising battery chemistry to power long-range, low-cost EVs. Sulfur is abundant in nature and nontoxic, which leads to low cost of the cell and environmental benefits. However, low active material utilization and poor cycle life hinder the practical application of Li-S batteries. The objective of this project is to develop new electrolyte materials to help overcome these challenges and enable high-efficiency Li-S batteries for vehicle application.

Project Impact. Development of novel functional electrolytes tailored for Li-S electrochemistry will enable improved materials utilization and longer cycle life as needed to take advantage of the high potential capacity of Li-S batteries to power long-range, low-cost EVs.

Approach. This project takes a new approach, combining organic synthesis and quantum chemistry computations to obtain an in-depth understanding of the interaction of the discharged lithium polysulfides with the electrolyte solvents and the lithium salt, aiming to develop new electrolyte materials for Li-S batteries. Based on the team's previous study, the fluorinated-ether-based electrolytes have shown very limited Li_2S_x solubility, and at the same time could effectively passivate the lithium anode surface affording a reversible electrochemistry with high CE. However, the low active material utilization compromises its advantages of high theoretical capacity and energy density. To overcome this, the team will investigate boron-containing fluorinated polyethers as a new class of electrolytes for Li-S batteries. To further improve the cycle life, the project also proposes to design and synthesize new polymer binders bearing a pentafluorophenyl group on the backbone. First principles DFT and wave-function based quantum chemistry methods will be employed to provide accurate atomic/molecular level insight into the experimental studies. The team will also employ *ab initio* molecular dynamics (AIMD) simulations of the solvents for different finite temperatures and concentrations. The AIMD simulations will provide information on the structures of the electrolytes based on the fluorinated ethers synthesized in the experimental part of this project.

Out-Year Goals. The out-year goals are to find electrolytes that promote longer cycle life through electrolytes to reduce material loss.

Collaborations. This project engages in collaboration with Prof. A. Salehi at University of Illinois at Chicago (UIC).

Milestones

1. Design and synthesis of new fluorinated borate electrolytes and baseline studies of sulfur utilization, CE, and cycle life. (Q1, FY 2019; Completed December 30, 2018)
2. Quantum chemical calculations of the chemical stability and reactivity properties of new borate solvents in electrolytes and with electrode surfaces. (Q2, FY 2019)
3. Electrochemical characterization of performance of the new fluorinated borate electrolytes in Li-S cells for comparison with baseline studies. (Q3, FY 2019)
4. Correlation of experimental and theoretical results with post test data on Li-S cells using the fluorinated borate electrolytes. (Q4, FY 2019)

Progress Report

One of the issues for Li-S battery is the dramatic loss of active materials in the form of insoluble Li_2S and Li_2S_2 species. These species are generated both on a full discharge and during parasitic shuttling reactions common in Li-S cells. It is the project goal to utilize various Lewis acids in hopes of resolving lost materials that were deposited away from the cathode in the forms of Li_2S or Li_2S_2. This report addresses work performed thus far on one of these additives, TFEB (Figure 20a).

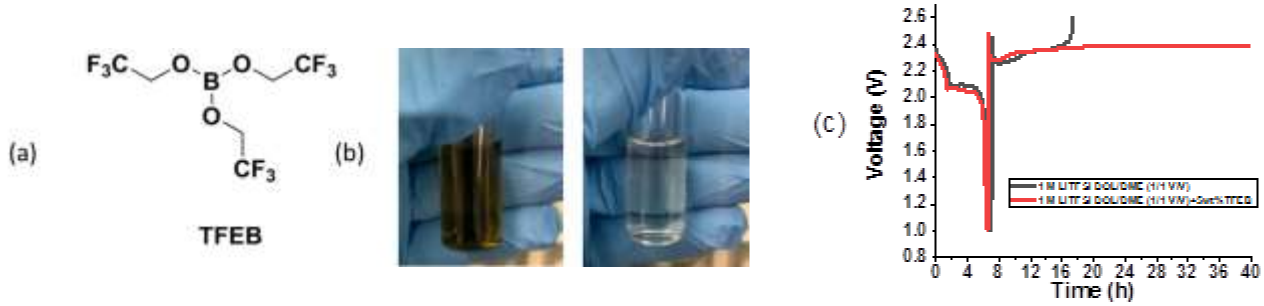

Figure 20. (a) Structure of tris(2,2,2-trifluoroethyl)borate (TFEB). (b) Chelating effect of TFEB with polysulfide anions (Li_2S_8); left: 50 mM of Li_2S_8 in DME, and right: 50 mM of Li_2S_8 with 0.6 EQ TFEB. (c) 1st cycle voltage profiles of 1 M LiTFSI DOL/DME (1/1) cell and 1 M LiTFSI DOL/DME (1/1) + 5% TFEB.

On addition of the TFEB additive to lithium polysulfide (Li_2S_8) solution in DME, the characteristic brown/dark color of polysulfide anions was reduced to light color. With further additive addition, all visible color in the solution disappeared (Figure 21b), showing a rapid interaction between TFEB and polysulfide anions. This interaction is caused by the Lewis acid-base reaction between the boron and the polysulfide anion forming a soluble polysulfide-borate complex. This strong chelation was also observed in the electrochemical performance in Li-S cell. Figure 21c shows the 1st cycle voltage profiles of Li-S cells with and without TFEB. The infinite charging plateau for the 5% TFEB cell further is due to the shuttling effect of the more dissolved polysulfides, confirming the strong interaction of additive and the polysulfide.

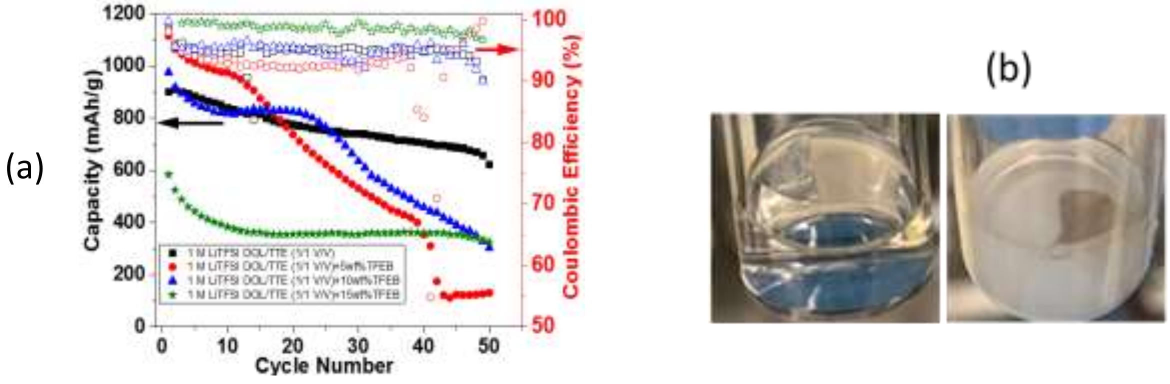

Figure 21. (a) Capacity retention and Coulombic efficiency of Li-S cells using 1 M LiTFSI DOL/TTE electrolyte with added 5%, 10%, and 15% TFEB additive. (b) Chemical reactivity of TFEB with lithium metal (left: lithium chip in TFEB; right: after 12 h).

1 M LiTFSI DOL/TTE has been reported as a high-efficiency, high-performance Li-S electrolyte. TTE is a fluorinated ether that could passivate the lithium anode and prevent severe shuttling effect with CE > 97% even without $LiNO_3$. To further evaluate the impact of TFEB, 1 M LiTFSI DOL/TTE electrolyte was selected instead of DOL/DME electrolyte. Figure 21a shows the capacity retention and CE of Li-S cells with 1 M LiTFSI DOL/TTE electrolyte plus different concentrations of TFEB. With 5% TFEB additive, the cell delivered much higher initial capacity, indicating improved sulfur utilization. However, increased additive amount, especially

the 15% additive cell, showed the opposite result. The team speculates this could be caused by the chemical reactivity of the additive with Li-metal anode, leading to the fast capacity fade. As confirmed by the results shown in Figure 21b, it is conclusive that TFEB is a strong anion-receptor as designed, but suffers from a lithium compatibility issue. New stable additives to address this are under development.

Patents/Publications/Presentations

The project has no patents, publications, or presentations to report this quarter.

TASK 2 – DIAGNOSTICS

Summary and Highlights

To meet the goals of the VTO Multi-Year Program Plan and develop lower-cost, abuse-tolerant batteries with higher energy density, higher power, better low-temperature operation, and longer lifetimes suitable for the next-generation of EVs, hybrid EVs (HEVs), and plug-in hybrid EVs (PHEVs), there is a strong need to identify and understand structure-property-electrochemical performance relationships in materials, life-limiting and performance-limiting processes, and various failure modes to guide battery development activities and scale-up efforts. In pursuit of batteries with high energy density, both high cell operating voltages and demanding cycling requirements lead to unprecedented chemical and mechanical instabilities in cell components. Successful implementation of newer materials such as silicon anode and high-voltage cathodes also requires better understanding of fundamental processes, especially those at the solid/electrolyte interface of both anode and cathode.

This Task takes on these challenges by combining model system *ex situ*, *in situ*, and *operando* approaches with an array of start-of-the-art analytical and computational tools. Three subtasks are tackling the chemical processes and reactions at the electrode/electrolyte interface. Researchers at LBNL use *in situ* and *ex situ* vibrational spectroscopy and far- and near-field scanning probe spectroscopy to understand the structure of active materials and the physio-chemical phenomena at electrode/electrolyte interfaces, particularly those of the high-voltage cathodes. GM is developing a number of *in situ* diagnostic techniques, including atomic force microscopy (AFM), nanoindentor, dilatometer, and stress-sensor, to be combined with atomic/continuum modeling schemes to investigate and understand the coupled mechanical/chemical degradation of the SEI layer on Li-metal anode. ANL aims to first understand the pathways/mechanisms of the parasitic reactions of the electrode/electrolyte interfaces and then stabilize them by developing functional surface coating and electrolyte additives. Subtasks at Brookhaven National Laboratory (BNL) and PNNL focus on the understanding of fading mechanisms in electrode materials, with the help of synchrotron-based X-ray techniques (diffraction and hard/soft X-ray absorption) at BNL and high-resolution transmission electron microscopy (HRTEM) and spectroscopy techniques at PNNL. UC San Diego (UCSD) is developing advanced diagnostic tools, including scanning transmission electron microscopy / electron energy loss spectroscopy (STEM/EELS), *operando* Bragg coherent diffraction imaging (BCDI) and *ab initio* computation, to probe anion redox and oxygen evolution in Li-excess NMC materials. At LBNL, model systems of electrode materials with well-defined physical attributes are being developed and used for advanced diagnostic and mechanistic studies at both bulk and single-crystal levels. These controlled studies remove the ambiguity in correlating a material's physical properties and reaction mechanisms to its performance and stability, which is critical for further optimization. The final subtask at Stanford University / Stanford Linear Accelerator Center (SLAC) develops and utilizes a correlative X-ray microscopy platform to investigate the lithiation dynamics and understand factors that determine the rate capability and degradation mechanisms in cathode materials. The diagnostics team not only produces a wealth of knowledge that is key to development of next-generation batteries, it also advances analytical techniques and instrumentation that have a far-reaching effect on material and device development in a variety of fields.

Task 2.1 – Model System Diagnostics for High-Energy Cathode Development (Guoying Chen, Lawrence Berkeley National Laboratory)

Project Objective. This project will use a rational, nonempirical approach to design and synthesize next-generation high-energy, high-voltage cathode materials. Combining a suite of advanced diagnostic techniques with model cathode materials and model electrode/electrolyte interfaces, the project will perform systematic studies to achieve the following goals: (1) obtain new insights into solid-state chemistry, particularly cationic and/or anionic redox activities during charge and discharge of high-capacity lithium TM oxides, (2) gain fundamental understanding on cathode/electrolyte interfacial chemistry and charge transfer process as a function of operating voltage, (3) reveal performance- and stability-limiting properties and processes in high-energy, high-voltage cathodes, and (4) develop strategies to mitigate the structural and interfacial instabilities.

Impact. The project will improve the commercial viability of next-generation high-energy cathode materials. The findings will enable more stable high-voltage cycling of existing Li-TM oxides as well as development of novel high-capacity cathode materials for advanced Li-ion batteries.

Approach. The project will prepare crystal samples of Li-stoichiometric and Li-excess TM oxides with well-defined physical attributes. It will perform advanced diagnostic and mechanistic studies at both bulk and single-crystal levels. Global properties and performance of the samples will be established from the bulk analyses, while the single-crystal-based studies will utilize time and spatially resolved analytical techniques to probe the material redox transformation process and failure mechanisms under battery operating conditions.

Out-Year Goals. In the out-years, the project will obtain fundamental knowledge on performance-limiting physical properties, phase transition mechanisms, parasitic reactions, and transport processes that prevent cathode materials from delivering higher capacities and achieving more stable cycling at high voltages. It will develop approaches to mitigate cathode structural and interfacial instabilities during high-voltage operation. Further, it will design and synthesize optimized Li-TM oxide cathodes as well as novel high-energy electrode materials.

Collaborations. This project collaborates with the following: G. Ceder, K. Persson, M. Doeff, B. McCloskey, and P. Ross (LBNL); V. Srinivasan (ANL); D. Nordlund and Y. Liu (Stanford Synchrotron Radiation Lightsource, SSRL); C. Wang (PNNL); C. Grey (Cambridge); and A. Huq and J. Nanda (Oak Ridge National Laboratory, ORNL).

`Milestones

1. Understand the interplay between cationic and anionic redox processes in model TM oxides. (Q1, FY 2019; Completed)
2. Characterize interfacial processes and surface changes on anion-active model oxides. (Q2, FY 2019; On schedule)
3. Evaluate the effect of particle size/morphology on oxygen redox chemistry and kinetics. (Q3, FY 2019; On schedule)
4. Develop design strategies to improve performance of anion-active oxide cathodes. (Q4, September 2019; On schedule)

Progress Report

Redox-inactive TMs that remain electrochemically inert during charge and discharge are considered essential in formation of the rock-salt phase with the cation disordered structure. It is unclear, however, what role they play during the cationic and anionic redox reactions. This quarter, three rock-salt oxides with the same redox-active manganese, but different inactive TMs of niobium, niobium/titanium, and titanium (namely, $Li_{1.3}Nb_{0.3}Mn_{0.4}O_2$, $Li_{1.25}Nb_{0.15}Ti_{0.2}Mn_{0.4}O_2$, and $Li_{1.2}Ti_{0.4}Mn_{0.4}O_2$) were synthesized and compared during the redox processes. Figure 22 shows the typical particle morphology (Figure 22a) and XRD patterns (Figure 22b) of the as-synthesized samples. All oxides had well-crystalized single primary particles with an average size of ~ 5 µm, and the phase-pure rock-salt crystal structure was confirmed by XRD.

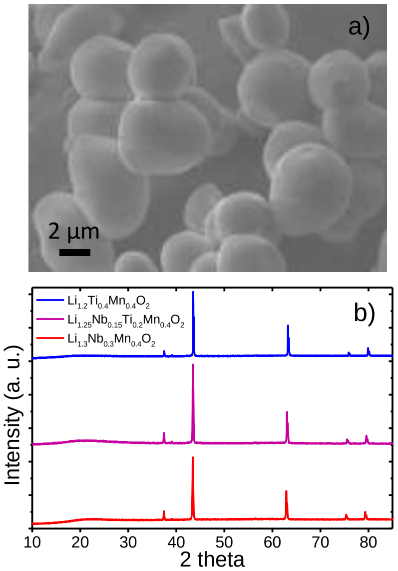

Figure 22. (a) Scanning electron microscopy image. (b) X-ray diffraction patterns of as-synthesized $Li_{1.3}Nb_{0.3}Mn_{0.4}O_2$, $Li_{1.25}Nb_{0.15}Ti_{0.2}Mn_{0.4}O_2$, and $Li_{1.2}Ti_{0.4}Mn_{0.4}O_2$ crystal samples.

Figure 23a-c compares the CVs collected during the first 10 cycles of the half cells. With cycling, the profiles followed a similar trend in peak evolution. During the anodic process, the peak arising from manganese oxidation (centered at ~ 3.5 V) gradually shifted toward higher voltages, while the intensity of the peak arising from oxygen oxidation (~ 4.5 V) gradually diminished. During the cathodic process, the current density of the primary reduction peak at ~ 3.2 V gradually decreased, while a lower voltage peak (~ 2.2 V) appeared and intensified. This results in an increasing voltage gap and an overall reduced current density with cycling. Compared to the niobium counterpart, the titanium substituted oxide appears to have a slower peak shift and reduced current decay, leading to improved stability. The changes in $Li_{1.25}Nb_{0.15}Ti_{0.2}Mn_{0.4}O_2$ cathode are somewhat in between. These differences were further evidenced in the charge/discharge cycling performance. Figure 23d-f shows the voltage profiles collected during the first 20 cycles of the half cells. Two voltage regions with the typical slopy and plateau profiles were observed in the first cycle of all three cells. The capacity obtained in each region, however, changed with the redox-inactive TM, even though all samples had the same amount of redox-active manganese. A more extended plateau region (known to be associated with oxygen oxidation) was observed with higher niobium substitution in the oxide. On the *d*Q/*d*V profile (Figure 23g-i), a split doublet peak (center at ~ 4.5 V) was observed during oxygen oxidation in $Li_{1.3}Nb_{0.3}Mn_{0.4}O_2$. The team's previous studies suggest that the higher voltage peak in the doublet is likely associated with oxygen oxidation via lattice oxygen loss. While this peak was responsible for a significant amount of capacity in $Li_{1.3}Nb_{0.3}Mn_{0.4}O_2$, its contribution was

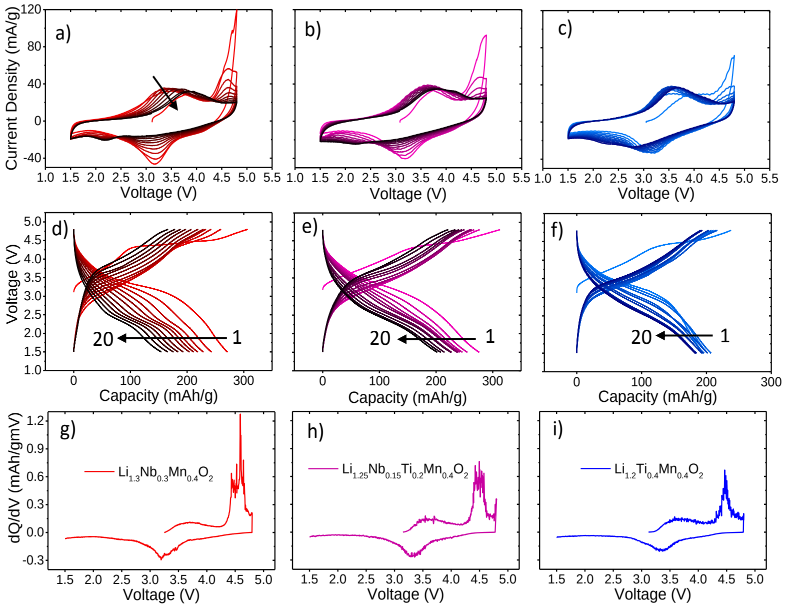

Figure 23. (a-c) Cyclic voltammograms of first 10 cycles; (d-f) voltage profiles of first 20 cycles; and (g-i) 1st cycle incremental capacity (*d*Q/*d*V) profiles obtained from $Li_{1.3}Nb_{0.3}Mn_{0.4}O_2$ (a/d/g), $Li_{1.25}Nb_{0.15}Ti_{0.2}Mn_{0.4}O_2$ (b/e/h), and $Li_{1.2}Ti_{0.4}Mn_{0.4}O_2$ (c/f/i) half cells. Cyclic voltammetry scan rate was 5 mV/min; charge/discharge current density was 10 mA/g.

greatly reduced in $Li_{1.25}Nb_{0.15}Ti_{0.2}Mn_{0.4}O_2$ and nearly negligible in $Li_{1.2}Ti_{0.4}Mn_{0.4}O_2$. As a consequence, the 1st cycle discharge capacities were ~ 280 and 200 mAh/g for $Li_{1.3}Nb_{0.3}Mn_{0.4}O_2$ and $Li_{1.2}Ti_{0.4}Mn_{0.4}O_2$, respectively. The large contribution of oxygen redox at higher voltage comes at the expense of stability. The capacity of $Li_{1.3}Nb_{0.3}Mn_{0.4}O_2$ decreased quickly with cycling, with only ~ 150 mAh/g remaining after 20 cycles. On the other hand, the discharge capacity was at ~ 190 mAh/g in $Li_{1.2}Ti_{0.4}Mn_{0.4}O_2$, nearly 95% capacity retention after 20 cycles. The results clearly suggest the dominant role of redox-inactive TMs in the performance of the cation-disordered rock-salt cathodes. Even though these cations do not directly contribute to charge storage capacity, they serve as a modulator and have a significant influence on the redox reactions, especially on the extent of oxygen redox.

Patents/Publications/Presentations

Publications

- Kan, W. H., C. Wei, D. Chen, T. Bo, B.-T. Wang, Y. Zhang, Y. Tian, J.-S. Lee, Y. Liu, and G. Chen. "Evolution of Local Structural Ordering and Chemical Distribution upon Delithiation of Rock-Salt Structured $Li_{1.3}Ta_{0.3}Mn_{0.4}O_2$ Cathode." Under review (2019).
- Cheng, L., M. Liu, R. Davis, A. Mehta, H. Xin, F. Lin, K. Persson, G. Chen, E. J. Crumlin, and M. Doeff. "Garnet Electrolyte Surface Degradation and Recovery." *ACS Applied Energy Materials* 1, no. 12 (2018): 7244. doi: 10.1021/acsaem.8b01723.
- Shin, Y., W. H. Kan, M. Aykol, J. K. Papp, B. McCloskey, G. Chen, and K. A. Persson. "Alleviating Oxygen Evolution from Li-Excess Oxide Materials through Theory-Guided Surface Protection." *Nature Communications* 9 (2018): 4597. doi: 10.1038/s41467-018-07080-6.

Task 2.2 – Interfacial Processes – Diagnostics
(Robert Kostecki, Lawrence Berkeley National Laboratory)

Project Objective. This collaborative project will develop and apply advanced experimental methodologies to study and understand the mechanism of operation and degradation of high-capacity materials for rechargeable cells for PHEV and EV applications. The objective is to develop and apply *in situ* and *ex situ* far- and near-field optical multi-functional probes and synchrotron-based advanced X-ray techniques to obtain detailed insight into the active material structure and physio-chemical phenomena at electrode/electrolyte interfaces at a spatial resolution corresponding to the size of basic chemical or structural building blocks. Through an integrated synthesis, characterization, and electrochemistry effort, the project aims to develop a better understanding of electrode and electrolyte materials so that rational decisions can be made as to their further development into commercially viable cathode materials.

Project Impact. Instability and/or high resistance at the interface of battery electrodes limits electrochemical performance of high-energy density batteries. A better understanding of the underlying principles that govern these phenomena is inextricably linked with successful implementation of high-energy-density materials in Li-based cells for PHEVs and EVs. Pristine and cycled composite and thin-film model electrodes are investigated using state-of-the-art techniques to identify, characterize, and monitor changes in materials structure and composition that take place during battery operation and/or storage. The proposed work constitutes an integral part of the concerted effort within the BMR Program, and it supports development of new electrode materials for high-energy, Li-metal-based rechargeable cells.

Approach. The pristine and cycled composite electrode and model thin-film electrodes will be probed using various surface- and bulk-sensitive techniques, including Fourier transform infrared (FTIR), attenuated total reflectance (ATR)–FTIR, near-field infrared (IR) and Raman spectroscopy and microscopy, and scanning probe microscopy to identify and characterize changes in materials structure and composition. Novel *in situ/ex situ* far- and near-field optical multifunctional probes in combination with standard electrochemical and analytical techniques are developed to unveil the structure and reactivity at interfaces and interphases that determine materials electrochemical performance and failure modes.

Out-Year Goals. In the out-years, the project aims to (1) understand the factors that control charge/discharge rate, cyclability, and degradation processes, (2) design and apply new diagnostic techniques and experimental methodologies capable of unveiling the structure and reactivity at hidden or buried interfaces and interphases that determine material, composite electrode and full-cell electrochemical performance and failure modes, and (3) propose effective remedies to address inadequate Li-metal-based battery calendar/cycle lifetimes for PHEV and EV applications.

Collaborations. Electrode materials and composite solid electrolytes tested under different cycling regimes by V. Battaglia and M. Doeff (LBNL) will be studied. The diagnostic studies will be carried out in sync with other diagnosticians in this research program.

Milestones

1. Manufacturing of model thin-film and composite LLZO and lithium thiophosphate (LPS) SSEs by pulsed laser deposition (PLD) as model systems for fundamental electrochemical studies of Li-metal battery systems. (Q1, FY 2019; See progress section)
2. Characterize the bulk and surface structure of lithium anode, NMC cathode electrodes, and SSEs and the relationship to electrochemical and interfacial properties. (Q2, FY 2019; On schedule)

3. Characterize the chemistry of SSE/Li and electrolyte/cathode interfaces with *ex situ* near-field IR, X-ray absorption spectroscopy (XAS) and XPS. (Q3, FY 2019; On schedule)
4. Design and develop new XAS/XPS experimental setup to characterize *in situ* solid/solid (for example, NMC/SSE Li/SSE) interfaces. *Go/No-Go Decision*: Demonstrate feasibility of *in situ* measurements of solid-solid electrochemical interfaces. (Q4, FY 2019; On schedule)

Progress Report

This quarter, the team initiated new diagnostic studies of chemical and electrochemical reactions at electrode/electrolyte interfaces in all-solid-state-battery systems. Model cells were assembled with NMC cathodes, lithium thiophosphate (LPS-Li_3PS_4 in this work) SSE and graphite anode. The cathode was assembled by pressing ion-conductive LPS solid-state electrolyte with NMC powder and a slight amount of conductive carbon additive, whereas the anode was manufactured by mixing and pressing LPS and graphite powder. NMC cathodes with different nickel contents, that is, NMC-333, NMC-523, NMC-811, and $LiNbO_3$-coated NMC-811, were built, tested, and characterized with XAS) in the Advanced Light Source (ALS) user facility at LBNL. The all-solid-state spectro-electrochemical cell was cycled between 2.5-4 V at 0.1C rate. The cell assembly and electrochemical measurements were carried out under argon atmosphere to avoid any possible interference of side reactions with oxygen or moisture.

Sulfur K-edge and phosphorous K-edge XAS spectra of the pristine and cycled NMC electrode were recorded *ex situ* (Figure 24). The sulfur K-edge XAS spectrum of pristine LPS electrolyte shows the absorption peak at 2470.2 eV, which corresponds to the occupied sulfur 1s orbital. The chemical shift of the sulfur K-edge is sensitive to changes in the ground state charge density around sulfur atom. It can be used to obtain information about the chemical bonding environment and related changes on chemical reaction(s) between LPS and NMC.

XAS spectra of NMC/LPS composites recorded after one day of storage in an argon glove box (Figure 24a) show that the sulfur K-edge shifts to higher energies with increasing nickel content in NMC. This effect is due to a decreasing shielding and lower negative net charge and electron density of the sulfur atom, for example, PS_4^{3-}(ortho-thiophosphate) may be transformed to other thiophosphates, such as $P_2S_7^{4-}$(pyro-thiodiphosphate), $P_2S_6^{4-}$(hypo-thiophosphate), and $P_2S_6^{2-}$(meta-thiodiphosphate). In ortho-thiophosphates, a negative net charge of three electrons is distributed equally over the four sulfur atoms. While for pyro-thiophosphates only two electrons over three sulfur atoms are distributed, one P–S–P bridge exists, which can affect photoelectron transition from occupied sulfur 1s orbitals to unoccupied sulfur 3p s* antibonding orbitals. However, the fact that no shift can be observed for the NMC-811 coated with $LiNbO_3$ demonstrates that interfacial side reactions can be effectively inhibited.

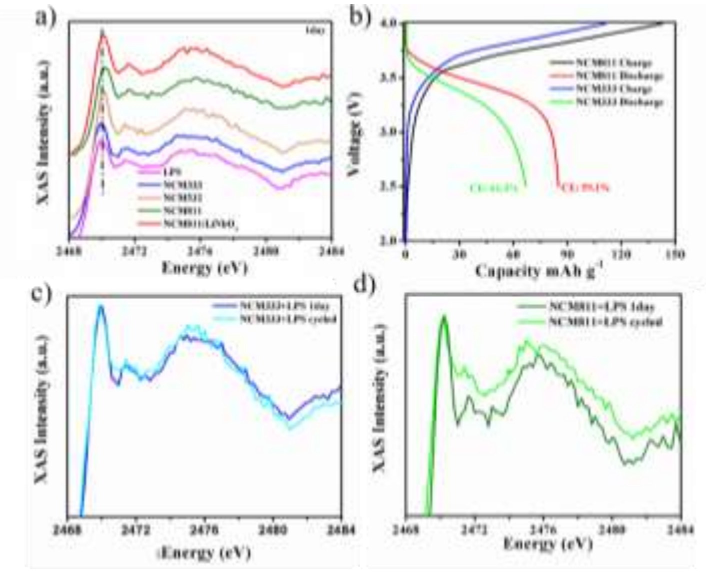

Figure 24. (a) Sulfur K-edge X-ray absorption near-edge spectroscopy (XANES) spectra of LPS mixed with NMC-333, -523, -811 and -811 coated with $LiNbO_3$. (b) 1st cycle charge/discharge profile of NMC-333 and NMC-811 cathode. Sulfur K-edge XANES spectra of cycled solid-state batteries assembled with (c) LPS-NMC-333 and (d) LPS-NMC-811.

The first charge discharge cycle of NMC-333 and NMC-811 based cells show rather low active material utilization ca. 46% and poor CE ca. 60%, which may result from inadequate electronic connectivity in the electrode composite and/or active material/electrolyte due to side reactions

(Figure 24b). However, the corresponding XAS spectra after one cycle (Figure 24c-d) look nearly identical to the pristine electrodes, that is, no clear evidence of additional LPS decomposition reactions was observed as compared to the pristine electrode after one day of storage.

This report concludes the project's efforts toward Milestone 1. The origins of NMC/LPS and Li/LPS interfacial instability will be further investigated.

Patents/Publications/Presentations

The project has no patents, publications, or presentations to report this quarter.

Task 2.3 – Advanced *In Situ* Diagnostic Techniques for Battery Materials
(Xiao-Qing Yang and Seong-Min Bak, Brookhaven National Laboratory)

Project Objective. The primary objective of this project is to develop new advanced *in situ* material characterization techniques and to apply these techniques to support development of new cathode and anode materials with high energy and power density, low cost, good abuse tolerance, and long calendar and cycle life for beyond Li-ion battery systems to power PHEVs and battery electric vehicles (BEV). The diagnostic studies will focus on issues relating to capacity retention, thermal stability, cycle life, and rate capability of beyond Li-ion battery systems.

Project Impact. The VTO Multi-Year Program Plan describes the goals for battery: "Specifically, lower-cost, abuse-tolerant batteries with higher energy density, higher power, better low-temperature operation, and longer lifetimes are needed for development of the next-generation of HEVs, PHEVs, and EVs." The knowledge gained from diagnostic studies through this project will help U. S. industries develop new materials and processes for next-generation Li-ion batteries in the effort to reach these VTO goals.

Approach. This project will use the combined synchrotron-based *in situ* X-ray techniques (XRD; and hard and soft XAS) with other imaging and spectroscopic tools such as HRTEM and MS to study the mechanisms governing performance of electrode materials.

Out-Year Goals. In the out years, the project will complete development of diagnostic techniques using X-ray pair distribution function (x-PDF), XRD, and XAS combined with neutron diffraction and neutron PDF (n-PDF), as well as STEM imaging and transmission X-ray microscopy (TXM) for cathode materials studies. It will then apply these techniques to study the structural changes of various new cathode materials.

Collaborations. The BNL team will work closely with material synthesis groups at ANL (Drs. Shin and Amine) for the high-energy composite and at PNNL for the S-based cathode and Li-metal anode materials, and with ORNL on neutron scatterings. This project will also collaborate with industrial partners at GM and Johnson Controls, as well as with international collaborators.

Milestones

1. Complete the *ex situ* soft x-ray absorption (sXAS) studies at oxygen K-edge of novel organic disulfide cathode material (1,2,4,5,6,7,9,10-octathia bis cyclopenta antraquinone-3,8-dithone, or TPQD) for Li-S batteries at different charged and discharged states. (Q1, FY 2019; Completed)
2. Complete the *ex situ* sXAS studies at sulfur K-edge of novel organic disulfide cathode material (1,2,4,5,6,7,9,10-octathia bis cyclopenta antraquinone-3,8-dithone, or TPQD) for Li-S batteries at different charged and discharged states. (Q2, FY 2019; In progress)
3. Complete XAS studies of sulfur electrode harvested from failed high-energy Li/S pouch cells after multiple cycling. (Q3, FY 2019; In progress)
4. Complete the spatially resolved XAS at sulfur K-edge and imaging of sulfur-based chemical species using XRF on the Li-metal anode in a cycled high energy Li/S pouch cell. (Q4, FY 2019; In progress)

Progress Report

The first milestone for FY 2019 was completed this quarter. BNL has been focused on the *ex situ* sXAS studies at oxygen K-edge of novel organic disulfide cathode material for Li-S batteries at different charged and discharged states. The BNL team has designed and synthesized novel organodisulfide electrode material 2,3,4,6,8,9,10,12- Octathia biscyclopenta [b,c]-5,11-antraquinone-1,7-dithone (TPQD) for Li-ion batteries. As shown in Figure 25, TPQD structure dithiolane group coordinated to a molecular benzoquinone skeleton through 1,4-dithiane; here, four-electron redox of disulfides and two-electron redox of 1-4-benzoquenone (BQ) are expected with a theoretical capacity of 324 mAh g^{-1}. The team's electrochemical results indicate that the TPQD electrode exhibits a high initial capacity of 251.7 mAh g^{-1}, which is corresponding to the 4.7 electron redox per formula unit. Thanks to the fast kinetics of BQ and π-conjugation structure, TPQD also delivers good high-rate capability (150 mAh g^{-1} at 5C) with stable cyclic performance. Oxygen K-edge XANES spectra were measured, as shown in Figure 26, and confirm the electrochemical mechanism of BQ in TPQD electrode. For the as-prepared TPQD, a sharp peak at 531 eV is observed, which is corresponding to the O1s- π^* (C=O) excitation that originates from the quinone. It can be clearly observed for the spectra at the 1st and 2nd discharge state that the peaks located at 531 eV markedly disappeared; meanwhile, two new peaks appeared at around 534 and 539 eV, attributed to the O1s-σ^* (O-C=C) and O1s-σ^* (O-Li) excitation, respectively. That means a successful transformation from C=O to C=C-O-Li during the lithiation process. When the electrodes are recharged back 3V, the characteristic peaks at 534 and 539 eV are obviously weakened and a strong peak at 531 eV appears again, indicating the reformation of C=O bonding.

Figure 25. Optimized structure and bond length of TPQD obtained by density functional theory calculation (grey denotes the carbon; yellow, the sulfur; and and red, the oxygen).

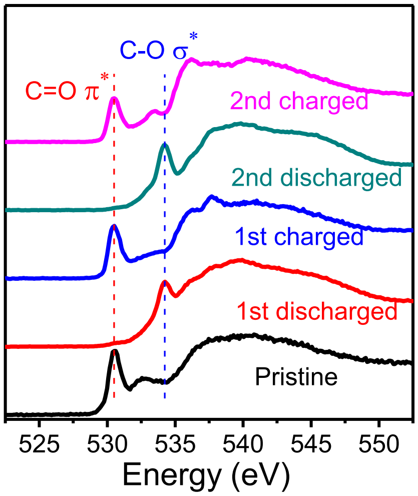

Figure 26. Oxygen K-edge X-ray absorption near-edge spectra of TPQD electrodes at different states of charge.

Patents/Publications/Presentations

Publications

- Wang, F., E. Hu, W. Sun, T. Gao, X. Ji, X. Fan, F. Han, X-Q. Yang*, K. Xu,* and C. Wang.* "A Rechargeable Aqueous Zn^{2+}-Battery with High Power Density and a Long Cycle-Life." *Energy & Environmental Science* (2018); Advance Article. doi: 10.1039/C8EE01883A (Communication), Publication Date: October 3, 2018.
- Yun, S., S-M. Bak, S. Kim, J. S. Yeon, M. G. Kim, X-Q. Yang, P. V. Braun*, and H. S. Park.* "Rational Design of Hierarchically Open-Porous Spherical Hybrid Architectures for Lithium-Ion Batteries." *Advanced Energy Materials*. doi: 10.1002/aenm.201802816, Publication Date (Web): December 20, 2018.
- Li, Y., X. Wang, Y. Gao, Q. Zhang, G. Tan, Q. Kong, S-M. Bak, G. Lu, X-Q. Yang, L. Gu, J. Lu, K. Amine, Z. Wang,* and L. Chen. "Native Vacancy Enhanced Oxygen Redox Reversibility and Structural Robustness." *Advanced Energy Materials*. doi: 10.1002/aenm.201803087, Publication Date (Web): December 5, 2018.

Presentations

- Materials Science and Engineering Colloquium, Department of Applied Physics & Applied Mathematics, Columbia University, New York, New York (November 16, 2018): "Using Synchrotron X-Ray and Neutron Based Scattering as well as TXM and TEM Imaging Techniques to Study the New Cathode Materials for Batteries and Studies on Li Metal Anode Protections"; Z. Shadike, R. Lin, E. Hu, S-M. Bak, X-Q. Yang,* H-S. Lee, X. Yu, Y. Chu, and Y. Liu. Invited.
- MRS Fall Meeting, Boston, Massachusetts (November 29, 2018): "Using Multi-Modal and Multi-Scale TEM and TXM Imaging Techniques to Study the Structural Stability of High Ni-Content Cathode Materials"; R. Lin, Z. Shadike, S-M. Bak, E. Hu, H. Xin, X. Huang, Y. Shin, H-S. Lee, Y. S. Chu, Y. Liu, and X-Q. Yang.* Invited.

Task 2.4 – Advanced Microscopy and Spectroscopy for Probing and Optimizing Electrode-Electrolyte Interphases in High-Energy Lithium Batteries
(Shirley Meng, University of California at San Diego)

Project Objective. The proposed research aims to develop advanced microscopy and spectroscopy tools to probe, understand, and optimize the anion activities that govern the performance limitations such as capacity and voltage stabilities in high-energy Li-excess TM (such as nickel, cobalt, manganese) oxides cathode materials. The approach uniquely combines atomic resolution STEM, EELS, *operando* BCDI, and first-principles computation to probe anion redox and oxygen evolutions in Li-excess NMC materials. Furthermore, the project will track the lithium and oxygen dynamics under electrochemical testing via *operando* neutron diffraction, which will enhance understanding of the overall structural changes due to anion activities. Ultimately, this will hone in on the synthesis efforts to produce the modified materials with optimum bulk compositions and surface characteristics at large scale for consistently good performance. The above-mentioned characterization tools will be extended to diagnose various anode types, such as Li-metal anode.

Project Impact. If successful, this research will enable *operando* imaging at the single-particle level by advanced microscopy imaging and high-energy-resolution oxygen K-edge EELS. This work will provide an in-depth understanding of anion activities in high-voltage electrode materials, which can lead to significant improvement in stabilizing operation voltage and electrode-electrolyte interface for future generation high-energy-density electrodes.

Approach. This unique approach combines STEM/EELS, *operando* BCDI, and *ab initio* computation as diagnostic tools for probing anion redox and oxygen evolutions in Li-excess NMC materials. This allows for pinning down the atomistic/molecular mechanism of anion oxidation and determining the speciation compositions and surface characteristics for enabling high rate and long life in the proposed materials. Neutron enables the characterization of bulk material properties to enhance and further optimize high-energy electrode materials.

Out-Year Goals. The goal is to improve the cycle life and efficiency of Li-excess NMC materials through the modification of both the cathode and the electrolyte. Single particle behavior of the modified Li-excess NMC with new electrolytes will be characterized.

Collaborations. This work funds collaborations on EELS (M. Chi, ORNL); neutron diffraction (K. An, ORNL); and soft XAS (M. Doeff, LBNL). It supports collaborative work with Z. Liu and Y. Xia at Ningbo Institute of Materials Technology and Engineering in China. It also supports collaboration with the Battery500 Consortium.

Milestones

1. Benchmarking electrochemical performance with the optimized Li-excess materials. (Q1, FY 2019; Completed)
2. Conducting XPS and differential electrochemical mass spectrometry (DEMS) characterization of anion evolution on modified Li-excess NMC. (Q2, FY 2019; In progress)
3. Carrying out STEM/EELS characterization on modified Li-excess NMC single particle using optimized electrolyte. (Q3, FY 2019; In progress)
4. Performing EELS and XPS characterization of SEI on electrochemically deposited lithium metal with new electrolyte systems. (Q4, FY 2019; In progress)

Progress Report

Benchmark Modified Li-Rich Layered Oxide (LRLO) Cathodes Performance

A gas-solid interface reaction (GSIR) was introduced to achieve delicate control of oxygen activity in LRLO. $Li[Li_{0.144}Ni_{0.136}Co_{0.136}Mn_{0.544}]O_2$ (denoted as LR-NCM) was synthesized through co-precipitation method (Figure 27a). Carbon dioxide gas was used to create uniform oxygen vacancies on LR-NCM particles' surface without affecting structural integrity. Figure 27b shows the Rietveld refined XRD pattern of LR-NCM after GSIR, in which all the peaks can be well indexed to R-3m space group. Li/Ni mixing of the sample is 3.32%. Element ratio of the modified LR-NCM was confirmed with ICP-OES as Li:Ni:Co:Mn=1.155:0.128:0.141:0.535.

The discharge capacity and energy density over cycling of the modified LR-NCM are shown in Figure 27c. All the cells were charged/discharged at C/20 (1C=250mAh/g) for two cycles as an activation process before the cycling at C/10 rate. After activation, it delivers a discharge capacity of 314 mAh/g and an energy density of 1109 mWh/g at the 1st cycle. The improved electrochemical performance is ascribed to the efficient utilization of oxygen activity through the creation of surface oxygen vacancies in the modified LR-NCM. After 25 cycles, the modified LR-NCM remains a specific capacity of 283 mAh/g (90.1% of the initial cycle) and an energy density of 940 mWh/g (84.7% of the initial cycle). The hysteresis between lithium insertion and removal in the modified LR-NCM is shown in Figure 27d. An increase of the hysteresis over cycling can be observed. Overall, the GSIR-modified LR-NCM has been chosen as the benchmark cathode for its high specific capacity and CE. Further improvement is needed to evade the decrease in energy density and the increase of hysteresis over cycling. Novel electrolyte will be introduced to create a more stable cathode electrolyte interface (CEI) in the system. One strategy is to add electrolyte additives such as LiBOB and LiDFOB. Another strategy will be using carbonate-free, sulfone-based electrolyte with high lithium salt concentration, which could support the system's fast ion exchange over a large voltage window. Both strategies are expected to improve the cycling performance in LR-NCM through the modification of CEI.

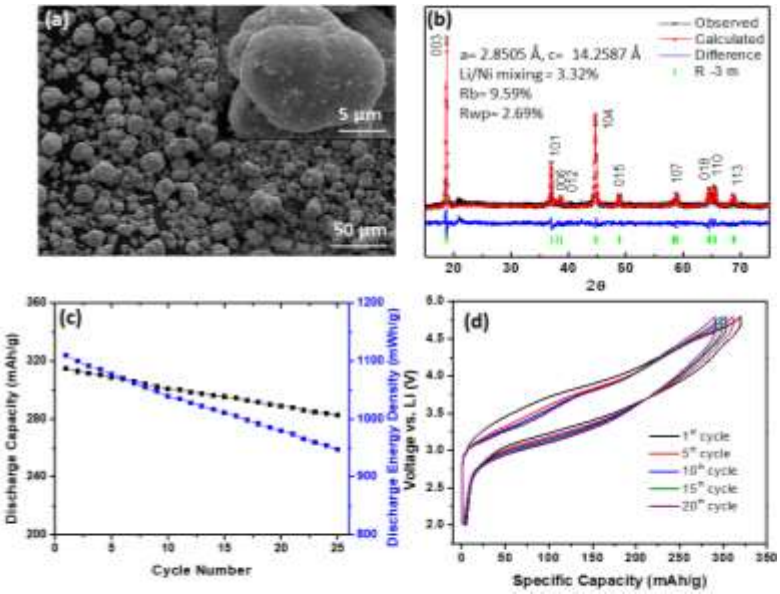

Figure 27. Characterization of the gas-solid interface reaction modified LR-NCM. (a) Scanning electron microscopy images taken at different magnifications. (b) Rietveld refinement of the X-ray diffraction pattern of LR-NCM. (c) The discharge capacity and energy density of the modified LR-NCM over cycling. (d) Voltage profiles of the modified LR-NCM at different cycle numbers.

In Situ Neutron Diffraction Study of the Performance Improvement in LRLO under Heat Treatment

Last quarter, the team explored the voltage and structural recovery of LRLO under heat treatment, which also provides another strategy in optimizing performance of LR-NCM. *In situ* neutron diffraction (ND) was conducted to further explore the reversible phase transformation in LR-NCM under real-time heating and cooling process. On heating from room temperature to 400°C, *in situ* ND and *in situ* sXRD exhibit a similar trend in the changes in a, c lattice. An "S" shape in the lattice a is observed in the *in situ* sXRD and *in situ* ND pattern (Figure 28a) with an increase in lattice parameter from room temperature to 100°C, a decrease from 100°C to 250°C, and an increase again from 250°C to 400°C. A flat region (or even decrease) in lattice c between 100°C to 200°C can be observed in Figure 28b. The flat region or decrease in both lattice parameter a and c from 100°C to 250°C indicates a phase transformation in the structure. The changes in the cooling process obtained through *in situ* ND show that both a and c shrink rapidly when cooling from 400°C to 80°C. After cooling, lattice parameter a and c are stable at a lower value than the cycled LR-NCM before heat treatment, indicating a structure recovery of the layered LR-NCM. The lithium and oxygen occupancy changes during *in situ* heating and cooling are obtained from Rietveld refinement. The occupancy of lithium in TM layer experiences an increase over heating and a small decrease over cooling (Figure 28c), which indicates that lithium returns to the TM layer under heat treatment. Even if a small amount of lithium would "escape" again from the TM layer, most would stay till the end of the cooling. The increased amount of lithium in TM layer could recreate the Li-excess environment and thus enable the oxygen activity in the following cycling. The changes in the oxygen occupancy (Figure 28d) are subtle, indicating that the heating treatment did not affect the oxygen concentration.

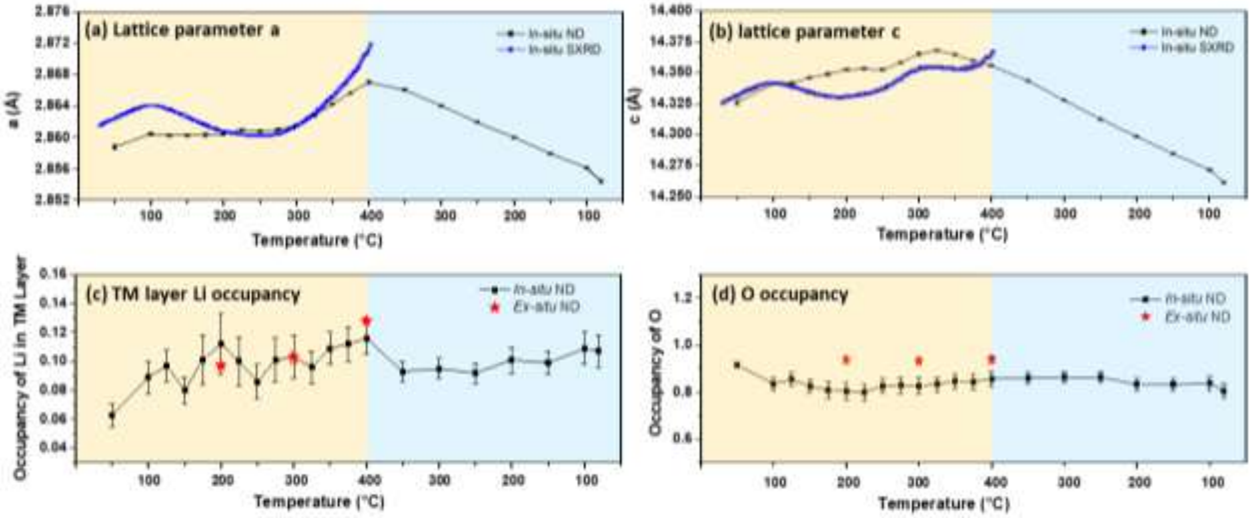

Figure 28. *In situ* neutron diffraction (ND), *in situ* soft X-ray diffraction, and *ex situ* ND of the initially cycled LR-NCM. Changes in (a) lattice parameter a, (b) lattice parameter c, (c) occupancy of lithium in transition-metal layer, and (d) occupancy of oxygen obtained from Rietveld Refinement.

Patents/Publications/Presentations

Publications

- Qiu, B., M. Zhang, Y. S. Meng, et al. "Structural and Voltage Recovery for Practicability of Anionic Redox in Li-Rich Layered Oxide Cathode Material." *Nature Communications*, under review.
- Wynn, T. A., C. Fang, M. Zhang, Y. S. Meng, et al. "Mitigating Oxygen Release in Anionic-Redox-Active Cathode Materials by Cationic Substitution through Rational Design." *Journal of Materials Chemistry A* 6 (2018): 24651.

Task 2.5 – *In Situ* Diagnostics of Coupled Electrochemical-Mechanical Properties of Solid Electrolyte Interphases on Lithium-Metal Rechargeable Batteries

(Xingcheng Xiao, General Motors; Brian W. Sheldon, Brown University; Yue Qi, Michigan State University; and Y. T. Cheng, University of Kentucky)

Project Objective. The project objective is to develop a comprehensive set of *in situ* diagnostic techniques combined with atomic/continuum modeling schemes to investigate and understand the coupled mechanical/chemical degradation of the SEI layer/lithium system during lithium cycling. The goal of this understanding is to develop a new coating design strategy to achieve dendrite-free high cycle efficiency and extend the cycle life of high-energy-density batteries with lithium as the anode for EV application.

Project Impact. The fundamental understanding of the coupled mechanical/chemical degradation of the SEI layer during lithium cycling will enable the project to identify the desirable mechanical properties on SEI/lithium as a system and the specific transport properties that enable the homogenous lithium stripping/plating while avoiding the mossy structure. Furthermore, it will allow the project to develop a highly impactful strategy to protect lithium metal and achieve dendrite-free high cycle efficiency, which can dramatically increase the energy density of lithium batteries for EV applications.

Approach. Different *in situ* techniques, including AFM, nano-indentor, dilatometer, and stress-sensor, will be developed to investigate the mechanical compatibility between SEI and soft lithium and the relationship between surface morphology and current density distribution that results in an inhomogeneous lithium plating/stripping process. Multiple strategies will be developed to tailor the mechanical and transport properties of SEI and to properly engineer the protective coating/lithium interface.

Out-Year Goals. The out-year goals involve using *in situ* electrochemical tools to reveal failure mechanisms of SEI/lithium as a whole electrode system, including correlating mechanical failure mechanisms of SEI/lithium, morphology evolution, cycle efficiency, and transport properties of SEI. Then, the project will develop continuum framework to establish the failure modes of SEI layer on lithium metal and provide the governing mechanical/material properties of SEI responsible for the critical failure mode based on the experimental results and atomic scale simulation.

Collaborations. Prof. H. Gao (Brown University) and Dr. Q. Zhang (GM) will be the key researchers involved in continuum simulation and postmortem analysis. Dr. C. Wang (PNNL), Dr. W. Yang (LBNL), and Dr. J. Xiao will be collaborators on advanced *in situ* analysis and electrolyte additives.

Milestones

1. Determine coating design window required to achieve mechanically stable coating on lithium metal. (Q1, FY 2019; Completed)
2. Determine impact of stress on morphological evolution of coated Li-metal surface, and identify failure modes of protective coatings on lithium. (Q2, FY 2019)
3. Vary coating modulus and investigate its impact on interfacial strength and cycle efficiency, and develop coating with desirable mechanical and transport properties. (Q3, FY 2019)
4. Establish a design strategy of protective coatings as artificial SEI on Li-metal electrode to achieve high cycle efficiency (> 99.8%). (Q4, FY 2019)

Progress Report

For high efficiency protection and practical operation, the chemical used for surface treatment should react with lithium surface fast and in high yield. Chlorosilane is a good candidate. It has been demonstrated that treating the Li-metal electrode with chlorotrimethylsilane (TMCS) to form an alkyl siloxane is a simple, effective method to avoid side reactions between lithium and electrolyte; however, this protecting film cannot survive in high current density cycling, which makes it less practical to use. The dense packing of small alkyl siloxane molecules resulting from the reaction of TMCS and lithium surface (LiOH, Li_2O) enables the effective isolation of lithium and electrolyte. However, the alkyl siloxanes have a low Young's modulus and are individually packed in the film, making the film easy to break under high current density cycling. Considering these facts, the team used chloro(dimethyl)-phenylsilane (PhDMCS) to treat the lithium surface, replacing one methyl group of TMCS with one phenyl ring. The reaction product of aryl siloxanes had much higher Young's modulus due to the rigid phenyl ring structures. The simulation results show the adjacent phenyl rings of siloxane molecules organized in an edge-to-face structure, indicating a strong electrostatic attraction due to π-π interaction (Figure 29). The double reinforcement of the aryl siloxane film due to high rigidity of phenyl ring structures and the π-π interaction of adjacent phenyl rings dramatically increased battery cycling life, even under high current density and areal capacity cycling (Figure 30).

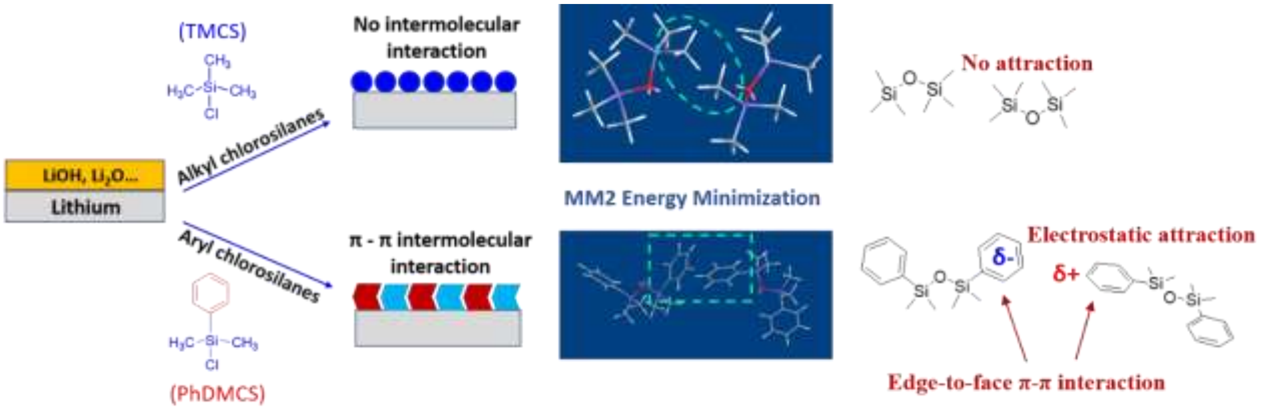

Figure 29. The reaction mechanism of lithium surface treatment with chlorosilanes, and simulation results of intermolecular interaction in resulting siloxane coating film on lithium surface.

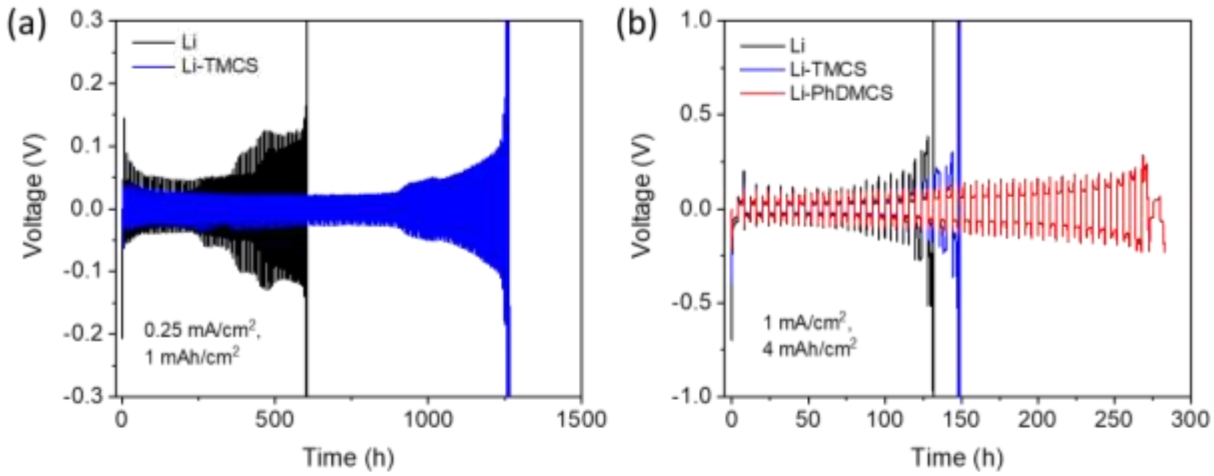

Figure 30. Galvanostatic cycling voltage profiles for symmetric cells using coated (chlorotrimethylsilane or chloro(dimethyl)-phenylsilane modified) or uncoated lithium electrodes under (a) low (0.25 mA/cm^2, 1 mAh/cm^2) and (2) high (1 mA/cm^2, 4 mAh/cm^2) current density and areal capacity. The electrolyte is 1 M $LiPF_6$ in EC/DEC 1:2 with 10% FEC by weight.

The success of this surface coating with aryl siloxanes provided an ideal system to figure out the mechanism of SEI protection by comparing the *in situ* characterization results of coated and uncoated Li-metal electrodes, and thus to develop and optimize *in situ* diagnostic techniques. Preliminary results by *in situ* impedance measurement indicate the PhDMCS-coated lithium electrode had a much smaller impedance increase during storage and cycling compared with uncoated lithium due to surface stabilization (Figure 31a-b). The *in situ* height change of lithium electrode by dilatometer showed the uncoated lithium electrode had much faster height increase compared to the PhDMCS-coated one under high current density cycling, indicating more dead lithium and SEI residues were generated on the uncoated lithium surface (Figure 31c-d). Further *in situ* characterization, such as SEM, nanoindentation, and multi-beam optical stress sensor (MOSS) evolution, is in progress. This, combined with simulation results, will help the team understand the relationship of SEI components and their impact on battery performance and thus, inversely, to develop the best *in situ* diagnostics techniques for Li-metal rechargeable batteries.

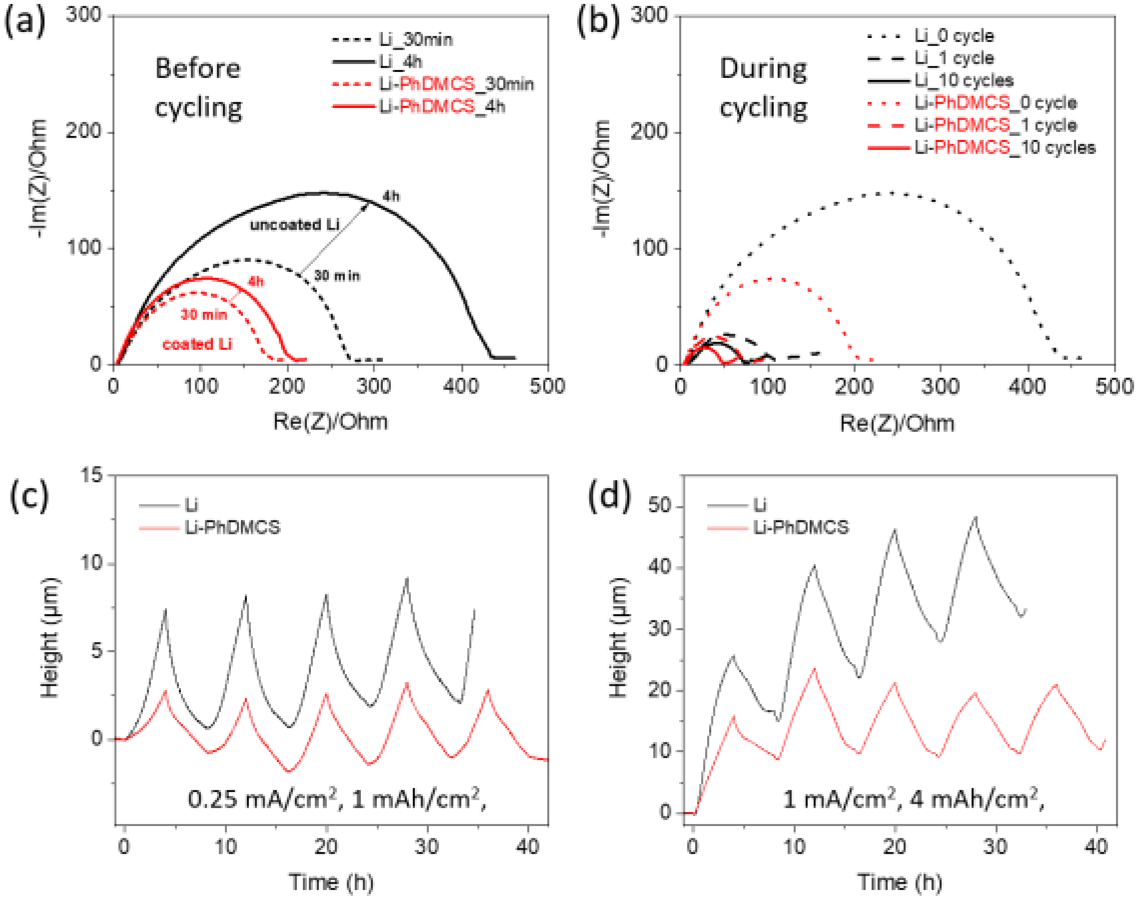

Figure 31. *In situ* characterization of symmetric cells using chloro(dimethyl)-phenylsilane (PhDMCS) treated or untreated lithium electrodes. (a) Impedance before and during cell cycling. Height change by dilatometer under (c) low (0.25 mA/cm^2, 1 mAh/cm^2) and (d) high (1 mA/cm^2, 4 mAh/cm^2) current density and areal capacity. The electrolyte is 1 M $LiPF_6$ in EC/DEC 1:2 with 10% FEC by weight.

Patents/Publications/Presentations

Publications

- Guo, K., W. Zhang, B. W. Sheldon, and H. Gao. "Concentration Dependent Properties Lead to Plastic Ratcheting in Thin Island Electrodes on Substrate under Cyclic Charging and Discharging." *Acta Materialia* 164: 261-271.
- Zhang, W., T. H. Cai, and B. W. Sheldon. "The Impact of Initial SEI Formation Conditions on Strain-Induced Capacity Losses in Silicon Electrodes." *Advanced Energy Materials* (2018): 1803066.

Presentations

- MRS Fall Meeting, Boston, Massachusetts (November 29, 2018): "*In Situ* Diagnostic of Coupled Mechanical and Chemical Degradation of Solid Electrolyte Interphase on Li Metal for Rechargeable Batteries"; X. Xiao. Invited.
- Materials Science & Technology (MS&T18), Columbus, Ohio (October 14–18, 2018): "Understanding the Mechanical Behavior of Electrode Materials for Improving the Performance and Durability of Lithium-Ion Batteries"; Y-T. Cheng.
- Materials Science & Engineering Seminar, University of Michigan, Ann Arbor, Michigan (October 18, 2018): "*In Situ* Mechanical Characterization for Understanding the Coupled Electrochemical-Mechanical Behavior of Battery Materials"; Y-T. Cheng.
- MRS Fall Meeting, Boston, Massachusetts (November 25–30, 2018): "*In Situ* Mechanical Characterization for Understanding the Coupled Electrochemical-Mechanical Behavior of Battery Materials"; Y-T. Cheng.
- Society of Engineering Science Annual Meeting, Madrid, Spain (October 10, 2018): "Chemo-Mechanical Degradation of Solid Electrolyte Interphases in Li Ion Batteries"; B. W. Sheldon. Keynote.
- MRS Fall Meeting, Boston, Massachusetts (November 25–30, 2018): "Stress Evolution in the SEI/Li Surface Layer and Its Impact on the Performance of Lithium Metal Batteries"; Juny Choi.

Task 2.6 – Microscopy Investigation on the Fading Mechanism of Electrode Materials (Chongmin Wang, Pacific Northwest National Laboratory)

Project Objective. This work will use a combination of *ex situ*, *in situ*, *operando* and cryo HRTEM and spectroscopy to probe the fading mechanism of both lithium and silicon as high-capacity anode as well as Ni-rich NMC as high-capacity cathode. For high-capacity anode, the research task will focus on revealing how lithium and silicon interact with liquid electrolyte to critically affect their fading process. For the Ni-rich NMC cathode, the project will focus on delineating the structural and chemical evolution of the Ni-rich NMC as their dependence on the operating voltage, charge rate ,and chemistry of electrolyte.

Project Impact. The proposed characterization work focuses on atomic-level structural and chemical analysis and direct correlation with battery fading properties. The work can be directly used to guide the designing of electrode materials with tailored microstructure and chemistry for enhanced properties of increasing the energy density of Li-ion batteries and to accelerate market acceptance of EVs, especially for PHEV as required by the EV Everywhere Grand Challenge.

Approach. Aberration-corrected STEM high-angle annular dark-field (STEM-HAADF) and cryo-TEM imaging combined with EELS / energy-dispersive X-ray spectroscopy (EDX) chemical analysis will be used to probe the microstructural and chemical evolution of both cathode and anode. TOF-SIMS, nano-SIMS, and XPS will be used to explore the chemistry and the thickness of SEI layer on cathode and anode material. These characterization results will be used to guide the materials optimization process and establish a solid knowledge base on the correlation between materials selections and structure evolution in the Ni-rich NMC layered cathode materials.

Out-Year-Goals. This project has the following out-year goals:

- Multi-scale *ex situ*/*in situ* and *operando* TEM and cryo-TEM investigation of failure mechanisms for energy-storage materials and devices. Atomic-level *in situ* TEM and STEM imaging to help develop fundamental understanding of electrochemical energy-storage processes and kinetics of electrodes.
- Extension of *in situ* TEM capability for energy storage technology beyond lithium ions, such as Li-S, Li-air, Li-metal, sodium ions, and multi-valence ions.

Collaborations. This project collaborates with G. Chen (LBNL); J. Nanda (ORNL); K. Amine (ANL); D. Wang (Pennsylvania State University); A. Manthiram (University of Texas at Austin, UT Austin); W. Tong (LBNL); G. Liu (LBNL); Y. Cui (Stanford University); J. Zhang (PNNL); J. Liu (PNNL); X. Xiao (GM); S. Meng (UCSD); and S. Whittingham (State University of New York, SUNY, at Binghamton).

Milestones

1. Resolve the true structural nature of the intragranular cracks in Ni-rich NMC and answer questions on the origin of such cracking behavior. (Q1, FY 2019; Completed)
2. Reveal the true structural and chemical information of Si-anode/liquid-SEI layer by integration of cryo-TEM and EELS. (Q2, FY 2019; On track)
3. Determine the critical factor that controls the correlation between charging rate and fading behavior of Ni-rich NMC. (Q3, FY 2019; On schedule)
4. Reveal the true structural and chemical information of Li-metal anode/liquid-SEI layer by cryo-TEM and EELS. (Q4, FY 2019; On schedule)

Progress Report

Doping of a trace amount of aluminum in NCA oxide has been noticed to dramatically enhance cycling stability. However, the functioning mechanism of the aluminum dopant remains unclear.

Using atomic-level imaging, spectroscopic analysis, and DFT simulation, the team demonstrates that the aluminum dopant in NCA is partially dissolved in the bulk lattice and partially exists as Al_2O_3 particles that epitaxially dress on the cathode particle surface. The Al_2O_3 particles play a role of surface coating at the site where they reside. The aluminum substitution lowers TM redox energy level and consequently promotes formation of a stable CEI layer. This prevents dissolution of TM from cathode and therefore eliminates deposition of TM on anode though cross talking on battery cycling.

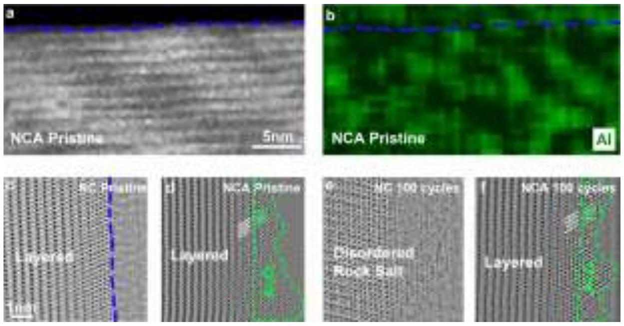

Figure 32. Formation of epitaxial Al_2O_3 layers on top of NCA surfaces. High-angle annular dark-field scanning transmission electron microscopy image (a) and corresponding EDS mapping (b) of pristine NCA sample. The blue dashed lines represent the surface boundary of NCA primary particle, and the green color depicts the aluminum elements distribution. (c, e) The zoom-in view of pristine and 100 cycled NC surfaces, respectively. The blue dashed lines depict the boundary of NC surfaces. (d, f) The zoom-in view of pristine and 100 cycled NCA surfaces, respectively. The green dashed lines outline the Al_2O_3 phase. The white and green lines represent the (01-2) planes of parent phase and (-120) planes of Al_2O_3 phase, respectively.

Specifically, the team uses two Ni-rich cathodes, one with the formula of $LiNi_{0.94}Co_{0.06}O_2$ (NC) and the other with 2% addition of aluminum in the NC materials ($LiNi_{0.92}Co_{0.06}Al_{0.02}O_2$, termed as NCA) to elucidate the origin of aluminum for enhanced cycling stability of NCA. The team reveals that the aluminum dopant enhances cycling stability through two aspects: improving the electrode structural stability, and modifying the cathode electronic property and thus reactivity. The STEM observations coupled with EDX mapping reveal that part of the aluminum segregates on the cathode surface, which leads to formation of Al_2O_3 islands with a size of a few nanometers. The atomistic simulations reveal that the aluminum dopant facilitates formation of phosphate-containing CEI layers in the Ni-rich cathode, resulting from the dopant-induced down shift of Fermi level. The CEI layers coupled with the scattered Al_2O_3 nano-islands work in synergy and enhance battery performance (Figure 32).

Through a systematic comparison study of NC and NCA, the team reveals that the dramatically improved cycling stability of NCA, as contrasted with that of NC, originates from the al-dopant-governed enhancement of CEI stability, due to modification of both crystallographic structural stability and electronic energy of cathode. Compared to NC, the NCA group shows a significantly improved interface behavior associated with several concurrent events: a much-reduced TM dissolution and reprecipitation; significantly thinner surface reconstruction layers; a less severe secondary particle pulverization on prolonged cycling; and a much-reduced SEI thickness in the graphite anode. This illustrates the vital roles of the aluminum doping in mitigating the detrimental reactions occurring at the CEI. Two consequences from aluminum doping contribute to improvement of interfacial reactivity: development of epitaxial Al_2O_3 nano-islands arising from the aluminum segregation, and formation of CEI layers on cycling. The results extend the understanding of dopant effects from bulk to solid liquid interface, and may be applicable in more general cathode systems.

Patents/Publications/Presentations

Publication

- Zou, L., Z. Liu, W. Zhao, H. Jia, J. Zheng, Y. Yang, G. Wang, J-G. Zhang, and C. Wang. "Solid−Liquid Interfacial Reaction Trigged Propagation of Phase Transition from Surface into Bulk Lattice of Ni-Rich Layered Cathode." *Chemistry of Materials* 30 (2018): 7016–7026.

Presentation

- MRS Fall Meeting, *In Situ/Operando* Analysis of Electrochemical Materials and Interfaces Symposium (CM03), Boston, Massachusetts (November 25–30, 2018): "*In-Situ* and *Ex-Situ* Electron Microscopy and Spectroscopy Diagnosis Guided Designing of Electrode Materials for Better Battery." Invited.

Task 2.7 – Correlative Microscopy Characterization of Electrochemical Hotspots in Oxide Electrodes (Yi Cui, William Chueh, and Michael Toney; Stanford/SLAC)

Project Objective. This project aims to develop and utilize a correlative microscopy platform to investigate the lithiation dynamics of lithium- and manganese-rich (LMR) NMC and NCA, with the specific goal of understanding factors that determine the rate capability and degradation mechanisms at the single primary particle length scale. By developing a nanoscale and single-particle understanding of lithiation, the project addresses specific engineering problems including electrochemical hotspot, electrode utilization, safety, and capacity/voltage fade.

Project Impact. Fundamental insights from this new diagnostic capability are expected to increase the power density and cycle life of oxide electrodes by improving electrode utilization, reducing electrochemical hotspots, decreasing capacity and voltage fade, and enhancing safety, which all improve the viability of Li-ion batteries for vehicle transportation. By understanding lithiation at the single-particle level, this project's success will contribute to improving on-vehicle battery management, such as charging/discharging protocol, and state-of-charge and state-of-health monitoring.

Approach. As stated, the project aims to develop a correlative microscopy platform to investigate the lithiation dynamics of LMR-NMC and NCA, with the goal of understanding factors that determine the rate capability and degradation mechanisms at the single primary particle length scale. On recharging time, the specific phenomena to be addressed include nonuniform current distribution and the correlation between surface property and the local lithiation rate. On degradation, phenomena to be addressed include correlating local chemistry and phases to capacity and voltage fading.

Out-Year Goals. Develop X-ray microscopy to investigate NMC and LMR-NMC cathodes at the single primary particle and single secondary particle level.

Collaborations. Commercial battery electrode particles are being supplied by Samsung.

Milestones

1. Quantify the local structure of Li-rich layered oxides using local X-ray probe. (Q1, FY 2019; Completed)
2. Assess the effect of synthesis condition of anion redox. (Q4, FY 2019)
3. Assess the effect of oxygen vacancies on anion redox. (Q4, FY 2019)

Progress Report

The team continued investigating model anion redox compound $Li_{2-x}Ir_{1-x}Sn_xO_3$. Understanding why tin substitution gives rise to these phenomena is central to uncovering the origin of the coupling between anion redox and metal migration/vacancy formation. Since the defect concentration is more reliably quantified in LISO25 ($x = 0.25$), the team focused DFT analysis on this composition. First, they examined evolution of the computed DOS in the control case of ordered, M_{Li}/V_M-free LISO25 as a function of lithium stoichiometry. The team observed that no unhybridized oxygen *2p* states are depopulated in the fully delithiated O1 structures; only hybridized Ir–O states are accessed, giving iridium a formal oxidation state of at least 6+, which is inconsistent with the XAS results. Thus, simple delithiation and the O3-O1 stacking change do not explain the high-voltage redox process in LISO. Importantly, the DFT calculations suggest that oxygen redox cannot occur in LISO25 or LISO50 after delithiating 1.5 lithium per formula unit if M_{Li}/V_M defects are not allowed to form.

Next, the team introduced the experimentally observed Sn_{Li}/V_M defects and examined their effect on the electronic structure and charge distribution of LISO. Out-of-plane tin migration into a lithium layer site creates a cation vacancy, V_M, and neighboring single-coordinate (dangling) oxygen atoms. Note that the team uses the term “single-coordinate” to refer to the number of covalent bonding partners, that is, counting iridium or tin, but not lithium. They find this stabilizes the delithiated structure significantly by 1.34-1.36 eV, whereas the formation of Ir_{Li}/V_M defect pairs are predicted to have a much smaller driving force of 0.02 eV.

The team attributes the Sn_{Li}/V_M stabilization to the response of the resulting M-O dangling bonds, which undergo one of two major transformations. As shown in Figure 33, when M=Ir, these bonds contract substantially, changing from ~ 1.94 Å to ~ 1.77 Å. Figure 33b shows that the bond contraction accompanies a splitting of the previously unhybridized oxygen *2p* states (shaded, top panel), with some states moving above the Fermi level and becoming oxidized (shaded, bottom panel), that is, the oxygen redox. The shifted states, approximately 1.5 eV higher in energy, rehybridize with the iridium *5d* states. These observations suggest the formation of short Ir–O π bonds (equivalently, terminal oxo ligands) through donation of oxygen lone pair electrons, approaching Ir=O double bonds (Figure 33b).

When M=Sn, on the other hand, the single-coordinate oxygens are predicted to instead pair up to form short (~ 1.44 Å) O–O dimers that straddle the V_M (Figure 33c). Again, this transformation results in a shift of the previously buried NB oxygen 2*p* states from below to above the Fermi level along with donation of electron density from oxygen to a neighboring iridium. The team stresses that these localized dimers are distinct from the long (~ 2.5 Å) dimers previously proposed for this material in that they are well within the range of typical bond lengths for O_2^{n-} species and, crucially, do not form in the absence of cation migration.

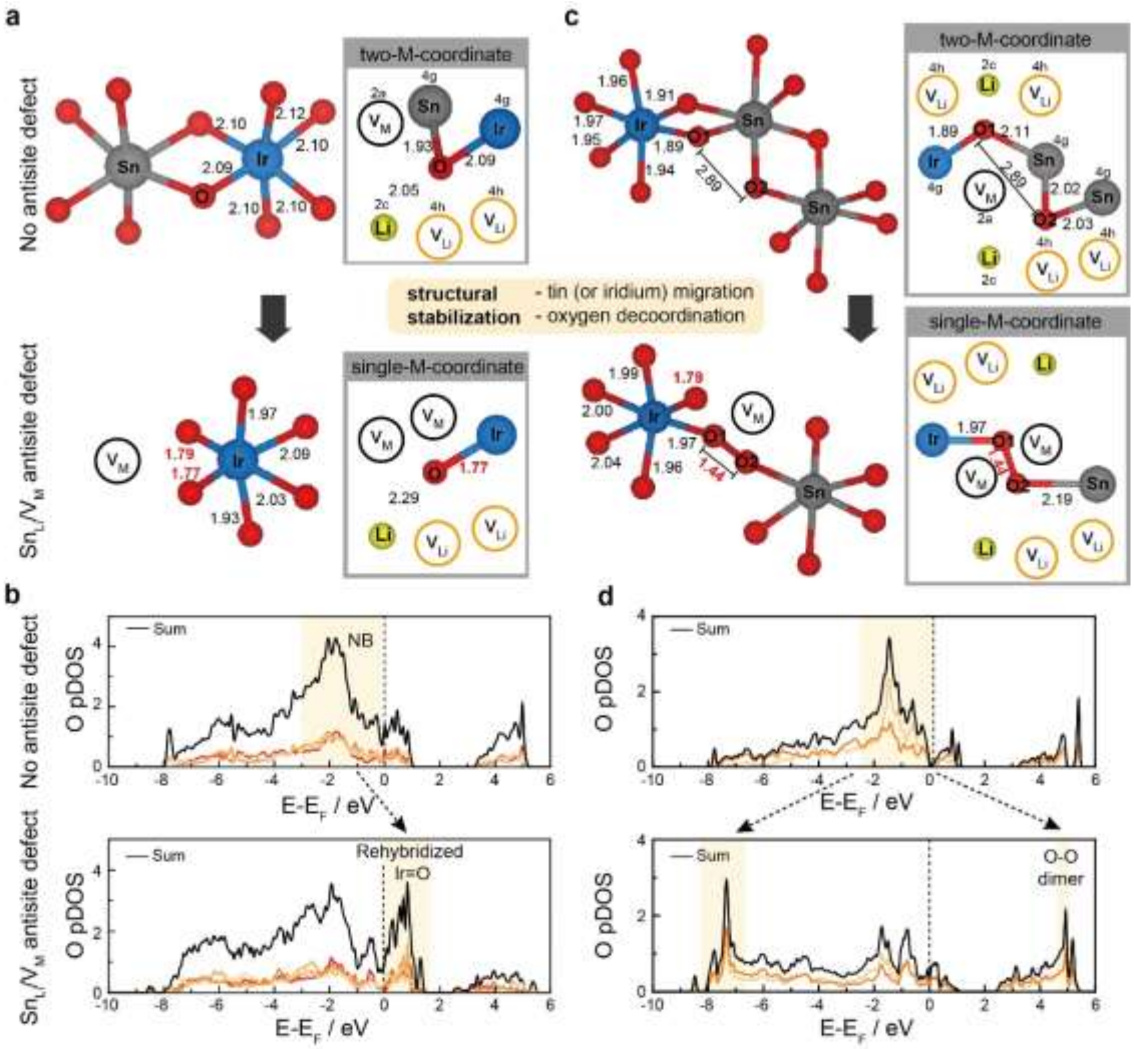

Figure 33. Computational predictions of M-O decoordination and Ir=O/O–O mediated anion redox. (a) Local coordination environments predicted by density functional theory in a $Li_{0.5}Ir_{0.75}Sn_{0.25}O_3$ structure showing the consequence of Sn_{Li}/V_M defect formation when the vacancy neighbors only iridium: contraction of the Ir—O bonds (left) and the resulting changes in local oxygen environment (right). Note that the presence of lithium neighboring oxygen negligibly affects the oxygen 2*p* states due to minimal hybridization between lithium and oxygen. (b) Projected DOS of the individual oxygen atoms involved in the Ir–O bond contraction before (top) and after (bottom) forming the Sn_{Li}/V_M defect, demonstrating the shift of the oxygen 2_p states above the Fermi level, indicating oxygen redox. (c) Local coordination environments when the migrating tin initially neighbors another tin, resulting in the formation of a 1.44 Å O–O dimer. (d) Projected DOS of the individual oxygen atoms involved in the O–O bond formation before (top) and after (bottom) forming the Sn_{Li}/V_M defect and O–O dimer, also showing a shift of the oxygen 2*p* states above the Fermi level.

Patents/Publications/Presentations

Publications

- Hong, J., W. E. Gent, P. Xiao, K. Lim, D-H. Seo, J. Wu, P. M. Csernica, C. J. Takacs, D. Nordlund, C-J. Sun, K. H. Stone, W. Yang, D. Prendergast, G. Ceder, M. F. Toney, and W. C. Chueh. "Metal-Oxygen Decoordination Stabilizes Anion Redox in Li-Rich Oxides." *Nature Materials* (2019). Accepted.
- Dai, K., J. Wu, Z. Zhuo, Q. Li, S. Sallis, J. Mao, G. Ai, C. Sun, Z. Li, W. E. Gent, W. C. Chueh, Y. Chuang, R. Zeng, Z. Shen, F. Pan, S. Yan, L. F. J. Piper, Z. Hussain, G. Liu, and W. Yang. "High Reversibility of Lattice Oxygen Redox Quantified by Direct Bulk Probes of Both Anionic and Cationic Redox Reactions." *Joule* (2019). Accepted.
- Gent, W. E. "Harnessing Oxygen Redox to Extend the Energy Density of Lithium-Ion Batteries." Ph.D. Thesis. Chemistry, Stanford University (2018).

Presentations

- MRS Fall Meeting, Boston, Massachusetts (November 28, 2018); W. C. Chueh.
- Royal Society Materials Challenges for Sustainable Energy Technologies, London, United Kingdom (September 19, 2018); W. C. Chueh.
- MRS Fall Meeting, Boston, Massachusetts (November 29, 2018): "Oxygen Redox, Cation Disorder, and a New Path Forward for Lithium-Rich Electrodes"; W. E. Gent, J. Hong, K. Lim, Y. Liang, P. Xiao, D-H. Seo, J. Wu, W. Yang, G. Ceder, D. Prendergast, M. F. Toney, and W C Chueh.

TASK 3 – MODELING

Summary and Highlights

Achieving the performance, life, and cost targets outlined by VTO will require moving to next-generation chemistries, such as higher capacity Li-ion intercalation cathodes, silicon and other alloy-based anodes, Li-metal anode, and sulfur cathodes. However, numerous problems plague development of these systems, from material-level challenges in ensuring reversibility to electrode-level issues in accommodating volume changes, to cell-level challenges in preventing cross talk between the electrodes. In this task, a mathematical perspective is applied to these challenges to provide an understanding of the underlying phenomenon and to suggest solutions that can be implemented by the material synthesis and electrode architecture groups.

The effort spans multiple length scales from *ab initio* methods to continuum-scale techniques. Models are combined with experiments, and extensive collaborations are established with experimental groups to ensure that the predictions match reality. Efforts also focus on obtaining parameters needed for the models, either from lower-length scale methods or from experiments. Projects also emphasize pushing the boundaries of the modeling techniques used to ensure that the task stays at the cutting edge.

In the area of intercalation cathodes, effort is focused on understanding working principles of high nickel layered materials with an aim of understanding structural changes and associated changes in transport properties. Coatings, an effective strategy for high-voltage operation, are being explored with the aim of providing a rational design approach for new coating materials. Focus is also paid both to assembling porous electrodes with particles to predict conduction behavior and to developing tools to measure electronic conduction.

Efforts also continue in predicting transport properties of liquid electrolytes, especially in the superconcentrated regime and understanding the nature of the silicon anode behavior.

In the area of Li-metal anodes, the focus is on understanding how materials can be designed to prevent dendrite growth using continuum modeling approaches, combined with calculations on mobility in solid conductors. The results are used to guide materials development by providing the properties needed to prevent dendrites while also achieving the energy and power goals. Models are also starting to examine the role of the SEI on the morphology of the dendrite and to describe the mechanical-electrochemical coupled effects that are critical for dendrite formation in both polymer and ceramic materials. In the area of sulfur cathodes, the task is aimed at modeling the dissolution-precipitation process and tracking the morphological changes during cycling.

Task 3.1 – Design of High-Energy, High-Voltage Lithium Batteries through First-Principles Modeling (Kristin Persson, Lawrence Berkeley National Laboratory)

Project Objective. This project supports VTO programmatic goals by developing next-generation, high-energy cathode materials and enabling stable cathode operation at high voltages through target particle morphology design, functional coatings, and rational design of electrolytes. The end-of-project goals include: (1) understanding of the factors that govern charge transport in nonaqueous, superconcentrated liquid electrolytes (2) new fundamental understanding of the Li-ion dynamics in Si-Sn electrode alloys (and their native oxides), with a design focus on improving stability of the silicon electrode through tin alloying, and finally (3) critical surface and coating design and optimization strategies that will improve cycling of Li-ion battery cathodes by reducing cathode degradation from oxygen loss.

Project Impact. To enhance performance of Li-ion systems, improvements on the cathode and the electrolyte side are needed. This project is aimed to result in an improved understanding of the atomistic mechanisms underlying surface behavior and performance of the Li-ion cathode materials, with the ultimate goal being to suggest strategies, such as coatings, surface protection, and particle morphology design. Furthermore, fundamental studies of electrolyte conductivity and transport mechanisms, as a function of solvent and salt concentrations, and components will be conducted.

Approach. First-principles calculations, both static and dynamic approaches, are used to model solid-state electrode material thermodynamics and kinetics. Liquid electrolytes are modeled through coupled classical molecular dynamics (MD) and first-principles methods to accurately capture solvation structure as well as reactivity of the liquid system.

Out-Year Goals. For the electrolyte development, work will be aimed toward understanding the atomistic interactions underlying the performance of lithium electrolytes specifically elucidating conductivity (as a function of salt concentration) and impact on the charge transport mechanisms at play. Stable interfaces will be determined by focusing initially on degradation mechanisms related to release of surface oxygen at high charge. Tuning particle morphology and coating materials—both of crystalline as well as amorphous structure—will be explored using the Materials Project. Li-ion conduction mechanisms and electrode stability of Si-Sn alloys will be determined, in addition to the reactivity and ionic conduction of the native oxide surface phases.

Collaborations. This project is highly collaborative between BMR PIs G. Chen (LBNL), G. Ceder (LBNL), and V. Srinivasan (ANL). Cathode design and synthesis will be performed by Chen and Ceder, surface design by Persson, and electrolyte design and testing by Persson and Srinivasan.

Milestones

1. Finish benchmarking of algorithms for obtaining reliable solvation structures and ionic conductivity in highly concentrated liquid electrolytes. (Q1, FY 2019; Completed)
2. Identify Li-ion conduction mechanisms in Si-Sn alloy anode, using first-principles modeling. (Q2, January 2019; In progress)
3. Evaluate SiO_2 and SnO_2 as surface phases from the perspective of ionic conduction and reactivity with lithium. (Q3, April–July 2019)
4. Conduct first evaluation of amorphous oxygen-retention and lithium diffusion enhancing coatings using the Materials Project infrastructure. (Q4, July 2019–November 2019)

Progress Report

This project is aimed toward cyclic organic carbonate-based electrolytes, specifically propylene carbonate (PC). In the superconcentrated regime (3 M), there is an absence of solvent exfoliation otherwise present at lower concentrations,[1] as well as a reported ability for fast charging and higher anodic stability.[2] However, concurrently, there is a significant decrease in the bulk conductivity. A bottom-up, molecular-level rational design for the superconcentrated regime requires an atomistic understanding of the solvation structure and charge transport in said systems. Therefore, a validated methodology for MD simulation in the superconcentrated regime is desirable.

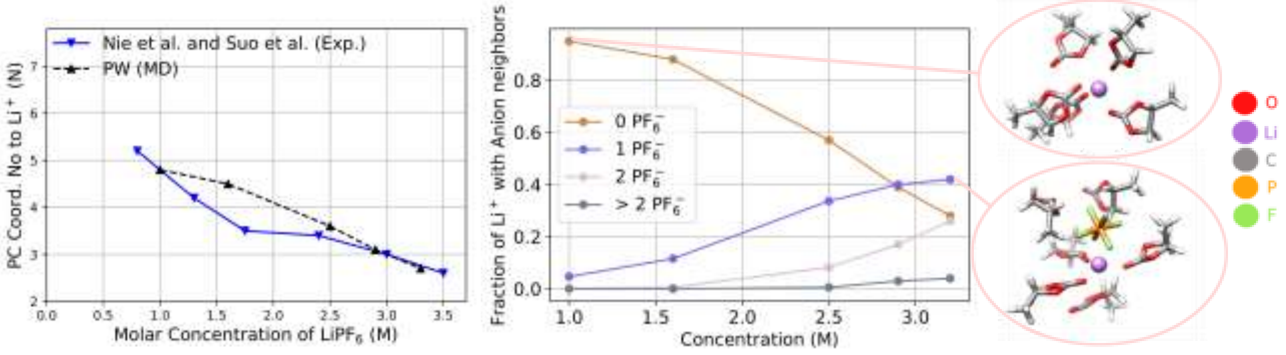

Figure 34. Coordination number of $\mathrm{Li^+}$ with propylene carbonate computed in the present work and compared to experimental values (left) and fraction of $\mathrm{Li^+}$ with n $\mathrm{PF_6^-}$ anions (middle). Representative solvation structures are shown on the right.

Assessment of electrolyte molecular-level structure was done via comparison to experiment of MD simulation-obtained coordination number of $\mathrm{Li^+}$ to the PC solvent, shown in Figure 34 (left). There is good agreement to experimental values from Nie et al., indicating a proper representation of concentration-dependent solvation structures in the MD simulations. The number of neighboring counter anions to the $\mathrm{Li^+}$ is shown in Figure 34 (center) as a function of $\mathrm{LiPF_6}$ concentration. The solvation environment of the $\mathrm{Li^+}$ is significantly altered in the superconcentrated regime, where a much larger fraction of $\mathrm{Li^+}$ cations are surrounded by anions in their primary solvation shell, consistent with the reported decrease in coordination number. However, even in the superconcentrated regime, there is still a non-negligible fraction of $\mathrm{Li^+}$ with no anions in the primary solvation shell. Representative solvation structures are illustrated in Figure 34 (right).

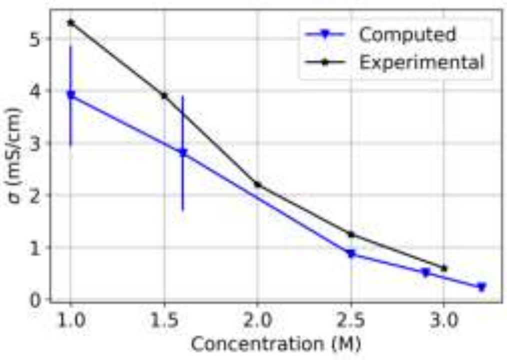

Figure 35. Bulk electrolyte conductivity of $\mathrm{LiPF_6}$ electrolyte as a function of salt concentration. Experimental data taken from Takeuchi et al. (2009).

The ability of the MD simulations to model transport of electrolyte species was validated by comparison of computed bulk conductivity σ to experimental σ, shown in Figure 35. There is good agreement between computed values and experiment, indicating that the herein employed methods are satisfactory for modeling such systems, thus providing a framework for further work in the molecular-level understanding and design of superconcentrated electrolytes.

[1] Nie, M., et al. "Role of Solution Structure in Solid Electrolyte Interphase Formation on Graphite with $\mathrm{LiPF_6}$ in Propylene Carbonate." *Journal of Physical Chemistry C* 117, no. 48 (December 5, 2013): 25381–89, https://doi.org/10.1021/jp409765w.

[2] Yamada, Y., and A. Yamada. "Review—Superconcentrated Electrolytes for Lithium Batteries." *Journal of The Electrochemical Society* 162, no. 14 (2015): A2406–A2423.

Patents/Publications/Presentations

Presentation

- Pacific Power Source Symposium (PPSS), Hawaii (January 2019): “The Impact of Minority as well as Majority Solvation Species on the Performance of Liquid Organic Electrolytes.” Invited.

Task 3.2 – Addressing Heterogeneity in Electrode Fabrication Processes
(Dean Wheeler and Brian Mazzeo, Brigham Young University)

Project Objective. The project goal is to better understand connections between fabrication conditions and undesired heterogeneity of thin-film electrodes by means of new nondestructive inspection (NDI) techniques and computer models.

Project Impact. This work will result in new diagnostic and modeling tools for rapidly and conveniently interrogating how well homogeneity has been maintained in electrodes during fabrication and in subsequent cycling. Real-time measurement of heterogeneity will enable manufacturer quality control improvements. The measurement and modeling tools will further enable researchers to compare different electrodes, improve formulations and processes, and anticipate cell performance of new designs.

Approach. Two NDI techniques will be developed or improved that will characterize electrochemical and mechanical uniformity of the electrodes. The first tool will be a flexible contact probe on a polymer substrate for rapidly measuring local electrical conductivity across electrodes of any geometry. The second tool will be a new acoustic probe that measures local elasticity and density of the composite film. These two prototyping efforts will be tied together by a particle-based microstructure model that allows prediction and correlation of electrode conductive and mechanical properties with fabrication conditions.

Out-Year Goals. This project was initiated October 2016 and concludes September 2019. Overall goals by fiscal year are as follows:

- **2017.** Fabricate first-generation flexible conductivity probe and proof-of-concept of acoustic probe. Improve microstructure model to match experiment.
- **2018.** Integrate flex probe with test fixtures suitable for assessment of large or continuous samples. Demonstrate measurement of localized ionic conductivity.
- **2019.** Assess affect of heterogeneity on cell charge and discharge performance. Further improve accuracy and reliability of probe and modeling technologies.

Collaborations. The following collaborators have provided battery materials for analysis: M. Wixom (Navitas), K. Smith (National Renewable Energy Laboratory, NREL), R. Subbaraman and J. Christensen (Bosch), S. Harris (LBNL), B. Polzin (ANL), and C. Kim (Hydro-Quebec, HQ). Other collaborations and the transfer of this technology to interested parties are being pursued.

Milestones

1. Quantify microstructure heterogeneity effects on overall cell performance. (Q1, FY 2019; Completed)
2. Create localized ionic conductivity maps on at least two candidate materials. (Q2, FY 2019; In progress)
3. Create design package for commercialization of the conductivity probe including associated control and computing hardware. (Q3, FY 2019; In progress)
4. Demonstrate the capacity of the smoothed particle hydrodynamics drying model to investigate the physics of the drying process for further optimization. (Q4, FY 2019; In progress)

Progress Report

Milestone 1 Completion. Li-ion battery electrodes possess local variations in microstructure that lead to variations in mechanical, transport, and kinetic properties. These variations, referred to as electrode heterogeneity, can adversely affect battery performance and lifetime as a result of non-uniform current, temperature, SOC, and aging. A combination of a Newman-type and equivalent circuit models was used to investigate the effect of heterogeneous electrodes in terms of non-uniform ionic resistance and active material loading on the performance and life of a baseline Li-ion cell.

In the model, the electrodes consisted of three parallel equal-area regions, each representing different internal resistances: high/hot, medium, and low/cold. These variations in the positive and negative electrodes were examined according to whether the different resistances were aligned or misaligned. The results for different charge and discharge rates show that higher rates increase non-uniformities of dependent properties such as temperature, current density, positive and negative electrode SOC, and charge and discharge capacities, especially in the case of charging.

Moreover, the results suggest that degradation takes place faster and to a higher degree during charging due to more non-uniformity compared to results from comparable discharging cases. In addition, for the discharging cases, the results show that the misaligned active material loading case has more negative effects on the cell performance and lifetime. In this case, the results suggest that high degradation takes place during discharge in the negative electrode.

Figure 36 shows the aligned resistances case at 5C charge. Sensitivity analysis for this case shows that structural heterogeneity affects charge capacity to the greatest extent and temperature to the least extent.

In conclusion, adequate homogeneity is needed in electrodes to enable fast charging capability with a good cycle life. Additional work is needed to experimentally confirm these model results.

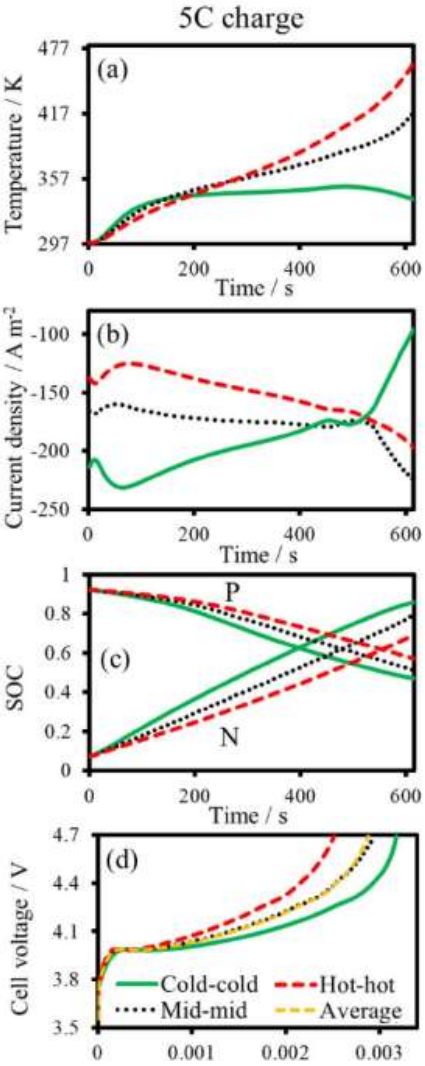

Figure 36. Temperature, current, and positive and negative electrodes states of charge (SOC) distributions, along with charge curves for the charging aligned resistances case (hot-hot, middle-middle, and cold-cold).

Patents/Publications/Presentations

The project has no patents, publications, or presentations to report this quarter.

Task 3.3 – Understanding and Strategies for Controlled Interfacial Phenomena in Lithium-Ion Batteries and Beyond

(Perla Balbuena and Jorge Seminario, Texas A&M University; Partha Mukherjee, Purdue University)

Project Objective. The project objective is to evaluate and characterize interfacial phenomena in lithiated silicon and Li-metal anodes and to develop guidelines for potential solutions leading to controlled reactivity at electrode/electrolyte interfaces of rechargeable batteries using advanced modeling techniques based on first principles.

Project Impact. Understanding SEI growth on constantly evolving silicon surfaces and on highly reactive Li-metal surfaces is expected to allow definition of the electrolyte properties required in high-performance cells. Strategies to control the silicon anode instability and pulverization issues and the well-known safety and short effective lifetimes of Li-metal anodes will be developed by tuning the electrolyte composition, structure, dynamic, and stability, as well as that of the electrode morphology and interactions with the electrolyte, based on multiple characterizations of interfacial phenomena.

Approach. A comprehensive multiscale modeling approach, including first-principles *ab initio* static and dynamics, classical MD, and coarse-grained mesoscopic models, will focus on the roles of the electrolyte's chemical, structural, and dynamical properties and of the electrode micro- and nano- structure on the formation and evolution of the SEI layer and the associated electrochemical performance on silicon and on Li-metal anodes.

Out-Year Goals. Work will progress toward characterizing lithiation and SEI formation at silicon surfaces as well as the subsequent cracking and reforming events under the most realistic modeling conditions. Similarly, the project will investigate electrolyte effects on reactivity and dendrite formation in Li-metal surfaces. The project aims to capture how the chemistry of the various electrolyte components (mainly liquids, but also solid polymers and gels) affects the main issues that influence the electrode performance.

Collaborations. This project funds work at Texas A&M University (TAMU). Other contributors include Prof. G. Somorjai (UC Berkeley), Prof. S. Yassar (UIC), and Dr. V. Murugesan (PNNL).

Milestones

1. Complete analysis of anode macroscopic effects during cycling. (Q1, FY 2019; Completed)
2. Complete study of improved electrolytes for silicon anodes. (Q2, FY 2019)
3. Complete study of improved electrolytes for lithium anodes. (Q3, FY 2019)
4. Complete evaluation of alternative charging strategies for lithium anodes. (Q4, FY 2019)

Progress Report

Macroscopic Effects during Cycling of Silicon and Lithium Metal Anodes. Silicon anodes exhibit massive volumetric changes with cycling (lithiation and delithiation), resulting in particle and SEI cracking and exposure of fresh anode surface for the formation of parasitic SEI. Figure 37a-b correlates the damage map in silicon anodes with surface film for crystalline silicon exhibiting multiphase transport with phase segregation and amorphous silicon exhibiting single-phase transport. Clearly, it demonstrates the need for going toward amorphous silicon to mitigate the fracture tendencies.

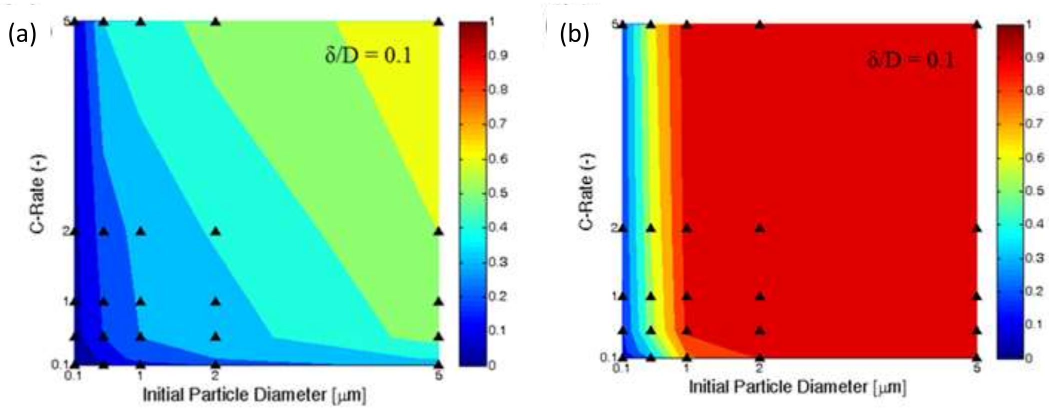

Figure 37. Damage map (see color scale for damage intensity) for variation of particle size and C-rate with film thickness (δ) to particle size (D) ratio, for (a) amorphous silicon with film and (b) crystalline silicon with film. Crystalline silicon exhibits much more severe fracture as compared to amorphous silicon with increase in particle size and C-rate.

Crystalline silicon particles beyond 100-200 nm show severe fracture at all C-rates, while amorphous silicon particles can sustain reasonably well up to 1-2 µm. Conversion of crystalline silicon to amorphous silicon is reported to occur over the first few lithiation-delithiation cycles. The team suggests extremely slow lithiation and delithiation (<C/100) of crystalline silicon particles with mid-ranged particle size (~ 1-2 µm) for the first few cycles to enable complete conversion into amorphous silicon with minimal fracture. The decreased fracture tendency of amorphous silicon is a desirable characteristic and then can then be utilized to cycle the electrodes at higher C-rates. For amorphous silicon, the damage density for 1-2 µm particles lies within the reasonable limit (< 0.2) for C-rates up to 2C. Hence, the team recommends an upper limit for C-rate of 2C for cycling of amorphous silicon particles. Thus, fracture inside the silicon active material can be minimized using the above cycling technique. However, surface film rupture is inevitable for both amorphous and crystalline silicon owing to the high volumetric expansion of the silicon particle and brittle mechanics of the film. Consequently, capacity fade due to SEI film breakdown cannot be mitigated unless surface film modification is done to obtain elastomeric films. A small improvement in the fracture characteristics is obtained by decreasing the Young's modulus of the brittle film layer; however, it is not enough to resolve the capacity deterioration of silicon electrodes due to film breakage and resulting fresh SEI formation.

For Li-metal anodes with SEI layer that exhibits a complex structure, comprising various components, spatial heterogeneities can exist that can affect the Li-ion transport and reduction at the Li-metal surface. The results of the mesoscopic model demonstrate that the maximum stress shows rapid increase with SEI inhomogeneities, while it has a relatively weak dependence on the electrochemical Biot number (ratio between diffusion resistance and interfacial charge transfer resistance) and, correspondingly, current density. For a fixed current density, increased SEI inhomogeneity facilitates the growth of lithium dendrite, as shown also with the atomistic models. For a specific SEI heterogeneity, the growth of lithium dendrite also shows direct correlation with current density increase. Maximum stress scales strongly with SEI inhomogeneity and shows mild increase with current density causing SEI fracture.

Patents/Publications/Presentations

Publications

- Galvez-Aranda, D. E.; A. Varma, K. Hankins, J. M. Seminario, P. P. Mukherjee, and P. B. Balbuena. "Chemical and Mechanical Degradation and Mitigation Strategies for Si Anodes: Multiscale Modeling." *Journal of Power Sources*. Under review.
- Tewari, D., and P. P. Mukherjee. "Mechanistic Understanding of Electrochemical Plating and Stripping of Metal Electrodes." Under review.

Presentations

- Americas International Meeting on Electrochemistry and Solid State Science (AiMES) 2018 Meeting, Cancun, Mexico (October 2, 2018): "Molecular Dynamics Simulations of Solid Electrolytes for Li-Ion Nanobatteries"; J. M. Seminario. Invited.
- Technische Universität, Braunschweig, Germany (October 25, 2018): "Analysis of New Materials for Rechargeable Batteries"; J. M. Seminario. Invited seminar.
- Technische Universität, Braunschweig, Germany (October 23, 2018): "Solid-Electrolyte-Interphase Formation and Effects on Li Metal Anodes"; P. B. Balbuena. Invited seminar.
- Battery500 Seedling Projects Meeting Review, Berkeley, California (August 1, 2018): "Identification of Efficient and Stable Solid-Solid Electrochemical Interfaces for Li-S Batteries"; P. B. Balbuena.
- Ulm University, Ulm, Baden-Württemberg, Germany (November 8, 2018): "Addressing Main Issues of Lithium-Sulfur Batteries"; J. M. Seminario. Invited talk.
- Universidad de Santiago de Chile, Santiago, Chile (December 5, 2018): "Nanobatteries for the Development and Analysis of New Materials for Rechargeable Batteries"; J. M. Seminario. Invited talk.
- AiMES 2018 Meeting, Cancun, Mexico (October 2, 2018): "Mesoscale Understanding of Lithium Electrodeposition"; P. P. Mukherjee. Invited.

Task 3.4 – Electrode Materials Design and Failure Prediction
(Venkat Srinivasan, Argonne National Laboratory)

Project Objective. The main objective of this project is development of computational models for understanding the various degradation mechanisms for next-generation Li-ion batteries. This year's goal is to use the continuum-based mathematical model to (1) investigate interfacial stability between electrodes and ceramic-based SSEs, and (2) experimentally measure and understand the impedance observed at the cathode/SSE interface. Ceramic-based SSEs are expected to enable high energy density and liquid-free, safe, next-generation Li-ion batteries. Li-metal anodes should be incorporated due to their substantially larger specific capacity, as compared to present day graphite-based anodes. During deposition, lithium dendrite growth through the SSEs and subsequent short circuit has been a major issue, limiting the successful implementation of SSEs. Similarly, on the cathode side, diffusion of TMs into the SSEs and delamination between cathode and SSE lead to increased interfacial resistance. The developed computational model will be used to investigate the impact of microstructural (grain size), physical (mechanical stiffness), and transport (conductivity) properties of the SSE on the overall interfacial degradation observed at both the cathode and anode sides. Due to the SOC-dependent electrochemical and mechanical properties of the cathode, an attempt will be made to experimentally measure the SOC dependent impedance at the cathode/SSE interface. The main focus of this project will be to elucidate the interfacial issues, observed at both anode and cathode sides, and devise strategies to enable the successful implementation of SSE in next-generation Li-ion batteries.

Project Impact. Findings from this research will give a better understanding of the factors, at the cathode/SSE interface, limiting the cycle life of solid-electrolyte-based Li-ion batteries. These results will help to enable incorporation of cathode particles within SSEs.

Project Approach. The approach used here is to develop mesoscale models, based on continuum modeling, to describe the critical processes in the materials, and combining them with electrochemical, microscopic, and spectroscopic data to ensure parameter estimation and model validation. The model is then used to provide insights on the impact of material properties on performance and life, and guidance for design of new materials.

Out-Year Goals. At the end of this project, a computational framework will be presented that is capable of estimating delamination and impedance at cathode/SSE interface.

Collaborations. The project has no collaborations this period.

Milestones

1. Investigate impact of grain-interior(GI)/grain-boundary(GB) microstructure on overall dendrite growth observed at SSE/lithium interface. (Q1, FY 2019; Completed)
2. Analyze effect of delamination at the cathode/SSE interface as a mode of degradation. (Q2, FY 2019; In progress)
3. *Go/No-Go Decision*: Estimate SOC-dependent impedance at cathode/SSE interface. If not possible, proceed with impedance measured at fixed SOC. (Q4, FY 2019)

Progress Report

Investigate Impact of GI/GB Microstructure on the Overall Dendrite Growth Observed at Li/SSE Interface. Even though the mechanical stiffness of the ceramic-based electrolytes is very high, lithium dendrite growth through SSEs has been one of the major bottlenecks preventing their widespread implementation in next-generation Li-ion batteries. Inhomogeneous GI/GB microstructure, variation in conductivity through the two different phases, and difference in their elastic stiffness—all of these factors contribute to the overall non-uniform current distribution observed at the Li/SSE interface. The majority of experimental studies and DFT-based, lower-length-scale calculations indicate that conductivity of lithium through the GB region is smaller in magnitude than the GI. However, several experimental observations reported enhanced lithium deposition at the GB regions. Using the concept of mechanical-stress-induced change in electrochemical potential, the team provides an explanation for why current focusing at the GB is possible in spite of slower ionic transport. Following the pioneering work conducted by Monroe and Newman (*Journal of the Electrochemical Society* 151 (2004): A880), the team derived a modified version of the Butler-Volmer equation that takes into account the stress-induced change in electrochemical potential, and is also applicable to ceramic-based, single-ion-conducting SSEs. The magnitude of mechanical stress has been estimated assuming deposition of a monolayer of lithium at the Li/SSE interface. Since newly deposited lithium metal pushes the existing metal electrode and SSE in opposite directions, compressive stress evolves in both of them. The modified Butler-Volmer equation indicates that higher compressive stress prevents lithium deposition. Since the elastic modulus of the GB region is a few orders of magnitude smaller than the elastic modulus of GI, lower compressive stress develops there. This results in enhanced lithium deposition at the GBs. Smaller magnitude of GB conductivity tends to minimize the current focusing, but net current density at GB still remains higher than the GI. Figure 38a-b demonstrates two different GI/GB microstructures that have been used to analyze the effect of grain size on the current focusing. Figure 38c clearly depicts that smaller sized grains, with multiple GBs, lead to uniform distribution of currents and reduced focusing at GBs.

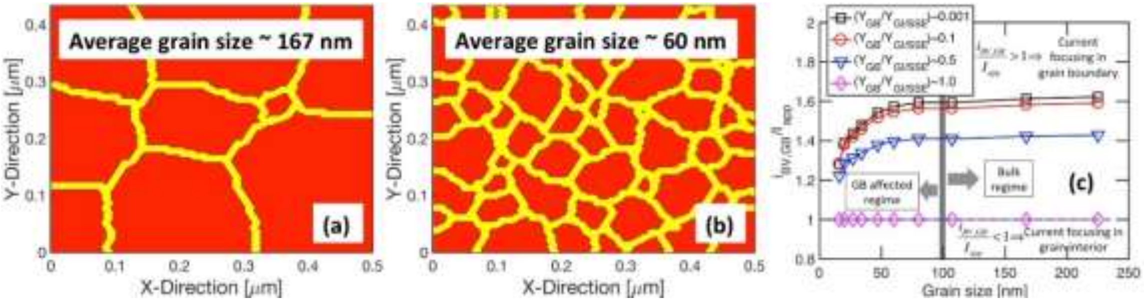

Figure 38. (a) Grain-interior/grain-boundary (GI/GB) microstructure with average grain size of 167 nm. (b) GI/GB microstructure with average grain size of 60 nm. (c) Current focusing observed at GB region plotted with respect to grain size. Decrease in grain size helps to distribute the current and reduce the current focusing observed at the GB regions.

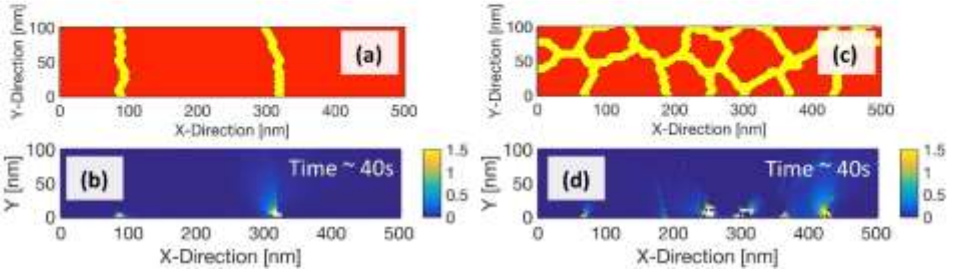

Figure 39. (a) Grain-interior/grain-boundary (GI/GB) microstructure with larger grains (LG). (b) Strain energy (SE) and cracking at GB for LG. (c) GI/GB microstructure with small grains (SG). (d) SE and cracks at GB for SG.

Figure 39 clearly demonstrates that enhanced lithium deposition at the GB region has the potential to initiate crack fronts, which can propagate through the brittle ceramic SSE and eventually short the cell. This provides a good explanation of enhanced lithium deposition and crack initiation at GB region. Development of a computational model and elucidation of lithium dendrite growth in ceramic-based SSEs satisfies the milestone for this quarter.

Patents/Publications/Presentations

The project has no patents, publications, or presentations to report this quarter.

Task 3.5 – First-Principles Calculations of Existing and Novel Electrode Materials (Gerbrand Ceder, Lawrence Berkeley National Laboratory)

Project Objective. Solid-state batteries are promising to achieve high energy density. The project objective is to determine the design principles needed to create SSEs with high Li-ion conductivity while also achieving stability against common Li-ion cathodes and Li-metal anodes.

Project Impact. The project will lead to understanding of the factors that control Li-ion motion in crystalline and amorphous solids and develop strategies to create stable interfaces against lithium metal and high-voltage cathode materials. The understanding of such processes is necessary to determine design principles to develop reliable all solid-state batteries.

Approach. High-throughput computation method is used to screen suitable solid electrolyte with high electrochemical stability and high ionic conductivity, by incorporating Nudged Elastic Band (NEB) and AIMD method. Meanwhile, DFT is used to calculate bulk elastic constants of materials, surface energies, and interface de-cohesion energies of grain boundaries. Thermodynamic interface stability is assessed from *ab initio* computed grand potential phase diagrams in which the lithium voltage can be controlled. Kinetic limits for solid electrolyte decomposition are assessed by topotactic lithium insertion and removal from the solid electrolyte.

Out-Year Goals. Future goals include the following: (1) gain insight into what creates high Li-ion conduction in sulfide and oxide solids, and (2) develop stable, processable solid-state conductors that can be applied in all solid-state batteries.

Collaborations. There are no current collaborations.

Milestones

1. Modeling of the Li_2S-P_2S_5 phase diagram for SSEs: solid phases correctly modeled. (Q1, FY 2019; Completed)
2. Modeling of the Li_2S-P_2S_5 phase diagram for SSEs: include correct modeling of amorphous phase. (Q2, FY 2019)
3. Model Li-ion conductivity in amorphous LPS (Li-P-S) systems and glass ceramics. (Q3, FY 2019)
4. Develop understanding on which structural and compositional features make LPS an excellent ionic conductor. (Q4, FY 2019)

Progress Report

The strongly constrained and appropriately normed (SCAN) meta generalized gradient approximation (GGA) exchange correlation functional[1, 2] has been applied to construct the phase diagram within the Li_2S-P_4S_7-S compositional space, as shown in Figure 40. The result agrees well with experiments showing that all ternary phases known to be metastable are also metastable in this diagram. As suggested by the computed phase diagram, $Li_4P_2S_6$ and Li_3PS_4 are the only two stable phases at 0K, while the remaining five metastable phases are marked by red points. To achieve accurate phase stability predictions in this chemical space, it was important to use novel DFT functionals. Figure 41 compares formation energies from the novel SCAN approach with the more classic GGA Perdew, Burke and Ernzerhof (PBE) functional. In comparison, the SCAN functional performs superiorly in several aspects.

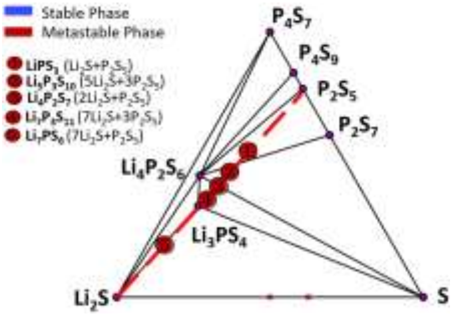

Figure 40. Calculated Li_2S-P_4S_7-S phase diagram using strongly constrained and appropriately normed (SCAN) functional.

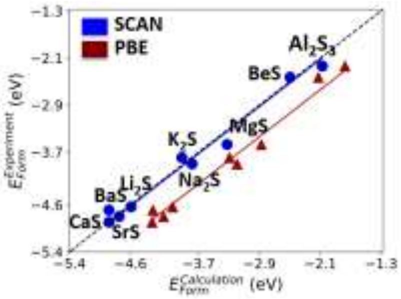

Figure 41. Comparison of binary sulfide formation energy calculated from Perdew, Burke, and Ernzerhof (PBE) and strongly constrained and appropriately normed (SCAN) with experimental measurement.

The binary sulfide formation energy calculated by PBE has a systematic error of -0.54 eV with respect to experiment. This problem is greatly corrected by SCAN, which gives a systematic error of only -0.03 eV, thus indicating that SCAN captures the bonding strength of sulfur with non-TM atoms much better. Meanwhile, the data in Figure 41 also indicate there is no need for sulfide correction when using the phase diagram or energetic data calculated from SCAN, which has been a problem issue for previous functionals such as PBE.

The SCAN functional also performs better in ranking the Li-P-S polymorphs. Taking Li_3PS_4 as an example, the PBE predicted ground state has P $\bar{4}$ 3m symmetry. This phase is an unusual hypothetical structure with a large void in the middle. This PBE-predicted ground state is inconsistent with the synthesis report in literature, since the real ground state of Li_3PS_4 is the γ phase with $Pmn2_1$ space group. The latter is correctly captured by the SCAN functional. The deviation of PBE prediction from experimental results may be because the PBE functional always over-stabilizes surfaces.[3] The SCAN functional also properly captures finite temperature variations in phase stability. Even though $Li_7P_3S_{11}$ and $Li_4P_2S_7$ are both metastable phases as shown in the 0K phase diagram, they become thermodynamically stable above 420K and 1010K as a result of vibrational entropy effects (Figure 42). These results are consistent with experimental synthesis reports.[4]

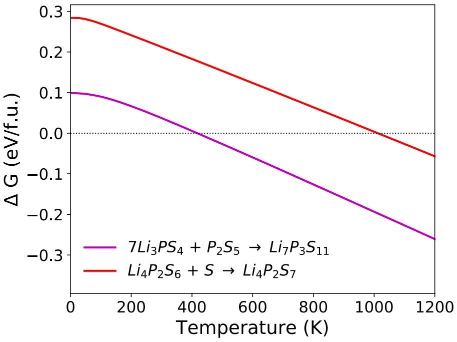

Figure 42. ΔG versus T for $Li_7P_3S_{11}$ and $Li_4P_2S_7$.

[1] Sun, et al. *Physical Review Letters* 115 (2015): 036402.

[2] Kitchaev, et al. *Physical Review B* 93 (2016): 045132.

[3] Patra, et al. *Proceedings of the National Academy of Sciences* (2017): 201713320.

[4] Dietrich, et al. *Journal of Materials Chemistry A* 34 (2017): 18111-18119.

Patents/Publications/Presentations

The project has no patents, publications, or presentations to report this quarter.

Task 3.6 – Dendrite Growth Morphology Modeling in Liquid and Solid Electrolytes
(Yue Qi, Michigan State University)

Project Objective. The project goal is to develop a validated model to predict lithium dendrite morphology evolution in both liquid and solid electrolytes during electrodeposition and stripping to accelerate the adoption of Li-metal electrodes in current and emerging battery technologies. To achieve this goal, the project has four objectives: (1) formulate a general framework that captures the electrochemical-mechanical driving forces for lithium morphology evolution; (2) consider the role of the nm-thin SEI in liquid electrolytes as well as the microstructures of μm-thick solid electrolytes for lithium morphology evolution; (3) connect micron-scale phase-field models and atomic-scale DFT-based simulations via parameter- and relationship-passing to predict lithium dendrite nucleation and growth kinetics and morphology; and (4) validate the key input parameters and main conclusions of the multi-scale model as new capabilities are being developed step-by-step.

Project Impact. This atomically informed, fully coupled, electrochemical-mechanical dendrite morphology evolution model will allow the project to design the desired properties of artificial SEI coatings, the microstructure of solid electrolyte materials, and the corresponding battery operating conditions, so as to avoid dendrite growth during cycling. It will accelerate design of durable and safe lithium anodes for Li-S, Li-air, and all-solid Li-ion batteries. Thus, it directly impacts emerging technologies, such as Li-S, Li-air, and all-solid Li-ion batteries, which aim to meet the DOE target of the high-energy-density battery cells (> 350 Wh/kg) for EV applications and to push the cost below \$100/kWh$_{\text{use}}$.

Approach. A multiscale model approach is taken to connect micron-scale phase-field models and atomic-scale DFT-based simulations via parameter- and relationship-passing.

Out-Year Goals. The second-year goal is to establish the model to simulate metallic lithium precipitation in solid electrolytes while further developing the understanding of lithium dendrite growth in liquid electrolytes. To reach this goal, mechanical and electrochemical driving forces for lithium dendrite growth in solid electrolytes will be coupled in phase-field model, while DFT is used to address the lithium plating tendency in various solid electrolyte and coating materials. Validation of the model will come from experiments to correlate the distinctive transport properties of artificial SEI layers with their impact on lithium dendrite morphology.

Collaborations. This project collaborates with UMD, Sandia National Laboratories (SNL), PNNL, University of Arkansas, and University of Houston.

Milestones

1. Identify an ideal microstructure of LLZO to avoid lithium dendrite growth. (Q1, FY 2019; It was predicted a coating layer, such as LiPON, between the Li/LLZO, will be more efficient in resisting lithium dendrite. A *Go* decision was made to experimentally vary this prediction.)
2. Develop a fully coupled Li/SEI/liquid electrolyte dendrite morphology model. (Q2, FY 2019; In progress)
3. Illustrate the relationship between Li/SEI interface roughness, adhesion, and dendrite morphology in a liquid electrolyte. (Q3, FY 2019; In progress)
4. Determine the effect of multicomponent SEI layer on dendrite morphology in a liquid electrolyte. (Q4, FY 2019; In progress)

Progress Report

Solid Electrolyte. To assess the lithium dendrite resistance in a solid electrolyte, β-Li_3PS_4, cubic-LLZO, $Li_{1.17}Al_{0.17}Ti_{1.83}(PO_4)_3$ (LATP), and an ALD LiPON form (Li_2PO_2N) were investigated with DFT calculations. The team believes the excess electrons located on the surface will likely reduce Li-ions to metallic lithium. Based on this hypothesis, the ranking of the resistance to lithium dendrites for these materials would be Li_2PO_2N > β-Li_3PS_4 > LATP > LLZO. The phase field model further incorporated the electrochemical-mechanical coupled Li-dendrite growth in an open crack and a GB (Figure 43). A design map was generated to demonstrate the impact of transport and mechanical properties (including GB adhesion energies, elastic moduli, excess e^- density, and Li^+ conductivities). Figure 43 shows that the excess electrolyte density on the crack surface and GB inside the solid electrolyte causes tremendously larger dendrite amount and deeper depth due to the isolated dendrite nucleation and growth.

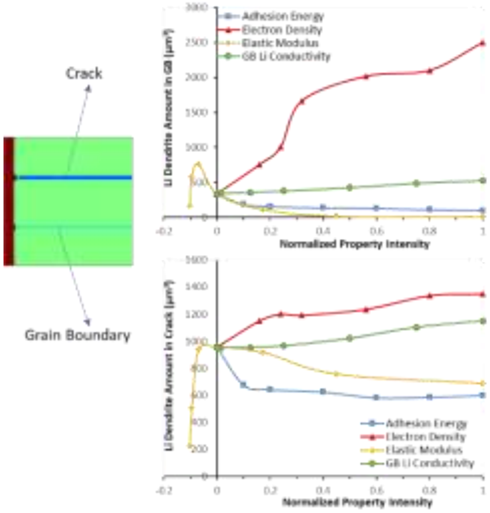

Figure 43. The lithium dendrite total amount in grain boundaries (GBs) and cracks.

Table 1. Material properties of solid electrolyte materials.

	Shear modulus (GPa)	Fracture energy (J/m^2)	Reduction potential vs. Li (V)	Bulk bandgap (eV)	Surface bandgap (eV)	Location of excess electrons
c-LLZO	59	1.72	0.05	4.04	1.87	Surface
β-Li_3PS_4	6	0.38	1.71	2.40	2.15	Bulk
LATP	55.6	0.88	2.16	2.08	0.88	Bulk
Li_2PO_2N	30	0.92	0.87	5.29	3.76	Bulk

Liquid Electrolyte. Based on the above analysis, varying the microstructure of the SE will not be as effective as a coating layer to prevent lithium dendrite growth. This strategy is similar to controlling the SEI layer on lithium in the liquid electrolyte. The team has demonstrated experimentally that, in traditional carbonate electrolyte, the new Li_2S formed in the inner part of the SEI layer by introducing electrolyte additive 1,2-propyleneglycol sulfite (PS) was more beneficial for the stability of SEI compared with Li_2O. DFT calculations show that Li_2S is mechanically more stable for preventing crack formation during SEI formation, based on volume mismatch, and Li_2S tends to trap fewer electrons on its fractured surface than Li_2O. Therefore, Li_2S can resist electron leakage through the SEI and prevent Li-electrolyte side reactions more efficiently than Li_2O. The electrochemical performance of a full cell ($LiFePO_4$ pairing with 20 µm lithium foil in 1 M $LiPF_6$-EC/DEC and 1 M $LiPF_6$-EC/DEC/ 5 wt% PS) demonstrated the capacity retention due to PS.

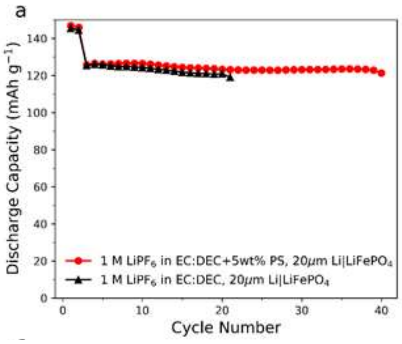

Figure 44. Cycle life of Li-$LiFePO_4$ full cell with EC/DEC electrolytes with and without the PS additives.

This confirmed that coating layer design is efficient in preventing lithium dendrite growth in both liquid (Li_2S) and solid electrolytes (ALD LiPON). Therefore, a *Go decision* was made this quarter.

Patents/Publications/Presentations

Publications

- Li, G., Z. Liu, Q. Huang, Y. Gao, M. Regula, D. Wang, L-Q. Chen, and D. Wang. “Stable Metal Anodes Enabled by Electrokinetic Effects in High-Zeta-Potential Porous Structures.” *Nature Energy* 3 (2018): 1076.
- Li, Y.S., and Y. Qi. “Energy Landscape of the Charge Transfer Reaction at the Complex Li/SEI/Electrolyte Interface.” Submitted to *Energy & Environmental Science*.
- Xu, J., H.-K. Tian, J. Qi, Y. Qi, Q. Zhang, and X. Xiao. “Mechanical and Electronic Stabilization of Solid Electrolyte Interphase with Sulfite Additive for Lithium Metal Batteries.” To be submitted to *Journal of Environmental Sciences*.
- Liu, Z., Y. Li, Y. Ji, Q. Zhang, X. Xiao, Y. Yao, L.-Q. Chen, and Y. Qi. “Atomically-Informed Phase-Field Modeling of Li and Mg Electrodeposition Morphologies.” In preparation.

Task 3.7 – First-Principles Modeling and Design of Solid-State Interfaces for the Protection and Use of Lithium-Metal Anodes
(Gerbrand Ceder, University of California at Berkeley)

Project Objective. The project objective is to determine the design principles that control the solid electrolyte/lithium electrode interfaces by determining the reaction products stemming from pairing solid electrolytes and lithium metal. The project will conduct rigorous analysis based on computing electrolyte phase-diagrams closed and open to lithium. Li-ion transport properties in bulk electrolytes and interfacial products will be assessed through AIMD and NEB calculations. Simultaneously, a robust framework will be developed to identify factors controlling lithium dendrite propagation within solid electrolytes and interfacial products by accounting for irregularities, defects, and GBs, through a model that includes elements of fracture mechanics, thermodynamics, and electrochemistry.

Project Impact. The project will lead to understanding of the complex evolution of lithium metal/SEI during electrochemical cycling. The understanding of this process is necessary to determine design principles to develop reliable all solid-state batteries.

Approach. By incorporating NEB and AIMD methods, high-throughput computation is used to screen candidate solid electrolyte with high electrochemical stability and high ionic conductivity. DFT is used to calculate bulk elastic constants of materials, surface energies, and interface de-cohesion energies of GBs; continuum theory (elastic-plastic-fracture mechanics) is used to assess the resilience of solid electrolytes and grain/particle boundaries toward lithium dendrite growth and propagation. The finite element method is used to couple several physical processes, including electrochemical deposition, ionic diffusion, thermal expansion, and mechanical contacting.

Out-Year Goals. The out-year goals include the following: (1) obtain design criteria for solid electrolytes that can resist unstable lithium propagation by computing elastic properties, surface energies, and decohesion energies, and (2) adapt fracture mechanics models describing crack propagation to lithium dendrite propagation in different scenarios.

Collaborations. There are no collaborative activities this quarter.

Milestones

1. Development of high-throughput framework to screen SSE materials based on phase stabilities. (Q1, FY 2019; Completed)
2. Adapt fracture models that describe crack propagation in materials to lithium dendrite propagation in perfect crystal with cracks. (Q2, FY 2019; On target)
3. Adapt fracture models that describe crack propagation in materials to lithium dendrite propagation in perfect crystal with GBs. (Q3, FY 2019; On target)
4. Adapt fracture models that describe crack propagation in materials to lithium dendrite propagation in pressed/porous electrolyte. (Q4, FY 2019; On target)

Progress Report

Figure 45. Solid electrolyte materials listed by conductivity.

High Throughput Screening of Stable Solid Electrolyte Materials

By integrating the project work on determining chemical and electrochemical stability windows of electrolyte materials against lithum metal, the team has developed a high throughput screening framework that has allowed them to explore material/chemical space in search of promising materials. Furthermore, by including Li-ion conductivity calculations in the framework, the team has been able to search for both stable and fast lithium conductors. Broadly, the screening framework consists of computing phase stability from multicomponent phase diagrams, chemical/electrochemical interface stability versus lithium, and Li-ion conductivity. Using the developed framework, the team has been able to explore candidate materials including variants of commonly used materials such as oxides and sulfides, in addition to less common chemistries involving phosphates, nitrides, and borates, as shown in Figure 45.

Deposition and Induced Stress States at Crack Tips

The project has developed a theoretical model to account for deposition at sharp cracks. This model accounts for current focusing effects at cracks and allows determination of the corresponding stress state. The current density inhomogeneity from sharp tips can occur additionally to that from interfacial contact loss, as the team has determined and reported previously. This becomes yet another source for high local deposition currents that can lead to higher stress conditions than depositions at flat interfaces.

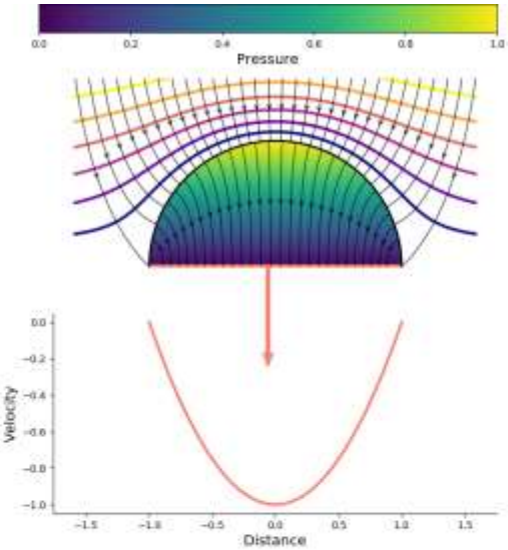

Figure 46. Crack tip normalized ion flux, potential, and pressure field.

The theoretical model quantifies the local distortion effects of sharp interfaces on potential, flux lines, and stress increases. Figure 46 shows normalized modeling results for local fields at a sharp defect. Furthermore, the study shows that deposition inhomogeneity at crack can lead to stress states with large deviatoric components that force deposited metal to plastically yield. Hence, the team obtained yet more evidence for the critical importance of lithium yielding and plastic properties.

Furthermore, the role of high ionic conductivity is an important aspect in determined possible stress states. High ionic conductivity can exacerbate current *hotspots*, but it also plays a role in potential ion redistribution, which becomes another stress relief mechanism present in the theoretical study. Thus, continued development of this theoretical framework will allow the team to determine critical values for material properties (that is, electrolyte conductivity, electrolyte elasticity and fracture toughness, and lithium yield) that play an important role in lithium propagation and cell.

Patents/Publications/Presentations

The project has no patents, publications, or presentations to report this quarter.

Task 3.8 – Large-Scale *Ab Initio* Molecular Dynamics Simulations of Liquid and Solid Electrolytes (Lin-Wang Wang, Lawrence Berkeley National Laboratory)

Project Objective. The project objective is to use AIMD simulations and other computational approaches to study the discharging mechanism in Li-S battery, especially for polysulfide interaction with liquid electrolyte solvent molecules, and cathode materials, as well as lithium diffusion mechanisms in various systems. The long-term goal is to use such theoretical understanding to provide guidance to develop better electrolyte and cathode systems to overcome the bottlenecks that prevent commercialization of the Li-S battery.

Project Impact. Making the Li-S battery a commercial reality will have a major impact on society and also help to realize the VTO goal of 500 km per charge for EV. However, the nature of chemical reaction makes it different from the traditional intercalation-based Li-ion battery. The molecular nature of Li_2S_n also allows solvation in the electrolyte. To address these problems, it is essential to have fundamental studies and understandings of the underlying mechanisms. The theoretical simulation can also play an important role in discovering and designing new cathode materials.

Approach. One major issue is solvation of Li_2S_n molecules in the electrolyte. The project seeks to solve this problem by both understanding the Li_2S_n-electrolyte interaction and discovering better cathode materials for optimal Li_2S_n-cathode binding. More specifically, it aims to develop reliable methods that combine classical force field (CFF) simulations with *ab initio* calculations to study the thermal dynamic properties of Li_2S_n in different electrolytes, as well as the interactions with different species within the electrolytes. It will also study Li_2S_n interaction with different cathode materials, especially for 2D cathode materials comprised with light elements in the right-upper corner of the periodic table. The goal is to have sufficient binding energy between the Li_2S_n molecules and the cathode material, so that, thermodynamically, the Li_2S_n will not be dissolved in the electrolyte. To study the Li_2S_n-electrolyte interaction, the project must accurately calculate the molecule entropy inside the solvent, which is a rather challenging task. It plans to use the bicanonical method to carry out the calculation. To design new cathodes, the project plans to focus on lightweight 2D materials. Genetic algorithm combined with DFT will be used to explore the structure and morphology of the Li_2S_n cluster on top of the 2D material. The stability of the solid electrolyte will be investigated by studying the surface reaction of such electrolytes.

Out-Year Goals. In outgoing years, the project will further develop the computational methods for more accurate entropy and interaction energy calculations for the electrolyte. This is a critical capability for studying the battery system. The project will also explore different cathode materials and morphologies. In particular, there is a vast space to explore using 2D materials as Li-S battery cathodes. Stability of the solid electrolyte is another topic to be investigated.

Collaborations. The project will collaborate with G. Liu and Y. Cui for cathode design. It has also collaborated with Prof. F. Pan of Beijing University for lithium battery research in general.

Milestones

1. Develop reliable ways to calculate the diffusion barrier of lithium in either crystal or amorphous structure. (Q1, FY 2019; Completed)
2. Continue calculation of Li_2Sn/cathode binding energies, and phase diagrams, discovering new adequate cathode materials and morphologies. (Q2, FY 2019; Initiated)
3. Investigate the solid electrolyte, its pathways and surface stabilities, and electrolyte/anode interface. (Q3, FY 2019)
4. Develop method to calculate Li-ion chemical energy in liquid electrolyte with *ab initio* calculations. (Q4, FY 2019)

Progress Report

The project has developed an algorithm that can help the team identify the lithium diffusion pathway in a solid electrolyte. Traditionally, the diffusion pathway can be theoretically investigated by *ab initio*, either through transition barrier calculations using the NEB method, or through direct AIMD. However, such simulations are expensive and thus cannot be used for high-throughput screening of the lithium transition pathway. To overcome this, the team has developed a fast empirical method that can be used to quickly reveal the lithium transition pathway in a solid electrolyte. The method is based on the bond valence (BV) method, in which the energy of lithium at a given spatial location is estimated by the charge neutrality principle. More specifically, the charge transfer between an anion and the lithium is assumed to depend exponentially on their distance with given parameters depending on the electron negativities and the radius of the anion. The total charge transfer from the lithium to neighboring anions should add up to 1. However, this method ignores the long-range Coulomb interactions, as well as the repulsion between lithium and other nearby positive cations in the system. This can lead to erroneous results. The team has thus added the Ewald energy on top of the BV model. This Ewald energy takes into account the Coulomb interactions, and the cation-Li repulsion. Proper mixing of the BV term and the Ewald energy term is used to take into account both effects. The team has used the resulting formula to evaluate the lithium transition path in any given crystal. They found that this BV-Ewald method provides a qualitatively similar path compared with *ab initio* results.

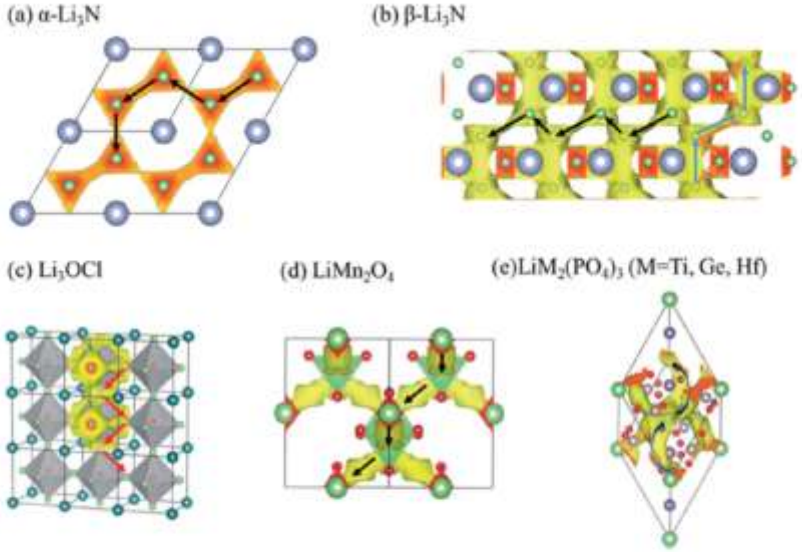

Figure 47. The lithium diffusion pathways for different solid electrolytes (the yellow isosurfaces), compared with the *ab initio* calculated transition pathways (the arrows).

Figure 47 shows the comparison between the BV-Ewald revealed lithium pathway and the *ab initio* calculated lithium transition pathways. They agree qualitatively with each other. Using this BV-Ewald method, the team has investigated 34 known SSEs. Although they are known as solid-state lithium electrolytes, not all of their paths are known. Using the BV-Ewald method, the team has identified some of them as 3D electrolyte (with all three directions connected with lithium channels), while others are 2D and 1D electrolytes (with only 2D or 1D channels).

In the future, the project plans to further improve this model to give the diffusion barrier height. Right now, the model still cannot provide adequate barrier height. Perhaps an analytical method like this can be combined with machine learning techniques to provide better predictive power for future solid electrolyte material. The goal is to use such tools to screen the possible candidates in the current crystal database. Using the BV-Ewald method, the lithium transition path can be generated in minutes, instead of days of simulations as for the *ab initio* method. This will make it possible for high-throughput screening.

Patents/Publications/Presentations

Publications

- Chen, D., J. Jie, M. Weng, S. Li, D. Chen, F. Pan, and L.W. Wang. “High Throughput Identification of Li Ion Diffusion Pathways in Typical Solid State Electrolytes and Electrode Materials by BV-Ewald Method.” *Journal of Materials Chemistry A* 7 (2019): 1300.
- Tsao, Y., M. Lee, E. C. Miller, G. Gao, J. Park, S. Chen, T. Katsumata, H. Tran, L. W. Wang, M. F. Toney, Y. Cui, and Z. Bao. “Designing a Quinone-Based Redox Mediator to Facilitate Li_2S Oxidation in Li-S Batteries.” *Joule*. https://doi.org/10.1016/j.joule.2018.12.018.

Task 3.9 – *In Operando* Thermal Diagnostics of Electrochemical Cells (Ravi Prasher, Lawrence Berkeley National Laboratory)

Project Objective. Effective heat dissipation in batteries is important for multiple reasons including performance, reliability, and safety. Currently, the thermal management of battery cells is provided at the system level by either forced air or liquid cooling, leading to reduced system-level energy densities and more failure-prone complex system designs. Furthermore, even given theoretically infinite system-level cooling applied to the external battery surface, peak temperature rise within a cell would still easily exceed acceptable threshold values due to the poor thermal transport properties within the cell itself. It has not yet been possible to thermally profile a real cell during operation to provide a spatially resolved map of heat transfer properties throughout the cell. The objective of this research is to create a metrology capable of spatially resolved *in operando* thermal property profiling, and then use this tool to reveal the largest thermal bottlenecks within a functioning Li-ion cell and create a complete materials-level cell thermal model.

Project Impact. The intrinsic thermal resistance of Li-ion cells is currently far higher than the theoretical value predicted by simply combining the known thermal properties of each macro component into an appropriate thermal model. The spatially resolved thermal transport property measurements from this project will reveal what key piece of information is missing. Preliminary data suggest that more than 75% of the total battery thermal resistance may be due to a single interface between the cathode and separator, previously unknown. An accurate understanding of the cell internal thermal transport is necessary to successfully optimize cell thermal performance to meet the challenges of extremely fast charging, mitigating thermal runaway, and improving battery performance, reliability, and safety.

Approach. To accomplish the project goals, the team will utilize two state-of-the-art thermal metrology techniques. They will build an in-house adapted 3*ω* technique to measure thermal transport properties throughout the bulk of a Li-ion cell while it is in operation, without affecting the operation of the cell. The 3*ω* system will work by using mm-scale sensors on the electrode current collectors to send variable-frequency thermal waves into the operational battery to quantitatively measure heat transport through different layers and interfaces. The team will also use the ultrafast optical time domain thermoreflectance (TDTR) technique to measure nanoscale thermal transport properties of constituent components of the cathode composite. They will then combine these results to create an "all-scale" accurate thermal model of the cell that—unlike existing models—agrees with the empirical measurements of cell thermal performance.

Out-Year Goals. In outgoing years, the project will design, build, and implement the adapted 3*ω* metrology. This will involve developing and testing the metrology itself along with accompanying theory, designing compatible battery samples, and finally applying the technique to live cells. The team will use the already built TDTR system at LBNL to measure epitaxially grown cathode materials provided by collaborators. Combined, this will provide enough data to construct and validate a realistic all-scale thermal model of the battery.

Collaborations. This project collaborates with two LBNL groups: V. Battaglia's for cell assembly for 3-Omega studies, and R. Kostecki's for pristine battery active material growths for TDTR studies.

Milestones

1. *Ex situ* high-accuracy measurements of thermal conductivity of individual battery components. (Q1, FY 2019; Completed)
2. Robust thermal model development. (Q2, FY 2019; On schedule)
3. *In situ* battery 3-omega thermal measurements from anode and cathode side. (Q3, FY 2019; On schedule)
4. Detailed *in operando* thermal measurements performed. (Q4, FY 2019; On schedule)

Progress Report

The project has successfully performed high-accuracy *ex situ* measurements of the thermal conductivity (*k*) of individual battery cathodes (NMC) and anodes, in both the dry and wet (with electrolyte) state. These measurements were necessary because a careful examination of the available literature revealed that currently available data for *k* of battery materials is sparse and highly variable and therefore unreliable. The team's 3-omega measurements require some of these values as inputs into the data analysis thermal model so as to measure other more important *in operando* thermal properties. Therefore, the team designed and built a new piece of equipment in-house to perform their own *ex situ* measurements of *k* of battery components. This new measurement system is a linear heat flow "Cut Bar" system (shown in Figure 48a), which was so named because the sample is placed in the middle of a "cut" copper bar through which heat flows. These Cut Bar measurements will be used to achieve more accurate analyses of the *in operando* 3-omega measurement data.

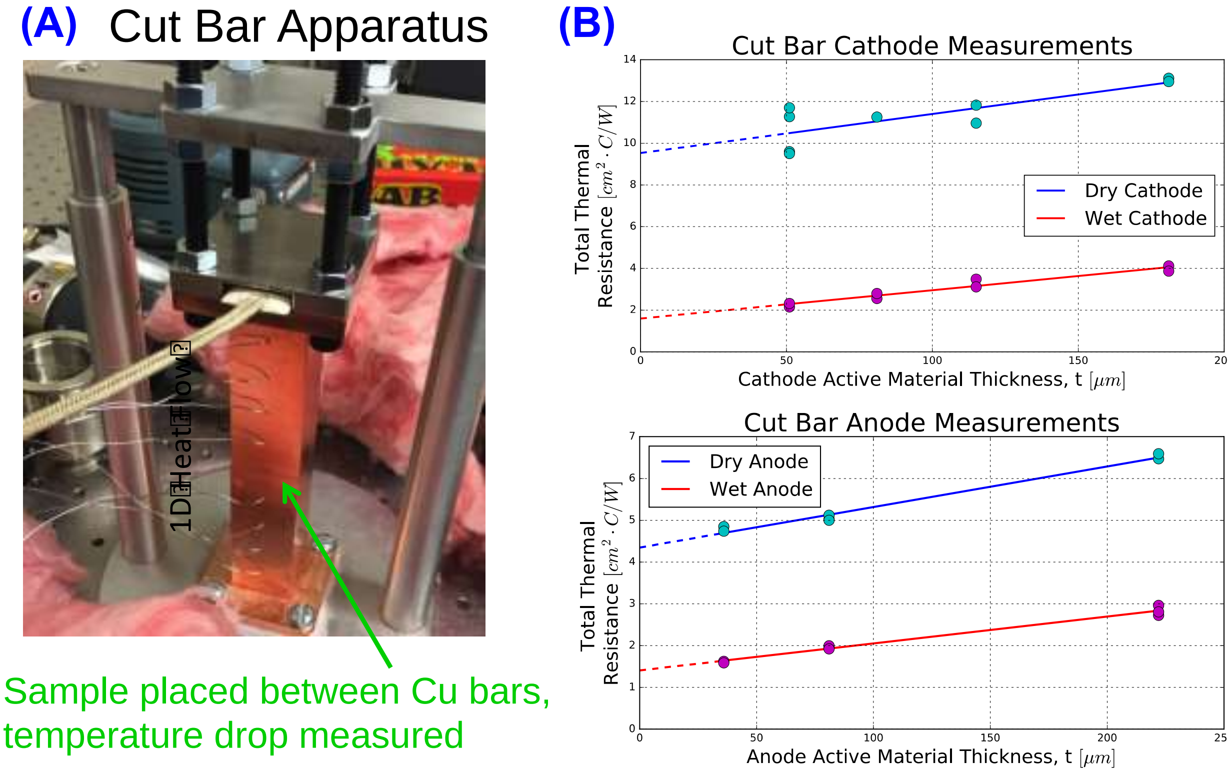

Figure 48. In-house built Cut Bar linear heat flow meter apparatus. (a) Picture of the new equipment. (b) Compilations of Cut Bar measurements on anodes and cathodes of varying thickness, both dry and wetted with delithiated electrolyte.

The Cut Bar works by sandwiching a sample between two highly thermally conductive copper bars. Thermocouples in the bars measure the temperature gradient from which both the heat flux and the temperature drop across the sample can be measured. The total thermal resistance at steady state can then be calculated. This includes both the thermal contact resistance between the sample and the bars as well as the thermal resistance of the sample itself. To separate out the thermal contact resistance from the sample's intrinsic thermal conductivity, the team measures samples of varying thicknesses. The thermal conductivity can then be independently extracted from the slope of these lines, as shown in Figure 48b. The team therefore fabricated battery electrodes of varying thicknesses. Measurements were performed multiple times at multiple different thicknesses in both a dry and wet state for both cathodes and anodes. For the wet state, the team saturated electrodes with the electrolyte solvent (equal parts DE and DEC) without lithium salts added. The extracted electrode thermal conductivities are:

$$k_{cathode\_dry} = \mathbf{0.54\ W/m\text{-}K},\ k_{cathode\_wet} = \mathbf{0.74\ W/m\text{-}K}$$

$$k_{anode\_dry} = \mathbf{1.03\ W/m\text{-}K},\ k_{anode\_wet} = \mathbf{1.55\ W/m\text{-}K}$$

To the team's knowledge, these are the most direct measurements of the cross plane thermal conductivity of battery cathode and anode active materials taken to date. All other measurements available in the literature were indirect measurements: either k was theoretically calculated from other properties, or a stack of multiple electrodes (including weak interfaces and sometimes current collectors) was measured and averaged in lieu of directly measuring k of an individual electrode.

Patents/Publications/Presentations

The project has no patents, publications, or presentations to report this quarter.

Task 3.10 – Multi-Scale Modeling of Solid-State Electrolytes for Next-Generation Lithium Batteries (Anh Ngo, Larry A. Curtiss, and Venkat Srinivasan, Argonne National Laboratory)

Project Objective. This project is part of a multi-scale modeling effort to obtain an in-depth understanding of the interaction of the electrode and the solid electrolyte aimed at developing highly efficient SSE batteries for vehicle applications. Input parameters needed for mesoscale (continuum) level calculations are being obtained from atomistic calculations including DFT and classical MD simulations. This atomistic input will enable a multi-scale computational procedure for SSEs that is capable of successfully capturing the physicochemical aspects during charge and discharge process including lithium transport mechanisms, interfacial phenomena during the insertion and extraction of lithium ions, and mechanical deformation of SSE.

Project Impact. A major safety concern experienced with commercially available Li-ion batteries under some scenarios is leakage of the liquid electrolyte, which can potentially catch fire. Replacement of the liquid electrolyte is necessary to decrease the fire hazard and improve safety associated with present-day Li-ion batteries. In addition, use of solid electrolytes provides a path to prevent dendrites in Li-metal anodes, thereby leading to batteries with significantly higher energy density. The impact of this project will be to help in development of good SSEs as a replacement for the commercially used organic liquid electrolytes to improve safety and energy density in Li-ion batteries.

Approach. Parameters needed for mesoscale modeling of grain-interior, grain-boundary, and electrode-electrolyte interface will be calculated by DFT-based calculations along with Monte Carlo (MC) and MD simulations. The calculations will be used to determine properties of the electrode with the solid electrolyte as well as in grain-boundary regions of the solid electrolyte. This will include calculations of structure, stability, ionic conductivity, Young’s modulus, fracture toughness, exchange current density, and other properties.

Out-Year Goals. The out-year goals of this work are to calculate other properties such as fracture toughness and include other SSEs and coatings in the multi-scale modeling.

Collaborations. This project collaborates with Y. Cui at Stanford.

Milestones

1. Computation of elastic – conductivity properties of interfaces between LLZO with lithium as function of applied electric field for input into multiscale modeling. (Q1, FY 2019; Completed)
2. Investigation of structure and stability of SSE interfaces with anode and cathode surfaces for input into multiscale modeling. (Q3, FY 2019)

Progress Report

To understand the metal deposition mechanism at the interface of lithium electrode and SSEs, it is important to determine the various transport properties and reaction kinetics at the interface. Due to the stiff nature of the SSEs, any non-uniform deposition of lithium can give rise to mechanical stress distribution within the electrolyte. Diffusivity, Young's modulus, and exchange current density for the SSEs have been calculated by atomistic methods used previously in this project. To elucidate the overall impact of all these properties on the lithium deposition, all the calculated parameters have been input into a continuum-level mesoscale model, where the conduction and deposition of lithium has been solved, along with the mechanical deformation and stress generation within the SSEs. The atomistic calculations reveal that the Young's modulus within the GB region is smaller than the bulk, whereas the Li-ion concentration within GB is slightly larger. Higher elastic modulus usually leads to generation of larger stress. Hence, the stress within GB is smaller in magnitude than that within the bulk domain. Due to deposition of lithium, compressive stresses generate at the Li/SSE interface.

Since, both the stress and lithium concentration affect the exchange current density, it is worthwhile to investigate the overall distribution of reaction current near a GB region. Figure 49a schematically depicts a possible Li/SSE interface, whereas, a zoomed-in view of a region close to the GB is shown in Figure 49b. Distribution of reaction current at the Li/SSE interface is clearly depicted in Figure 49c. Even though the conductivities of the GB and bulk have been assumed to be equal, higher magnitudes of exchange current density at the GB lead to larger reaction current and eventually to current focusing at the GB regions. Please note that the effective exchange current density at the GB region has been affected by both the local concentration and the mechanical-stress-induced effects.

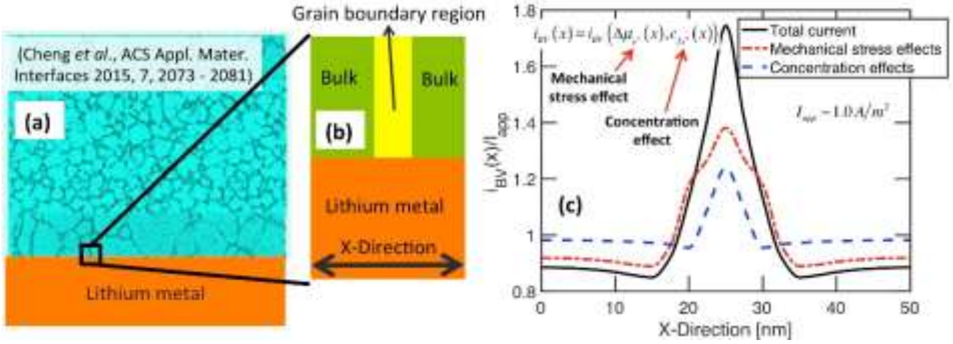

Figure 49. (a) Schematic of Li/SSE interface where various grain boundaries (GBs) stay in contact with lithium metal. (b) Zoomed-in view of a small portion in vicinity of a GB. (c) Reaction current at the Li/SSE interface, with current focusing at GB, even though bulk and GB conductivities are equal.

Incorporating this variation in exchange current density into a larger microstructure, it is possible to estimate the non-uniformity in lithium deposition and propensity of crack formation within SSEs. Figure 50a demonstrates the applied current profile and corresponding voltage response observed with respect to time. Based on stress calculations as cracks start to propagate, the simulation is stopped. Figure 50b shows how the fracture initiation current density (FICD) varies with respect to grain size. For very small grains, reduced current focusing at GB leads to higher FICD. For larger grains, decreased inhomogeneous deposition leads to increase in FICD. Hence, the various grain sizes can be divided into "bulk regimes" and "GB affected regimes."

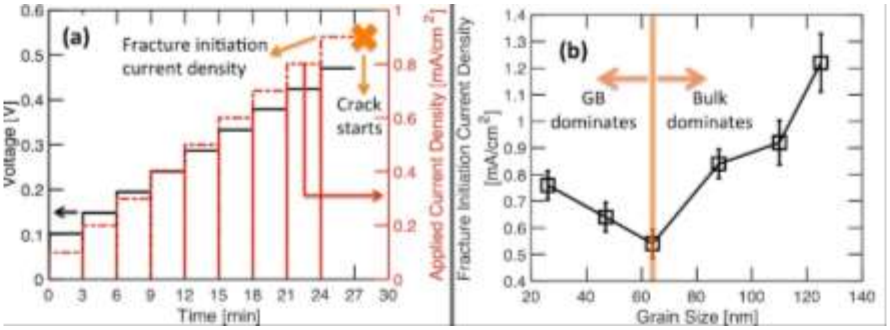

Figure 50. Evolution of voltage and current over time for a particular grain boundary microstructure. Simulation stops as soon as cracks start to propagate. (b) Variation in "fracture initiation current density" with respect to grain size. For both small and large grains, fracture initiation occurs at high current densities.

Patents/Publications/Presentations

Publication

- Barai, P., A-T. Ngo, K. Higa, L. A. Curtiss, and V. Srinivasan. “Mechanical Stress Induced Current Focusing and Fracture in Grain Boundaries.” Submitted.

TASK 4 – METALLIC LITHIUM

Summary and Highlights

The use of a metallic lithium anode is required for advanced battery chemistries like Li-ion, Li-air, and Li-S to realize dramatic improvements in energy density, vehicle range, cost requirements, and safety. However, the use of metallic lithium with liquid and polymer electrolytes has so far been limited due to parasitic SEI reactions and dendrite formation. Adding excess lithium to compensate for such losses effectively negates the high energy density for lithium in the first place. For a long lifetime and safe anode, it is essential that no lithium capacity is lost either (1) to physical isolation from roughening, dendrites, or delamination processes, or (2) to chemical isolation from side reactions. The key risk and current limitation for this technology is the gradual loss of lithium over the cycle life of the battery.

BMR, Battery500, and other DOE programs are addressing this challenge with many innovative and diverse approaches. Key to all is the need for a much deeper analysis of the degradation processes and new strategies to maintain a dense, fully connected lithium and a dendrite-free electrolyte so that materials can be engineered to fulfill the target performance metrics for EV application, namely 1000 cycles and a 15-year lifetime, with adequate pulse power. Projecting the performance required in terms of just the lithium anode, this requires a high rate of lithium deposition and stripping reactions, specifically about 30 µm of lithium per cycle, with pulse rates up to 10 and 20 nm/s (15mA/cm^2) charge and discharge, respectively, with little or no excess lithium inventory. This is daunting in the total mass and rate of material transport that must be achieved without failures.

The efficient and safe use of metallic lithium for rechargeable batteries is then a great challenge, and one that has eluded R&D efforts for years. This Task takes a broad look at this challenge for both solid-state batteries and batteries continuing to use liquid electrolytes. For the liquid electrolyte batteries, MIT with Carnegie Mellon is investigating fluoridated components and other additives to form self-healing SEI coatings at the lithium surface. At University of Pittsburgh, alternatives to a standard Li-metal anode are being explored, including metal alloys and templated structures. Researchers at PNNL are pivoting from liquid electrolytes to hybrid electrolytes, with addition of a polymer component to a concentrated solvent-in-salt electrolyte. For solid-state batteries, programs are addressing both the electrolytes and the lithium interface. The stability of the garnet ceramic electrolyte with lithium is being investigated at ANL with materials from University of Michigan. The different mechanical and electrochemical mechanisms leading to the formation of shorting lithium features through the solid electrolytes is under study at ORNL, University of Michigan, and Michigan Technological University. And new ceramic-polymer composite electrolytes formed with scalable processing are investigated to reveal the properties of both the ceramic electrolyte / polymer electrolyte interface and contacts of the solid electrolyte with the solid composite cathode and thin lithium anode.

Highlights. Promising Li-metal cycling was reported using electrolytes of organic solvent salt solutions with additive and different salts, highly concentrated solutions, and pure dense ceramic and glass electrolytes. The project shows how using thin (6- and 20-µm) lithium as one contact can provide a rapid assessment of the lithium stability.

For the solid electrolyte systems:

- For the LLZO ceramic, continued work focuses on comparing the redox stability with various dopants: aluminum, niobium, and tantalum. The niobium is reduced throughout the bulk of the garnet LLZO after contacting lithium metal, whereas Zr^{4+} is reduced somewhat near the interface for the dopants. The aluminum showed no significant change before/after reaction with lithium, and the EIS is stable for extended contact time. (Task 4.6)

- Also for Al-doped LLZO, new results identify a critical voltage leading to internal Li-metal precipitation. This is related to Li-metal penetration in the ceramic electrolyte leading to shorts. (Task 4.7)
- Solid-state cells of $LiFePO_4$ versus lithium were tested with two different dry-composite, polymer-ceramic electrolytes. Cells were fabricated with thick lithium foil and thin 6-µm lithium films, and were then compared. Capacity loss is faster for cells with thin films, but the mechanism needs further study. The interface between the solid LFP composite cathode and the composite ceramic electrolyte is improved with an intervening polymer layer to provide full contact between the ceramic composites. (Task 4.4)

For liquid electrolyte system:

- Highly concentrated (> 3 M) lithium salt in organic electrolyte solutions was probed, specifically comparing carbonate, ether, and phosphate solvents. This is an effort to identify alternative solvents to use for both hybrid polymer-in-salt electrolytes and composite hybrid polymer-in-salt electrolytes. (Task 4.1)
- Asymmetric Li-Li and Li-$LiCoO_2$ cells were evaluated using 20-µm thick lithium on copper to limit the excess lithium when cycling to an areal capacity of 3 mAh/cm^2. The electrolyte composed of $LiPF_6$ (1M) in FEC+DMC + X, X being a new additive, performed best, demonstrating self-forming, self-healing SEI properties. (Task 4.2)
- A practical separator was created by spray-coating nanopowder of silica directly onto the $LiCoO_2$ cathode surface. This, combined with the standard polypropylene sheet separator, provided a Li-ion battery with improved cycling in $LiClO_4$(EC-DMC-FEC) electrolyte. (Task 4.5)

For the lithium anode:

- A suitable host for lithium was comprised of a metal that forms a structurally isomorphous alloy (SIA) with lithium plus a nucleating agent. This has provided stable cycling for 200 cycles at currents to 2 mA with no observable dendrites. (Task 4.3)

Task 4.1 – Lithium Dendrite Prevention for Lithium Batteries
(Wu Xu and Ji-Guang Zhang, Pacific Northwest National Laboratory)

Project Objective. Enable lithium metal to be used as an effective anode in rechargeable Li-metal batteries for long cycle life. The investigation in FY 2019 will focus on effects of various organic solvents, inorganic solid electrolytes, and polymers on ionic conductivity, lithium CE, lithium anode morphology, and battery performances in terms of long-term cycling stability and rate capability at room temperature and elevated temperatures. The compatibility of such electrolytes with 4-V, high-Ni, NMC cathode will also be investigated.

Project Impact. Lithium metal is an ideal anode material for rechargeable batteries. Unfortunately, uncontrollable dendritic lithium growth and limited CE during repeated lithium stripping/deposition processes have prevented practical application. This work will explore the new hybrid composite electrolytes that can lead to dendrite-free lithium deposition with high CE. The success of this work will increase energy density of Li-metal and Li-ion batteries and accelerate market acceptance of EVs, especially of PHEVs as required by the EV Everywhere Grand Challenge.

Approach. The approach will encompass several areas. (1) Develop appropriate high-concentration electrolytes (HCEs) that have high lithium CE over 99% and are stable with high-Ni NMC (for example, NMC-532) cathodes. (2) Add a small amount of inorganic solid electrolytes and proper polymers into the HCEs to form uniform mixtures, which will be cast into thin films. (3) Solid-state polymer-in-salt electrolyte will be prepared through the hot-pressing method. The effects of the type and content of inorganic fillers and polymers on the ionic conductivity, the electrochemical window, the lithium CE and the morphology will also be tested.

Out-Year Goals. The long-term goal of the proposed work is to enable lithium and Li-ion batteries with > 120 Wh/kg (for PHEVs), 1000 deep-discharge cycles, 10-year calendar life, improved abuse tolerance, and less than 20% capacity fade over a 10-year period.

Collaborations. This project collaborates with C. Wang of PNNL on characterization by TEM/SEM; Drs. K. Xu and M. Ding of ARL on solvent purification and differential scanning calorimetry (DSC) measurements; and Dr. B. Polzin at ANL on coated electrode sampling.

Milestones

1. Achieve over 300 cycles for 4-V Li||NMC batteries with ~ 2 mAh/cm^2 cathode loading. (Q4, September 30, 2018; Completed)
2. Investigate effects of high-concentration electrolytes on lithium CE and deposited lithium morphology. (Q1, January 15, 2019; Completed)
3. Investigate effects of polymers in hybrid electrolytes on lithium CE and deposited lithium morphology. (Q2, March 31, 2019; In progress)
4. Develop an HCE with lithium CE > 98% and oxidation potential up to 4.4 V. (Q3, June 30, 2019; In progress)
5. Achieve over 100 cycles for Li||NMC-532 batteries with medium cathode loading. (Q4, September 30, 2019; In progress)

Progress Report

This quarter, the team completed milestones for both last quarter and this quarter. The 4-V Li||NMC-333 coin cells with ~ 2 mAh cm^{-2} cathode loading and using hybrid "polymer-in-salt" composite electrolytes have reached 300 cycles at C/5 charging and C/3 discharging at 60°C, as well as at C/3 charging and 1C discharging at 60°C.

For this quarter, three types of HCEs were investigated based on organic carbonate, ether, and phosphate solvents, where the salt was LiFSI. The conductivity, electrochemical stability, lithium CE, and deposited lithium morphology were studied systematically; part of the results are shown in Figure 51. The average CE was assessed as $CE_{avg.} = \frac{nQ_{cycle,strip}+Q_{strip}}{nQ_{cycle,plate}+Q_{reservoir}}$, a method developed by PNNL.

For the two carbonate solvents DMC and $EC_{0.3}$-$DMC_{0.7}$ at the same salt/solvent molar ratio of 1:1.1, LiFSI-1.1DMC has slightly higher conductivity of 1.09 mS cm^{-1} at 30°C, electrochemical oxidation voltage of 4.55 V versus Li/Li^+ (with the cutoff current density of 0.01 mA cm^{-2}), and average lithium CE (99.3%) in comparison to the LiFSI-1.1($EC_{0.3}$-$DMC_{0.7}$) that has a conductivity of 0.78 mS cm^{-1} at 30°C, oxidation voltage of 4.4 V, and lithium CE of 98.8%. Large nodule-like and compact lithium particles can be observed for LiFSI-1.1DMC. The thickness of the lithium film deposited in LiFSI-1.1DMC is around 12 µm.

For the HCEs of LiFSI-nDME at different molar ratios, the molar ratio of the highest concentration of the LiFSI-DME electrolyte is 1:0.7. With the increase of the solvent content, the conductivity increases (that is, 1.15, 1.71, 2.36, 3.16, and 4.52 mS cm^{-1} at 30°C for 1:0.7, 1:0.8, 1:0.9, 1:1, and 1:1.2, respectively), the lithium CE also slightly increases from 98.0% for 1:0.8 to 98.5% for 1:1.2 (where the 1:0.7 could not be tested due to unknown reasons), but oxidation voltage decreases from 4.59 V for 1:0.7 to 4.18 V for 1:1.2. Lithium particles deposited in LiFSI-1.2DME are very compact, and lithium film thickness is 13 µm.

For the HCEs with two alkylphosphates (TMPa and TEPa) and two salt/solvent molar ratios (1:1.1 and 1:1.3), LiFSI-1.1TMPa and LiFSI-1.3TMPa have slightly higher conductivities than those with TEPa (0.63 and 0.83 mS cm^{-1} at 30°C versus 0.43 and 0.58 mS cm^{-1}, respectively). Both TMPa-based HCEs exhibit 5 V stability, but the TEPa-based HCEs have only about 4.7 V oxidation stability when the current density is set at 0.01 mA cm^{-2}, much higher than the carbonate-based HCEs and DME-based HCEs. The highest CE (98.7%) of the TMPa-based HCEs is obtained in LiFSI-1.3TMPa. Fibrous and nodule-like lithium particles can be observed, and the deposited lithium film is looser than those from carbonate and ether HCEs. The thickness is ~ 18 µm.

Both LiFSI-1.1DMC and LiFSI-0.8DME HCEs have conductivity higher than 1 mS cm^{-1} at 30°C. They are stable above 4.5 V versus Li/Li^+ and have lithium CE larger than 98%, so they are currently used in the study of hybrid polymer-in-salt electrolytes.

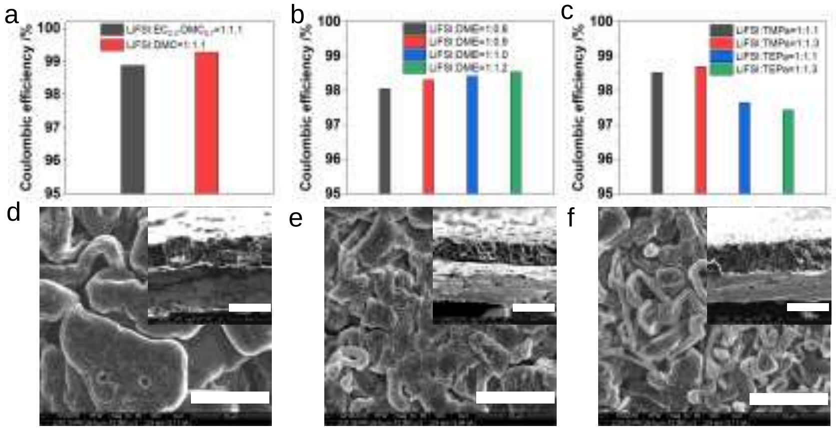

Figure 51. Coulombic efficiency of Li||Cu cells at 0.5 mA cm^{-2} with (a) carbonate high-concentration electrolytes (HCEs), (b) ether HCEs, and (c) alkylphosphate HCEs. Scanning electron microscopy images of deposited lithium particles at 0.1 mA cm^{-2} with capacity of 1.5 mAh cm^{-2} with (d) carbonate HCEs, (e) ether HCEs, and (f) alkylphosphate HCEs. Scale bar for the top view is 10 µm; for the cross-section view, it is 20 µm.

Patents/Publications/Presentations

Presentation

- BMR Electrolyte Discussion, Berkeley, California (October 11, 2018): "Lithium Dendrite Prevention for Lithium Batteries"; W. Xu and J.-G. Zhang.

Task 4.2 – Self-Assembling and Self-Healing Rechargeable Lithium Batteries (Yet-Ming Chiang, Massachusetts Institute of Technology; Venkat Viswanathan, Carnegie Mellon University)

Project Objective. The project objectives are as follows: (1) investigate formation of lithium halide containing SEI, (2) characterize the structure and composition of the SEI surface film and morphology of the electrochemically deposited lithium, and (3) develop combinations of electrolytes (solvents + salts) and electrolyte additives that produce a highly Li-ion conducting, mechanically robust, and self-healing SEI to suppress lithium dendrite formation and improve CE.

Project Impact. Efforts to achieve practical use of the Li-metal anode in rechargeable lithium batteries have long been plagued by lithium dendrite formation and low CE. Lithium dendrites cause battery short-circuits, leading to serious safety hazards. The low CE of Li-metal anodes demands use of excess lithium to offset the lithium loss during cycling, which lowers the overall energy density of the battery. If successful, this project will enable self-forming and self-healing SEI containing alkali and/or alkaline earth halides that can suppress dendrite formation and improve CE. This will eventually enable high-energy-density (> 400 Wh/kg) and long-cycle-life (> 500 cycles, 80% capacity retention) Li-metal batteries.

Approach. The project approach involves the following: (1) identifying suitable combinations of solvents, Li-electrolyte salts, and halide and other additives that can produce highly Li-ion conducting, mechanically robust, and self-healing SEI, (2) using integrated theory and experiment, and (3) assembling and testing symmetric and asymmetric cells and Li-metal batteries comprising a high areal-capacity cathode (> 3 mAh/cm^2) and a capacity-limited Li-metal anode (< 130% lithium excess).

Out-Year Goals. The project will down-select electrolyte compositions, develop designs for prototype full cells of > 10 mAh capacity, and fabricate/deliver cells to DOE-specified laboratories for testing and evaluation.

Collaborations. This project collaborates with 24M Technologies Inc. on 18 cm^2/80 cm^2 pouch cell fabrication and tests.

Milestones

1. *Go/No-Go Decision*: Demonstrate Li-Li symmetric cells that meet established criteria cycling at ≥ 3 mAh/cm^2 at C/5 rate over 30 cycles. (Q1, FY 2019; Completed ahead of schedule)

Progress Report

This quarter, cycling results are reported for asymmetric Li-Li cells and Li-$LiCoO_2$ full cells utilizing the electrolytes developed in this project. As shown in previous reports, an asymmetric Li-Li cell test was developed that is able to quantify both the CE and area-specific impedance (ASR) of Li-metal electrodes, whereas conventional symmetric Li-Li cell tests can only quantify ASR. Furthermore, "soft" short circuits can be difficult to differentiate from a low ASR in symmetric Li-Li cells, whereas the asymmetric configuration will often yield unrealistically high CE when short circuits are present. Thus, in this quarter, efforts were focused on testing both asymmetric Li-Li cells and Li-$LiCoO_2$ full cells, under conditions where the area capacity is ≥ 3 mAh/cm^2 at C/5 rate.

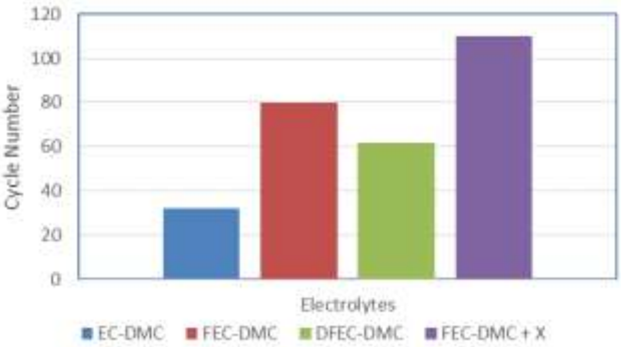

Figure 52. Results from asymmetric Li-Li cell tests. The four electrolytes are 1 M $LiPF_6$ dissolved in EC-DMC, FEC-DMC, DFEC-DMC, and FEC-DMC + additive X, respectively.

The asymmetric Li-Li cells were assembled using Li-metal electrodes having different thicknesses and area-capacities. The working electrode is a 20-µm-thick lithium film coated on a copper foil (area capacity ~ 4.12 mAh cm^{-2}) while the counter electrode is a 750-µm-thick lithium foil. The two electrodes were assembled in a CR2032-type coin cell with a Tonen polyethylene separator and 40-µL electrolyte. The cells were cycled at a current density of 0.6 m/cm^{-2} to an area capacity of 3.0 mAh cm^{-2} per deposition/stripping cycle. With each cycle, any Coulombic inefficiency consumes a portion of the initial 4.12 mAh cm^{-2} capacity of the working electrode, and when all of the initial capacity is consumed, the voltage of the cell rises sharply during the stripping cycle. Thus, the cells were cycled until the overpotential on Li-stripping exceeds 0.5 V versus Li^+/Li, indicating that there is no available lithium for stripping at the working electrode. Results are shown in Figure 52 for asymmetric Li-Li cells using an EC-DMC baseline electrolyte; three fluorinated electrolytes identified as having self-forming, self-healing SEI properties are also shown in the Figure. While the baseline electrolyte barely reaches this quarter's milestone criteria of cycling at 3 mAh cm^{-2} at C/5 rate over 30 cycles, the three other electrolytes have significantly better performance.

Li-metal full cells were assembled using a "high-voltage" $LiCoO_2$ cathode (area-capacity ~ 4.2 mAh/cm^2 when charged to 4.5 V versus Li^+/Li), a 20-µm-thick lithium anode coated on a copper foil (areal capacity ~ 4.12 mAh/cm^2), and a single-layer polyethylene separator. The tests were performed inside a temperature chamber set at 30°C ± 0.2°C. 2025-type coin cell cases made of 316L-grade stainless steel were used for the tests, which are stable at the 4.5 V upper cutoff voltage of the tests. The full cells were first cycled at 0.1 C rate for 3 cycles, and then cycled at 0.2 C charge-0.5 C discharge (in the project's tests, 1 C = 170 mA/g = 3.91 mA/cm^2). As shown in Figure 53, the $LiCoO_2$ full cell containing the 1 M $LiPF_6$ FEC-DMC + X additive electrolyte, which performed the best of the electrolytes in Figure 52, showed ~ 150 cycles to 80% of initial capacity. Additional details regarding the additive X will be provided in future reports.

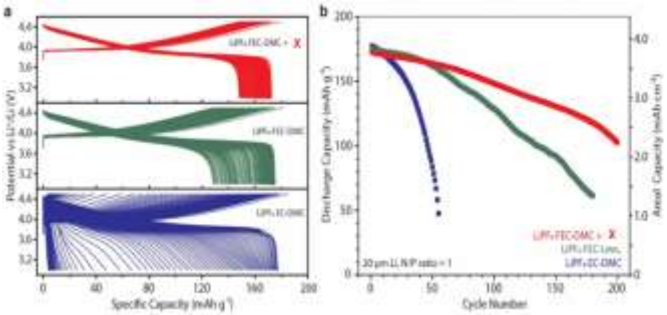

Figure 53. Cycling results for Li-$LiCoO_2$ full-cell tests using three electrolytes from the standardized Li-metal full-cell tests.

Patents/Publications/Presentations

Patent

- Y-M. Chiang, V. Viswanathan, L. Li, V. Pande, D. Krishnamurthy, Z. Ahmad, and W. H. Woodford. “Lithium Metal Electrodes and Batteries Thereof.” U.S. Patent Application No. 20170288281A1.

Task 4.3 – Engineering Approaches to Dendrite-Free Lithium Anodes (Prashant Kumta, University of Pittsburgh)

Project Objective. This project will yield Li-metal anodes with specific capacity ≥ 2000 mAh/g (≥ 4 mAh/cm^2), ~ 1000 cycles, and CE ≥ 99.99% with superior rate capability. The goal is to (1) systematically characterize different approaches for generation of dendrite-free Li-metal anodes while also providing understanding of the scientific underpinnings, and (2) evaluate the microstructure and electrochemical performance of dendrite-free Li-metal anodes. Generation of high-performance, dendrite-free Li-metal anodes will successfully demonstrate generation of novel sulfur cathodes, affording fabrication of Li-S batteries meeting the targeted gravimetric energy densities ≥ 350 Wh/kg and ≥ 750Wh/l with a cost target $125/kWh and cycle life of at least 1000 cycles for meeting the EV Everywhere Grand Challenge blueprint.

Project Impact. Dendrite formation in electrochemical systems occurs due to inhomogeneous current densities coupled with local diffusion gradients, surface roughness, and kinetic roughening. Lithium dendrite formation and growth are, however, not well understood; adding to the complexity is SEI formation. Control and elimination of Li-metal dendrite formation is a challenge. If overcome, it would render universal adoption of Li-anode batteries for stationary and mobile applications. This project is a scientific study of novel approaches to address dendrite formation in Li-anode batteries, electrolyte decomposition, and associated cell failure. Development of dendrite-free, high-performance lithium anodes will enable use of Li-free cathodes, opening a myriad of possibilities to push the envelope in terms of cathode capacity and battery energy density.

Approach. This project will explore several approaches focused on engineering new structurally isomorphous metallic alloys combined with engineering the surface of metallic lithium as well as the current collectors, including developing novel high Li-conducting conjugated polymers and composite structures. The unifying theme is to initiate a uniform nucleation with homogenous growth, eliminating preferential reversible plating and de-plating, and thus resulting in dendrite-free, high-energy-density Li-metal anodes. This project comprises three major phases to be successfully completed in three years. In the first year, the team developed foams as templates for lithium deposition. This year, the team will focus on developing Li-rich SIA anodes and generating composite multilayer anodes (CMAs).

Out-Year Goals. The out-year goal is to utilize the novel anode architectures discovered in this project to design full batteries, likely Li-S, that achieve advanced high-energy-density, high-rate, extremely cyclable cell development.

Collaborations. The project works with Dr. M. K. Datta and Dr. O. I. Velikokhatnyi (University of Pittsburgh) as co-PIs. It also collaborates with Dr. A. Manivannan (Global Pragmatic Materials), XPS analysis; Dr. D. Krishnan Achary (University of Pittsburgh), solid-state magic angle spinning NMR (MAS-NMR) characterization; and Dr. J. R. Gaines (Kurt Lesker), thin-film system fabrication/ characterization.

Milestones

1. Integrated electrode (IE) generation to be accomplished through utilizing this project's coating development. (Q4, FY 2019; In progress)
2. Novel configurations (PF) development to optimize utilization of lithium with no dendrite formation. (Q4, FY 2019; In progress)
3. Novel alloys (SIA) exhibiting high capacity with no dendrite formation at high rates. (Q4, FY 2019; In progress)
4. Fabrication/characterization of 10-mAh cell configurations. (Q4, FY 2019; In progress)

Progress Report

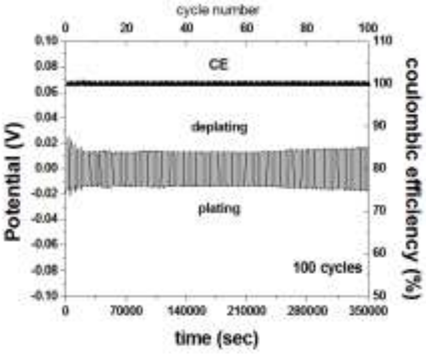

Figure 54. Plating/stripping behavior of lithium metal using novel metal alloys as current collector.

This quarter, the team conducted experiments to verify the minimum heterogeneous nucleation barrier surface of the novel current collectors identified, thus demonstrating minimum nucleation barrier/nucleation underpotential. These experiments verified formation of a smooth homogeneous surface across the “zero nucleation underpotential” current collector due to significantly high nucleation rate. Accordingly, the team conducted further experiments to determine the lithium growth front morphology and study the long-term lithium cycling performance. Thus, the team conducted Li-metal plating/stripping at a current density of 1 mA/cm^2 for 4 h with up to 100 cycles. The electrolyte used for this test was 1.8 M LiTFSI + 0.2 M $LiNO_3$ in DOL:DME electrolyte (Figure 54), which shows stable cycling to 100 cycles with a CE of ~ 100%. SEM micrograph of the Li-metal growth front obtained after 100 cycles, shown in Figure 55, displays the evolution of a planer morphology with no presence of dendritic structures. These results clearly suggest that the current collector exhibits good wetting and high capillarity with lithium metal inhibiting the “non-planar cellular/dendrite” growth at high plating current density. A detailed scientific study of the nucleation and growth behavior of lithium metal on the developed novel multicomponent metal alloys will be reported next quarter.

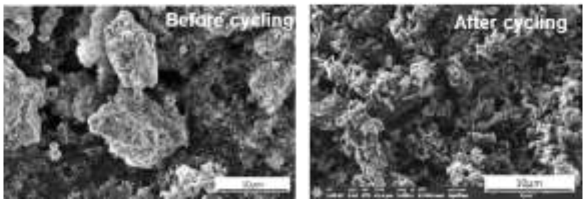

Figure 55. Scanning electron micrograph of Li-metal growth front obtained after 100 cycles.

Additionally, the team developed SIAs to replace copper/carbon systems with the ability to modify the lithium plating morphology by altering the nucleation and growth mechanisms. The alloy host was chosen to match the crystallographic registry of the lithium metal combined with the addition of a nucleating agent to enable homogeneous nucleation. These new alloys were made by high-energy mechanical milling (HEMM), and the phase evolution was studied by XRD. The lithiated alloy was examined for lithium plating/stripping in a CR2025 coin cell, with lithium as the counter/reference electrode and 1 M $LiPF_6$ in EC:DEC:FEC electrolyte at different areal current/charge densities (Figure 56a). The lithium alloy host improves the electrochemical processes of reversible lithium plating/stripping, yielding a high ~ 99.6% CE after 200 cycles (Figure 56a). The plating/de-plating potential reduces to ~ 20-40 mV with the electrode, stabilizing after 40 cycles (Figure 56b). Post cycled electrode SEM images (Figure 56c) show no dendrites, due to efficient nucleation and uniform lithium growth during plating and stripping processes, demonstrating the efficacy of this new alloy system.

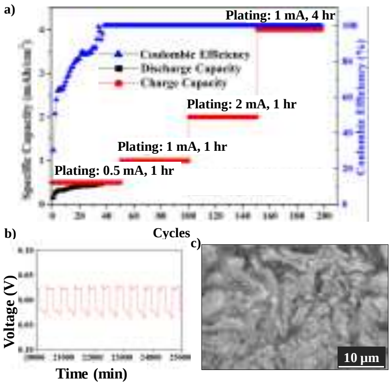

Figure 56. (a) Electrochemical cycling. (b) Voltage profile after 40 cycles. (c) Scanning electron microscopy after 200 cycles showing absence of dendrites; scale bar 10 microns.

Patents/Publications/Presentations

The project has no patents, publications, or presentations to report this quarter.

Task 4.4 – Composite Electrolytes to Stabilize Metallic Lithium Anodes (Nancy Dudney and X. Chelsea Chen, Oak Ridge National Laboratory)

Project Objective. The project has several objectives: (1) prepare composites of representative polymer and ceramic electrolyte materials to achieve thin membranes that have the unique combination of electrochemical and mechanical properties required to stabilize the metallic lithium anode while providing for good power performance and long cycle life, (2) understand the Li-ion transport at the interface between polymer and ceramic solid electrolytes, which is critical to effective conductivity of the composite membrane, (3) identify key features of composite composition, architecture, and fabrication that optimize performance, and (4) using practical and scalable processing, fabricate thin electrolyte membranes to use with a thin metallic lithium anode to provide good power performance and long cycle life.

Project Impact. A stable lithium anode is critical to achieve high energy density with excellent safety, lifetime, and cycling efficiency. This study will identify key design strategies that should be used to prepare composite electrolytes to meet the challenging combination of physical, chemical, and manufacturing requirements to protect and stabilize the Li-metal anode for advanced batteries. By utilizing well characterized and controlled component phases, design rules developed for composite structures will be generally applicable toward substitution of alternative and improved solid electrolyte component phases as they become available. Success will enable DOE technical targets: 500-700 Wh/kg, 3000-5000 deep discharge cycles, and robust operation.

Approach. This project seeks to develop practical solid electrolytes to provide stable, long-lived protection for the Li-metal anode. Current electrolytes have serious challenges when used alone; oxide ceramics are brittle, sulfide ceramics are air sensitive, polymers are too resistive and soft, and many electrolytes react with lithium. Composites provide a clear route to address these issues. While work continues to emphasize study of ceramic electrolyte/polymer electrolyte interfaces, this effort has expanded to address (1) practical processing routes to fabricate full batteries using better composite electrolytes with a composite cathode and thin Li-metal anode, and (2) introduction of alternative polymer and ceramic phases to replace well-known model materials and develop improved composite electrolytes. In addition to solid-state devices, hybrid batteries are investigated using a fluid or gel catholyte within the porous cathode. Coatings have also been employed to stabilize electrode interfaces. These directions increase complexity of the studies, but are needed to improve cycling stability and rate performance and to advance practical implementation of the solid electrolyte and Li-anode technology.

Out-Year Goal. The goal is to use advanced manufacturing processes where the architecture of the composite membrane can be developed and tailored to maximize performance and cost-effective manufacturing.

Collaborations. Work is conducted by Dr. Y. Zhang and Dr. X. Chen. Ceramic electrolyte powders are obtained from Ohara Corporation and Prof. J. Sakamoto (University of Michigan). Polymer electrolytes are provided by Prof. Z. Bao (Stanford University) and T. Saito (ORNL). The team will work with new partners from U.S.-German Cooperation on Energy Storage.

Milestones

1. Fabricate full cell using thin evaporated lithium anodes. Compare full cell performance using thick and thin evaporated lithium anodes. (Q1, FY 2019; Completed)
2. Fabricate gel composite electrolytes with a target room temperature conductivity of 1×10^{-4} S/cm. Thoroughly evaluate ion transport, and thermal and structural properties. (Q2, FY 2019)
3. Expand composite materials portfolio to include non-PEO type of polymer electrolytes. Identify promising polymer ceramic systems with interfacial ASR less than 10 ohm. (Q3, FY 2019)
4. Work with partners from US-German Cooperation on Energy Storage on WP3, Interface of Lithium with Polymer Electrolyte. Complete milestones as detailed in the proposal. (Q4, FY 2019)

Progress Report

The project continued using the composite $LiFePO_4$ (LFP) composite cathode. The team tested two new cells, Li|PE|CPE|PE|LFP and Li|PE|CPE2|PE|LFP, to compare with previous cells, Li|PE|LFP and Li|PE|CPE|LFP. Note that LiTFSI/[EO] = 1/16 in CPE and LiTFSI/[EO] = 1/8 in CPE2. All cells were built using the protocol from last quarter, but this period the team compared cells with 6-μm vapor-grown lithium films to cells with a thick lithium foil. Based on the active cathode loading, the theoretical capacity of each cell is 1.1 mAh/cm^2.

Figure 57 summarized cells with thicker lithium. The team cycled the cells at 70 μA/cm^2, and then by 90 μA/cm^2 for cycles 21-40 at 75°C. All cells achieve near theoretical capacity. Notably, the capacity of Li|PE|CPE|LFP cell increased slightly from 0.99 to 1.19 mAh/cm^2 during the first 10 cycles (Figure 57b, inset) and remained until cycle 20. Addition of a PE layer between CPE and LFP improved initial performance, likely by ensuring a full contact area between the electrolyte and cathode composites, both having high ceramic-loading. The capacity retention rate for 40 cycles of PE, CPE, CPE|PE, and CPE2|PE cells is 80%, 92%, 91%, and 95%, respectively. In all cases, after 10 or 20 cycles the charge curve became noisy and with excess charge capacity. The cause(s) may relate to leakage current, lithium reaction, or poor contact. The team believes that the noisy behavior during charge leads to cell failure.

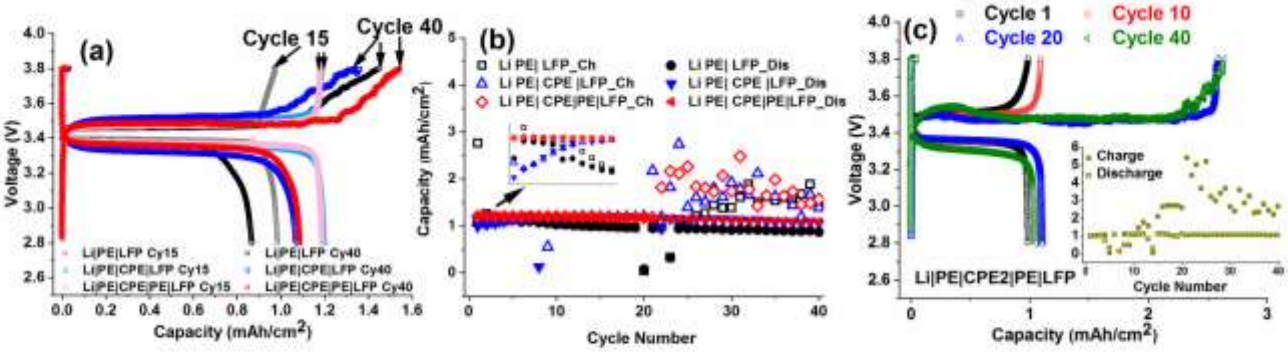

Figure 57. (a) Discharge and charge at cycle 15 and 40 for Li|PE|LFP, Li|PE|CPE|LFP, and Li|PE|CPE|PE|LFP. (b) Charge and discharge cyclability of these cells. (c) Voltage profiles for Li|PE|CPE2|PE|LFP cell, with cell cycability in the inset.

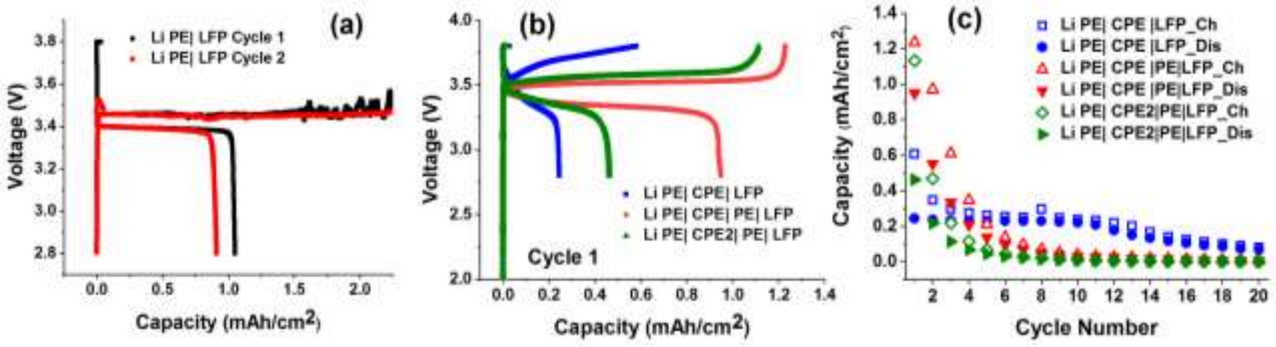

Figure 58. (a) The voltage profiles for Li PE|LFP cell at cycles 1 and 2. (b) Charge and discharge curve in the initial cycle for cell lithium PE|CPE|LFP, Li PE|CPE|PE|LFP, and Li PE|CPE2|PE|LFP. (c) Cyclability of these three cells.

To tackle this problem, the team used vapor-deposited thin lithium anode to study behavior of the full cells. A 6-μm by 0.9-cm^2 lithium film was deposited onto the 120-μm PE layer; otherwise, the team used the same configuration as above, that is, Li PE|LFP, Li PE|CPE|LFP, Li PE|CPE|PELFP, and Li PE|CPE2|LFP. As shown in Figure 58a, the PE cell achieved the theoretical capacity of 1.1 mAh/cm^2 in the first discharge, even though the charge curve is noisy. This cell remains under test. In Figure58b, the PE layer between CPE and LFP helps to decrease cell resistance, as observed in the Li-foil cell. The first discharge capacities for CPE, CPE|PE, and CPE2|PE cells are 0.22, 0.98, and 0.48 mAh/cm^2, respectively. However, the capacity fades severely for both CPE|PE and CPE2|PE cells; at cycles > 5, capacities are close to 0 (Figure 58c). For the Li PE|CPE|LFP cell, the discharge capacity remains at 0.21 mAh/cm^2 for first the 10 cycles and starts fading afterward. From this data, the teams see that degradation is much more apparent when the lithium capacity is limited.

Patents/Publications/Presentations

Publication

- Chen, X. C., A. S. Pandian, X. Liu, K. Liu, F. M. Delnick, and N. J. Dudney.* “Determining and Minimizing Resistance for Ion Transport at the Polymer/Ceramic Electrolyte Interface.” In review.

Task 4.5 – Lithium Batteries with Higher Capacity and Voltage (John B. Goodenough, University of Texas at Austin)

Project Objective. The project objective is to develop an electrochemically stable alkali-metal anode that can avoid SEI layer formation and alkali-metal dendrites during charge/discharge. To achieve the goal, a thin and elastic solid electrolyte membrane with a Fermi energy above that of metallic lithium and an ionic conductivity $\sigma > 10^{-4}$ S cm^{-1} will be tested in contact with alkali-metal surface. The interface between the alkali-metal and the electrolyte membrane should be free from liquid electrolyte, have a low impedance for alkali-metal transport and plating, and keep a good mechanical contact during electrochemical reactions.

Project Impact. A safe alkali-metal anode that can be plated/stripped reversibly at low resistance and high rates over many thousands of charge/discharge cycles would maximize the volumetric energy density for a given cathode of a rechargeable battery for powering an all-electric road vehicle. Such a battery could also be used for stationary back-up storage of electric power from energy sources other than fossil fuels.

Approach. The project will design, make, and test cells. The approach is to introduce a solid-electrolyte interfacing the anode and a coating on the anode current collector that is wet by a lithium anode. The solid electrolyte should also be wet by the anode to create a bond that is strong enough to constrain the anode volume changes to be perpendicular to the anode/electrolyte interface.

Out-Year Goals. The out-year goal is to develop coin cells that are safe and low-cost with a long cycle life at a voltage $V > 3.0$ V that can compete with the internal combustion engine for powering a road vehicle.

Collaborations. This project collaborates with A. Manthiram at UT Austin and K. Zaghib at HQ.

Milestones

1. Test a new, low-cost ceramic separator concept with a liquid electrolyte and an alkali metal anode. (Q1, FY 2019; Completed)
2. Test redox energies and cyclabilities of novel NASICON-structured cathode materials in a Na-ion battery. (Q2, FY 2019)
3. Synthesize and evaluate solid sulfide electrolytes. (Q3, FY 2019)
4. Investigate oxygen redox chemistry for reversible high-voltage Na^+ intercalation. (Q4, FY 2019)

Progress Report

The team has tested a low-cost separator concept that could reduce the long-standing cost of commercial rechargeable batteries while also improving some important properties of a separator. Polymer separators have long been treated as a staple in the Li-ion battery technology, with the majority of interest in technological advancement falling to the three main components: the cathode, the anode, and the electrolyte. However, the polymer separator is one of the major cost hurdles for large-scale productions. To reduce the cost of current Li-ion battery technology, cheaper alternatives to the traditional polymer separators that still maintain the necessary properties for a separator must be explored.

The team started with a survey of current literature on ceramic materials with a large electronic energy band gap large enough such that the Fermi levels of the two electrodes fall within it. This requirement coupled with a need for cheap material processing yielding a useful morphology such as uniform nanospheres left the team with the obvious choice of silica, SiO_2. Rather than sintering a pellet to attempt to serve as a separator or mixing with a binder polymer, the team developed the idea of spraying the uniform nanoparticles onto the surface of the cathode. This coating gives a much better plasticity over a sintered ceramic pellet, allowing a much more robust ceramic separator. These coated $LiCoO_2$ electrodes were first tested against a graphite anode with 1 M $LiClO_4$ in EC/DMC/FEC (45:45:10) as the electrolyte for proof of concept.

Full cells with an SiO_2-coated $LiCoO_2$ electrode cycled very well at a current density of 1 mA/cm^2 (corresponding to ~ 1C rate) when compared to control cells using a standard polypropylene sheet as a separator (Figure 59). Initial results indicate that the reduced capacity fade exhibited by the SiO_2 coating is owing to superior wetting of the electrolyte by the SiO_2 nanoparticles over the polypropylene separator stemming from a much higher overall surface area of the close-packed SiO_2 nanoparticle film, as opposed to the simple "pin-hole" morphology of the polypropylene separator (Figure 60).

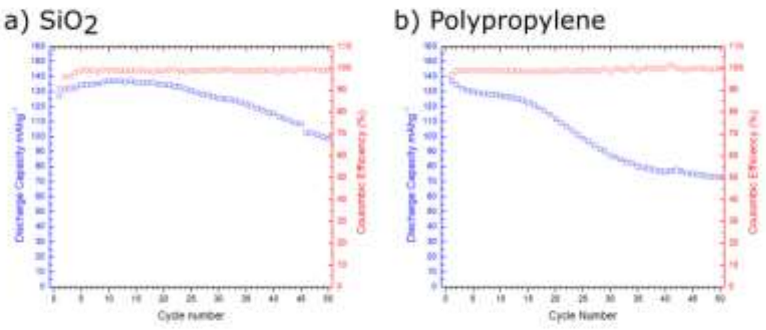

Figure 59. Discharge capacity and Coulombic efficiency of full cells with SiO_2 electrode coating as a separator (a) and a sheet of polypropylene as a separator (b).

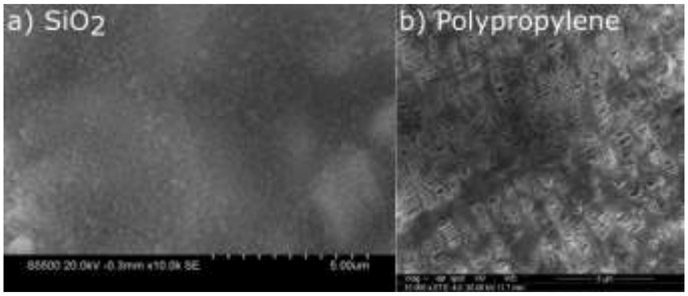

Figure 60. Scanning electron microscopy images of SiO_2 electrode coating and a sheet of polypropylene representative of the separator schemes used for cells, as shown in Figure 59.

Patents/Publications/Presentations

The project has no patents, publications, or presentations to report this quarter.

Task 4.6 – Advancing Solid-State Interfaces in Lithium-Ion Batteries
(Nenad M. Markovic and Larry A. Curtiss, Argonne National Laboratory)

Project Objective. The project objectives are multifaceted, including development of a new mechanically and chemically stable and Li-ion conductive ($\geq 2 \times 10^{-4}$ S/cm at 298 K) solid electrolyte for a solid-state battery encompassing a Li-metal anode, Li-oxide-based cathode, and nonflammable crystalline and amorphous solid electrolytes that can operate at cathode potentials > 5 V (denoted as a S_{Li}-S_{EL}-S_C system).

Project Impact. Protective organic and inorganic compounds can enhance stability of the interface, improve Li-ion interfacial transport, minimize dendrite formation, and increase safety in Li-ion batteries.

Approach. The project proposes to develop and use interdisciplinary, atomic-/molecular-level insight obtained from integrating both experimental- and computational-based methodologies to define the landscape of parameters that control interfacial properties for a new generation of the Li-ion solid-solid battery systems. The strategy will involve transferring knowledge gained from well-characterized thin-film materials to real-world materials. This strategy forms a closed loop wherein the knowledge gained from model systems is used to design more complex, real-world materials, and vice versa. The work will focus on utilizing existing in-house synthesis and characterization methods to enable rapid transition from fundamental science to realistic cells.

Out-Year Goals. The out-year goals are to use and develop the physical and chemical synthesis methods for design of solid-solid interfaces with unique chemical/mechanical/conductivity properties. The proposed work will develop and exploit a variety of *ex situ* and *in situ* experimental optical and surface sensitive techniques and electrochemical methods to explore and explain bulk and interfacial properties of the selected materials. The results will serve to unravel many puzzling bulk and interfacial properties of S_{Li}-S_{EL}-S_C systems, including various types of ceramic and glass materials.

Collaborations. This project funds work at ANL. It will establish collaboration with J. Sakamoto at University of Michigan.

Milestones

1. Understand the impact of different dopants in LLZO (niobium versus tantalum versus aluminum) on reactivity by surface and bulk sensitive techniques and spectroscopic methods. (Q1, FY 2019; Completed)
2. Determine the impact of solid electrolyte crystallinity (single crystal versus polycrystalline versus amorphous) on electrolyte reactivity by surface- and bulk-sensitive techniques and spectroscopic methods. (Q2, FY 2019)
3. Distinguish chemical versus electrochemical reactivity at the interface and bulk of model solid-state electrochemical systems with Li-metal anodes and $LiCoO_2$ cathodes by electrochemical testing and characterization. (Q3, FY 2019)
4. Determine dopant-dependent impact on chemical reactivity of different interfaces of solid-state electrolytes with lithium metal by computational characterization. (Q4, FY 2019).

Progress Report

LLZO-Li Bulk Stability. Cubic garnet $Li_7La_3Zr_2O_{12}$ (LLZO) stabilized with aluminum, niobium, or tantalum dopants is a particularly promising solid electrolyte for all-solid-state Li-metal batteries. The last report showed that the intrinsic reactivity of the Li-LLZO interface is dopant dependent. The team has determined that some degree of zirconium reduction takes place for all three dopant types and that significant reduction of niobium also takes place for Nb-doped LLZO. To determine whether the redox reaction is surface-limited, valence changes in the bulk were characterized. LLZO samples reacted with lithium were polished to remove surface layers, and XPS measurements of repolished samples reveal significant reduction of niobium species in the bulk of Nb-doped LLZO (Figure 61a). This suggests that lithium inserts into the niobium LLZO bulk as a result of the reaction with lithium metal, transforming Nb-doped LLZO from a solid electrolyte into a cathode material. In contrast to the niobium species, only Zr^{4+} is observed in the zirconium 3d core level spectrum of Al-, Nb- or Ta-doped repolished samples (Figure 61b), indicating that reduction of zirconium does not proceed further into the bulk and supporting the hypothesis that Zr^{4+} reduction is unrelated to Li^+ insertion at the LLZO-Li interface. Due to low aluminum doping concentration and spectrum overlapping with stronger copper 3s peak from copper impurities in the lithium target, it was not possible to analyze the aluminum valence state in Al-doped LLZO with XPS. Therefore, soft X-ray absorption measurements in total fluorescence yield mode (characterization depth > 100 nm from surface) were used to scan aluminum K edge to track valence change of aluminum. The XAS spectrum (Figure 61c) showed no significant changes before/after reaction with lithium. This result suggests that, unlike niobium, the aluminum species is at least stable in the bulk of LLZO and indicating the reaction is surface-limited.

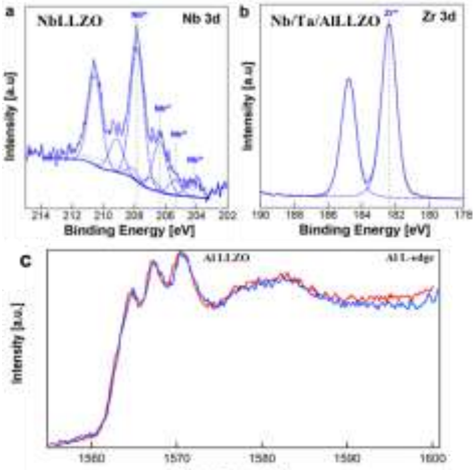

Figure 61. (a) Niobium 3d and (b) zirconium 3d core level X-ray photoelectron spectra and (c) aluminum L-edge X-ray absorption spectra reveal (a) the reduction of niobium and (b) no reactivity of zirconium for all doped LLZO and (c) no reactivity of aluminum.

Aluminum LLZO-Li Interfacial Impedance. Differences in bulk stability between LLZO dopant species are further highlighted when comparing the evolution of interfacial impedance with time. The previous report showed niobium LLZO-Li impedance increasing along with time, while tantalum LLZO-Li impedance is stable over 3 days of measurements. As for aluminum LLZO, EIS spectra (Figure 62a) exhibit two semicircles and a low-frequency tail/semicircle, and the best fit for these spectra was obtained using an (LR)-(RQ)-W equivalent electrical circuit model. The high-frequency region fit is provided in the inset of Figure 62. This model indicates an incomplete, first semicircle with a peak at ~ 300 kHz that corresponds to GB conduction in LLZO pellets. Resistance and capacitance value fittings of EIS spectra are summarized in the table in Figure 62, further demonstrating that the spectra for aluminum LLZO are essentially unchanged. To verify this assignment, a separate EIS measurement was carried out from 7-250 mHz using symmetric Au||LLZO||Au cells (Figure 62b), which further revealed the bulk impedance contribution and yielded GB impedance response similar to that in Li-Li symmetric cells.

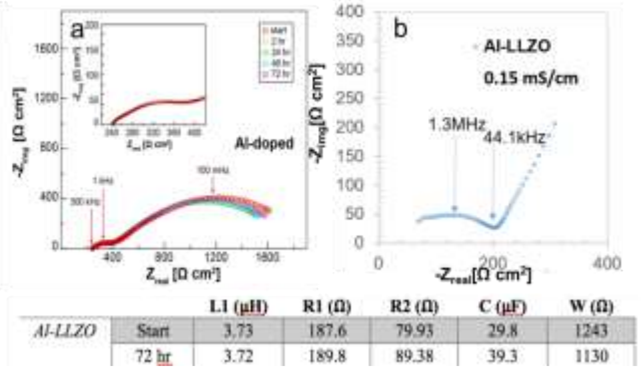

		L1 (μH)	R1 (Ω)	R2 (Ω)	C (μF)	W (Ω)
Al-LLZO	Start	3.73	187.6	79.93	29.8	1243
	72 hr	3.72	189.8	89.38	39.3	1130

Figure 62. Electrochemical impedance spectroscopy (EIS) results for (a) Li-Li symmetric cell with Al-doped LLZO and tracking the change in impedance of 72 hours. (b) Au||Al LLZO||Au cell measured in 7-250 mHz to determine bulk ionic conductivity. Induction, resistance, capacitance, and Warburg impedance value for fittings of EIS shown in the table.

Patents/Publications/Presentations

Publication

- Zhu, Y., J. G. Connell, S. Tepavcevic, P. Zapol, R. Garcia-Mendez, N. Taylor, J. Sakamoto, B. J. Ingram, L. A. Curtiss, D. D. Fong, J. W. Freeland, and N. M. Markovic. "Dopant-Dependent Stability of Garnet Solid Electrolyte Interfaces with Lithium Metal." Submitted to *Advanced Energy Materials*.

Task 4.7 – Mechanical and Defect Properties at the Protected Lithium Interface (Nancy Dudney, Oak Ridge National Laboratory; Erik Herbert, Michigan Technological University; Jeff Sakamoto, University of Michigan)

Project Objective. The project objective will be to understand the evolution of lithium metal on cycling in contact with a generic solid electrolyte under various intrinsic and extrinsic conditions. The team plans to construct a set of stability maps that will describe the predominate mass transport process and defect structure evolution in lithium metal. Simple maps may address current density, areal capacity, and layer thickness. Then, maps extending to many other cell designs, interfacial factors, and duty cycle parameters are envisioned. A key activity in FY 2018 will be to develop experimental tools with which to probe lithium morphology in real time. While initial work will focus on experimental characterization, modeling will be introduced to interpret kinetic processes and extrapolate for alternative properties and designs and extended cycling.

Project Impact. Stability maps can guide realistic design choices for solid electrolytes and cell design. Ideally, lithium is deposited and removed uniformly to maintain a fully dense anode in good contact with the solid electrolyte. However, in practice, this may not be realized depending on cycling conditions, nature of the electrolyte, nature of the lithium, and cell architecture. Mapping the lithium defect evolution will offer insight for when, how, and why the lithium structure is altered, along with a much deeper analysis of the degradation. With this insight, the team can realistically project the performance of optimized Li-metal anodes. Materials and cells can be engineered to fulfill the target level of performance for EV batteries, namely 1000 cycles, 15-year lifetime, with adequate pulse power.

Approach. The project will work to develop experimental tools to probe the lithium structure and its interfaces with mechanical, imaging, and electrochemical methods during mass transport and relaxation. Different constructions for the stability maps will be explored to identify the most useful graphical representation of what is expected to be a rich and detailed analysis of the formation and annealing of lattice and extended defects in the lithium metal.

Out-Year Goals. In the out-years, modeling efforts will be integrated to interpret and extrapolate the results to wide cycling conditions and detailed analysis of the solid electrolytes being used to stabilize the lithium metal.

Collaborations. This project funds work at ORNL, Michigan Technological University, and University of Michigan.

Milestones

1. Analysis of creep tests for glassy LiPON electrolyte, assessing dependence on the temperature and displacement of the indenter. (Q1, FY 2019; Completed)
2. Analysis of neutron imaging for lithium transport in LLZO using isotope exchange. (Q2, FY 2019; On schedule)
3. Evaluation of defect and microstructure formed in the cycled lithium metal and at the interfaces with the solid electrolyte. (Q3, FY 2019)
4. With German partners, assess whether dynamic impedance will detect early onset of voids in the lithium. (Q4, FY 2019)

Progress Report

The study to analyze the low-voltage stability of $Li_{6.25}Al_{0.25}La_3Zr_2O_{12}$ was completed (R. Garcia-Mendez, PhD candidate). Lithium three-electrode cells were assembled and tested to evaluate the Li-LLZO interface at and below 0 V versus Li/Li^+. This study controlled the potential and measured the current. At low under potentials, stable cycling was observed in which the Li-LLZO interface exhibited Ohmic behavior, confirmed by EIS measurement. However, at greater under potentials, deviation from Ohmic behavior was observed. The team hypothesizes that there is a critical voltage above which electronic conduction occurs within the solid electrolyte leading to internal Li-metal precipitation. The mechanism could be governed by quantum mechanics. This work can help understand the conditions under which lithium metal penetrates ceramic electrolyte and can enable solutions to stabilize metal anodes.

Nanoindentations of LiPON thin films were completed and reported last quarter. To reiterate, creep measurements were conducted at several temperatures and analyzed as viscoplastic flow behavior described by the constitutive equation $\dot{\varepsilon} = B\,\sigma^n$ where $\dot{\varepsilon}$ is the normalized strain rate, σ the stress, and n the stress exponent. To date, the stress exponent for LiPON films is a high number, ~ 20, and independent of temperature and displacement. Such a high value may be understood as the rearrangement of small atomic clusters in the material, rather than single atoms. The exponent indicates an activated volume of 112 $Å^3$, whereas a possible cluster unit of LiPON, being 3 Li^+ plus a PO_4^{-3} unit, would occupy 81 $Å^3$ in the dense glass. These characteristics of the glassy LiPON electrolyte are being incorporated into a mathematically tractable and transparent model that relates a 2D state of stress at the lithium/SSE interface to the average current density, the length scale of an interfacial defect, and lithium diffusional creep and/or dislocation plasticity stress relaxation mechanisms.

Patents/Publications/Presentations

Presentations

- MRS Fall Meeting, Boston, Massachusetts (November 2018): "Examining the Low Voltage Stability of $Li_{6.25}Al_{0.25}La_3Zr_2O_{12}$"; R. Garcia-Mendez. Invited.
- University of South Florida, Department of Physics, Department Seminar, St. Petersburg, Florida (November 2018): "Enabling Metallic Li Anodes through Solid-State Electrolytes"; J. Sakamoto.
- 59th Battery Symposium, Osaka, Japan (November 2018): "Enabling Metallic Li Anodes through Solid-State Electrolytes"; J. Sakamoto. Invited.
- Bunsen Colloquium on Solid-State Batteries, Frankfurt, Germany (November 2018): "Enabling Metallic Li Anodes through Solid-State Electrolytes"; J. Sakamoto. Plenary talk.
- Massachusetts Institute of Technology, Department of Materials Science, Department Seminar, Cambridge, Massachusetts (December 2018): "Enabling Metallic Li Anodes through Solid-State Electrolytes"; J. Sakamoto.

TASK 5 – SULFUR ELECTRODES

Summary and Highlights

The collected work reported for this Task involves six projects that have focused on the following:

- Developing new electrolytes, additives, and electrode compositions to prevent polysulfide dissolution in Li-S battery.
- Enabling sulfur cathodes with high capacity and long cycle life by developing sulfur cathodes from the perspective of nanostructured materials design, which will be used to combine with Li-metal anodes to generate high-energy Li-S batteries.
- Developing a novel S_xSe_y cathode material for rechargeable lithium batteries with high energy density and long life, as well as low cost and high safety.
- Delivering an electrochemically responsive self-formed hybrid LIC as a protective layer for Li-metal anodes, enabling Li-metal anodes to cycle with a high efficiency.
- Conducting focused fundamental research on the mechanism of "shuttle effect" inhibition for rechargeable Li-S batteries and to develop the electrode and electrolyte systems that can mitigate the "shuttle effect," enabling long cycle life.
- Exploring the fundamental reaction mechanism of polysulfide under the electrical field by applying advanced characterization techniques to accelerate development of Li-S battery technology.

Highlights. The reports detail considerable work conducted in both Li-S and Li-metal battery technologies. The salient results of these efforts are highlighted below:

- Research by Dr. G. Liu and his coworkers from LBNL have used RTIL 1-butyl-1-methyl-pyrrolidinium-bis(trifluorome-thanesulfonyl) imide as an electrolyte component to control polysulfide dissolution in Li-S batteries. The initial results demonstrate better capacity retention.
- Dr. Y. Cui and his group from Stanford University have combined a dark-field light microscopy (DFLM) technique with a planar electrochemical cell fabricated on a glass slide to visualize sulfur electrochemistry reactions *in operando*.
- Dr. K. Amine and researchers from ANL have determined that the parasitic reactions inside the Li-S battery have been significantly mitigated in concentrated siloxane electrolytes because of the solid-solid lithiation process, as is evident from the *in situ* selenium K-edge XANES measurements.
- Dr. D. Wang and fellow researchers from Pennsylvania State University have developed a 3D cross-linked polyethylenimine Li-ion-affinity sponge (3D PPS) as the Li-metal anode host using electrokinetic phenomena to mitigate the issues of Li-metal anode. They also demonstrate an electrokinetic surface conduction and electro-osmosis process occurring within the high-zeta-potential sponge change concentration and current density profiles, enabling dendritic-free plating/stripping of lithium with high CE at high deposition capacities and current densities, even at low temperatures.
- Dr. D. Qu (UWM) and Dr. X-Q. Yang (BNL) have together investigated various electrolyte compositions and have exploited the *in situ* electrochemical high-performance liquid chromatography (HPLC)/MS technique to understand chemical and electrochemical reactions of polysulfide species in these electrolytes.
- Dr. D. Lu and J. Liu (PNNL) have developed a new low-temperature phase of $Li_7P_2S_8Br_{0.5}I_{0.5}$ (LT-LPSBI) solid-state Li^+ conductor that possesses high Li^+ conductivity, and decent interfacial compatibility with sulfur active materials to enable fast sulfur/sulfide conversion at low-weight proportions of the electrode.

Task 5.1 – Novel Chemistry: Lithium Selenium and Selenium Sulfur Couple (Khalil Amine, Argonne National Laboratory)

Project Objective. The project objective is to develop a novel S_xSe_y cathode material for rechargeable lithium batteries with high energy density and long life, as well as low cost and high safety.

Project Impact. Development of a new battery chemistry is promising to support the goal of PHEV and EV applications.

Approach. The dissolution of lithium polysulfides in nonaqueous electrolytes has been the major contribution to the low energy efficiency and short life of Li-S batteries. In addition, the insulating characteristics of both end members during charge/discharge (sulfur and Li_2S) limit their rate capacity. To overcome this problem, sulfur or Li_2S is generally impregnated in a carbon-conducting matrix for better electronic conductivity. However, this makes it difficult to increase the loading density of practical electrodes. It is proposed to solve these barriers using the following approaches: (1) partially replace sulfur with selenium, (2) nano-confine the S_xSe_y in a nanoporous conductive matrix, and (3) explore advanced electrolytes with suppressed shuttle effect.

Out-Year Goals. This new cathode will be optimized with the following goals:

- A cell with nominal voltage of 2 V and energy density of 600 Wh/kg.
- A battery capable of operating for 500 cycles with low capacity fade.

Collaborations. This project engages in collaboration with the following: Professor C. Wang of UMD, Dr. Y. Ren, and Dr. C. Sun of Advanced Photon Source at ANL, and Dr. L. A. Curtiss at ANL.

Milestones

1. Leakage current measurement of Li/Se and Se-S systems in different electrolytes. (Q1, FY 2019; Completed)
2. Interfacial understanding on cycled lithium metal in different electrolytes. (Q2, FY 2019; In progress)
3. Computational understanding on the interactions of cations/anions with solvents in electrolytes. (Q3, FY 2019; In progress)
4. Rational cathode design for high areal loading Li/Se and Se-S systems. (Q4, FY 2019; In progress)

Progress Report

This quarter, the team investigated the parasitic reactions inside Li-S battery under different electrolytes. During charge (Figure 63a), the long-chain polysulfides will migrate from sulfur cathode to lithium anode and get the electrons from lithium metal, and then be reduced to short-chain polysulfides. These short-chain polysulfides will be migrated back to sulfur cathode due to concentration gradient difference and then oxidized back to long-chain polysulfides. This loop will continuously occur and eventually cause the capacity fading of Li-S battery. Thus, the measured static current will be proportional to the rate of parasitic reactions and can be correlated with the capacity fading of Li-S battery. Figure 63b shows a typical current relaxation curve collected; an exponential decay function was used to extract static current (y_0 in Figure 63b). Figure 63c compares the measured static current of Li-S battery in different electrolytes. As shown, in the ether-based electrolytes (both dilute and concentrated), the leakage current is much higher than that in the concentrated siloxane electrolytes. This indicates that the parasitic reactions inside Li-S battery have been significantly mitigated in the concentrated siloxane electrolytes. This is because of the solid-solid lithiation process as observed from the *in situ* selenium K-edge XANES measurement reported last quarter.

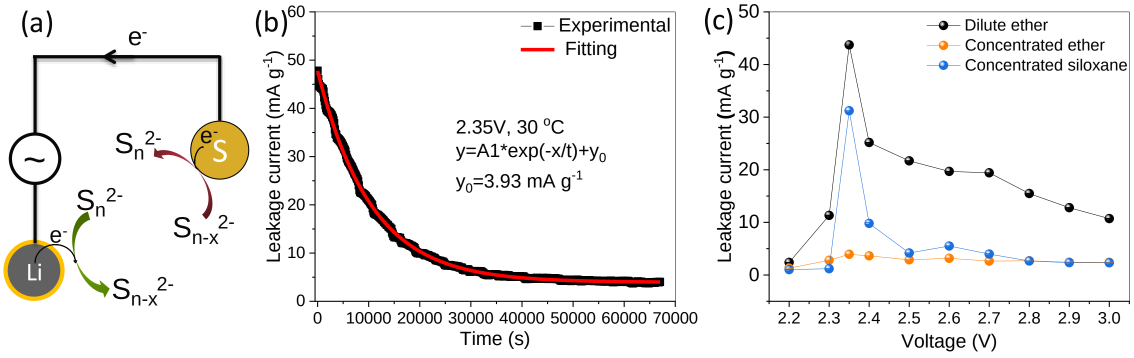

Figure 63. (a) Scheme for parasitic reactions inside Li-S battery during charge. (b) Representative current relaxation curve collected to extract static leakage current. (c) Leakage current measurement of Li-S battery in different electrolytes.

The team has further conducted *in situ* high-energy X-ray diffraction (HEXRD) on Li-S battery when charge/discharged in concentrate siloxane electrolytes. As shown in Figure 64a, the pristine sulfur cathode showed distinct diffraction peaks belong to crystalline sulfur. During discharge, it can be clearly seen that it is discharged to form amorphous Li_2S. During the charge process, no crystalline sulfur can be observed, confirming there is no dissolution of crystalline sulfur or Li_2S outside carbon matrix. Furthermore, the team has conducted *in situ* extended X-ray absorption fine structure (EXAFS) selenium K-edge measurement of Li/Se battery during cycling in concentrated siloxane electrolytes, as EXAFS is sensitive to the local environment, whether crystalline or amorphous. Figure 64b exhibits the standard EXAFS data of selenium and Li_2Se, which showed distinct features on bond distance. Figure 64c displays the contour plot of *in situ* EXAFS selenium K-edge data during cycling. As shown, the pristine Li/Se battery exhibited distinct features of selenium, remaining constant at the plateau region. At the end of the first discharge, one can clearly see formation of Li_2Se, but in amorphous state (confirmed by HEXRD). At the end of the first charge process, one can see the re-formation of amorphous selenium. The EXAFS study has further confirmed the two-phase transition process of Li/S and Li/Se battery when cycled in concentrated siloxane electrolytes. The team will further explore the interfacial property of cycled lithium metal under different electrolytes next quarter to uncover the relationship between electrolyte structures and performance.

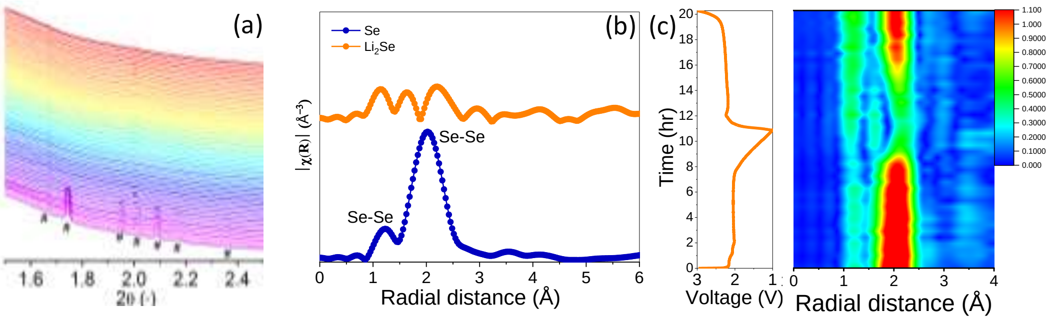

Figure 64. (a) ***In situ*** **high-energy X-ray diffraction measurements of Li/S battery in the concentrated siloxane electrolytes. (b) Extended X-ray absorption fine structure (EXAFS) selenium K-edge data of amorphous selenium and Li_2Se. (c) Contour plot of** ***in situ*** **EXAFS selenium K-edge data of Li/Se battery at C/10 in the concentrated siloxane electrolytes.**

Patents/Publications/Presentations

Publication

- Xu, G. L., H. Sun, C. Luo, L. Estevez, M. H. Zhuang, H. Gao, R. Amine, H. Wang, X. Zhang, C. J. Sun, Y. Z. Liu, Y. Ren, S. Heald, C. S. Wang, Z. Chen, and K. Amine. "Solid-State Lithium/Selenium-Sulfur Chemistry Enabled a Robust Solid-Electrolyte Interphase." *Advanced Energy Materials* (2018): 1802235.

Presentation

- Meeting Abstract, ACS National Meeting, Orlando, Florida (March 31–April 4, 2019): "Novel Chemistry for Automotive Application: Lithium-Selenium and Selenium-Sulfur Couple"; G-L. Xu, Z. Chen, and K. Amine.

Task 5.2 – Development of High-Energy Lithium-Sulfur Batteries
(Jun Liu and Dongping Lu, Pacific Northwest National Laboratory)

Project Objective. The project objective is to develop high-energy, low-cost Li-S batteries with long lifespan. All proposed work will employ thick sulfur cathode (≥ 2 mAh/cm^2 of sulfur) at a relevant scale for practical applications. The diffusion process of soluble polysulfide out of thick cathode will be revisited to investigate cell failure mechanism at different cycling. The fundamental reaction mechanism of polysulfide under the electrical field will be explored by applying advanced characterization techniques to accelerate development of Li-S battery technology.

Project Impact. The theoretical specific energy of Li-S batteries is ~ 2300 Wh/kg, which is almost three times higher than that of state-of-the-art Li-ion batteries. The proposed work will design novel approaches to enable Li-S battery technology and accelerate market acceptance of long-range EVs required by the EV Everywhere Grand Challenge.

Approach. The project proposes to (1) identify and address key issues of applying high-energy sulfur cathodes including materials, binders, electrode architectures, and functional electrode additives, (2) advance mechanism study of sulfur cathode and electrolyte by using *in situ*/*ex situ* techniques and custom-designed hybrid cell setup, and (3) verify effectiveness of the new approaches with coin/pouch cells by using high-loading electrodes (> 4 mg/cm^2), limited lithium (< 200% lithium excess), and lean electrolyte (E/S < 4 μL/mg).

Out-Year Goals. This project has the following out-year goals:

- Fabricate Li-S pouch cells with thick electrodes to understand sulfur chemistry/electrochemistry in environments similar to real application.
- Leverage the Li-metal protection project funded by the DOE and PNNL advanced characterization facilities to accelerate development of Li-S battery technology.
- Develop Li-S batteries with a specific energy of 400 Wh/kg at cell level, 1000 deep-discharge cycles, improved abuse tolerance, and less than 20% capacity fade over a 10-year period to accelerate commercialization of EVs.

Collaborations. This project engages in collaboration with the following: Dr. X-Q. Yang (BNL), Dr. D. Qu (UWM), Dr. G. Zhang (University of Alabama), and Dr. J Tao (PNNL).

Milestones

1. Synthesize high Li^+ conductivity sulfide based Li^+ conductors with room-temperature conductivity > 1 mS/cm for sulfur cathodes. (Q1, FY 2019; Completed)
2. Develop electrode preparation method for sulfur/Li^+-conductor cathodes with sulfur mass loading > 4 mg/cm^2 and sulfur > 75 wt% in whole electrode. (Q2, FY 2019; In progress)
3. Complete electrode composition and architecture optimization for low porosity sulfur electrodes (electrode density >1 g/cm^3). (Q3, FY 2019; In progress)
4. Complete electrochemical evaluation of high-loading sulfur electrodes (> 4 mg/cm^2) at E/S < 3 μL/mg, and identify compatible liquid electrolytes with the cathodes. (Q4, FY 2019; In progress)

Progress Report

Under practical conditions of high-loading cathode and lean amount of electrolyte, cycle life of Li-S battery is very limited. The excessive electrolyte consumption during deep Li-metal stripping/plating causes continuous increase of cell impedance. This leads to both capacity decay and shortened cell cycle life. Therefore, it remains a challenge to construct and maintain stable Li-ion conductive networks of cathode for long-term cycling. To address the issue of dependence of Li^+ transport solely on liquid electrolyte, additional solid Li^+ conductors were introduced into the electrode architectures, forming solid/liquid hybrid Li^+ conductive networks after adding a small amount of liquid electrolyte. To realize such a design, it is critical to develop solid-state Li^+ conductors that possess high Li^+ conductivity, and decent interfacial compatibility with sulfur active materials. High ionic conductivity is a prerequisite for the Li^+ conductors to enable fast sulfur/sulfide conversion at a low weight proportion of the electrode.

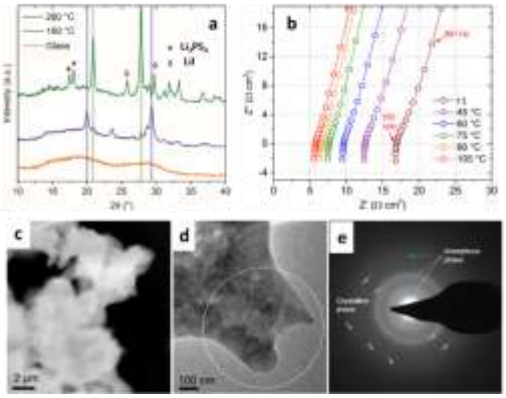

Figure 65. (a) X-ray diffraction patterns of the glass phase (bottom), LT-LPSBI (middle), and HT-LPSBI (top). (b) Nyquist plot of an In-SE-In (SE = LT-LPSBI) cell tested at various temperatures. (c) Scanning transmission electron microscopy (TEM) of LT-LPSBI powder. (d) Low magnification TEM image of the primary particle edge. (e) Electron diffraction of the circled region in (b).

This quarter, a new low-temperature phase of $Li_7P_2S_8Br_{0.5}I_{0.5}$ (LT-LPSBI) was synthesized by mechanical mill of precursors followed by annealing. The precursor mixture was completely reduced to the amorphous state after mechanically ball-milling as shown in Figure 65a. On heating, the amorphous product underwent two exothermic events according to the differential thermal analysis (DTA), with onsets at around 180°C and 230°C, respectively. The two events correspond to crystallization of the metastable LT-LPSBI phase and crystallization of high-temperature phase LPSBI (HT-LPSBI). To minimize the conversion to HT-LPSBI, LT-LPSBI was obtained by annealing at 160°C for 60 h. Three major diffraction peaks were observed at 20.0°, 23.6° and 29.3°, which are ascribed to diffraction of LT-LPSBI phase (Figure 65a). The peaks of LT-LPSBI were broader than those of HT-LPSBI, indicating the presence of nanocrystals or amorphous phase along with the crystalline phase. This is proved by the STEM and selected area electron diffraction (SAED) characterization (Figure 65c-e). The LT-LPSBI shows loosely interconnected morphology composed of micro-sized primary particles. Results of SAED indicate the existence of both crystalline and amorphous phases, which is consistent with the XRD analysis results. This is the first time that these two phases have been identified. The ionic conductivities of the glass, LT-LPSBI, and HT-LPSBI were characterized by impedance spectroscopy. A typical impedance plot consisted of a straight line that intercepts with the real axis at high frequency, representing the electrode response. The bending below the real axis above 100 kHz was due to stray inductance. The ionic conductivity of LT-LPSBI was measured 4.7 mS/cm at room temperature (Figure 65b), which is comparable to LGPS-type materials or crystalline $Li_7P_3S_{11}$ in cold-pressed state. In comparison, the room-temperature conductivities of the glass phase and HT-LPSBI were 0.8 mS/cm and 0.05 mS/cm, respectively. The activation energy E_a of the three phases was calculated based on the Arrhenius equation, $\sigma = \sigma_0/T \exp(-E_a/kT)$, and the E_a of the three phases follows the inverse trend of the ionic conductivities: 0.31 eV, 0.26 eV, and 0.20 eV for HT, glass, and LT, respectively. The LT-LPSBI was used for preparation of high Li^+ conductive sulfur cathodes.

Patents/Publications/Presentations

Publication

- Wang, Y., D. Lu, J. Xiao, Y. He, C. Wang, J. Zhang, and J. Liu. "Superionic Conduction and Interfacial Properties of the Low Temperature Phase $Li_7P_2S_8Br_{0.5}I_{0.5}$." *Energy Storage Materials*. Under revision.

Presentation

- International Coalition for Energy Storage and Innovation and Pacific Power Source Symposium (ICESI-PPSS 2019), Waikoloa Village, Hawaii (January 2019): "Development of High Energy Lithium-Sulfur Batteries: From Materials to Pouch Cell"; D. Lu, J. Xiao, L. Shi, A. Baranovskiy, J. Zhang, and J. Liu.

Task 5.3 – Nanostructured Design of Sulfur Cathodes for High-Energy Lithium-Sulfur Batteries (Yi Cui, Stanford University)

Project Objective. The charge capacity limitations of conventional TM oxide cathodes are overcome by designing optimized nano-architectured sulfur cathodes. This study aims to enable sulfur cathodes with high capacity and long cycle life by developing sulfur cathodes from the perspective of nanostructured materials design, which will be used to combine with Li-metal anodes to generate high-energy Li-S batteries. Novel sulfur nanostructures as well as multi-functional coatings will be designed and fabricated to overcome issues related to volume expansion, polysulfide dissolution, and the insulating nature of sulfur.

Project Impact. The capacity and the cycling stability of sulfur cathode will be dramatically increased. This project's success will make Li-S batteries to power EVs and decrease the high cost of batteries.

Approach. The approach comprises the three main parts shown below, with primary activities listed.

- ***Advanced Nanostructured Sulfur Cathodes Design and Synthesis.*** (1) Engineer empty space into sulfur cathode to solve the problem of electrode volume expansion; (2) Develop novel sulfur nanostructures with multi-functional coatings for the confinement of sulfur/lithium polysulfides to address the issues of active materials loss and low conductivity; (3) Develop/discover optimal nanostructured materials that can capture the polysulfide dissolved in the electrolyte; (4) Develop space efficiently packed nanostructured sulfur cathode to increase the volumetric energy density and rate capability; and (5) Identify the interaction mechanism between sulfur species and different types of oxides/sulfides, and find the optimal material to improve the capacity and cycling of sulfur cathode.
- ***Structure and Property Characterization.*** (1) *Ex situ* SEM; (2) XPS analysis; and (3) *In operando* XRD and optical microscopy.
- ***Electrochemical Testing.*** (1) Coin cells and pouch cells; and (2) a set of electrochemical techniques.

Out-Year Goals. The cycle life, capacity retention, and capacity loading of sulfur cathodes will be greatly improved (200 cycles with 80% capacity retention, > 0.3 mAh/cm^2 capacity loading) by optimizing material design, synthesis, and electrode assembly.

Collaborations. This project engages in collaboration with the following: BMR PIs; SLAC National Accelerator Laboratory: Dr. M. Toney (*In situ* X-ray); and Stanford: Professor Nix (mechanics) and Professor Bao (materials).

Milestones

1. Build *in situ* characterization platform to monitor nucleation/dissolution of sulfur/Li_2S_n. (Q1, FY 2019, October 2018; Completed)
2. Develop a non-invasive imaging method with sub-micron, sub-second resolution for Li-S battery in label-free, native organic liquid electrolyte. (Q2, FY 2019, January 2019; Completed)
3. Demonstrate the substrate-dependent electrochemical formation of super-cooled liquid sulfur and crystals, as well as rapid solidification of a super-cooled sulfur droplet. (Q3, FY 2019, April 2019; Ongoing)

Progress Report

Last quarter, the team built *in situ* characterization platform to monitor nucleation/dissolution of sulfur to provide direct evidence about a long-debated reaction pathway for sulfur. This quarter, using this technique, the team was able to directly observe multiple new phenomena in Li-S batteries for the first time, including electrochemical generation of metastable liquid sulfur at room temperature on different substrates, and the growth of sulfur crystals on commonly used carbon materials.

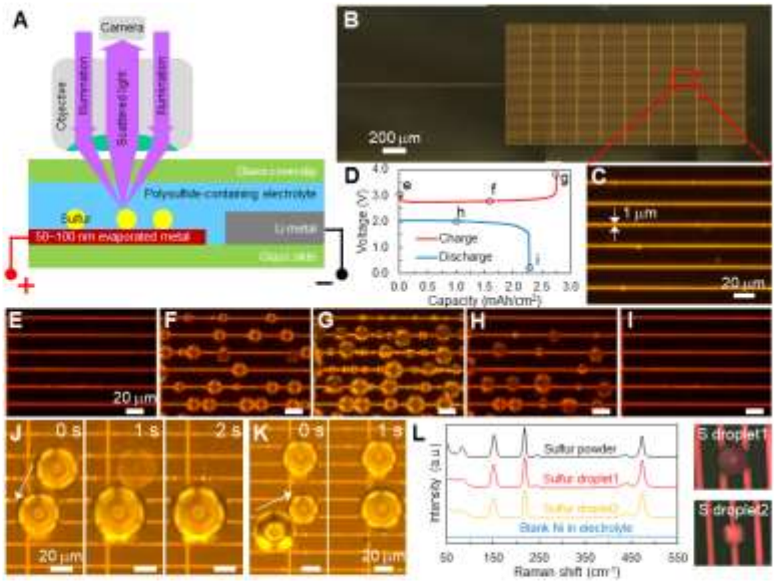

Figure 66. (a) Schematic of the electrochemical cell design that allows *in operando* dark-field light microscopy (DFLM) observation. (b-c) DFLM images of the metal grid (50-nm thick, 1-µm wide) fabricated on glass slide as a substrate for the electrochemical cell. (d) Voltage profile of the cell. Time-lapse DFLM images (e-i) showing the formation and dissolution of super-cooled sulfur droplets. (j/k) Two sets of time-lapse images showing rapid merging of neighboring droplets and relaxation to spherical shape within one second, indicating the liquid nature of sulfur. (l) *In situ* Raman spectra of super-cooled sulfur droplets. Corresponding bright-field light microscopy images captured by the Raman microscope are shown on the right. The spectra match that of solid S_8 powder, and the signals are not from electrolyte or substrate.

This quarter, the project reports on combining DFLM and a planar electrochemical cell fabricated on a glass slide to visualize sulfur electrochemistry *in operando*. A metal grid electrode (1 µm in line width, 50 nm in height) was deposited on a glass substrate via e-beam lithography for galvanostatic charging/discharging at room temperature (Figure 66a-d). During electrochemical cycling, liquid-like sulfur microspheres formed on nickel grids toward the end of charging (formation starts at ~ 2.8 V), and reversibly reduced into soluble polysulfide on discharging (Figure 66e-i). Well-separated nickel grids allowed sulfur microspheres to be individually resolved and monitored. The microspheres are spherical, semi-transparent to light, and form over the entire surface of nickel grid electrode. As they grew larger and approached each other, neighboring droplets occasionally merged into larger droplets that relaxed rapidly to a spherical shape to minimize surface energy (Figure 66j-k). To confirm the chemical composition of microdroplets, micro Raman spectroscopy was performed on the same sealed electrochemical cell. The Raman spectrometer had sufficient spatial resolution to collect spectra on individual sulfur microdroplets (Figure 66l). The spectra of the droplets match that of solid sulfur powders but not polysulfides, indicating the liquid droplets are chemically cyclo-sulfur (S_8). Eutectic alloys of sulfur with other elements can significantly alter the freezing temperature, but the Raman spectra rule out this possibility. On the other hand, it is well known that small amounts of impurities serve as heterogeneous nucleation sites that limit the degree of supercooling. Sulfur in its molten state is also known to form polymeric chains, but earlier Raman spectroscopy investigations of the polymerization of S_8 monomers into higher order S_n polymers concluded that polymerization occurs at temperatures greater than 140°C.

In addition to nickel, these super-cooled liquid sulfur microdroplets electrochemically form on various other metal-containing substrates, including palladium, platinum, indium tin oxide (ITO), and cobalt sulfide (CoS_2) (Figure 67a). In contrast, carbon substrate (polished glassy carbon) leads to the formation of irregular crystalline solid sulfur particles that do not undergo significant changes when contacting with each other (Figure 67b). Therefore, the electrochemical formation of super-cooled sulfur is both generic and substrate-dependent. It should be noted that the super-cooling reported here is unlikely to stem from a size effect. Liquid-like behaviors have been shown to accompany extremely small (< 10 nm) particles, but the droplets reported here are micron-scale, whose melting point is close to bulk according to Gibbs-Thomson equation.

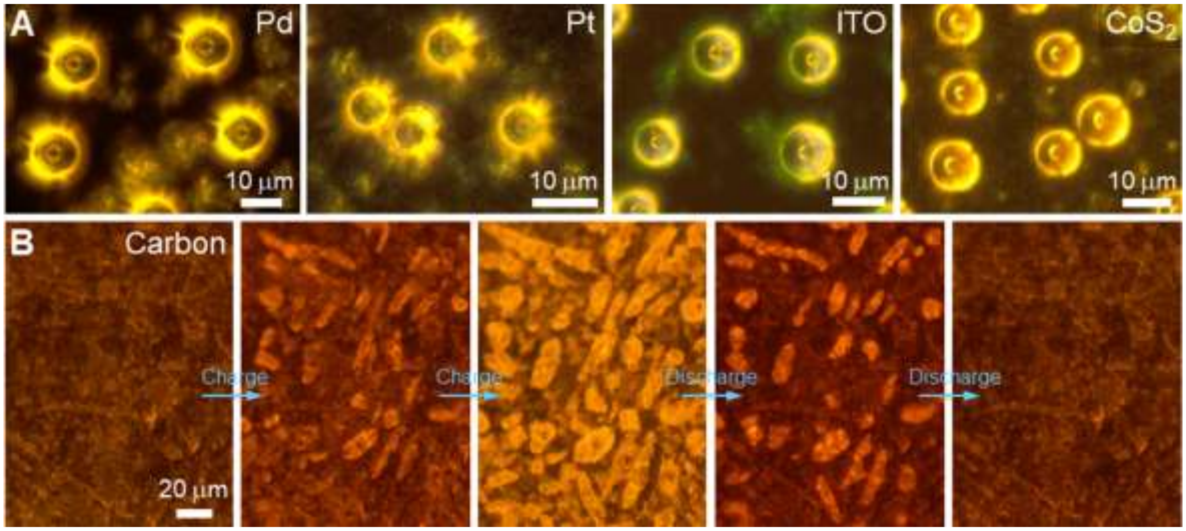

Figure 67. (a) *In operando* dark-field light microscopy (DFLM) images of sulfur droplets electrochemically formed on palladium, platinum, indium tin oxide (ITO), and cobalt sulfide (CoS_2) substrates. (b) Time-lapse *in operando* DFLM images of crystalline sulfur formation and dissolution on glassy carbon substrate.

Patents/Publications/Presentations

The project has no patents, publications, or presentations to report this quarter.

Task 5.4 –Investigation of Sulfur Reaction Mechanisms (Deyang Qu, University of Wisconsin at Milwaukee; Xiao-Qing Yang, Brookhaven National Laboratory)

Project Objective. The primary objectives are:

- To continue conducting focused fundamental research on the mechanism of "shuttle effect" inhibition for rechargeable Li-S batteries;
- To continue developing the electrode and electrolyte systems that can mitigate the "shuttle effect" so low self-discharge and long cycle life can be achieved.
- To synthesize sulfur composite material with an emphasis on polymer sulfur composite materials.
- To develop creative electrode making processes to improve processability and aerial capacity; for example, polymeric sulfur composite may be unsuitable for the traditional slurry casting process.

The ultimate goal of this project is to develop a practical rechargeable Li-S battery that meets the challenges of powering the next generation of EVs beyond Li-ion technologies.

Project Impact. With the unique *in situ* electrochemical-HPLC/MS and *in situ* electrochemical microscopic techniques developed in this project, the mechanisms of all reactions in a Li-S cell can be further understood. Better understanding the sulfur redox reaction will lead to mitigation of the "shuttle effect." The project results will thus guide development of polymer sulfur cathode and Li-S designs for EVs.

Approach. This project will use *in situ* electrochemical-HPLC/MS, XPS, SEM, and XRD to study electrochemical reactions associated with sulfur electrodes. Electrochemical techniques such as AC impedance, rotation ring disk electrode, and galvanostat will be used to study the electrode process kinetics. The project will use an *in situ* electrochemical optical method to investigate the surface of lithium anode during cycling of a Li-S cell. It will develop thicker sulfur electrode with high areal capacity using dry process.

One-Year Goals. The one-year goals include the following: Complete the investigations of new electrolytes for the mitigation of the "shuttle effect" and improvement of the Li-anode performance. Complete preliminary design of new electrode processes and tests of polymeric sulfur composite electrodes.

Collaborations. The PI, D. Qu, is the Johnson Controls Endowed Chair Professor; thus, the UWM and BNL team has close collaboration with Johnson Controls' scientists and engineers. This collaboration enables the team to validate the outcomes of fundamental research in pilot-scale cells. This team has been closely working with top scientists on new material synthesis at ANL, LBNL, and PNNL, with U. S. industrial collaborators at GM, Duracell, and Johnson Controls as well as international collaborators in China, Japan, and South Korea. These collaborations will be strengthened and expanded to give this project a vision on both today's state-of-the-art technology and tomorrow's technology in development, with feedback from the material designer and synthesizers upstream and from industrial end users downstream.

Milestones

1. Literature review and molecular design of polymeric sulfur compounds. (Q1, FY 2019; Completed)
2. Complete screening electrolyte and additives for the Li-S batteries. Start synthesis of polymeric sulfur compounds. (Q2, FY 2019)
3. Complete preliminary designs of electrode manufacture process and start to explore feasibility for the synthesized polymeric sulfur composite. (Q3, FY 2019)
4. Complete initial design of electrode manufacture processes and tests of synthesized polymeric sulfur materials. (Q4, FY 2019)

Progress Report

This quarter, the team continued investigating various electrolyte compositions, used established *in situ* electrochemical HPLC/MS technique to understand the chemical and electrochemical reactions of polysulfide species in those electrolytes, and conducted an extensive literature review for polymer sulfur chemistry. Based on findings from the literature research, polymer sulfur materials were synthesized and tested as Li-S cathode.

An example of a typical synthesis mechanism of a sulfur-polymer is shown in Figure 68, with selective unsaturated cross-linkers for sulfur-containing polymers shown in Figure 69.

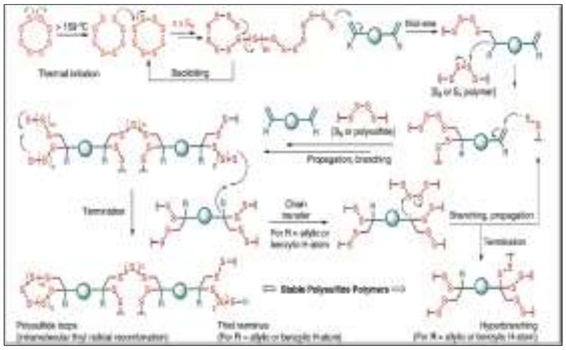

Figure 68. Example of synthesis route of a sulfur co-polymer compound. Chalker, et al., *Green Chemistry* 19 (2017): 2748.

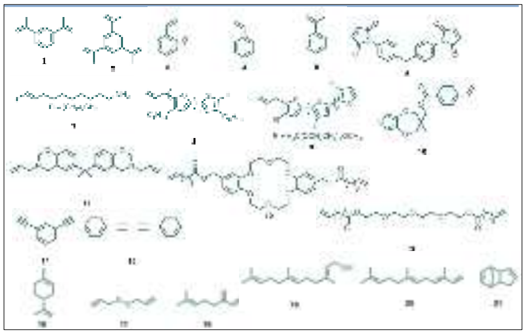

Figure 69. The selection of possible cross-linking groups for the co-polymers.

To ensure entrapment of all polysulfides in the cathode matrix, the binding energy between polysulfides and backbone (polymer) or the matrix must be stronger than the solvation energy of polysulfide and lithium ion with solvent. Cross linking is an effective way for restriction of polysulfides with the electrode matrix, since the mobility of polysulfides can be limited by chemical bonding or relatively strong Van de Waals forces. However, engineering challenges remain, especially in material processing. The copolymer compounds are elastic in nature and thus have a low packing density. Many of those compounds are also difficult to dissolve in solvent, so the traditional slurry casting technique widely used in Li-ion electrode manufacture may be inadequate for making sulfur copolymer electrodes. Table 2 and Figure 70 show performance of the ten copolymer cathodes reported last quarter, but made with improved processes. Improvement can be demonstrated.

Table 2. Test results of ten synthesized co-polymers reported last quarter, but with improved electrode processes.

	1st Dischage Capacity (mAh/g)	100th Discharge Capacity (mAh/g)	200th Discharge Capacity (mAh/g)
1	632.9	467.8	340.7
2	671.2	359.3	371.8
3	783.2	374.8	n/a
4	252.3	242.3	201.1
5	1091.8	580.7	n/a
6	210.9	68.5	56.7
7	696.6	323.4	274.8
8	749.9	319.0	178.7
9	227.3	190.3	133.4
10	743.5	374.9	290.2
S8	1364.0	300.9	207.5

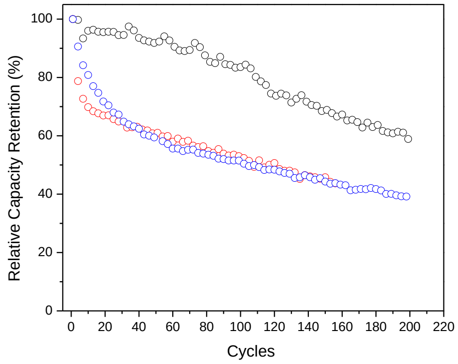

Figure 70. Comparison of relative capacity retention of three selected copolymer cathodes.

Patents/Publications/Presentations

The project has no patents, publications, or presentations to report this quarter.

Task 5.5 – Electrochemically Responsive, Self-Formed, Lithium-Ion Conductors for High-Performance Lithium-Metal Anodes
(Donghai Wang, Pennsylvania State University)

Project Objective. The project objective is to develop and deliver an electrochemically responsive self-formed hybrid LIC as a protective layer for Li-metal anodes, enabling Li-metal anodes to cycle with a high efficiency of ~ 99.7% at high electrode capacity (> 6 mAh/cm^2) and high current density (> 2 mA/cm^2) for over 500 cycles. The project will also demonstrate prototype ~ 300 mAh Li-S battery cells with energy densities of ~ 200 Wh/kg and ~ 80% capacity retention for ~ 300 cycles at ~ 80% depth of discharge using Li-metal anodes with this protective layer.

Project Impact. This project aims to develop a new hybrid LIC that enables safe and high-performance Li-metal anodes. Use of these anodes in turn enables Li-S batteries with high energy density and long cycling life. Such anodes can also lead to a 50% increase in the energy density of conventional Li-ion batteries with Li-metal oxide cathodes. Meeting the technical targets will potentially develop a new high-energy-density lithium battery, promote increased adoption of EVs and PHEVs, and reduce petroleum consumption in the transportation sector by helping battery-powered vehicles become accepted by consumers as a reliable source of transportation.

Approach. The novel multiphase organo-Li_xS_y or organo-$Li_xP_yS_z$ hybrid ion conductors with tunable multi-functional organic components and controlled Li_xS_y and $Li_xP_yS_z$ inorganic components will be designed and prepared, and thus enable safe use of lithium metal with high CE. In the third year, the team will develop the organo-Li_xS_y/organo-$Li_xP_yS_z$ composite lithium protection layers with tuned functionality: (1) finding appropriate composition, (2) developing appropriate synthesis and fabrication methods, and (3) optimizing organo-Li_xS_y/organo-$Li_xP_yS_z$ components in a protection layer to improve CE and Li-S battery performance.

Out-Year Goals. The project is working toward developing the organo-Li_xS_y/organo-$Li_xP_yS_z$ composite lithium protection layers with tuned functionality. Characterization, performance, and compatibility tests on materials and systems will be conducted. Uniform, dendrite-free lithium deposition under protection of organo-Li_xS_y/organo-$Li_xP_yS_z$ composite lithium protection layers will be demonstrated; CE will be improved.

Collaborations. There are no active collaborations.

Milestones

1. Develop the organo-Li_xS_y/organo-$Li_xP_yS_z$ composite lithium protection layers with tuned functionality. Conduct characterization and performance tests on the materials. (Q1, FY 2019; In progress)
2. Demonstrate uniform and dendrite-free lithium deposition under protection of the organo-Li_xS_y/organo-$Li_xP_yS_z$ composite lithium protection layers. (Q2, FY 2019)
3. Optimize the organo-Li_xS_y/organo-$Li_xP_yS_z$ composite lithium protection layers and demonstrate lithium anodes cycling with ~ 99.4% CE for ~ 200 cycles. (Q3, FY 2019)
4. Demonstrate lithium anodes with optimized organo-Li_xS_y/organo-$Li_xP_yS_z$ composite lithium protection layers and ~ 99.7% CE for ~ 300 cycles. (Q4, FY 2019)

Progress Report

The team is developing a 3D cross-linked polyethylenimine lithium-ion-affinity sponge (3D PPS) as the Li-metal anode host and uses electrokinetic phenomena to mitigate issues of Li-metal anode. They show that electrokinetic surface conduction and electro-osmosis within the high-zeta-potential sponge (Figure 71a) change concentration and current density profiles, enabling dendritic-free plating/stripping of lithium with high CE at high deposition capacities and current densities, even at low temperatures. The use of Li-hosting sponge leads to a significantly improved cycling stability of Li-metal batteries with a limited amount of lithium (for example, N/P ratio = 0.6) at commercial-level areal capacity.

The 3D PPS was prepared directly on copper foil by an ice-templating method through crosslinking of branched polyethylenimine (PEI) by 1, 4-butanediol diglycidyl ether (BGE) (Figure 71c). SEM investigation of the 3D PPS host on copper foil (3D PPS@Cu) along top and cross-section views (Figure 71d-e, respectively) reveals sponge-like porous structure containing irregularly shaped pores. The pores in 3D PPS have a high interconnectivity. The 3D PPS has a pore volume of ~ 5.5 cm^3 g^{-1} and a porosity of 87%, and therefore can accommodate deposited lithium as high as 74.6 wt% within the sponge host. 3D PPS has many polar groups (amine and ether) that have strong affinity with lithium ions and self-concentrate lithium ions (self-concentrating feature). The Li-ion-affinity groups direct formation of EDL in 3D PPS with a high zeta potential of approximately +42 mV in the electrolyte (1.0 M LiTFSI in 1, 3-dioxolane (DOL) and 1, 2-dimeth-oxyethane (DME) with a volume ratio of 1:1). The existence of EDL promotes electrokinetic phenomena, such as electrokinetic surface conduction and electro-osmosis (electrokinetic pumping feature), within the sponge under an electric field. The Li-ion electrokinetic self-concentrating and pumping features of the 3D PPS can synergistically overcome diffusion limited current (Figure 72a), reduce the concentration polarization (Figure 72b-h), and therefore regulate the Li-ion concentration difference in deionization area to enable a uniform Li-ion distribution (Figure 72f).

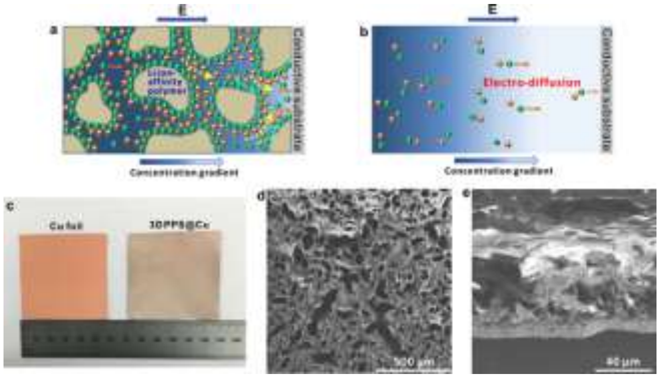

Figure 71. (a) Electrokinetic phenomena (for example, electrokinetic surface conduction and electro-osmosis) in 3D PPS under electric field. (b) Electro-diffusion of lithium ions in traditional cells under electric field. (c) Photograph of bare copper foil and 3D PPS@Cu. (d) Scanning electron microscopy (SEM) morphology of 3D PPS@Cu (top view). (e) SEM morphology of 3D PPS@Cu (cross-section view).

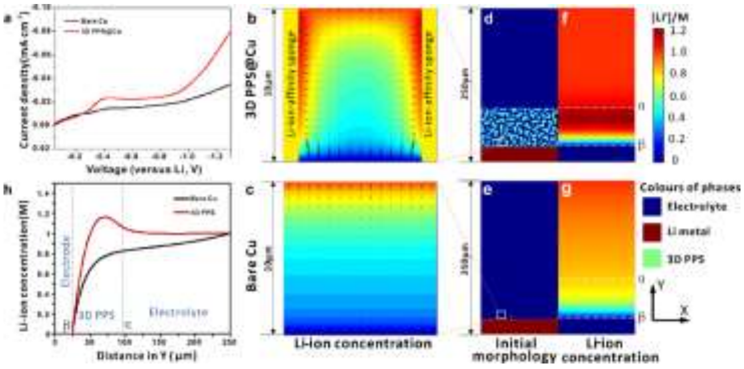

Figure 72. The Li-ion electrokinetic self-concentrating and pumping features of the 3D PPS. (a) Linear sweep voltammetry of 3D PPS@Cu and bare copper electrode. (b-c) Equilibrium Li-ion concentration profiles with constant-reaction-current electrode surfaces at enlarged 10×10 $\mu m2$ sponge-pore scale for (b) 3D PPS@Cu and (c) bare copper electrode. (d-e) Initial phase morphologies of 250×250 $\mu m2$ (d) 3D PPS@Cu and (e) bare copper half-cell systems. (f-g) Equilibrium Li-ion concentration profiles with constant-reaction-current electrode surfaces at the 250×250 $\mu m2$ scale for (f) 3D PPS@Cu and (g) bare copper electrode. (h) 1D cross-sectional equilibrium Li-ion concentration profiles along Y direction in 3D PPS@Cu and bare copper electrode.

Benefiting from the Li-ion electrokinetic self-concentrating and pumping effects of 3D PPS, dendrite-free Li plating/stripping on 3D PPS@Cu at both high deposition capacity and high current density are achieved in various electrolytes. Compared with bare copper electrode typical of mossy dendritic structure of lithium (Figure 73a-b), 3D PPS@Cu exhibits a uniform, compact, and dendrite-free lithium conformally deposited within 3D PPS at various deposition capacities and current densities in ether-based electrolyte (2 mA h cm^{-2} and 2 mA cm^{-2} in Figure 73c-f; 2 mA h cm^{-2} and 4 mA cm^{-2}

in Figure 4a-d; 4 mA h cm^{-2} and 4 mA cm^{-2} in Figure 4e-h; 4 mA h cm^{-2} and 6 mA cm^{-2} in Figure 4i-l). Remarkably, at extremely high deposition capacities and current densities (6 mA h cm^{-2} and 6 mA cm^{-2} in Figure 3i-l; 4 mA h cm^{-2} and 12 mA cm^{-2} in Figure 5a-d; 4 mA h cm^{-2}, and 20 mA cm^{-2} in Figure 5e-h), the deposited lithium still shows a uniform, compact morphology and a conformal structure within 3D PPS. Strikingly, even at low temperatures, uniform and dendrite-free lithium deposition is still observed within 3D PPS at a high current density of 20 mA cm^{-2} and a deposition capacity of 4 mA h cm^{-2} (0°C and -10°C, as shown in Figures 76 and 77, respectively).

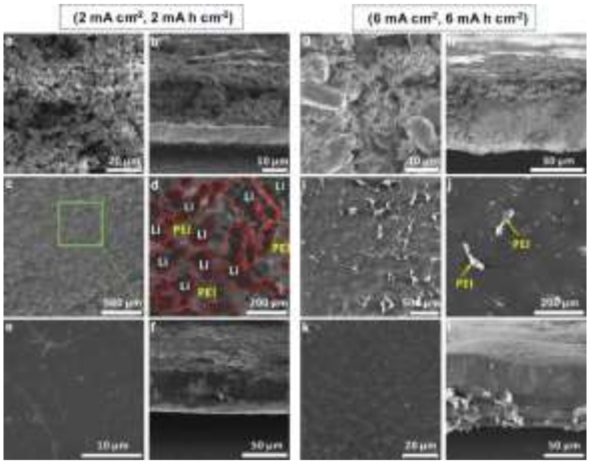

Figure 73. The morphology of lithium metal deposited on the different electrodes. Scanning electron microscopy (SEM) images of lithium metal deposited on the bare copper electrode (a-b) and 3D PPS@Cu (c-f) at a deposition capacity of 2 mA h cm^{-2} and current density of 2 mA cm^{-2}. SEM images of lithium metal deposited on the bare copper electrode (g-h) and 3D PPS@Cu (i-l) at a deposition capacity of 6 mA h cm^{-2} and current density of 6 mA cm^{-2}. The electrolyte used here is 1.0 M LiTFSI in DOL and DME (V/V = 1) with 1 wt% $LiNO_3$.

The uniform and dendrite-free lithium within 3D PPS@Cu leads to significantly improved CE and cycling stability of lithium plating/stripping. When measured at a deposition capacity of 2 mA h cm^{-2} and a current density of 2 mA cm^{-2}, the cells with 3D PPS@Cu electrodes exhibit a long cycle life over 800 cycles with an average CE as high as 99.1% (Figure 78a). When elevating the deposition capacity to 4 mA h cm^{-2} and the current density to 4 mA cm^{-2}, a high average CE of 99% over 450 cycles is achieved (Figure 78b). More notably, under extremely high deposition capacity and current density (6 mA h cm^{-2} and 6 mA cm^{-2}), the 3D PPS@Cu electrodes show a peerless lithium plating/stripping performance undemonstrated to date with an average CE of 98.9% for more than 300 cycles (Figure 78c).

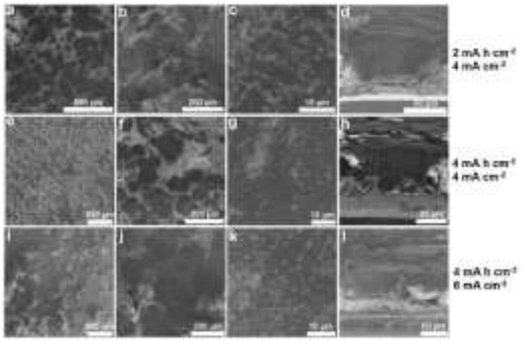

Figure 74. The morphology of lithium metal deposited on the 3D PPS@Cu at different deposition capacities and current densities. The electrolyte used here is LiTFSI/DOL+DME+1 wt% $LiNO_3$.

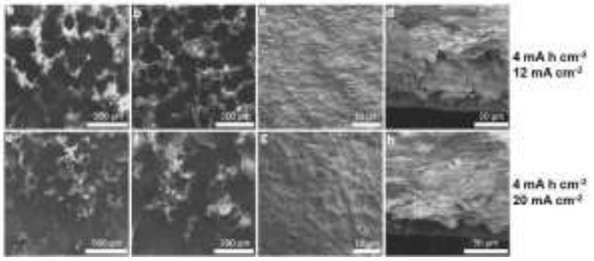

Figure 75. The morphology of lithium metal deposited on the 3D PPS@Cu at extremely high current densities and a deposition capacity of 4 mA h cm^{-2}. (a-d) Current density of 12 mA cm^{-2}. (e-h) Current density of 20 mA cm^{-2}. The electrolyte used here is 1.0 M LiTFSI/DOL+DME+1 wt% $LiNO_3$.

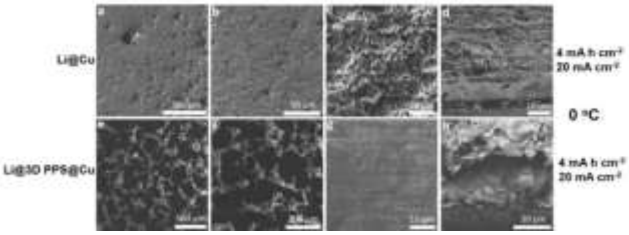

Figure 76. The morphology of lithium metal deposited on the bare copper electrode and 3D PPS@Cu at 0°C with a high current density of 20 mA cm^{-2} and a deposition capacity of 4 mA h cm^{-2}.

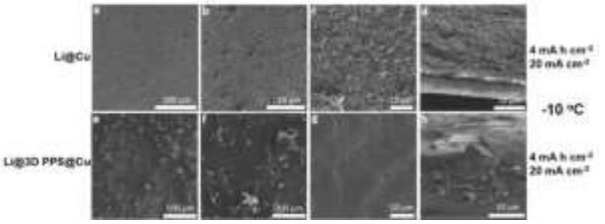

Figure 77. The morphology of lithium metal deposited on the bare copper electrode and 3D PPS@Cu at -10°C with a high current density of 20 mA cm^{-2} and a deposition capacity of 4 mA h cm^{-2}.

The high CE of lithium plating/stripping within 3D PPS@Cu allows the team to fabricate 3D PPS@Cu with limited amount of lithium (designated as Li@3D PPS@Cu) as anode, potentially achieving a high-energy-density Li-metal battery with excellent cycling life. The team demonstrated this advantage in full cells assembled using Li@3D PPS@Cu anodes and $LiFePO_4$ cathodes. At a low N/P ratio of 0.6 (areal lithium amount ratio of negative to positive electrodes, termed N/P ratio), the full cell exhibits an initial capacity of 146.7 mA h g^{-1} (areal capacity of 2.5 mA h cm^{-2}) and maintains a stable cycling performance over 200 cycles with an average CE of ~ 99.7% (Figure 78d). The team attributes the excellent cycling performance of full cells to stable Li@3D PPS@Cu anodes confirmed by their dendrite-free morphology after 50 cycles, as shown in SEM images (Figure 78e-h). When the high-areal-capacity $LiFePO_4$ cathodes (3.8 mA h cm^{-2}) were used, the full cells deliver an initial capacity of 149 mA h g^{-1} and show excellent cyclability of 400 cycles with average CE of ~99.78% at a N/P ratio of 2 (Figure 78i); this confirms the excellent cycling stability of Li@3D PPS@Cu anodes in a practical cycling condition.

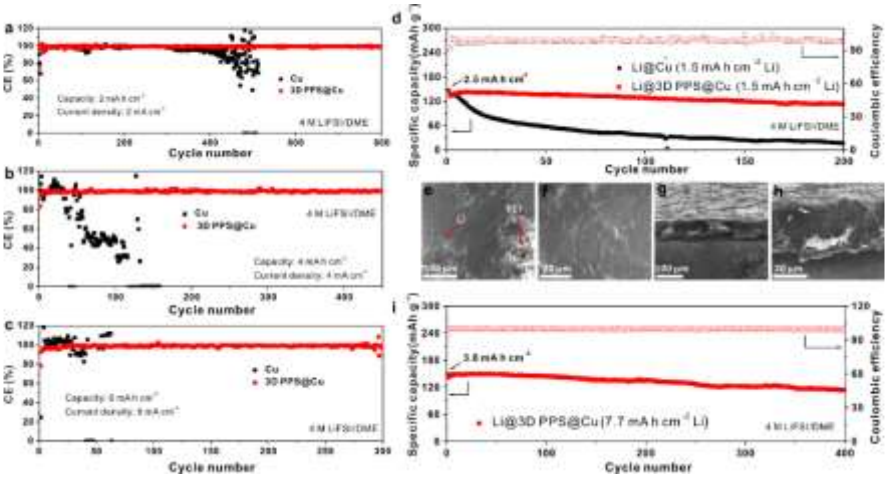

Figure 78. (a) Coulombic efficiency (CE) of lithium deposition on 3D PPS@Cu and bare copper electrode at a current density of 2 mA cm^{-2} and a deposition capacity of 2 mA h cm^{-2}. (b) CE of lithium deposition on 3D PPS@Cu and bare copper electrode at a current density of 4 mA cm^{-2} and a deposition capacity of 4 mA h cm^{-2}. (c) CE of lithium deposition on 3D PPS@Cu and bare copper electrode at a current density of 6 mA cm^{-2} and a deposition capacity of 6 mA h cm^{-2}. (d) Cycling performance of full cells (N/P ratio: 0.6) using 1.5 mA h cm^{-2} lithium on 3D PPS@Cu and bare copper electrode as anodes, respectively. (e-h) SEM images of Li@3D PPS@Cu in full cell after 50 cycles. (i) Cycling performance of full cells (N/P ratio: 2) using 7.7 mA h cm^{-2} lithium on 3D PPS@Cu as anodes and high-areal-capacity $LiFePO_4$ as cathodes (3.8 mA h cm^{-2}).

Patents/Publications/Presentations

Publication

- Li, G. X., Z. Liu, Q. Q. Huang, Y. Gao, M. Regula, D. W. Wang, L. Q. Chen, and D. H. Wang. "Stable Metal Battery Anodes Enabled by Polyethylenimine Sponge Hosts by Way of Electrokinetic Effects." *Nature Energy*, 3 (2018): 1076–1083.

Presentation

- MRS Fall Meeting, Boston, Massachusetts (November 2018): "Stable Li Anodes Enabled by Interfacial Functionalization for Li-S Batteries"; D. Wang.

Task 5.6 – New Electrolytes for Lithium-Sulfur Battery (Gao Liu, Lawrence Berkeley National Laboratory)

Project Objective. The project objective is to develop new electrolytes, additives, and electrode compositions for Li-S battery with high ion-conductivity, stable towards polysulfide and promoting the polysulfide affiliation with the electrode substrate to prevent polysulfide dissolution.

Project Impact. This work will address the high cost and low energy-density of the Li-ion rechargeable batteries. The emerging Li-S batteries could be both high energy-density and low cost. This project enables the applications of low cost and abundant sulfur element as a major chemical component for electrical energy storage. This project will develop new approaches for electrolytes and electrode compositions of Li-S rechargeable batteries.

Approach. This project aims to develop new electrolytes and additives for Li-S battery. The properties of the ideal electrolyte for sulfur electrode would be high ion conductivity, stable towards polysulfide, and promoting the polysulfide affiliation with the electrode substrate to prevent polysulfide dissolution. The project is designed to first understand the electrode substrate interaction with the polysulfides in different electrolytes. This will lead to better understandings of the polysulfide nucleation and precipitation mechanisms in common electrolytes. The second stage of the project will focus on chemically modifying the structures of the solvent and salt electrolyte molecules to increase electrolyte stability and ionic conductivity and to prevent polysulfide dissolution and promote polysulfides precipitation.

Out-Year Goals. The team will also investigate the contribution of Li-metal electrodes to the overall Li-S battery performance and develop methods to stabilize Li-metal surface.

Collaborations. This project collaborates with Dr. J. Guo and Dr. W. Yang (ALS/LBNL), Prof. A. Minor (National Center for Electron Microscopy at LBNL/UC Berkeley), and Dr. L.-W. Wang (LBNL).

Milestones

1. Identify the baseline electrolyte compositions and electrode composition and configuration for Li-S study. (Q1, FY 2019; Complete)
2. Develop polymer binders with different affiliation functional groups with polysulfides, and use baseline electrolytes to investigate dissolution and precipitation of polysulfides. (Q2, FY 2019; In progress)
3. Develop the *in situ* cells for synchrotron analysis with improved spatial resolution. (Q3, FY 2019; In progress)
4. Formulate one composition of the new electrolyte for Li-S battery and test its performance. (Q4, FY 2019)

Progress Report

This project began this quarter, with a focus on electrolyte and electrode interaction and new electrolyte development. An extensive literature review and a review of the team's past research results on electrolyte compositions and electrode composition and configuration for Li-S were conducted.

Electrode Configurations

Sulfur Materials. For pure sulfur materials, both micro-sized and nano-sized sulfur particles have been used for sulfur electrodes. At low sulfur loading in the electrode, the micro-sized sulfur particle electrode performs better than that of the nano-sized sulfur particles. However, the nano-sized sulfur electrode tends to give higher gravimetric capacity compared to the micro-sized sulfur particles at the initial cycling with higher sulfur loading electrode. This is mainly due to better utilization of sulfur active materials for the electrode based on nano-sized sulfur particles. Micro-sized particles tend not to be fully utilized in a high-loading electrode, leaving behind unreacted sulfur particles in the electrode after the first few cycles. The high electrical resistivity of the sulfur is largely to blame.

Binders. Non-functional binder, functional binder with strong binding/affiliation to the polysulfide, conductive binder, and conductive and functional binder have all been applied to improve performance of sulfur electrodes. It is demonstrated that the strong binding between the binders and polysulfide is one of the most important factors for enhanced sulfur electrode.

Electrolyte. Many electrolyte compositions have been applied to Li-S batteries. Carbonate-based electrolytes used in the Li-ion battery chemistry are not stable toward polysulfide. Ether-based electrolyte is the choice for Li-S rechargeable batteries. DME, DOL with LiTFSI salt is among the best electrolyte for Li-S chemistry. RTIL, such as 1-butyl-1-methyl-pyrrolidinium-bis(trifluorome-thanesulfonyl)imide, has also been used as an electrolyte component to control polysulfide dissolution.

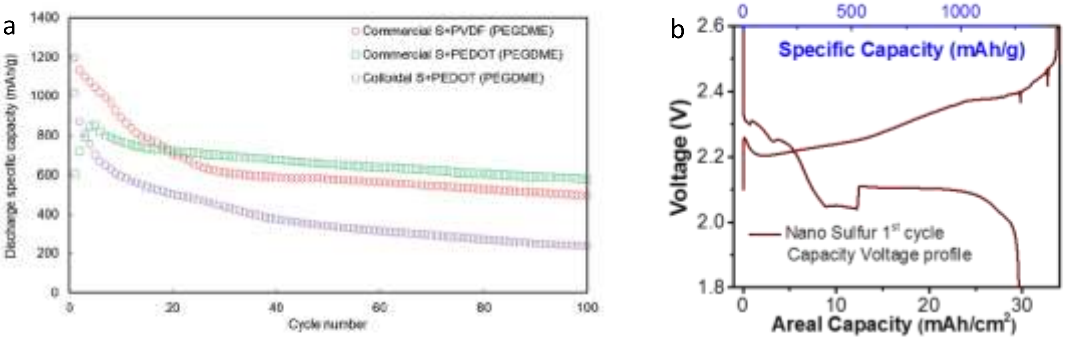

Figure 79. (a) Electrochemical performance of three low-loading (~ 1mg/cm^2) sulfur electrodes using PEGDME-based electrolyte [*Journal of Material Research* 29 (2014): 1027]. (b) Initial capacity voltage profile of carrageenan-based nano-sulfur electrode with the sulfur mass loading of 24.6 mg/cm^2 [*Nano Energy* 38 (2017): 82].

Patents/Publications/Presentations

Publication

- Yang, C., Q. Du, Z. Li, M. Ling, X. Song, V. Battaglia, X. Chen, and G. Liu. "*In-Situ* Covalent Bonding of Polysulfides with Electrode Binders *In Operando* for Lithium–Sulfur Batteries, *Journal of Power Sources* 402 (2018): 1–6.

TASK 6 – AIR ELECTRODES / ELECTROLYTES

Summary and Highlights

High-density energy storage systems are critical for EVs required by the EV Everywhere Grand Challenge. Conventional Li-ion batteries still cannot fully satisfy the ever-increasing needs because of their limited energy density, high cost, and safety concerns. As an alternative, the rechargeable lithium-oxygen (Li-O_2) battery has the potential to be used for long-range EVs. The practical energy density of a Li-O_2 battery is expected to be ~ 800 Wh kg^{-1}. The advantages of Li-O_2 batteries come from their open structure; that is, they can absorb the active cathode material (oxygen) from the surrounding environment instead of carrying it within the batteries. However, the open structure of Li-O_2 batteries also leads to several disadvantages. The energy density of Li-O_2 batteries will be much lower if oxygen must be provided by an onboard container. Although significant progress has been made in recent years on fundamental properties of Li-O_2 batteries, research in this field is still in an early stage, with many barriers to be overcome before practical applications. These barriers include:

- Instability of electrolytes—The superoxide species generated during discharge or O_2 reduction process is highly reactive with electrolyte and other components in the battery. Electrolyte decomposition during charge or O_2 evolution process is also significant due to high over-potentials.
- Instability of air electrode (dominated by carbonaceous materials) and other battery components (such as separators and binders) during charge/discharge processes in an O-rich environment.
- Corrosion of Li-metal anode in an electrolyte saturated with oxygen.
- Low energy efficiency associated with large over-potential and poor cyclability of Li-O_2 batteries.
- Low power rate capability due to electrode blocking by the reaction products.
- Absence of a low-cost, high-efficiency oxygen supply system (such as oxygen selective membrane).

The main goal of this Task is to provide a better understanding on the fundamental reaction mechanisms of Li-O_2 batteries and identify the required components (especially electrolytes and electrodes) for stable operation of Li-O_2 batteries. This task will investigate several new approaches to improve stability of Li-metal anode in Li-O_2 batteries:

- Li-metal anodes will be protected using two approaches: (1) *in situ* formation of a stable SEI layer before Li-O_2 cell operation through various electrolyte formulations and treatment protocols, and (2) *ex situ* formation of stable inorganic/polymeric hybrid electrolyte layers through dip-coating or tape-casting method to coat the inorganic/polymeric hybrid electrolyte layer on Li-metal surface.
- A joint theoretical/experimental approach for design and discovery of new cathode and electrolyte materials will act synergistically to reduce charge overpotentials and increase cycle life. Synthesis methods, in combination with design principles developed from computations, will be used to make new cathode architectures. Computational studies will be used to help understand decomposition mechanisms of electrolytes and how to design electrolytes with improved stability.
- A new cathode will be developed based on high-efficiency catalyst such as two-dimensional TM dichalcogenides. These cathode materials will be combined with new electrolyte blends and additives that work in synergy to reduce charge potentials and increase stability of the Li-air system.

State-of-the-art characterization techniques and computational methodologies will be used to understand charge and discharge chemistries. Success of this Task will establish a solid foundation for further development of Li-O_2 batteries toward practical applications for long-range EVs. The fundamental understanding and breakthrough in Li-O_2 batteries may also provide insight on improving performance of Li-S batteries and other energy storage systems based on chemical conversion process.

Task 6.1 – Rechargeable Lithium-Air Batteries
(Ji-Guang Zhang and Wu Xu, Pacific Northwest National Laboratory)

Project Objective. The objective of this project is to develop rechargeable lithium-oxygen (Li-O_2) batteries with long-term cycling stability. In FY 2019, the team will pay more attention to lithium anode stabilization and building a more stable Li-O_2 battery based on the protected lithium anode and optimized air-electrodes to develop practical Li-O_2 batteries with stable, long-term cycling capability.

Project Impact. Li-air batteries have a theoretical specific energy more than five times that of state-of-the-art Li-ion batteries and are potential candidates for use in next-generation, long-range EVs. Unfortunately, the poor cycling stability and low CE of Li-air batteries have prevented their practical application. This work will explore well-protected Li-metal anodes, new electrolytes, and high-loading air-electrodes that could lead to long cyclability and high CE in high-energy Li-air batteries that can be used in the next-generation EVs required by the EV Everywhere Grand Challenge.

Approach. Li-metal anodes will be protected using highly elastic and stable protective composite layers and gel-polymer crosslinked electrolytes. These membranes will be prepared through dip-coating or tape-casting method to coat the inorganic/polymeric hybrid electrolyte layers. Stable host structures for lithium metal will also be investigated to stabilize Li-metal anode in oxygen atmosphere. The electrochemical performances of Li-O_2 batteries using the protected Li-metal anodes and the previously developed carbon/catalyst composite air electrodes based on CNTs and TM oxides such as RuO_2 will be evaluated. The lithium anodes, air-electrodes, and Li-O_2 cells at different stages of cycling (including as-prepared, after discharge, after recharge, and after cycling) will be analyzed by microscopy and spectroscopy techniques such as SEM, EDX, TEM, XRD, and XPS.

Out-Year-Goals. The long-term goal is to enable rechargeable Li-air batteries with a specific energy of 800 Wh/kg at cell level, 1000 deep-discharge cycles, improved abuse tolerance, and less than 20% capacity fade over a 10-year period to accelerate commercialization of long-range EVs.

Collaborations. This project collaborates with C. Wang of PNNL on characterization of cycled air electrodes by TEM/SEM.

Milestones

1. Develop highly elastic and stable protective composite layers for lithium anode in Li-O_2 batteries. (Q1, FY 2019; Completed)
2. Protect Li-metal anode by using gel-polymer crosslinked electrolytes Li-O_2 batteries. (Q2, FY 2019)
3. Develop stable host structure to protect lithium anode in oxygen rich environment. (Q3, FY 2019)
4. Complete evaluation of cycling performance of Li-O_2 batteries with protected Li-metal anodes and optimized air-electrodes. (Q4, FY 2019)

Progress Report

This quarter, the milestone on development of highly elastic and stable protective composite layers for lithium anode used in Li-air batteries was accomplished. A new composite polymer layer (CPL) consisting of a novel polymer and LiFSI (mass ratio is 2.2:1.5) has been developed. As illustrated in Figure 80a, some gaps always exist if a free-standing protective membrane is placed on commercial lithium metal that is not completely flat due to production defect. These gaps inevitably lead to increased interfacial resistance on Li-metal anode. In this work, a slurry of novel polymer, lithium salt was dissolved in DME and directly cast on lithium surface followed by thermal solidification process (120ºC in vacuum to remove solvent) to enable a good contact between lithium and CPL and to decrease interfacial resistance on lithium metal (Figure 80a). After casting, the as-obtained uniform and highly elastic CPL forms a reliable protection layer for Li-metal surface (Figure 80b). This novel CPL is highly stable against reactive lithium metal. Figure 80c shows that lithium is still shining one week after it was coated with CPL even when stored in an elevated environment (60°C).

The ionic conductivity of CPL is 1.1×10^{-4} S cm^{-1} at 25ºC measured by placing a ~ 2-mm-thick CPL between two pieces of stainless-steel spacers in a coin-cell configuration (Figure 80d, inset). The cyclic stability of Li||Li cells with or without the CPL-coated Li-metal electrodes (CPL coating thickness is ~ 25 µm) was tested in a coin cell containing 1 M LiFSI-DME electrolyte at a current density of 0.2 mA cm^{-2} at 25°C (Figure 80e). It can be seen that Li||Li cell without CPL protection exhibits significant voltage increase as a function of time (or cycle number) due to continuous side reaction between lithium metal and liquid electrolyte. In contrast, the Li||Li cells with CPL on lithium electrode surface demonstrated excellent stability, as shown in Figure 80e. The protected Li-metal anode will be used in Li-O_2 cells to improve their cycling stability next quarter.

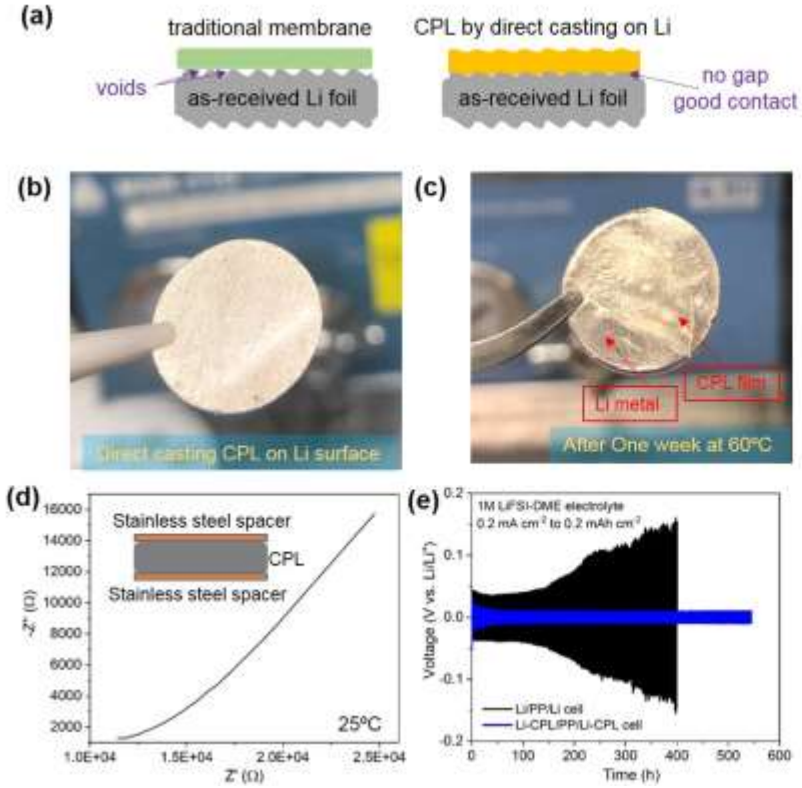

Figure 80. (a) Schematic of traditional artificial membrane on as-received Li-foil surface and current composite polymer layer (CPL) formed by direct casting on lithium foil. (b) Corresponding photo of as-prepared, uniform, highly elastic CPL coated on Li-metal surface. (c) Photo of Li-metal surface coated by CPL after one week at 60°C. Lithium metal with CPL was recovered from coin cell for stability test. (d) Ionic conductivity test of CPL placed between two pieces of stainless-steel spacers tested in coin cells at room temperature (25°C). (e) Cyclic stability tests based on Li||Li cells with or without CPL on lithium metal tested in a coin cell containing 1 M LiFSI-DME electrolyte at 25°C. Current density: 0.2 mA cm^{-2}.

Patents/Publications/Presentations

Publication

- Liu, B., W. Xu, L. Luo, J. Zheng, X. Ren, H. Wang, M. H. Engelhard, C. Wang, and J.-G. Zhang. “Highly Stable Oxygen Electrodes Enabled by Catalysts Redistribution through an *In-Situ* Electrochemical Method.” *Advanced Energy Materials* (2018). Under review.

Task 6.2 – Lithium-Air Batteries
(Khalil Amine and Larry A. Curtiss, Argonne National Laboratory)

Project Objective. This project will develop new cathode materials and electrolytes for Li-air batteries for long cycle life, high capacity, and high efficiency. The goal is to obtain critical insight that will provide information on the charge and discharge processes in Li-air batteries to enable new advances to be made in their performance. This will be done using state-of-the-art characterization techniques combined with state-of-the-art computational methodologies to understand and design new materials and electrolytes for Li-air batteries.

Project Impact. The instability of current nonaqueous electrolytes and degradation of cathode materials limits performance of Li-air batteries. The project impact will be to develop new electrolytes and cathode materials that are stable and can increase energy density of electrical energy storage systems based on lithium.

Approach. The project is using a joint theoretical/experimental approach for design and discovery of new cathode and electrolyte materials that act synergistically to reduce charge overpotentials and increase cycle life. Synthesis methods, in combination with design principles developed from computations, are used to make new cathode architectures. Computational studies are used to help understand decomposition mechanisms of electrolytes and how to design electrolytes with improved stability. The new cathodes and electrolytes are tested in Li-O_2 cells. Characterization, along with theory, is used to understand the performance of materials used in the cell and make improved materials.

Out-Year Goals. The out-year goals are to find catalysts that promote discharge product morphologies that reduce charge potentials and find electrolytes for long cycle life through testing and design.

Collaborations. This project engages in collaboration with Prof. K. C. Lau (UC at Norridge), Prof. Y. Wu (Ohio State University), Dr. D. Zhai (China), and R. Shahbazian-Yassar (UIC).

Milestones

1. Synthesis and testing of low-cost TM catalysts that give low charge potentials in Li-O_2 batteries. (Q1, FY 2019; Completed)
2. Investigation of dependence of discharge product properties on electrolytes with mixtures of sodium and lithium salts. (Q2, FY 2019)
3. Computational and experimental studies of charge and discharge mechanisms involving mixtures of salts in electrolytes. (Q3, FY 2019)
4. Computational and experimental studies of new electrolyte additives for increased efficiency Li-O_2 batteries. (Q4, FY 2019)

Progress Report

Catalysts play a significant role in the oxygen evolution reaction (OER) of lithium peroxide in Li-O_2 batteries and the right catalyst can reduce the over-potential during charge and increase efficiency. So far, attractive OER performances are mostly reported for catalysts using expensive noble metals such as iridium, ruthenium, platinum, and palladium, which could limit the large-scale applications of Li-O_2 batteries. Hence, it is desirable to explore low-cost and effective alternative catalysts for the OER. TM-based catalysts such as Co_3O_4, NiO, $Co(OH)_2$, and $Ni(OH)_2$ have attracted much attention because of their low cost and earth abundancy. However, most synthesis methods not only involve multiple processes, but also have problems with the aggregation or contamination of catalysts.

The project has designed a simple approach to prepare ultrafine cobalt and nickel nanoparticles dispersed in a porous LiOH structure (denoted as Co_2Ni@LiOH) by an *in situ* lithiation strategy. The team lithiated cobalt-nickel layered double hydroxide (Co-Ni LDH) nanoplates by a discharge process under argon in a Swagelok cell, leading to formation of cobalt and nickel metal nanoparticles in a LiOH composite (Co_2Ni@LiOH). Then, the Co_2Ni@LiOH composite-based electrode was directly employed as the cathode in a Li-O_2 cell after filling the glass chamber with pure oxygen. The metal particles have ultrafine size (~ 2 nm), and the composite has a uniform 3D porous structure with enhanced surface area and good electrical conductivity.

As the oxygen cathode for the Li-O_2 cell, the Co_2Ni@LiOH exhibits a high discharge voltage of 2.7 V and a very low charge potential of 3.4 V at a current density of 50 µA cm^{-2}, which results in a much higher roundtrip efficiency of ~ 79% compared with that of pristine Co-Ni LDH (~ 59%). This high roundtrip efficiency is comparable to that of the well-known noble metals. The Co_2Ni@LiOH-based Li-O_2 cell is stable and can last 40 cycles with a 3.6 V charge potential at the current density of 50 µA cm^{-2}. The team investigated the discharge and charge products in the Li-O_2 cell from different cycles at a current density of 50 µA cm^{-2}. After the 1st discharge, the SEM image (Figure 81a) shows that the Co_2Ni@LiOH electrode is covered by toroidal structures, which is the common morphology for Li_2O_2. After charging the cell, all the toroidal structures have disappeared and the interconnected structure is exposed, which is Co_2Ni@LiOH (Figure 81b). The XRD and Raman spectra for various cycles are shown in Figures 81c-d.

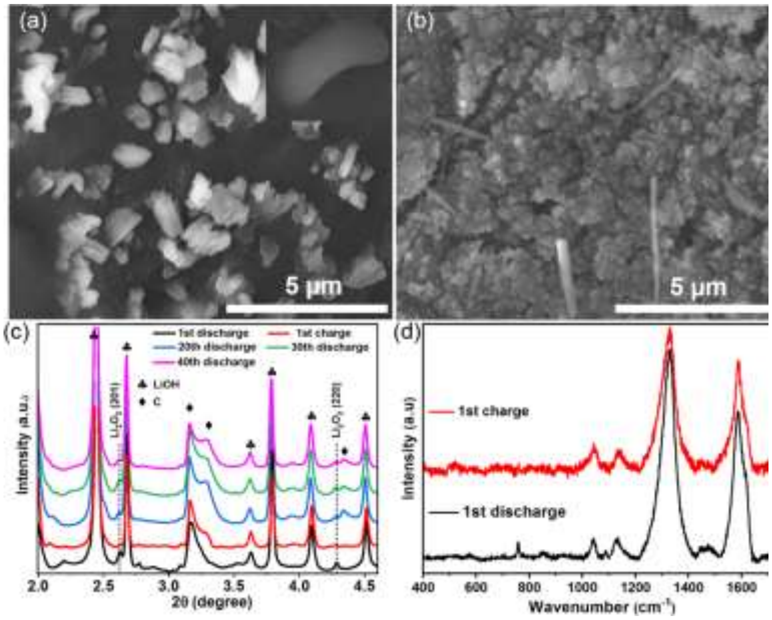

Figure 81. Scanning electron microscopy of (a) 1st discharge and (b) charge products in Li−O_2 batteries with the Co_2Ni@LiOH cathode. (c) X-ray diffraction of the 1st, 20th, 30th, and 40th discharge and the 1st charge products. (d) Raman spectrum of the 1st discharge and charge products in Li−O_2 battery.

The well-aligned network facilitates the oxygen diffusion and the electrolyte penetration into the electrode. The enhanced electrical conductivity network improves the charge transport kinetics and more active sites are exposed, which facilitate the adsorption and dissociation of oxygen during the oxygen reduction reaction (ORR) and the OER. This new catalyst design is important for development of effective non-noble metal catalysts for Li-O_2 batteries.

Patents/Publications/Presentations

Publication

- Guo, Y., Z. Dai, J. Lu, X. Zeng, Y. Yuan, X. Bi, L. Ma, T. Wu, Q. Yan, and K. Amine. "Lithiation Induced Non-Noble Metal Nanoparticle for Li-O_2 Batteries." ACS *Applied Materials & Interfaces* 11 (2019): 811−818.

Task 6.3 – Development of Long Cycle Life Li-O_2 Batteries that can Operate in an Air Atmosphere (Larry A. Curtiss/Anh Ngo, Argonne National Laboratory; Amin Salehi-Khojin, University of Illinois at Chicago)

Project Objective. The objective of this work is to develop new materials for Li-O_2 batteries that give longer cycle life and improved efficiencies in an air environment. New electrolyte blends and additives will be investigated the can reduce clogging and at the same time promote the cathode functionality needed to reduce charge overpotentials. New cathode and anode materials will be investigated that can work in conjunction with the electrolytes to improve cycle life in the presence of air components.

Project Impact. Li-air batteries are considered as a potential alternative to Li-ion batteries for transportation applications due to their high theoretical specific energy. The major issues with the existing Li-O_2 systems include degradation of the anode electrode, reactions with air components, clogging of the cathode, and electrolyte instability. Thus, this project is using a comprehensive approach to improve cycle life and efficiency through development of new materials for electrodes, anodes, and electrolytes that work in synergy.

Approach. The experimental strategy is to use cathode materials based on 2D TM dichalcogenides (TMDCs) that the team has found to be among the best oxygen reduction and evolution catalysts. These cathode materials will be combined with new electrolyte blends and additives that work in synergy to reduce charge potentials and increase stability of the Li-air system. DFT and *ab initio* MD simulations are used to gain insight at the electronic structure level of theory of the electrolyte structure and function both in the bulk and at interfaces with the cathode, anode, and discharge product. Classical MD is used to obtain understanding at longer length and time scales of processes occurring in the electrolyte and growth mechanisms of discharge products. The team will also utilize a high-throughput screening strategy based on experiment and theory to develop a large database of properties and outcomes of electrolyte combinations that can be analyzed using machine learning to predict electrolytes and additives that will have the best performance.

Out-Year Goals. The out-year goal is to find electrolytes for Li-O_2 batteries that give high capacities and long cycle life in an air atmosphere using high-throughput screening.

Collaborations. This project engages in collaboration with Z. Zhang (ANL), R. Assary (ANL), B. Narayanan (University of Louisville), and R. Klie (University of Illinois at Chicago).

Milestones

1. Investigate possible lithium anode protection additives and redox mediators for electrolyte blends that can work with MoS_2 cathode to extend cycle life and reduce charge overpotentials of Li-O_2 cells. (Q1, FY 2019; Completed)
2. Develop and assess additives for electrolyte additives that will work in concert with MoS_2 cathode in Li-O_2 cells. (Q2, FY 2019)
3. Investigate additives for electrolyte blends that will work in concert with MoS_2 cathode for increased efficiency of Li-O_2 cells running in a realistic air environment. (Q3, FY 2019)
4. Using machine learning techniques, develop reactive force fields for lithium oxides that will enable realistic modeling of charge and discharge processes in the MoS_2 based Li-O_2 system. (Q4, FY 2019)

Progress Report

Li-air batteries are considered as a potential alternative to Li-ion batteries for transportation applications due to their high theoretical specific energy. Thus far, research on the Li-air battery has been largely limited to the short life cycle in a pure oxygen environment (Li-O_2 batteries). The major issues with the existing Li-O_2 systems include degradation of the anode electrode, clogging of the cathode electrode, and electrolyte instability. In the presence of actual components of air such as nitrogen, carbon dioxide, and moisture, the issues become even more complex since a small concentration of such reagents could influence reaction pathways and discharge products at the cathode. Another major problem with Li-O_2 systems is that their volumetric energy density, due to the necessity of the storing of oxygen, may be too small for practical applications. Recently, the team demonstrated a Li-O_2 battery comprised of a lithium carbonate-based protected anode, a molybdenum disulfide (MoS_2) cathode, and dimethyl sulfoxide (75%)/ionic liquid (25%) electrolyte that all work together to give a long life of up to 700 cycles and that can run in an air-like atmosphere for the first time [*Nature* 555 (2018): 502], although it required a high charge potential (~ 4 V).

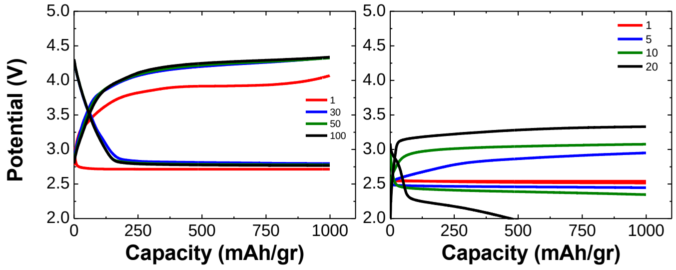

75% TEGDME/25 % IL
1 M LiNO3

75% TEGDME/25 % IL
1 M LiI

Figure 82. Voltage profiles for Li-O_2 battery with $LiNO_3$ additive (left) and LiI redox mediator (right).

This quarter, as a first step in improving battery efficiency, that is, lowering charge potential, the team investigated modifying the cell configuration based on a molybdenum disulfide cathode. They replaced the ionic liquid in the electrolyte blend with tetraglyme (TEGDME). In addition, the team is initially using pure O_2 with no other air components for this systematic study on reducing charge potential. They have explored separately two additives to the electrolyte blend, including lithium nitrate and lithium iodine. These two additives were chosen as they were beneficial in some systems. Lithium nitrate was found to provide lithium anode protection in Li-S systems, and lithium iodine has been found to act as a redox mediator in some Li-O_2 systems. These were used in combination with a LiTFSI salt. The voltage profiles for both additives are shown in Figure 82. Results for lithium nitrate indicate that it provides for long cycle life, as it ran for 100 cycles, which is probably due to formation of a protective coating on the anode. Results for lithium iodine indicate that it gives a low charge potential, but poor cycle life. The team is carrying out characterizations of the processes to fully understand the role of these additives and how to simultaneously improve both cycle life and efficiency.

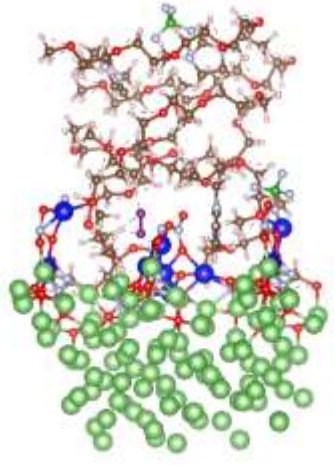

Figure 83. *Ab initio* molecular dynamics simulation of eight $LiNO_3$ molecules added to electrolyte showing them forming a layer on the lithium anode.

The team is also carrying out computation simulations to help investigate the role of the additives in the Li-O_2 cell. This has included AIMD simulations of the interface between the electrolyte and a Li-metal surface when lithium nitrate is added. Figure 83 shows the result when eight lithium nitrate molecules are added to the AIMD cell. The lithium nitrate molecules react strongly with the lithium surface to form a layer on the lithium surface. The team also added an oxygen molecule to the system, and it was found that the lithium-nitrate layer prevented the reaction of O_2 with the lithium surface, which occurs if it is free to interact with the surface. This strong reaction with the lithium surface of the lithium nitrate is consistent with experimental results showing that lithium nitrate gives long cycle life. The team is also investigating the role of lithium iodine as a redox mediator in the project's system.

Patents/Publications/Presentations

The project has no patents, publications, or presentations to report this quarter.

TASK 7 –SODIUM-ION BATTERIES

Summary

During FY 2019, the BMR will add five new projects, including several in the area of Na-ion batteries. The Na-ion battery will require investigations to identify optimal electrode materials, electrolytes, separators, and binders to reach its full potential. The BMR program will therefore have a limited effort directed toward identifying Na-ion battery materials that have potential value for vehicle applications. These projects will be included in this new section as they get underway. More detailed information on this BMR Task will be provided in upcoming reports.

Task 7.1 – Exploratory Studies of Novel Sodium-Ion Battery Systems
(Xiao-Qing Yang and Enyuan Hu, Brookhaven National Laboratory)

Project Objective. The objective of this project is to develop new advanced *in situ* material characterization techniques and apply these techniques to explore the potentials, challenges, and feasibility of new rechargeable battery systems beyond the Li-ion batteries, namely the sodium-ion battery systems for EVs, such as PHEV and BEV. To meet the challenges of powering PHEVs and BEVs, new rechargeable battery systems with high energy and power density, low cost, good abuse tolerance, and long calendar and cycle life need to be developed. This project will use the synchrotron based *in situ* x-ray diagnostic tools, combined with TEM, STEM, and TXM imaging techniques developed at BNL to evaluate the new materials and redox couples to obtain fundamental understanding of the reaction mechanisms of these materials aiming for improvement of and guidance for new material and new technology development regarding Na-ion battery systems.

Project Impact. In the VTO MYPP, the goals for battery are described as: "Specifically, lower-cost, abuse-tolerant batteries with higher energy density, higher power, better low-temperature operation, and longer lifetimes are needed for the development of the next-generation of HEVs, PHEVs, and EVs." The knowledge learned from diagnostic studies and collaborations with U. S. industries through this project will help U. S. industries to develop new materials and processes for new generation of rechargeable battery systems, namely Na-ion battery system in their efforts to reach the VTO goals.

Approach. This project will use the synchrotron-based *in situ* X-ray diagnostic tools developed at BNL to evaluate the new materials and redox couples to enable a fundamental understanding of the mechanisms governing performance of these materials and provide guidance for new material and new technology development regarding Na-ion battery systems.

Out-Year Goals. Complete the synchrotron based *in situ* XRD and *ex situ* absorption (XAS) studies of low-cost P2-type iron-based cathode materials ($Na_{0.7}[Cu_{0.15}Fe_{0.3}Mn_{0.55}]O_2$) as new cathode materials for Na-ion batteries during charge-discharge cycling.

Collaborations. The BNL team has been closely working with top scientists on new material synthesis at ANL, LBNL, and PNNL and with U. S. industrial collaborators at General Motors and Johnson Controls, as well as international collaborators.

Milestones

1. Complete *in situ* XRD studies of new low-cost P2-type iron based cathode materials ($Na_{0.7}[Cu_{0.15}Fe_{0.3}Mn_{0.55}]O_2$) for Na-ion batteries during charge-discharge cycling. (Q1, December 2018; Completed)
2. Complete the synchrotron-based XAS studies and XAS analysis of $Na_{0.7}[Cu_{0.15}Fe_{0.3}Mn_{0.55}]O_2$ and $Na_{0.7}[Cu_{0.2}Fe_{0.2}Mn_{0.6}]O_2$ electrodes at different SOCs at iron K-edge, copper K-edge, and manganese K-edge. (Q2, March 2019; In progress)
3. Complete the sXAS studies of $Na_{0.7}[Cu_{0.15}Fe_{0.3}Mn_{0.55}]O_2$ and $Na_{0.7}[Cu_{0.2}Fe_{0.2}Mn_{0.6}]O_2$ electrodes at different SOCs at iron L-edge, copper L-edge, and oxygen K-edge. (Q3, June 2019; In progress)
4. Complete *in situ* XRD studies of new stabilized global P2 phase cathode material ($Na_{0.72}[Li_{0.24}Mn_{0.76}]O_2$) for Na-ion batteries during charge-discharge cycling. (Q4, September 2019; In progress)

Progress Report

This quarter, the first milestone for FY 2019 was completed. BNL has been focused on the *in situ* XRD studies on the structural evolution of $Na_{0.7}[Cu_{0.15}Fe_{0.3}Mn_{0.55}]O_2$ and $Na_{0.7}[Cu_{0.2}Fe_{0.2}Mn_{0.6}]O_2$ materials. The *in situ* XRD results for $Na_{0.7}[Cu_{0.15}Fe_{0.3}Mn_{0.55}]O_2$ during the first cycle are shown in Figure 84a. The (002) peak located at 15.8° continuously shifts to lower 2θ angle, suggesting a solid-solution reaction. Along with the deintercalation of Na^+ ion, the *c* lattice parameter increases significantly, which is caused by the increased Coulombic repulsion between two adjacent oxygen layers. However, when the *in situ* cell is further charged to 4.2 V, the (002) peak shifts back to higher 2θ angles quickly, indicating new phase formation during the high-voltage charge process. In contrast, the *in situ* XRD results for $Na_{0.7}[Cu_{0.2}Fe_{0.2}Mn_{0.6}]O_2$ shown in Figure 84c have different structural evolution than $Na_{0.7}[Cu_{0.15}Fe_{0.3}Mn_{0.55}]O_2$; no new diffraction peaks beyond P2 structure were observed during sodium deintercalation and intercalation at high charging cut-off voltage, but only gradual shift of peak position. This suggests a solid-solution reaction mechanism during the full charge/discharge process in the voltage range of 2.5 V and 4.2 V, which is consistent with CV results and electrochemical charge/discharge curves.

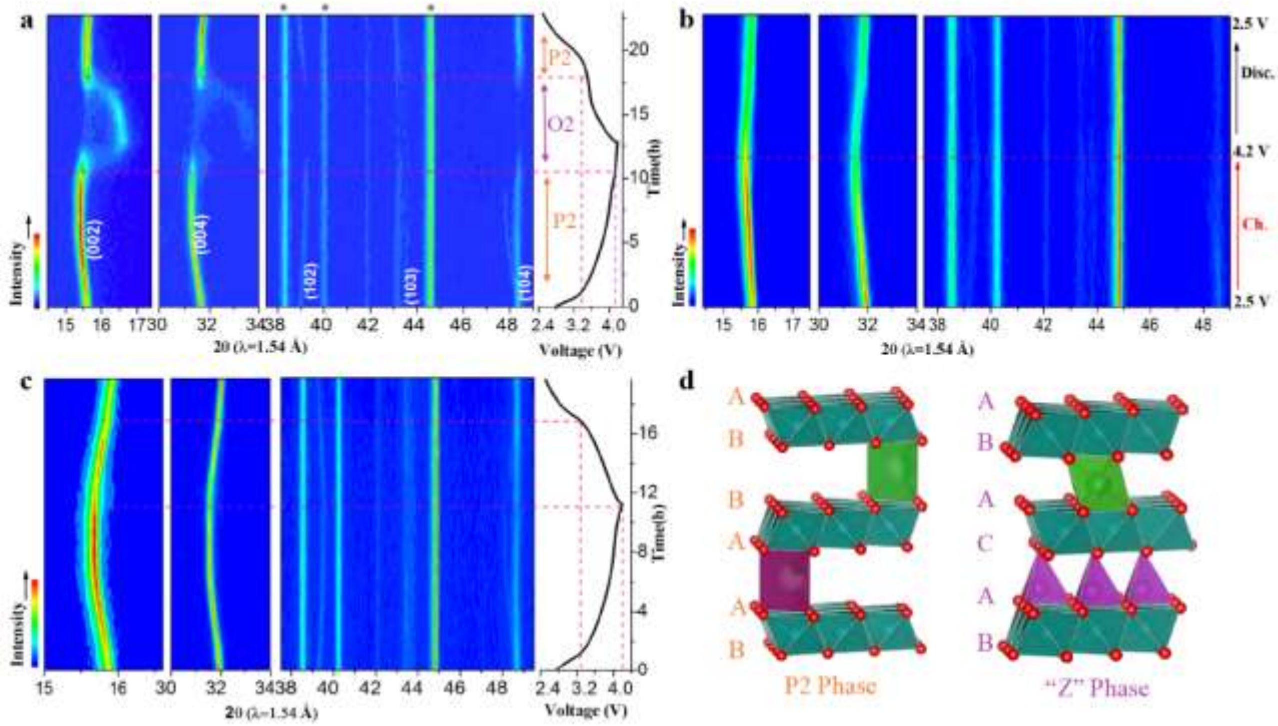

Figure 84. Structure evolution during sodium extraction and insertion. *In situ* X-ray diffraction (XRD) patterns of $Na_{0.7}[Cu_{0.15}Fe_{0.3}Mn_{0.55}]O_2$ electrode collected during (a) the 1st and (b) the 5th charge/discharge process. (c) *In situ* XRD patterns of $Na_{0.7}[Cu_{0.2}Fe_{0.2}Mn_{0.6}]O_2$ electrode collected during the 1st charge/discharge. All cycled between 2.5 and 4.2 V under a current rate of C/15.

Patents/Publications/Presentations

Publications

- Song, B., E. Hu, J. Liu,* Y. Zhang, X-Q. Yang, J. Nanda, A. Huq,* and K. Page.* "A Novel P3-Type $Na_{2/3}Mg_{1/3}Mn_{2/3}O_2$ as High Capacity Sodium-Ion Cathode Using Reversible Oxygen Redox." *Journal of Materials Chemistry A*. doi: 10.1039/C8TA09422E, Publication Date (Web): December 10, 2018.
- Q-C. Wang, J-K. Meng, X-Y. Yue, Q-Q. Qiu, Y. Song, X-J. Wu, Z-W. Fu, Y-Y. Xia, Z. Shadike, J. Wu, X-Q. Yang, and Y-N. Zhou.* "Tuning P2-Structured Cathode Material by Na-Site Mg Substitution for Na-Ion Batteries." *Journal of American Chemical Society*. doi: 10.1021/jacs.8b08638, Publication Date (Web): December 18, 2018.

Presentation

- Hong Kong Symposium of Batteries, Hong Kong Polytechnic University, Kowloon, Hong Kong (December 17, 2018): "Using Synchrotron X-ray and Neutron Based Scattering Combined with TEM and TXM Imaging Techniques to Study the New Cathode Materials for Batteries"; E. Hu, R. Lin, X. Yu, Z. Shadike, S-M. Bak, H. S. Lee, Y. Liu, K. Page, J. Liu, H. Xin, X. Wang, and X-Q. Yang.* Invited.

Innovation Center for Battery500
(Jun Liu, PNNL; Yi Cui, Stanford University)

Project Objective. The project aims to develop commercially viable lithium battery technologies with a cell-level specific energy of 500 Wh/kg through innovative electrode and cell designs that enable the extraction of the maximum capacity from advanced electrode materials. In addition to achieving high specific energy, the project aims to be able to achieve 1,000 cycles for the developed technologies.

Project Impact. The Battery500 Consortium will develop the next-generation lithium battery technologies that will significantly increase energy density, improve cycle life, and reduce cost. This will greatly accelerate deployment of EVs and reduce carbon emission associated with fossil fuel consumption. The consortium will utilize first-class expertise and capabilities in battery research in the United States and develop an integrated and multidisciplinary approach to accelerate development and deployment of advanced electrode materials in commercially viable high-energy batteries. The advances made in this consortium will also benefit the improvement of current Li-ion battery technologies.

Approach. This project will utilize an assortment of national resources located at the national laboratory level and university level. The lithium anode combined with a compatible electrolyte system and two cathodes—one high-Ni $LiNi_xMn_yCo_zO_2$ and another sulfur—will be studied and developed to reach high-energy density. The project focus is to design novel electrode and cell architectures to meet the 500 Wh/kg goal. The consortium will work closely with R&D companies, battery/materials manufacturers, and end users/OEMs to ensure that the developed technologies are aligned with industry needs and can be transitioned to production.

Out-Year Goals. This project aims for the following out-year goals. (1) Integrate materials and components developed in FY 2018 into 1-Ah pouch cell and demonstrate 400-Wh/kg cell with more than 30 charge discharge cycles, and provide analytical results for materials selection, cell design and fabrication, and further refinement for FY 2019. (2) Evaluate the seedling projects for key findings.

Collaborations. The collaboration among consortium team members will be well coordinated by the leadership team, which includes the keystone project leads and co-leads along with PIs at all member institutions. Collaboration with the community outside of this consortium and with industry will be facilitated by the executive committee, the advisory board, and the industry committee.

Milestones

1. Synthesize high-nickel layered oxide cathodes (nickel content > 90%) with a capacity of > 210 mAh/g and test. (Q1, December 2018; Completed)
2. Implement lithium protection approaches to demonstrate 20% cycle life improvement. (Q2, March 2019; In progress)
3. Fabricate and test a pouch cell capable of 350 Wh/kg and 250 cycles. (Q3, June 2019; In progress)
4. Fabricate and test a pouch cell capable of 400 Wh/kg and 30 cycles. (Q4, September 2019; In progress)

Progress Report

This quarter, the first milestone for FY 2019 was completed, and progress toward other milestones was made. High-nickel layered oxide cathodes (nickel content > 90%) with a capacity of > 210 mAh/g were synthesized and tested using Battery500 protocols.

The consortium PIs delivered 33 invited talks and published 11 papers in peer-reviewed journals during this quarter, as well.

The technical portion of this report is organized under three Keystone projects, as presented below.

Keystone Project 1: Materials and Interfaces

Li-Metal Anode

This quarter, the consortium focused on developing further understanding of the SEI layer to further inform the conception of advanced electrolyte systems, electrode design, and interfacial engineering and to support efforts on improving current pouch-cell performance to reach the project goal of 500 Wh/kg specific energy. Some work on Li-metal SEI is also highlighted in the Keystone Project 2.

Characterization of SEI Formation at Different Potentials. The consortium recognizes the critical dependence of battery performance on the nanostructure and electrochemical properties of the SEI. However, knowledge of how the SEI nanostructure forms and of its impact on ionic transport is limited due to difficulties in direct probing. Using cryogenic-electron microscopy (cryo-EM) and EIS, the team tracked the voltage-dependent, stepwise evolution of the SEI formed on CuO nanowires in carbonate electrolytes. They find that the SEI in 1 M $LiPF_6$ EC:DEC electrolyte forms as a 3-nm thick amorphous layer at 1.0 V versus Li/Li^+ and grows in thickness with decreasing anode potential, to a thickness of 8 nm upon reaching 0.0 V versus Li/Li^+ (Figure 85a-c). With the addition of 10% FEC to the electrolyte, the SEI thickness evolves similarly (Figure 85d-f). However, the nanostructure of the layer changes in the presence of the FEC additive; with 10% FEC, an inverted multilayer structure forms, whereas with no additives, a mosaic-type structure is formed instead (Figure 85c/f). By correlating the observed nanostructures with refined EIS measurements, the team finds that the mosaic nanostructure causes continuous increases in impedance during growth (Figure 85g), while the inverted layered nanostructure formed with FEC improves SEI conductivity and maintains its interfacial impedance (Figure 85h).

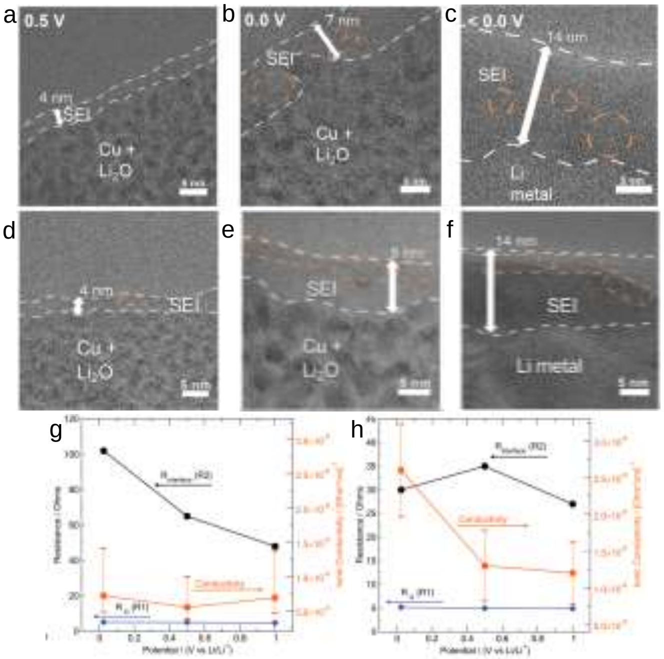

Figure 85. (a-c) Cryogenic electron microscopy (cryo-EM) images of SEI formed in 1 M $LiPF_6$ in EC/DEC without FEC on CuO nanowires at electrode potentials of (a) 0.5 V, (b) 0.0 V, and (c) below 0.0 V versus Li/Li^+. (d-f) Cryo-EM images of SEI formed in 1 M $LiPF_6$ in EC/DEC with 10% FEC on CuO nanowires at electrode potentials of (a) 0.5 V, (b) 0.0 V, and (c) below 0.0 V versus Li/Li^+. (g-h) Series resistance (R1), SEI ionic conductivity, and interfacial resistances (R2) extracted from EIS measurements for SEI formed in electrolyte (g) without and (h) with 10% FEC additive.

Li-S Batteries

Redox Mediator for Li_2S Activation in Li-S Cells. The initial oxidation of Li_2S in cathodes of Li-S batteries is characterized by an undesirable high overpotential barrier during charging. By engineering the functional groups and structure of small molecule quinones, the team designed a redox mediator molecule to improve efficiency and fast initial activation of Li_2S microparticles. By tailoring the quinone derivative properties, such as oxidation potential, solubility, and electrochemical stability, initial charging of Li_2S electrodes occurs below 2.5 V at a 0.5C rate with a subsequent discharge capacity as high as 1300 mAh/g (Figure 86). Furthermore, the team finds that deposition of dead, disconnected Li_2S is effectively prevented with the addition of the redox mediator, avoiding the primary cause of increasing polarization and decreasing reversible capacity of Li-S batteries on cycling.

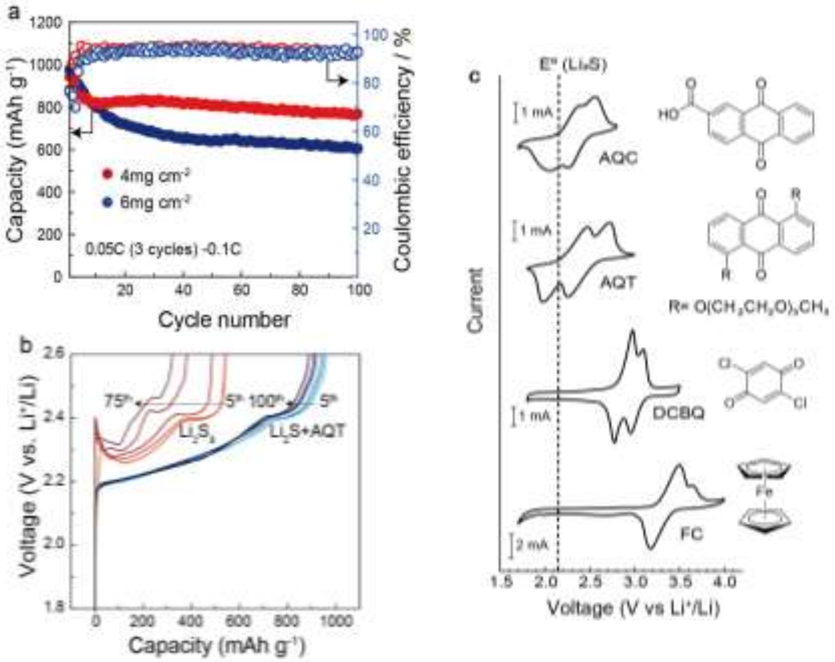

Figure 86. (a) Cycle performance of Li_2S electrodes with high sulfur mass loading. (b) Voltage profiles of Li_2S charging with and without quinone redox mediator. (c) Comparison of redox potentials of different redox mediator candidates.

Highlights. The highlights for this keystone project are as follows:

- Elucidated voltage-dependent formation of SEI using cryo-EM by observing its nanostructure and impedance.
- Developed Li-S redox mediator to enable low polarization charging of Li_2S and improved reversible capacity.

Keystone Project 2: Electrode Architecture

The project goal is to design, model, fabricate, and characterize the effects of electrode architecture on electrode and cell performance in support of reaching the project goal of 500 Wh/kg cell specific energy. Included in this project are architecture design of thick cathodes (UCSD), Li-metal electrode architectures (PNNL and Stanford), inorganic (UT-Austin) and polymer (Stanford) electrolytes, and electrode performance modeling (UW). Highlighted this quarter is the recent progress at UCSD on thick cathode and Li-metal anode.

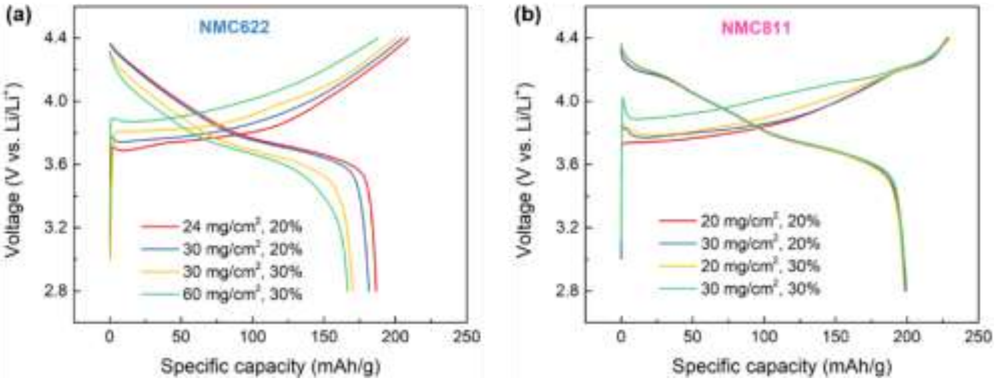

Figure 87. First-cycle voltage profiles of (a) NMC-622 and (b) NMC-811 thick electrodes with various active mass loading and porosity, at C/10, 2.8-4.4 V. Electrodes are provided by Maxwell Technologies.

S. Meng and P. Liu led groups at UCSD in examining electrochemical performances of thick electrodes, which are necessary to achieve a cell-level energy density of 400 Wh/kg, by studying the influence of active mass loading and porosity for both NMC-622 and NMC-811, as shown in Figure 87. To further improve rate performance of the NMC-811 cathode, Liu's group recently performed chemical modification of the carbon additive. While improvement under C/3 rate is minor versus the baseline, at a C/2 rate, the benefit becomes more pronounced.

Meng's group applied XPS on the cycled Li-metal electrode and found that the SEI layer that is formed in the fluoromethane-based liquefied gas electrolytes with tetrahydrofuran is composed of LiF and Li_2CO_3, which previously showed contributions to an ideal SEI layer with a highly ionically conducting pathway. Liu's group designed a new electrolyte for lithium metal. The new electrolyte delivers initial CE of 91.92% for the first cycle, and subsequently, it rapidly approaches CE of 99% after only 15 cycles (Figure 88a). Over the course of 900 cycles, the average CE of lithium in this electrolyte is 99.37%. Although the cell continues to have high CE, the charge/discharge voltage profiles show increased polarization (Figure 88b), which is caused by the consumption of electrolyte and accumulation of "dead" lithium.

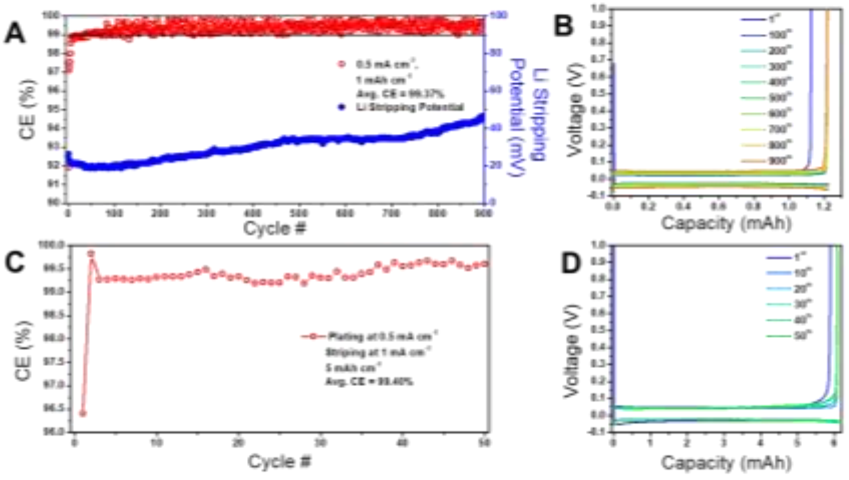

Figure 88. Li-metal Coulombic efficiency (CE) tests of Li||Cu cell in a new electrolyte. (a) CE cycled at 0.5 mA cm^{-2} for 1 mAh cm^{-2}. (b) Plating/ stripping voltage profiles at 0.5 mA cm^{-2} for 1 mAh cm^{-2}. (c) CE plating at 0.5 mA cm^{-2} and stripping at 1 mA cm^{-2} for 5 mAh cm^{-2}. (d) Plating/stripping voltage profiles plating at 0.5 mA cm^{-2} and stripping at 1 mA cm^{-2} for 5 mAh cm^{-2}.

In summary, the consortium continues to make advancements in both thick cathodes and lithium anode architectures and electrolyte. The performance of NMC thick cathodes with different active mass loadings and porosities has also been studied. The effect of carbon additives and the SEI layer has been studied. In addition, work on models to study the effect of external pressure has begun at UW.

Highlights. Highlights of this project are as follows:

- Implemented a thick NMC cathode that can be integrated in a 400 Wh/kg pouch cell.
- Studied SEI composition and new electrolyte compositions using 50-µm thick lithium.

Keystone Project 3: Cell Fabrication, Testing, and Diagnosis

This quarter, the project focused on several distinct points. First, the consortium worked to refine understanding on safety for Li-metal cells, including both lithium handling and evaluation of testing protocols. Other areas of advancement were on diagnostics and characterization of performance fade for Li-metal systems including characterization of cells undergoing both calendar- and cycle-life evaluation. Lastly, continued evaluation of FY 2019 deliverables occurred, and design metrics for Li-S cells were refined.

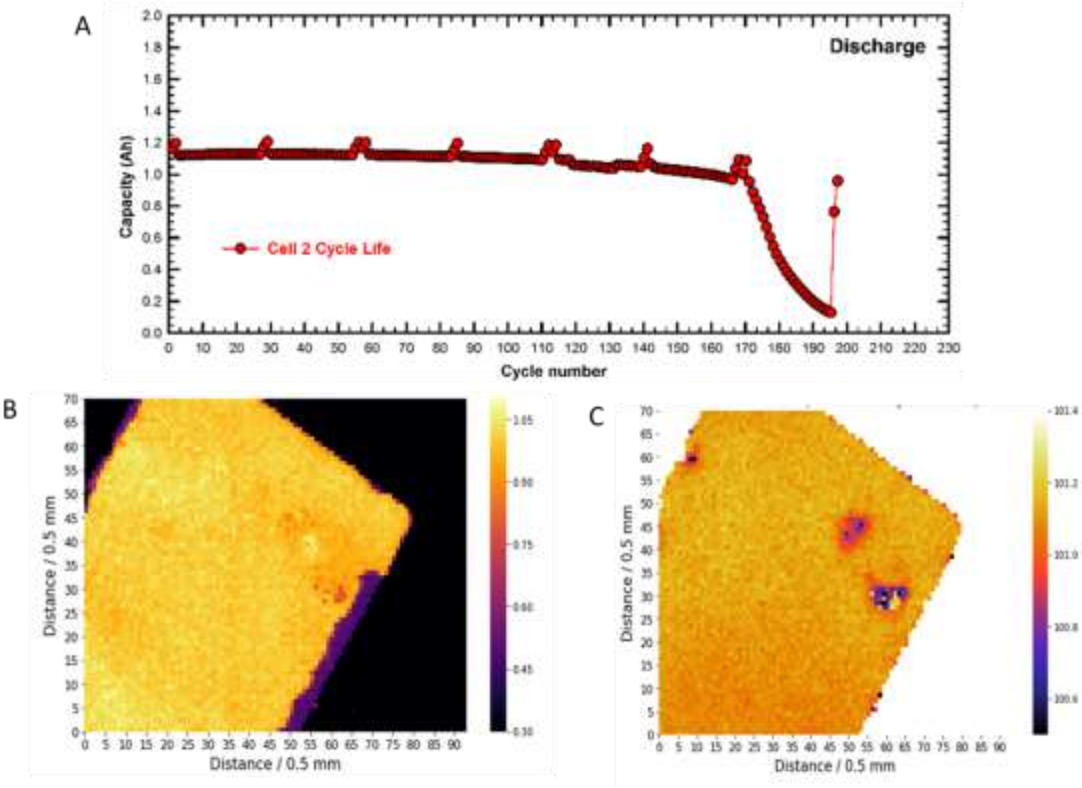

Figure 89. (a) Cycling data for a Li/NMC-622 cell developed in FY 2017. The cell achieved 200 cycles. (b) Variation in NMC loading content from *ex situ* X-ray diffraction (XRD) analysis following completion of testing. (c) State of charge in the NMC cathode from *ex situ* XRD analysis.

Characterization of cells and electrodes is necessary to understand the reasons for performance fade and to highlight key challenges in achieving high cycle life. A key outcome when performing post-testing evaluation of a cell that started undergoing testing in FY 2017 (with a specific energy of 310 Wh/kg and completing 200 cycles) was that low levels of SOC variation in the NMC-622 cathode were observed (Figure 89). Despite less than 3% variation in distribution across the electrode as determined using *ex situ* XRD lateral mapping analysis, specific areas on the electrode were not fully lithiated during discharge of the cell near the end of life. Based on electrochemical cycling data and other post-test analysis, this variation is likely due to distinct and evolving heterogeneity in the cell during cycling, which results in poor transport and hence low capacity (0.15 Ah at C/3) at moderate rates, but that enables relatively high retention at low rates (1.0 Ah at C/20) at the end of cycling (Figure 89a).

In addition to analysis of cells from FY 2018, evaluation continued for cells developed to meet the FY 2019 milestone that have a specific energy of 400 Wh/kg; these continue to cycle and currently have over 30 cycles with greater than 85% capacity retention (< 15% fade). Calendar life evaluation of Li||NMC cells has shown that over the course of more than a year, less than 7% fade is observed.

This quarter's milestone is related to refining understanding on safety and disseminating best practices to the Battery500 Consortium. Along those lines, a compilation of practices and concerns was presented to the Battery500 team, and a draft report was prepared. Both focused on understanding safety thresholds and means to minimize risk to research personnel, spanning from the receipt of lithium to post-test activities. It covered safety both with respect to use of lithium and to testing of larger 1-Ah+ cells. One significant highlighted consideration was understanding the state of the lithium metal after disassembly, as the potential for shorting the cell (even if in an Ar-filled glovebox) is enhanced due to loose lithium, as shown in Figure 90. As seen in the post-test image, key areas where lithium is disconnected from the copper current collector provide opportunity to short the cell; hence, added caution is needed during characterization to minimize risk to researchers.

Figure 90. Post-test Li-metal electrode at completion of 200+ cycles. Circles indicate areas of disconnected lithium after cycling.

Highlights. The highlights of the project are as follows:

- Protocols for safe operation and use of lithium were developed and shared across the Battery500 team.
- Characterization of cathodes after cycling indicate isolated areas of incomplete lithiation near end of life.

Patents/Publications/Presentations

Patent

- U.S. Provisional Patent Application.

Publications

- Yu, X., G. Zhou, and Y. Cui. “Mitigation of Shuttle Effect in Li-S Battery Using a Self-Assembled Ultrathin Molybdenum Disulfide Interlayer.” ACS *Applied Materials & Interfaces*. doi: 10.1021/acsami.8b19354, Publication Date (Web): December 27, 2018.
- Huang, W., D. T. Boyle, Y. Li, Y. Li, A. Pei, H. Chen, and Y. Cui. “Nanostructural and Electrochemical Evolution of the Solid-Electrolyte Interphase on CuO Nanowires Revealed by Cryogenic-Electron Microscopy and Impedance Spectroscopy.” ACS *Nano* 13, no. 28 (2018): 737–744. Publication Date (Web): December 27, 2018.
- Li, Y., Y. Li, and Y. Cui. “Catalyst: How Cryo-EM Shapes the Development of Next-Generation Batteries.” *Chem* 4, no. 10 (2018): 2250–2252. Publication Date (Web): October 11, 2018.
- Yin, L., G. Mattei, Z. Li, J. Zheng, W. Zhao, F. Omenya, C. Fang, W. Li, J. Li, Q. Xie, J-G. Zhang, M. Whittingham, Y. S. Meng, A. Manthiram, and P. G. Khalifah. “Extending the Limits of Powder Diffraction Analysis: Diffraction Parameter Space, Occupancy Defects, and Atomic Form Factors.” *Review of Scientific Instruments* 89, no. 9 (2018): 093002. doi: 10.1063/1.5044555.
- Yun, S., S-M. Bak, S. Kim, J. S. Yeon, M. G. Kim, X-Q. Yang, P. V. Braun,* and H. S. Park.* “Rational Design of Hierarchically Open-Porous Spherical Hybrid Architectures for Lithium-Ion Batteries.” *Advanced Energy Materials*. doi: 10.1002/aenm.201802816, Publication Date (Web): December 20, 2018.
- Li, Y., X. Wang, Y. Gao, Q. Zhang, G. Tan, Q. Kong, S-M. Bak, G. Lu, X-Q. Yang, L. Gu, J. Lu, K. Amine, Z. Wang,* and L. Chen. “Native Vacancy Enhanced Oxygen Redox Reversibility and Structural Robustness.” *Advanced Energy Materials*. doi: 10.1002/aenm.201803087, Publication Date (Web): December 5, 2018.
- Li, J., W. Li, Y. You, and A. Manthiram. “Extending the Service Life of High-Ni Layered Oxides by Tuning the Electrode-Electrolyte Interphase.” *Advanced Energy Materials* 8, no. 29, (2018): 1801957. Publication Date (Web): October 15, 2018.
- Xu, H., Y. Li, A. Zhou, N. Wu, S. Xin, Z. Li, and J. B. Goodenough. “Li_3N-Modified Garnet Electrolyte for All-Solid-State Lithium Metal Batteries Operated at 40°C.” *Nano Letters* 18, no. 11 (2018): 7414–7418. Publication Date (Web): October 23, 2018.
- Lee, H., H.-S. Lim, X. Ren, L. Yu, M. H. Engelhard, K. S. Han, J. Lee, H.-T. Kim, J. Xiao, J. Liu, W. Xu,* and J. Zhang*. “Detrimental Effects of Chemical Crossover from the Lithium Anode to Cathode in Rechargeable Lithium Metal Batteries.” ACS *Energy Letters* 3, no. 12 (2018): 2921–2930. doi:10.1021/acsenergylett.8b01819, Publication Date (Web): November 9, 2018.
- Lee, H., S. Chen, X. Ren, A. Martinez, V. Shutthanandan, V. Murugesan, K. S. Han, Q. Li, J. Liu, W. Xu,* and J. Zhang.* “Electrode Edge Effects and the Failure Mechanism of Lithium-Metal Batteries.” *ChemSusChem* 11, no. 21 (2018): 3821–3828. doi: 10.1002/cssc.201801445, Publication Date (Web): October 11, 2018.
- Nagpure, S. C., T. R. Tanim, E. J. Dufek, V. V. Viswanathan, A. J. Crawford, S. M. Wood, J. Xiao, C. C. Dickerson, and B. Liaw. “Impacts of Lean Electrolyte on Cycle Life for Rechargeable Li Metal Batteries.” *Journal of Power Sources* 407 (2018): 53–62. Publication Date (Web): October 23, 2018.

Presentations

- MRS Fall Meeting, Boston, Massachusetts (November 25–30, 2018): “Materials Science Challenges for High Energy Li Cells”; J. Liu. Invited.
- MRS Fall Meeting, Boston, Massachusetts (November 25–30, 2018): “Electrolyte Chemistry for Li and Zn Batteries”; J. Liu. Invited.
- MRS Fall Meeting, Boston, Massachusetts (November 27, 2018): “Stabilization of Metal Anodes by Localized High Concentration Electrolytes”; X. Cao, S. Chen, X. Ren, J. Zheng, L. Yu, W. Xu, and J. Zhang (presenter). Invited.
- Sixth International Renewable and Sustainable Energy Conference, Rabat, Morocco (December 2018): “Fundamental Challenges of Rechargeable Lithium Metal Batteries”; J. Xiao (speaker) and J. Liu. Keynote.
- 11th International Conference on Advanced Lithium Battery for Automobile Applications (AABA), Huzhou, China (October 2018): “Challenges and Opportunities of Employing Li Metal Anode for the Next-Generation Battery Technologies”; J. Xiao (presenter) and J. Liu. Invited.
- Materials Science and Engineering Colloquium, Department of Applied Physics & Applied Mathematics, Columbia University, New York, New York (November 16, 2018): “Using Synchrotron X-Ray and Neutron Based Scattering as well as TXM and TEM Imaging Techniques to Study the New Cathode Materials for Batteries and Studies on Li Metal Anode Protections”; Z. Shadike (presenter), R. Lin, E. Hu, S-M. Bak, X-Q. Yang (presenter),* H-S. Lee, X. Yu, Y. Chu, and Y. Liu. Invited.
- MRS Fall Meeting, Boston, Massachusetts (November 29, 2018): “Using Multi-Modal and Multi-Scale TEM and TXM Imaging Techniques to Study the Structural Stability of High Ni-Content Cathode Materials”; R. Lin (presenter), Z. Shadike, S-M. Bak, E. Hu, H. Xin, X. Huang, Y. Shin, H-S. Lee, Y. S. Chu, and Y. Liu, and X-Q. Yang (presenter).* Invited.
- Hong Kong Symposium of Batteries, Hong Kong Polytechnic University, Kowloon, Hong Kong, (December 17, 2018): “Using Synchrotron X-Ray and Neutron Based Scattering Combined with TEM and TXM Imaging Techniques to Study the New Cathode Materials for Batteries”; E. Hu, R. Lin, X. Yu, Z. Shadike, S-M. Bak, H. S. Lee, Y. Liu, K. Page, J. Liu, H. Xin, X. Wang, Xiao-Qing Yang (presenter).* Invited.
- 11th AABA, Huzhou, China (October 14, 2018): “Can Multi-Electron Intercalation Batteries Replace Today’s Li-Ion Batteries? (The Ultimate Limits of Intercalation, as Exemplified by NMC and 2e Cathodes)”; M. S. Whittingham. Invited.
- Energy Storage Review, Nanjing, China (October 16, 2018): “Approaching 50 Years of Li-Ion Batteries (from Solid State Ionics to Domination of Portable Storage)”; M. S. Whittingham. Invited.
- Director’s Lecture, PNNL, Richland, Washington (October 30, 2018): “Solid State Ionics – The Key to the Discovery and Domination of Lithium Batteries”; M. S. Whittingham. Invited.
- Harvard University, Cambridge, Massachusetts (November 14, 2018): “What are the Materials Limitations to Advancing Li-Batteries to the Next Level”; M. S. Whittingham. Invited.
- MRS Meeting, Boston, Massachusetts (November 26, 2018): “Materials for High Energy Li and Li-Ion Batteries”; M. S. Whittingham. Invited.
- MRS Meeting, David Turnbull Award Lecture, Boston, Massachusetts (November 27, 2018): “Solid State Ionics – The Key to the Discovery and Domination of Lithium Batteries for Portable Energy Storage Leading to a Multi-Billion Dollar Industry”; M. S. Whittingham. Invited.
- MRS Meeting, Boston, Massachusetts (November 29, 2018): “1D, 2D and 3D Defect Dynamics in Li Intercalation Compounds”; Y. S. Meng. Invited.
- Departmental Seminar, Materials Science and Engineering, University of Washington, Seattle, Washington (November 19, 2018): “Future Mobility – How Battery Changes Electrification”; B. Liaw. Invited.

- 9th Annual Battery Safety Conference, Arlington, Virginia (October 30–31, 2018): "Cross-Platform Analysis to Improve Cell Design for Safety"; B. Liaw. Invited Featured Presentation.
- Departmental Seminar, Electrical Engineering, San Diego State University, San Diego, California (October 19, 2018): "A Broad Perspective on Future Mobility – How Battery Changes Electrification"; B. Liaw. Invited.
- Materials Science Seminar, Northwestern University, Evanston, Illinois (October 2, 2018): "Nanomaterials Design for Energy Storage and Catalysis"; Y. Cui. Invited.
- 19th Annual Vanderbilt Nanoscience and Nanotechnology Forum, Vanderbilt University, Nashville, Tennessee (October 3, 2018): "Nanomaterials Design for Energy and Environment"; Y. Cui. Invited keynote talk.
- 6th Nano Israel Conference, Jerusalem, Israel (October 10–11, 2018): "Nanomaterials Design for Energy and Environment"; Y. Cui. Invited plenary talk.
- Fall Fiber Society Conference, University of California, Davis, California (October 29–31, 2018): "Fibers Across Multiple Length Scale from Energy, Environment to Electronics"; Y. Cui. Invited Plenary Talk.
- Global Energy Forum, Stanford University (November 1–2, 2018): "How Far Can Batteries Go"; Y. Cui. Invited.
- Stanford Chinese Faculty & Family Club, Quarterly Speaker Series, Stanford University, Stanford, California (November 4, 2018): "Batteries Now and Future"; Y. Cui. Invited.
- Stanford University, Department of Energy Resources Engineering Seminar (November 5, 2018): "Pathways of Batteries Towards Sustainable Electric Transportation and Stationary Storage"; Y. Cui. Invited.
- International Symposium on Functional Materials for Energy Storage and Conversion – Carbon Energy, Wenzhou, China (November 12–13, 2018): "Materials Technology Innovation and Commercialization"; Y. Cui. Invited Plenary Talk.
- University of Chinese Academy of Sciences Seminar, Beijing, China (November 14, 2018): "Nanotechnology for Energy and Environment"; Y. Cui. Invited.
- Xiangshan Meeting on Hollow Materials, Beijing, China (November 15–16, 2018): "Hollow Materials Design for Energy"; Y. Cui. Invited keynote talk.
- MRS Fall Meeting, Symposium ET09, Boston, Massachusetts (November 25–30, 2018): "Nanoscale Design for Lithium-Sulfur Batteries"; Y. Cui. Invited.
- MRS Fall Meeting, Symposium ET01, Boston, Massachusetts (November 25–30, 2018): "Nanoscale Composite Polymer Electrolyte Batteries"; Y. Cui. Invited.
- 4th International Symposium on Energy Chemistry & Materials (ISECM 2018), Xiamen University, Xiamen, Fujian, China (December 10–13, 2018): "Nanomaterials and Interfacial Design for Energy Storage"; Y. Cui. Invited plenary talk.
- MRS Fall Meeting, Boston, Massachusetts (November 28, 2018): "Understanding the Many Length Scales of Ion Insertion Solids"; W. C. Chueh. Invited.
- SNL Colloquium, (December 17, 2018): "X-Rays Show How Sustainable Energy Materials Function"; M. F. Toney. Invited.